

Testing and Optimization of Manufacturing Procedures Using Regression Modeling Techniques

Submitted to the Graduate School of Natural and Applied Sciences
in partial fulfillment of the requirements for the degree of

Master of Science

in Mechanical Engineering

by

Emre Görkem ÖZTÜRK

ORCID 0000-0002-6004-9098

August, 2021

This is to certify that we have read the thesis **Testing and Optimization of Manufacturing Procedures Using Regression Modeling** submitted by **Emre Görkem Öztürk**, and it has been judged to be successful, in scope and in quality, at the defense exam and accepted by our jury as a MASTER'S THESIS.

APPROVED BY:

Advisor: **Assoc. Prof. Dr. Levent Aydın**

 İzmir Kâtip Çelebi University

Committee Members:

Assist. Prof. Dr. Ebubekir Atan

 İzmir Kâtip Çelebi University

Prof. Dr. Alper Taşdemirci

 İzmir Institute of Technology

Date of Defense: August 24, 2021

Declaration of Authorship

I, **Emre Görkem Öztürk**, declare that this thesis titled **Testing and Optimization of Manufacturing Procedures Using Regression Modeling** and the work presented in it are my own. I confirm that:

- This work was done wholly or mainly while in candidature for the Master's degree at this university.
- Where any part of this thesis has previously been submitted for a degree or any other qualification at this university or any other institution, this has been clearly stated.
- Where I have consulted the published work of others, this is always clearly attributed.
- Where I have quoted from the work of others, the source is always given. This thesis is entirely my own work, with the exception of such quotations.
- I have acknowledged all major sources of assistance.
- Where the thesis is based on work done by myself jointly with others, I have made clear exactly what was done by others and what I have contributed myself.

Signature:

Date: 24.08.2021

Testing and Optimization of Manufacturing Procedures Using Regression Modeling

Abstract

With the developments in manufacturing methods over time, the need for precision manufacturing methods in sectors such as automotive and aerospace is increasing. In order to increase precision in manufacturing methods, product performance and minimize the margin of error in production, the relationship between the design parameters of the process and the process outputs is examined.

Outputs such as surface roughness, cutting forces and tool wear are essential in manufacturing. Optimization methods have the most important role in the analysis of these outputs.

In this thesis, a new design optimization strategy is proposed to improve the analytical performance of surface roughness, cutting forces, tool wear and tool life by considering structural and experimental parameters as design variables. In order to overcome inadequate approaches to modeling-design-optimization of data outputs, a detailed study has been carried out methodologically on multiple nonlinear neuro-regression analysis. For this purpose, data set was selected from 12 different literature studies. A hybrid method was used to test the accuracy of the predictions of the proposed functional structures modeling the data. In order to reveal whether the model is realistic or not, the limitation of the candidate models was checked after calculating with 13 different models. Then, using four different optimization algorithms, suitable models were optimized for different optimization scenarios. This new optimization approach is also suitable for another modeling-design-optimization problem in analytical applications.

Keywords: Optimization, Neuro-Regression Modeling, Stochastic Method, Surface Roughness, Cutting Forces, Tool Wear

Regresyon Modelleme Tekniklerinin Kullanıldığı İmal Usülleri Çalışmalarının Sınanması ve Optimizasyonu

ÖZ

Zaman içerisinde imalat yöntemlerinde sağlanan gelişmelerle birlikte otomotiv ve uzay gibi sektörlerde hassas imalat yöntemlerine ihtiyaç giderek artmaktadır. İmalat yöntemlerinde hassasiyeti arttırabilmek, ürün performansını arttırabilmek ve üretimdeki hata payını minimize edebilmek adına prosesin dizayn parametreleri ve proses çıktıları ile olan ilişkileri incelenmektedir.

Yüzey pürüzlülüğü, kesme kuvvetleri ve takım aşınması gibi çıktılar imalatta önem teşkil etmektedir. Bu çıktıların incelemelerinde ise optimizasyon yöntemleri en önemli role sahiptir.

Bu tez kapsamında, tasarım değişkenleri olarak yapısal ve deneysel parametreler dikkate alınarak yüzey pürüzlülüğünün, kesme kuvvetlerinin, takım aşınmasının ve takım ömrünün analitik performansını arttırmak için yeni bir tasarım optimizasyon stratejisi önerilmiştir. Veri çıktılarının modellenmesi-tasarımı-optimizasyonu konusundaki yetersiz yaklaşımların üstesinden gelmek için metodolojik olarak çoklu doğrusal olmayan nöro-regresyon analizi üzerinde ayrıntılı bir çalışma yapılmıştır. Bu amaçla veriler 12 farklı literatür çalışmasından seçilmiştir. Verileri modellemek için önerilen fonksiyonel yapıların tahminlerinin doğruluğunu test etmek için hibrit bir yöntem kullanılmıştır. Modelin gerçekçi olup olmadığını ortaya çıkarmak için 13 farklı model ile hesaplanmasından sonra aday modellerin sınırlılığı kontrol edilmiştir. Daha sonra dört farklı optimizasyon algoritması kullanılarak uygun modeller farklı optimizasyon senaryoları açısından optimize edilmiştir. Bu yeni optimizasyon yaklaşımı, analitik uygulamalarda başka bir modelleme-tasarım-optimizasyon problemi için de uygundur.

Anahtar Kelimeler: Optimizasyon, Nöro-Regresyon Modelleme, Stokastik Metot, Yüzey Pürüzlülüğü, Kesme Kuvvetleri, Takım Aşınması

To my family...

Acknowledgment

First and foremost, I would like to express my endless thanks to my academic advisor Assoc. Prof. Dr. Levent Aydın, who has always supported me, who has been working hard on me for about 7 years. He never withheld his knowledge from me, rather he worked patiently to teach something more. I will always be proud to work with him and to be his student.

I would like to thank also Prof. Dr. Alper Taşdemirci who helped me with his valuable suggestions and guidance has been helpful in every phases of the completion of my study.

I should state that I am grateful to my family who supported me in my nearly 20 years of education under all circumstances, who always stood behind me and who did not spare their moral support.

Lastly, I am very thankful to my beloved friend Alp Emre Yaşar for his friendship, caring, support, and motivation.

Table of Contents

Declaration of Authorship	ii
Abstract	iii
Öz	iv
Acknowledgment	vi
List of Figures	xiii
List of Tables.....	xiv
List of Abbreviations.....	xix
List of Symbols	xx
1 Introduction	1
1.1 Literature Survey	1
1.2 Objectives and Motivation.....	6
2 Machining Process.....	12
2.1 Milling.....	12
2.2 Turning.....	14
2.3 Surface Roughness.....	17
2.4 Cutting Forces.....	19
2.5 Tool Wear	21
3 Regression Analysis.....	24
3.1 Regression Models.....	24
3.2 Purpose of Regression Analysis.....	26
3.3 Non-Linear Regression Analysis	26
4 Neuroregression Approach.....	29

4.1	Design of Experiments (DOE).....	29
4.1.1	DOE Techniques.....	30
4.1.1.1	Randomized Complete Block Design	31
4.1.1.2	Full Factorial Design	31
4.1.1.3	Fractional Factorial Design	32
4.1.1.4	Central Composite Design.....	32
4.1.1.5	Box-Behnken Design	32
4.1.1.6	Taguchi Design.....	32
4.1.1.7	Latin Hypercube Design.....	33
4.1.1.8	Optimal Design (D-Optimal).....	34
4.2	Mathematical Modeling	34
4.2.1	Coefficient of Determination.....	35
4.2.2	Training and Testing.....	36
5	Optimization Process	38
5.1	Introduction.....	38
5.2	Simulated Annealing.....	41
5.3	Differential Evolution	43
5.4	Nelder-Mead	44
5.5	Random Search	45
6	Mathematica Implementation	47
6.1	Global and Local Optimization by Mathematica.....	47
6.1.1	FindMinimum.....	49
6.1.2	NMinimize and NMaximize Functions	51
6.2	Random Search	52
6.3	Simulated Annealing.....	56
6.4	Differential Evolution	60
6.5	Nelder-Mead	62

7 Case Studies	65
7.1 Mathematical Models.....	65
7.2 Case Study #1	67
7.2.1 Optimization Scenarios.....	70
7.2.1.1 Scenario 1	71
7.2.1.2 Scenario 2	71
7.2.1.3 Scenario 3	71
7.2.1.4 Scenario 4	71
7.2.2 Results and Discussion	72
7.3 Case Study #2	90
7.3.1 Optimization Scenarios.....	93
7.3.1.1 Scenario 1	94
7.3.1.2 Scenario 2	94
7.3.1.3 Scenario 3	94
7.3.1.4 Scenario 4	94
7.3.2 Results and Discussion	94
7.4 Case Study #3	110
7.4.1 Optimization Scenarios.....	112
7.4.1.1 Scenario 1	112
7.4.1.2 Scenario 2	112
7.4.1.3 Scenario 3	112
7.4.2 Results and Discussion	113
7.5 Case Study #4	117
7.5.1 Optimization Scenarios.....	119
7.5.1.1 Scenario 1	119
7.5.1.2 Scenario 2	119
7.5.1.3 Scenario 3	119

7.5.2	Results and Discussion	120
7.6	Case Study #5	123
7.6.1	Optimization Scenarios.....	125
7.6.1.1	Scenario 1	125
7.6.1.2	Scenario 2	125
7.6.1.3	Scenario 3	125
7.6.2	Results and Discussion	125
7.7	Case Study #6	129
7.7.1	Optimization Scenarios.....	131
7.7.1.1	Scenario 1	131
7.7.1.2	Scenario 2	131
7.7.2	Results and Discussion	132
7.8	Case Study #7	135
7.8.1	Optimization Scenarios.....	138
7.8.1.1	Scenario 1	139
7.8.1.2	Scenario 2	139
7.8.1.3	Scenario 3	139
7.8.1.4	Scenario 4	139
7.8.2	Results and Discussion	140
7.9	Case Study #8	153
7.9.1	Optimization Scenarios.....	156
7.9.1.1	Scenario 1	156
7.9.1.2	Scenario 2	156
7.9.1.3	Scenario 3	157
7.9.1.4	Scenario 4	157
7.9.2	Results and Discussion	157
7.10	Case Study #9	164

7.10.1 Optimization Scenarios.....	166
7.10.1.1 Scenario 1	166
7.10.1.2 Scenario 2	166
7.10.1.3 Scenario 3	167
7.10.2 Results and Discussion	167
7.11 Case Study #10	171
7.11.1 Optimization Scenarios.....	173
7.11.1.1 Scenario 1	173
7.11.1.2 Scenario 2	173
7.11.1.3 Scenario 3	174
7.11.2 Results and Discussion	174
7.12 Case Study #11	178
7.12.1 Optimization Scenarios.....	180
7.12.1.1 Scenario 1	180
7.12.1.2 Scenario 2	181
7.12.1.3 Scenario 3	181
7.12.2 Results and Discussion	181
7.13 Case Study #12	185
7.13.1 Optimization Scenarios.....	188
7.13.1.1 Scenario 1	188
7.13.1.2 Scenario 2	188
7.13.1.3 Scenario 3	189
7.13.2 Results and Discussion	189
8 Conclusion.....	201
References	204
Appendices	215
Appendix A Explicit Model Expressions of the Case Studies	216

Curriculum Vitae 231

List of Figures

Figure 2.1 Milling types (a) face milling (b) shoulder milling.....	13
Figure 2.2 Milling types (a) peripheral (or flank) milling (b) ball-end milling.....	13
Figure 2.3 Groove or slot milling operation with different types of end mill	14
Figure 2.4 Basic turning operations.....	15
Figure 2.5 Basic motions in turning operations.....	16
Figure 2.6 Fundamental motions in boring process.....	16
Figure 2.7 Basic motions in boring operations	17
Figure 2.8 Roughness left on the machined surface	18
Figure 2.9 Various tool nose radius	19
Figure 2.10 Cutting force and its elements: (a) as exerted to the workpiece, (b) as exerted to the tool.....	20
Figure 2.11 Cutting speeds in milling for different materials	22
Figure 2.12 Comparison between the workpiece surfaces (a) new cutting tool and (b) worn cutting tool	22
Figure 2.13 Central wear and flank wear at the cutting edges are monitored by SEM with original magnification 100 times	23
Figure 4.1 Flow diagram of design process.....	30
Figure 5.1 Flowchart of Simulated Annealing algorithm.....	42
Figure 5.2 Flowchart of Differential Evolution algorithm	43
Figure 5.3 Flowchart of Nelder-Mead algorithm	45
Figure 5.4 Flowchart of Random Search algorithm	46
Figure 6.1 Mathematica optimization process.....	49

List of Tables

Table 1.1	Number and names of the case studies.....	9
Table 1.2	Literature studies on the modeling of surface roughness, cutting forces, tool wear and tool life.....	10
Table 6.1	Optimization methods and instructions.....	49
Table 7.1	Multiple regression model names, numbers, nomenclatures and formulas	66
Table 7.2	Experimental results of arithmetic mean and total roughness with different experimental conditions	69
Table 7.3	Results of the Neuro-regression models for the arithmetic mean roughness for Ra_{CC670}	72
Table 7.4	Results of the Neuro-regression models for the total roughness for Rt_{CC670}	73
Table 7.5	Results of the Neuro-regression models for the arithmetic mean roughness for Ra_{CC650}	73
Table 7.6	Results of the Neuro-regression models for the total roughness for Rt_{CC650}	74
Table 7.7	Results of the Neuro-regression models for the arithmetic mean roughness for $Ra_{CBN7020}$	74
Table 7.8	Results of the Neuro-regression models for the total roughness for $Rt_{CBN7020}$	75
Table 7.9	Optimization problem results of selected model CS1-O1-SON for arithmetic mean roughness (Ra_{CC670}).....	84
Table 7.10	Optimization problem results of selected model CS1-O2-LR for total roughness (Rt_{CC650}).....	85
Table 7.11	Optimization problem results of selected model CS1-O3-SON for arithmetic mean roughness (Ra_{CC650})	86

Table 7.12 Optimization problem results of selected model CS1-O4-L for total roughness (R_{tCC650}).....	87
Table 7.13 Optimization problem results of selected model CS1-O5-LR for arithmetic mean roughness ($R_{aCBN7020}$).....	88
Table 7.14 Optimization problem results of selected model CS1-O6-SOTN for total roughness ($R_{tCBN7020}$).....	89
Table 7.15 Experimental results of tool wear, surface roughness and cutting force components with different experimental conditions.....	92
Table 7.16 Results of the Neuro-regression models for the tool wear (VB).....	95
Table 7.17 Results of the Neuro-regression models for the surface roughness (Ra)	96
Table 7.18 Results of the Neuro-regression models for the cutting force (F_a).....	96
Table 7.19 Results of the Neuro-regression models for the cutting force (F_c).....	97
Table 7.20 Results of the Neuro-regression models for the cutting force (F_p).....	97
Table 7.21 Optimization problem results of selected model CS2-O1-LR for tool wear (VB).....	105
Table 7.22 Optimization problem results of selected model CS2-O2-SON for surface roughness (Ra).....	106
Table 7.23 Optimization problem results of selected model CS2-O3-L for cutting force (F_a).....	107
Table 7.24 Optimization problem results of selected model CS2-O4-SONR for cutting force (F_c).....	108
Table 7.25 Optimization problem results of selected model CS2-O5-SON for cutting force (F_p).....	109
Table 7.26 Experimental results of tool life and volume removed with different experimental conditions.....	111
Table 7.27 Results of the Neuro-regression models for the tool life (cutting time)	113
Table 7.28 Results of the Neuro-regression models for the volume removed.....	114
Table 7.29 Optimization problem results of selected model CS3-O1-TON for tool life (cutting time).....	116
Table 7.30 Experimental results of resultant force with different experimental conditions.....	118
Table 7.31 Results of the Neuro-regression models for the cutting force in terms of fitting performance and boundedness.....	120

Table 7.32	Optimization problem results of selected model CS4-O-FOTN for cutting force (resultant force)	122
Table 7.33	Experimental results of resultant force with different experimental conditions	124
Table 7.34	Results of the Neuro-regression models for the surface roughness	126
Table 7.35	Optimization problem results of selected model CS5-O-SON for surface roughness.....	128
Table 7.36	Experimental results of resultant force with different experimental conditions	130
Table 7.37	Results of the Neuro-regression models for the surface roughness in terms of fitting performance and boundedness	132
Table 7.38	Optimization problem results of selected model CS6-O-SOLNR for surface roughness	134
Table 7.39	Experimental results of surface roughness and cutting forces with different experimental conditions	137
Table 7.40	Results of the Neuro-regression models for the surface roughness	140
Table 7.41	Results of the Neuro-regression models for the cutting force (F_x , feed force)	141
Table 7.42	Results of the Neuro-regression models for the cutting force (F_y , thrust force)	141
Table 7.43	Results of the Neuro-regression models for the cutting force (F_z , tangential force)	142
Table 7.44	Optimization problem results of selected model CS7-O1-L for surface roughness (R_a).....	148
Table 7.45	Optimization problem results of selected model CS7-O2-L for feed force (F_x).....	149
Table 7.46	Optimization problem results of selected model CS7-O3-TON for thrust force (F_y).....	150
Table 7.47	Optimization problem results of selected model CS7-O4-SON for tangential force (F_z)	151
Table 7.48	Experimental results of surface roughness and cutting force with different experimental conditions	155
Table 7.49	Results of the Neuro-regression models for the cutting force.....	158

Table 7.50	Results of the Neuro-regression models for the surface roughness	158
Table 7.51	Optimization problem results of selected model CS8-O1-FOTN for cutting force.....	162
Table 7.52	Optimization problem results of selected model CS8-O2-L for surface roughness.....	163
Table 7.53	Experimental results of surface roughness with different experimental conditions	165
Table 7.54	Results of the Neuro-regression models for the surface roughness	168
Table 7.55	Optimization problem results of selected model CS9-O-L for surface roughness.....	170
Table 7.56	Experimental results of surface roughness with different experimental conditions	172
Table 7.57	Results of the Neuro-regression models for the surface roughness	174
Table 7.58	Optimization problem results of selected model CS10-O-L for surface roughness.....	177
Table 7.59	Experimental results of surface roughness with different experimental conditions	179
Table 7.60	Results of the Neuro-regression models for the surface roughness	182
Table 7.61	Optimization problem results of selected model CS11-O-FOTNR for surface roughness	184
Table 7.62	Experimental results of surface roughness and cutting forces with different experimental conditions	187
Table 7.63	Results of the Neuro-regression models for the cutting force (F_x , infeed force)	190
Table 7.64	Results of the Neuro-regression models for the cutting force (F_y , crossfeed force)	190
Table 7.65	Results of the Neuro-regression models for the cutting force (F_z , thrust force)	191
Table 7.66	Optimization problem results of selected model CS12-O1-SOTN for infeed force (F_x).....	195
Table 7.67	Optimization problem results of selected model CS7-O3-TON for thrust force (F_y).....	196

Table 7.68 Optimization problem results of selected model CS7-O4-SON for tangential force (Fz)	197
--	-----

List of Abbreviations

ANN	Artificial Neural Network
GA	Genetic Algorithm
DoE	Design of Experiment
ANOVA	Analysis of Variance
RSM	Response Surface Methodology
DE	Differential Evolution
SA	Simulated Annealing
RS	Random Search
NM	Nelder Mead
MDE	Modified Differential Evolution
MSA	Modified Simulated Annealing
MRS	Modified Random Search
MNM	Modified Nelder Mead

List of Symbols

V_c	Cutting speed
f	Feed
a_p	Depth of cut
n	Spindle speed
r	Tool nose radius
Ra	Surface roughness

Chapter 1

Introduction

1.1 Literature Survey

A great variety of machining methods have been introduced as the accuracy and precision required by the consumer has been increased in relation to the working condition of the workpieces, requiring high quality workpieces for industry. Demand for metalworking has gradually increased over the last few decades [1].

In the 1960s, the copying of work pieces was based on two distinct approaches. Via turning centers and machining centers, the work parts were machined. In order to conduct special processing operations, many instruments have been researched and the tool industry has thus expanded simultaneously. Owing to the high-cost investment budget, the devices have been extensively run in order to maximize efficiency. The need for high-speed centers has increased as a requirement of this [1].

In these days' industrial development and academic study, cutting tempered steels is a matter of excellent attention. In the aerospace, automotive, gear and bearing industry, they are commonly used. Grinding process has wide range use for strengthened steels. Nevertheless, grinding applications are time consuming and the geometry to be produced with this process is limited. Therefore, turning and milling are the technologies that give many possible advantages over grinding, which remains the traditional method of finishing vital hardened steel surfaces [2,3]. The material of the tool is usually chosen from high-speed steel, solid carbide or carbide inserts. Thermal properties of the material, machining parameters, cutting fluids and environmental conditions influence the surface quality of the work piece. [4].

The Taguchi method has been studied for analyzing the effects of manufacturing factors on surface roughness in turning and milling operations. Taguchi method has been used in determining the optimal cutting parameters that match the minimum surface roughness. The tests have been performed using the coated carbide insert on hardened steel bars AISI 4140 [5]. Taguchi parameter design method has been used in turning process to reach the required extending the tool life and targeted surface roughness with the optimal machining parameters. Feed rate has a significant effect on surface roughness, while cutting speed has a lower effect [6]. Taguchi's robust design method has been used for optimizing the process parameters to get minimum surface roughness and resultant force values in end milling process for the material strengthened steel AISI H13. High cutting speed, low feed rate and low cutting depth contribute to improved surface texture and low cutting force [7]. To minimize surface roughness the machining parameters such as nose radius, cutting speed, feed rate, axial depth of cut and radial depth of cut are considered using Taguchi's L50 orthogonal array. Improvement of surface roughness is 44.22% [8]. Mahapatra et al. used Taguchi method and Genetic Algorithm to find the ideal parametric composition that reach required quality of the manufactured good. As a result, the ideal outcome estimated by GA is unable to be reached in reality, due to nonbeing of the ideal parameter composition in the cutting mechanism. Therefore, in reality an arrangement must be made to choose the following potential feature composition; so near to the ideal [9]. In a further study, Taguchi method is utilized to reach the ideal cutting parameters to minimize surface roughness in turning. The vertical sequence, signal-to-noise ratio and analysis of variance (ANOVA) are used to examine the effects of the three cutting parameters: insert radius, feed rate and depth of cut, in turning processes of AISI 1030 steel bars utilizing TiN covered tools [10]. In an alternative study based on ANOVA, a study on surface roughness in hard turning of AISI D2 tool steel with ceramic cutting tools using experimental and statistical techniques is performed. Turning tests are conducted by using cutting speed feed rate and time as main parameters and analysis was done based on the responses. ANOVA is used to see the influence of cutting parameters on flank wear, specific cutting force and surface roughness [11].

Design of experiment (DoE) is a branch of applied statistics which deals with preparation, behavior, analysis and interpretation of controlled tests in order to evaluate those parameter or parameter group factors that control their value. It is a

valuable instrument for the collection and analyze of data that can be used in different experimental circumstances. The design of experiments (DoE) is the most significant element of Response Surface Methodology (RSM). RSM is a commonly used approximation for modeling and analyzing mathematical and statistical processes where the interest response has an impact on different variables. The main purpose of this method is to optimize the response. RSM technique has been used to show coherence between experimental and predicted results. Some of the previous RSM based researches can be listed as given in the following paragraph.

The study shows that there is a grateful coherence between results. In addition, the study observed that surface roughness is directly proportional with feed and inversely proportional with cutting speed [12]. Another study used RSM optimization technique to show effects of variables in drilling of Al-7075 alloy. The results clarified that cutting speed is less effective than feed rate on thrust force and cutting torque [13]. In order to show the influences of design variables (cutting speed, feed rate, radial depth and axial depth of cut) on cutting force in end milling process with RSM, first and second order models are built. The study showed that the most effective variable was feed rate and less was the cutting speed [14]. The RSM was also adopted by another study; they have examined that influences of Al_2O_3/TiC tool geometry on the surface roughness of AISI 1040 steel in turning process. To determine the geometry variables' ideal outcomes, the researchers also utilized an RSM second order model and the compound desirability measure [15]. In processing Hadfield steel, an experiment has been performed to simulate the assessment of formability using the Response Surface Methodology (RSM). On the flank wear and surface roughness, the connected impacts of cutting speed, feed rate, depth of cut, and tool corner radius has been examined. Ideal outcomes of machining parameters were determined using a second order RSM model and sequential approximation optimization (SAO) [16].

Two of the most hopeful natural calculation approaches are the Artificial Neural Network (ANN) and the Genetic Algorithm (GA) in engineering. ANN has become a highly potential and effective approach for modeling extremely complicated non-linear structures [17–21], and GA is used in a variety of study disciplines for parameter optimization in modern times [18,19,21,22]. Artificial neural network (ANN) and genetic algorithm (GA) are used in a recent study in order to identify the ideal cutting

parameters for end milling operations. The MATLAB ANN toolbox was used to construct ANN models depending on the feed-forward back-propagation method. It has been found that the combined ANN-GA technique decreased the time required to find an ideal result in comparison with the standard GA approach [23]. One other work used genetic algorithm (GA) with response surface methodology (RSM) for optimization of cutting parameters in high-speed ball-end milling with dry circumstances of A112014-T6 [24]. A multi-objective optimization method depending on genetic algorithms is integrated into a recent study in order to use of design variables (cutting speed, feed rate and depth of cut) optimization in turning operation. Although tool life and operation time are contradictory parameters, they are optimized at the same time [25]. In order to achieve minimum tool wear, minimum surface roughness and optimal cutting parameters, a study performs combination of RSM, ANN and GA. Machining parameters are developed by using RSM and the optimization procedure has been performed by using GA-RSM and GA-ANN combination. The results show that GA-ANN combination is much better and precise method [26]. Another study aims to develop a predictive model to minimizing surface roughness by using ANN and GA combination. Minimum surface roughness value has been determined with the optimal design variables. The predicted surface roughness value determined by ANN-GA approach model is very close to the experimentally obtained value [27]. In addition to this, another study has an aim to minimize surface roughness by optimizing turning process design variables. To achieve the machining conditions for targeted surface finish, the response surface methodology (RSM) and genetic algorithm (GA) are combined and used [28]. In other published paper, a genetic algorithm with binary coding is utilized to optimize design variables. The method optimizes design variables that affect manufacturing cost, time, and product quality [29]. For predicting the surface roughness, on the basis of a back-propagation learning method, an artificial neural network (ANN) model has built for the end milling process. As a result of the study, The two-hidden-layer ANN model estimates surface roughness more correctly and effectively than the one-hidden-layer model [30]. Another study is employed to show how ANN works on projection of surface roughness of 600 BHN steel, which is hard turned with minimal lubrication (MQL). 97,5% percent of the accuracy is achieved by the model that is depending on ANN [31].

There are several engineering areas that use regression analysis to describe the connection between a response variable and one or more independently-varying variables. A statistical and mathematical method is used in combination with empirical research to create this modeling strategy. According to Subramanian et al., ideal end mill process design parameters were determined using a regression cutting force model combined with a genetic algorithm [32]. Using nonlinear regression analysis with logarithmic data conversion, Feng and Wang (2002) presented an analytical model for the prediction of surface roughness during finishing process. Also, they analyzed the influence of workpiece hardness, feed, tool angle, depth of cut, spindle speed and cutting time on the output [33]. In another study, the several coating and tool types and specific cutting parameter effects were investigated and optimized to get the minimum average roughness of the milling surfaces. Due to results, a general linear regression model has been used to predict the process with the determination coefficient of 0.90 [34].

Multiple nonlinear neuro-regression approach can be performed to show the effects of nonlinear influences of the input parameters. This approach includes linear, quadratic, trigonometric, logarithmic, and their rational forms of the response values. A study has performed multiple nonlinear neuro-regression analysis to enhance the performance of a biosensor. The study aims enhance the performance of biosensor with overcome insufficient approaches by using neuro-regression approach and modeling-design-optimization studies. According to optimization results, 8,5% improvement of biosensor performance has been observed [35]. In another study, multiple nonlinear neuro-regression approach has been performed to study heat transfer optimization problem of a ground source heat exchanger. In the approach, the major aim is minimizing the error between objective function results and exact results. Optimization results show that heat transfer at a rate of reach 220 W per unit length in this problem. Also, it is reached its maximum value when all design variables (inputs) are maximum except borehole depth [36].

Hybrid optimization techniques are used to increase the search ability and to make the results more accurate. This new approach is based on the principle of simultaneously using stochastic optimization techniques such as differential evolution to bring solution to machining problems. Two authors conclude that the modeling of surface

performance in manufacturing operations has largely utilized Artificial Neural Networks and fuzzy set theory [37, 38]. Another author investigated the impact of manufacturing design variables integration to get high surface quality in turning process and to estimate the surface roughness values applied fuzzy modeling [39]. In another study, it is used a hybrid multi objective optimization technique, Fuzzy-Technique for Order Preference by Similarity to Ideal Solution (TOPSIS) to obtain optimal cutting parameters and their effect on Kerf Width (KW) together with Material Removal Rate (MRR) during processing AISI P20 tool steel [40].

The optimum machining parameters have been selected to minimize a machining cost by two stage Differential Evolution optimization method. With this method, better results have been obtained compared to single use of Differential Evolution. Significant results have been obtained that hybrid robust differential evolution can be used to optimize machining parameters [41]. Genetic algorithm and simulated annealing have been studied for multi-pass milling as a hybrid approach to minimize the production time which is the total time to produce a completed part from preparation to machining. For all four time periods mathematical equations were investigated. Five different constraints have been chosen for the machine and apparatus limits. Genetic simulated annealing algorithm have better results than genetic algorithm and geometric programming in milling operation for different objective functions [42].

Optimization methods are commonly used in several engineering problems to create or design complex systems to improve the performance of the structure in the field of aerospace, automotive, marine and chemical industries. Some of their applications are cost-friendly machining processes, high efficiency energy consumptions processes or lightweight product design. Even though most engineering design problems can be clarified using stochastic programming techniques like Differential Evaluation, Nelder-Mead, Random Search, Simulated Annealing which are most suitable [43].

1.2 Objectives and Motivation

In this thesis, optimization study of surface roughness minimization, cutting forces minimization, tool wear and tool life (cutting time) minimizations have been

performed considering experimental results of twelve different literature studies. Optimization of turning and milling process design variables cutting speed, spindle speed, depth of cut, feed, cutting time and tool nose radius have been accomplished by four different stochastic algorithms, Differential Evolution (DE), Simulated Annealing (SA), Random Search (RS), and Nelder Mead (NM).

The objectives of this study can be considered as follows;

- Defining the phenomenon and finding the coefficient of determination by mathematical model in the best way
- The possibility of experimental parameters selected and commenting behavior of machine for different machine parameters
- Determination of new objective function
- Investigating optimum surface roughness, cutting forces, tool wear and tool life value for different machining parameters
- Comparison of four different stochastic optimization algorithms

It should be noted that defining the best mathematical model is not simple for any machining parameters as well as another machining process turning, drilling etc. Because different disturbances dominate the system at different levels. Therefore, the mathematical model might be built according to other parameters such as material of cutting tool, cooling flowrate, workpiece material etc. However, if some of input values are selected to decrease the average roughness value, it would be more accurate to define the optimization problem.

In the current study, the results of 12 different literature studies were examined, and optimization process studies were carried out in order to show the deficiencies in these studies, to report the problems and to make improvements in the results. If we briefly mention about why the results of these literature studies are examined and why these studies are carried out, the R^2 value cannot be evaluated by using only one or two regression models as a decision criterion. It is not usually the case that a strong R^2 correlation equates to a fine match for acceptable structures. Determining the basic

actions of the phenomenon requires fresh modeling experiments using alternative regression techniques. Furthermore, the models established in the academic research have no limitedness control. For this reason, limitedness must be controlled if the engineering parameter ranges relate to the selected models.

As a result of this goal, all of the response values as cutting forces, surface roughness, tool wear, and tool life (cutting life) has been examined using multiple nonlinear neuro-regression approach. After that, the limitedness of potential models was examined in order to provide accurate results. Eventually, the different direct search techniques, including stochastic optimization methods, were carefully implemented.

In this present study, the experimental datas are taken from the studies of “Aouici, H., Fnides, B., Elbah, M., Benlahmidi, S., Bensouilah, H., & Yallese, M. (2016) [44]; Bouacha, K., Yallese, M. A., Khamel, S., & Belhadi, S. (2014) [45]; Davoodi, B., & Eskandari, B. (2015) [46]; Hanief, M., Wani, M. F., & Charoo, M. S. (2017) [47]; Jena, J., Panda, A., Behera, A. K., Jena, P. C., Das, S. R., & Dhupal, D. (2019) [48]; Kovac, P., Rodic, D., Pucovsky, V., Savkovic, B., & Gostimirovic, M. (2013) [49]; Meddour, I., Yallese, M. A., Bensouilah, H., Khellaf, A., & Elbah, M. (2018) [50]; Qu, S., Zhao, J., & Wang, T. (2017) [51]; Paturi, U. M. R., Devarasetti, H., & Narala, S. K. R. (2018) [52]; Sahoo, A. (2014) [53]; Sahoo, A., Rout, A., & Das, D. (2015) [54]; Subramanian, M., Sakthivel, M., Sooryaprakash, K., & Sudhakaran, R. (2013) [55]” is used for analysis and optimization processes. The names and numbers of case studies are listed in Table 1.1. These data sets have the cutting parameters as cutting speed, spindle speed, depth of cut, axial depth of cut, feed rate, feed per tooth, tool nose radius, cutting time and width of flank wear the corresponding values. First, the mathematical model predicting the data was investigated for the outputs by performing regression analysis. The accuracy of the model has also been verified by regression test methods. Then, cutting parameters were optimized for minimum surface roughness, minimum cutting forces, minimum tool wear and minimum tool life (cutting time) utilizing optimization methods. Table 1.2 contains the various optimization approaches to optimize various design variables of the literature studies of the present study.

Table 1.1: Number and names of the case studies

Number of Case Study	Name of Case Study
1	Aouici, H., Fnides, B., Elbah, M., Benlahmidi, S., Bensouilah, H., & Yallese, M. (2016) [44]
2	Bouacha, K., Yallese, M. A., Khamel, S., & Belhadi, S. (2014) [45]
3	Davoodi, B., & Eskandari, B. (2015) [46]
4	Hanief, M., Wani, M. F., & Charoo, M. S. (2017) [47]
5	Jena, J., Panda, A., Behera, A. K., Jena, P. C., Das, S. R., & Dhupal, D. (2019) [48]
6	Kovac, P., Rodic, D., Pucovsky, V., Savkovic, B., & Gostimirovic, M. (2013) [49]
7	Meddour, I., Yallese, M. A., Bensouilah, H., Khellaf, A., & Elbah, M. (2018) [50]
8	Qu, S., Zhao, J., & Wang, T. (2017) [51]
9	Paturi, U. M. R., Devarasetti, H., & Narala, S. K. R. (2018) [52]
10	Sahoo, A. (2014) [53]
11	Sahoo, A., Rout, A., & Das, D. (2015) [54]
12	Subramanian, M., Sakthivel, M., Sooryaprakash, K., & Sudhakaran, R. (2013) [55]

Table 1.2: Literature studies on the modeling of surface roughness, cutting forces, tool wear and tool life

Reference	Aim of the study	Input Parameters	Modeling Method	Result
Aouici et al (2015)	Check the validity of multiple linear regression models and determine the effects of machining parameters on the arithmetic mean roughness and total roughness	Cutting speed, feed rate and depth of cut	Response Surface Methodology (RSM) and Regression Analysis	Machining parameters are determined to obtain minimum surface roughness.
Bouacha et al (2014)	Investigate the effects of process parameters on surface roughness and cutting forces	Cutting speed, feed rate, depth of cut and cutting time	Response Surface Methodology (RSM)	The parameters that affect the surface roughness and cutting forces the most and the least are determined. The best combination has been achieved.
Davoodi et al (2015)	Investigate and optimize the effects of cutting parameters on tool life and volume of workpiece material removed during the machining	Cutting speed and feed rate	Response Surface Methodology (RSM)	The optimal machining parameters after optimization of cutting parameters for tool life and volume of material removed has been achieved.
Hanief et al (2016)	Develop a model to investigate the effects of cutting parameters on the cutting forces	Cutting speed, feed rate and depth of cut	Artificial Neural Network (ANN) and Multiple Regression Approach	The cutting force increases with increase in all the three parameters.
Jena et al (2019)	Minimizing surface roughness	Cutting speed, axial feed and depth of cut	Response Surface Methodology (RSM)	Minimum surface roughness has been obtained according to experimental conditions and optimization results.
Kovac et al (2012)	Presenting a novel mathematical model for determination of the surface roughness	Cutting speed, feed per tooth, depth of cut and width of flank wear land	Fuzzy Logic and Regression Analysis	Surface roughness values were taken at both the minimum and maximum levels.
Meddour et al (2018)	Modeling and optimization procedure for surface roughness and cutting forces	Cutting speed, feed rate, depth of cut and tool nose radius	Response Surface Methodology (RSM) and ANN	Minimum response parameters have been obtained according to experimental conditions and optimization results.

Table 1.2: Literature studies on the modeling of surface roughness, cutting forces, tool wear and tool life (continued)

Qu et al (2016)	Presenting an optimization procedure to determine and validate the optimum surface roughness and cutting force	Spindle speed, feed per tooth and axial depth of cut	Regression Analysis	The regression models of response values are developed and the influences of machining parameters on response parameters are also investigated.
Paturi et al (2018)	Presenting an approach for predicting and modeling the surface roughness	Cutting speed, feed and depth of cut	ANN	ANN model predictions have closer correlation than RA model.
Sahoo et al (2013)	Predicting and modeling of surface roughness	Cutting speed, feed rate and depth of cut	Regression Analysis	A mathematical model is developed and the influences of machining parameters on surface roughness are also investigated.
Sahoo et al (2014)	Predicting and modeling of surface roughness	Cutting speed, feed and depth of cut	Response Surface Methodology (RSM) and ANN	Both the RSM and the ANN prediction models are capable of properly estimating surface roughness.
Subramanian et al (2013)	Develop a model to predict the effects of cutting parameters on the cutting forces	Cutting speed, feed and depth of cut	Response Surface Methodology (RSM) and Genetic Algorithm (GA)	The regression model of cutting force is developed and the influences of design variables on cutting force are also studied.

Chapter 2

Machining Process

2.1 Milling

Machining refers to any of many techniques that use a checked material-removal operation to cut a section of raw material into a desired eventual form and dimension. There are a lot of types of machining such as turning, milling, drilling etc.

Milling process has a different technique from turning operation. Tools have multiple cutting profiles. These cutting edges move along the tool path in order to obtain flat or required surface profiles. The feed direction is vertical to the rotation of the center line of the tool [56].

The cutting tool is made of harder material than the workpiece material. Relative motion is necessary to machine the workpiece. The first motion is achieved with a specific speed as called cutting speed. Besides the cutting speed, the tool also moves with the terms of feed. The remaining parameter is how far the tool travels into the workpiece called depth of cut. These three terms are completely known as cutting conditions. The machine tool holds the workpiece, orients the machine tool according to the work, and supplies the energy for the process at the given speed, feed, and depth [56].

Early 1960s milling had been used for single purpose as obtaining flat surface. However, after machine center technology with desired accuracy and precision any desired tool path geometry is processed. Nowadays there are four types of milling

operations such as face milling, shoulder milling, peripheral milling (or known as flank milling), and ball end milling shown in Figure 2.1 and Figure 2.2 [57].

For reaching the required geometry, the number of types of milling operations has increased for more specific machining such as profile milling, square shoulder milling, slot milling. In slot milling tool generates a tool path within slot by various types of end mill as shown in Figure 2.3 [57].

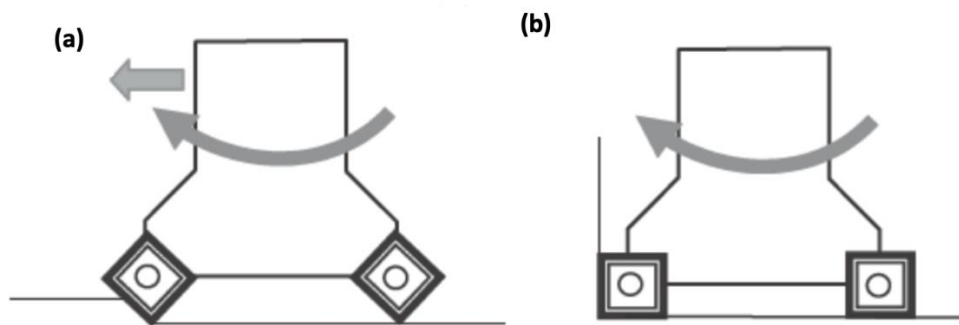


Figure 2.1: Milling types (a) face milling (b) shoulder milling (Source: [57])

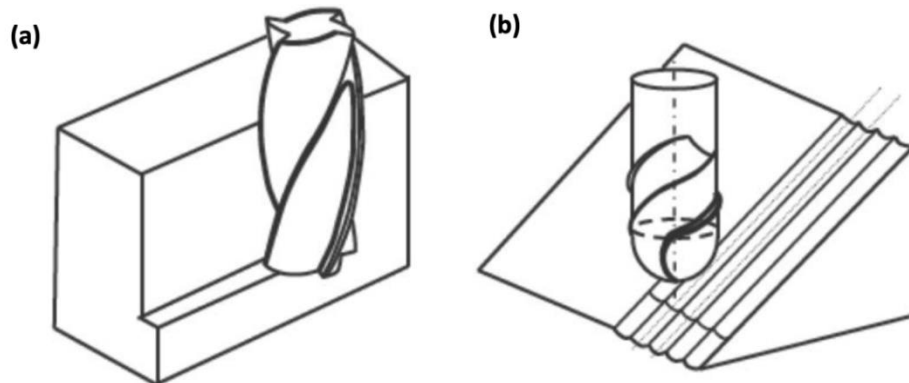


Figure 2.2: Milling types (a) peripheral (or flank) milling (b) ball-end milling
(Source: [57])

With the increasing of machining technologies and processing speeds, the wear of the tool is increasing. Machine tools need to be renewed due to the reduced workpiece surface quality with the wear of the tools. This leads to increased tool costs. On the other hand, due to the reason that the surface quality values are desired, the effect of the tool wear on the surface quality is increasing.

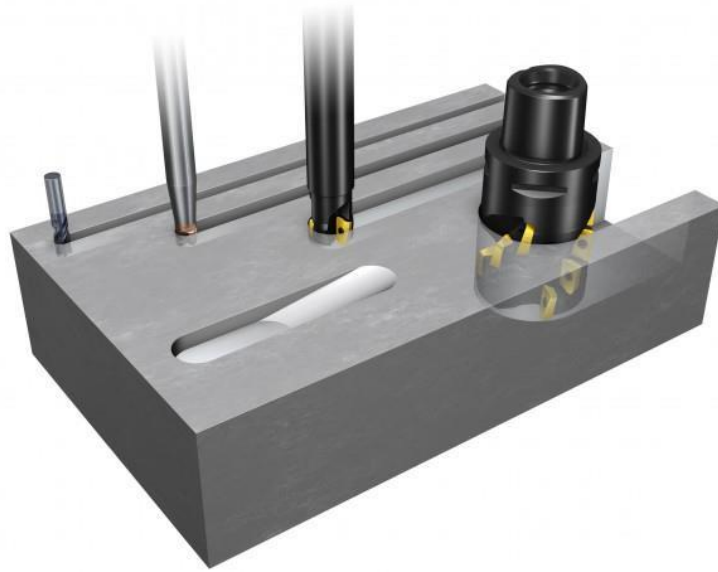


Figure 2.3: Groove or slot milling operation with different types of end mill
(Source: [58]).

2.2 Turning

Tool and workpiece must move relative to one other in order to execute machining processes. There are numerous fundamental parameters that combine to create this relative motion, including the primary as cutting speed and secondary as cutting feed. In conjunction with these actions, tool geometry and tool setup relative to the workpiece determines the form of the so many processed surfaces.

Workpiece rotation and tool feed movement are the principal revolution motions during processes, which are referred to as turning. This motion conjunction is used to process outside and inside of the workpiece. Known as a lathe, this machine tool performs the basic turning motions necessary. It has taken centuries for the lathe to evolve. Through a computer-style menu-driven, CNC lathes are controlled electronically by a computer-based software that can be changed and shown on the machine, along with an imitated manufacturing view.

Cylindrical surfaces are machined using the turning process. Figure 2.4 depicts the fundamental turning motions. These motions are:

- The rotation of the workpiece on all sides of the turning centerline is the main move.

- The tool's translatory move, often called as the feed motion, is the subsidiary motion.

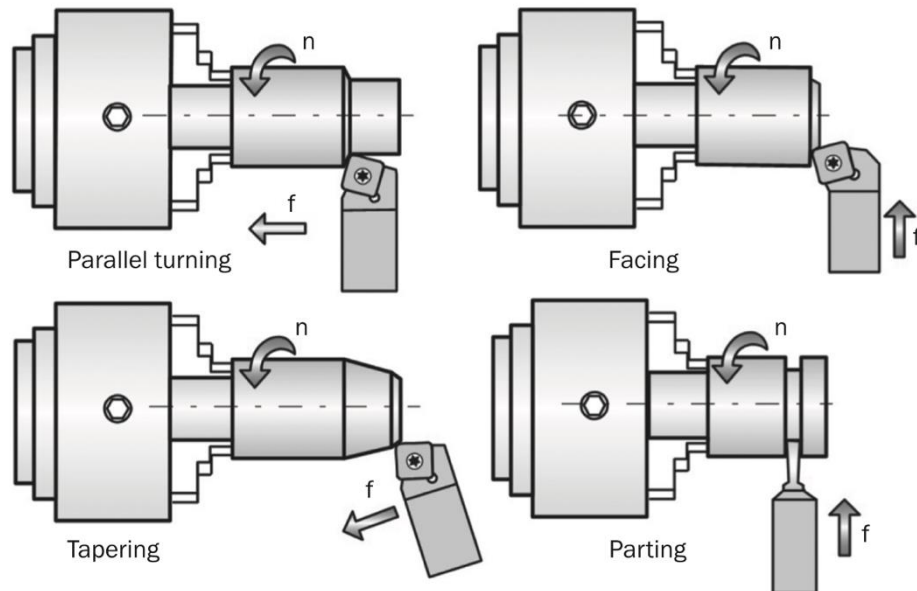


Figure 2.4: Basic turning operations (Source: [56]).

The orientation of the feed motion regarding the turning centerline and the form of the tool varies in fundamental turning activities depicted in Figure 2.4. The feed orientation is parallel to the turning centerline in parallel turning (also called longitudinal turning). The feed orientation is the vertical align to the turning centerline while facing and parting. The feed orientation in tapering is at an angle to the turning centerline. On a contemporary CNC lathe, Figure 2.5 depicts a range of turning processes.

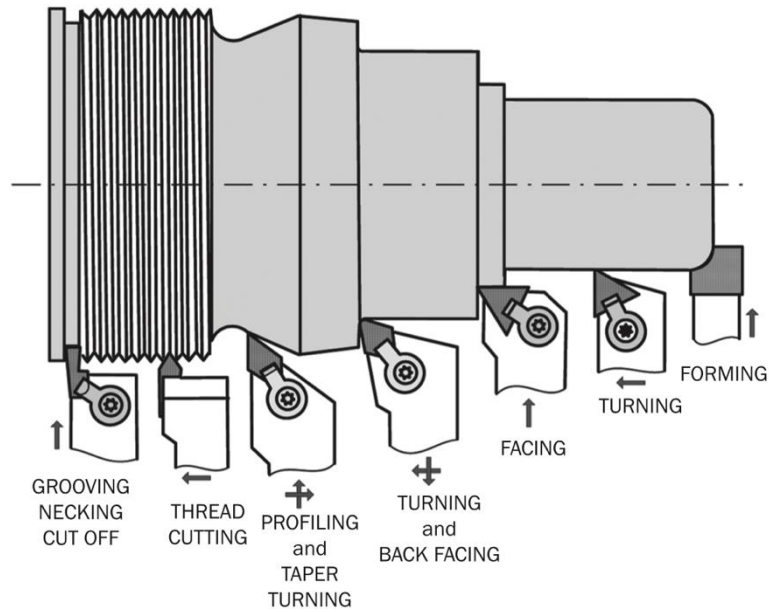


Figure 2.5: Basic motions in turning operations (Source: [56]).

Boring is a type of internal turning that is applied to expand the interior diameter of an existing hole drilled with a drill or a cored hole in a casting. Boring follows exactly similar fundamental motions as turning, as seen in Figure 2.6.

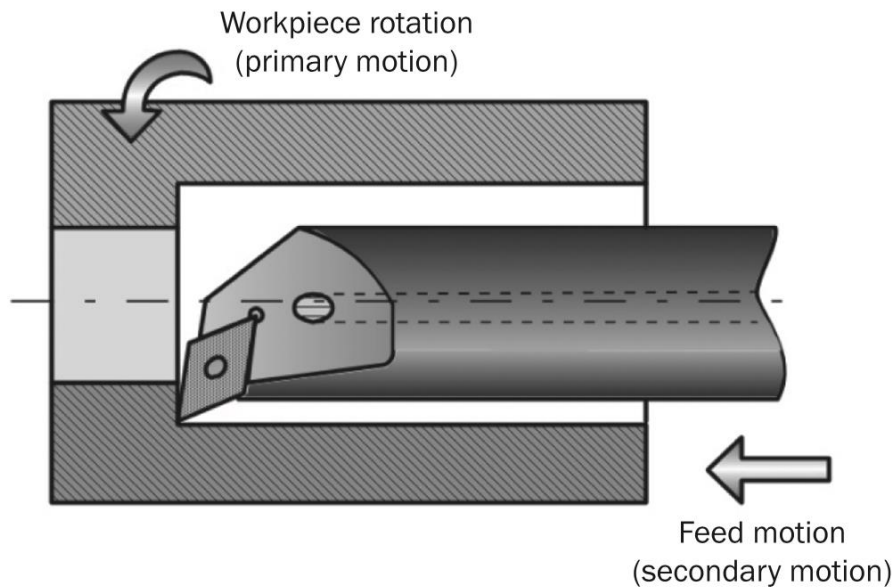


Figure 2.6: Fundamental motions in boring process (Source: [56]).

Boring accomplish these essential goals:

- **Dimensioning:** In the process of boring, the hole is made the right dimension and the surface quality is improved.

- Levelness: Boring rectifies a hole that has already been drilled or cast.
- Centering: Rotary holes are made coaxial by boring.

Figure 2.7 indicates that many of the turning actions that occur during external turning also occur during boring. If the workpiece is turned externally, the tool overhang and tool holder dimension are not influenced by the workpiece's extent. On the other hand, when it comes to internal turning, or boring, the diameter and extent of the workpiece's hole severely limit the tool's option.

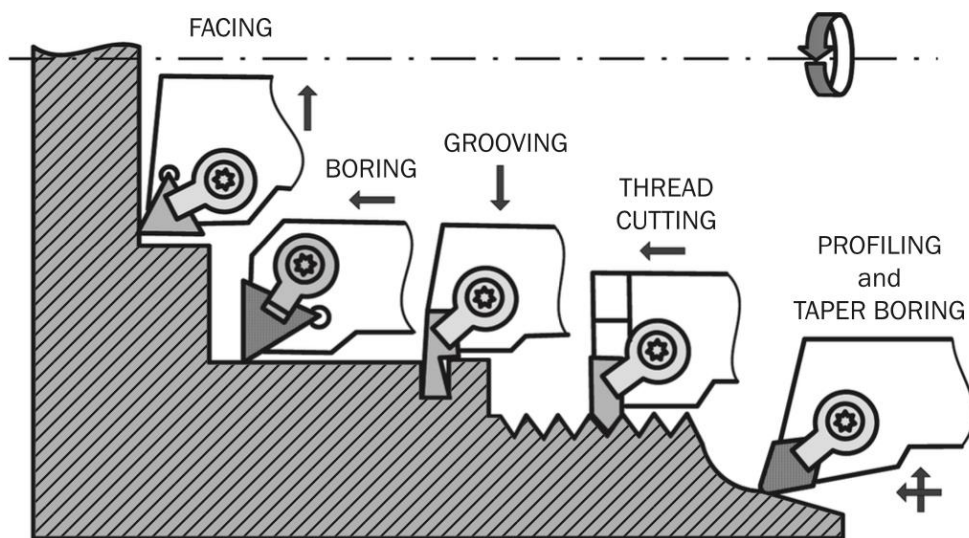


Figure 2.7: Basic motions in boring operations (Source: [56]).

2.3 Surface Roughness

Surface roughness is defined as the average of surface levels throughout the surface. The vertical variations of an actual surface from its absolute shape are used to calculate it. The surface is rough if these variances are substantial; the surface is smooth if they are modest. Surface roughness has a significant impact on how a machine affects its surroundings. Rough surfaces tend to wear down faster than smooth surfaces, and their contact has greater friction coefficients. As a result, surface roughness is a common surface integrity characteristic given by the component drawing. Even though roughness is generally undesirable, reducing the roughness of a machined surface will almost always raise its performance and production costs enormously.

The arithmetic mean roughness is the most commonly used roughness parameter, and its brief description is Ra. The additional most used parameters are Rt and Rz. Rz is ten-point mean roughness and Rt is the highest point of the sample surface evaluated in accordance with Standard ISO 468:1982: Surface roughness – Parameters, their rates, and basic guidelines for establishing requirements.

The cutting edge angles κ_r and κ_{r1} have the greatest impact on the surface roughness of processed components (Shaw, 1984). Figure 2.8 shows the most understandable situation where the nose radius is zero to understand this effect. Surface roughness is depicted by triangle ABC as a result of tool progress owing to cutting feed f . Triangle having edges AC, BC, and AB. AC is exactly the same with the cutting feed per cycle, BC is aligned with the main cutting edge AD, AB is collinear with the subsidiary cutting edge AE.

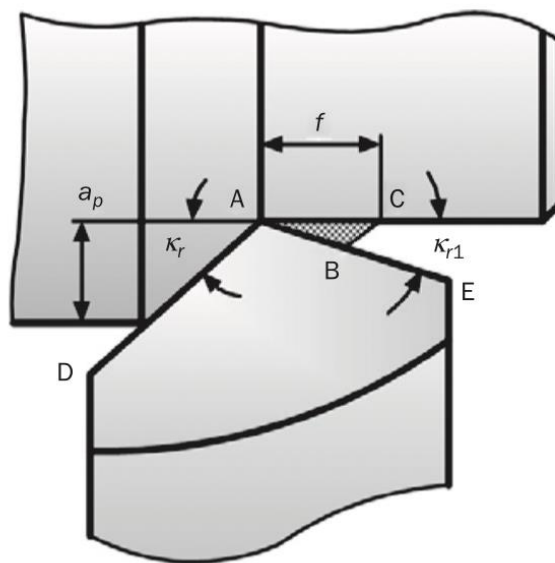


Figure 2.8: Roughness left on the machined surface (Source: [59]).

According to the Figure 2.8, surface roughness is either theory-based or geometrical. κ_r and κ_{r1} are cutting edge angles that affect roughness distance Rt and roughness profile (theory-based arising from feed markings). Using the highest peak-to-valley length, this roughness may be calculated for the tool without nose radius (Figure 2.9 (a)):

$$R_t = \frac{f \sin \kappa_r \sin \kappa_{r1}}{\sin(\kappa_r + \kappa_{r1})} \quad (2.1)$$

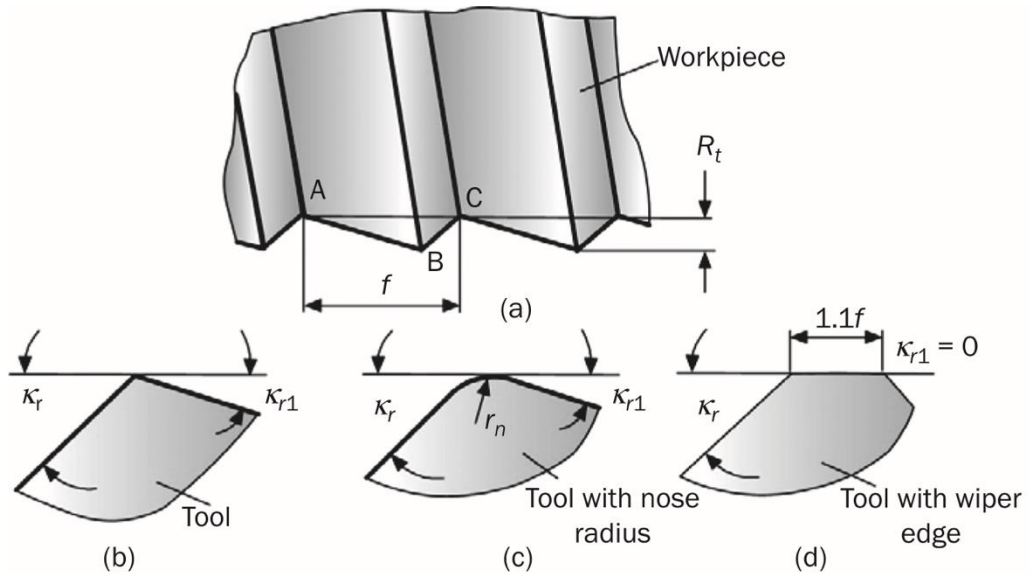


Figure 2.9: Various tool nose radius (Source: [59]).

Determine the roughness while using an entirely-radius tool is implemented (Figure 2.9 (b)) may be as:

$$R_t \approx \frac{f^2}{8r_n} \quad (2.2)$$

2.4 Cutting Forces

When a cutting tool is introduced into a substance, it causes the material to resist. This resistance is called as cutting force. Machining procedures for cutting such as turning, milling, and drilling are carried out on production using unlike force orientations and magnitudes. Although cutting processes change, standard finishing parameters remain for the material surface. Leading to this production trends are: considerable minimizing in production costs, shorter manufacturing times, better surface entireness, minimizing or eliminating the usage of ecologically hazardous cooling mediums, and heat treatment-induced component disfigurements [1–4].

A specific amount of force is exerted by the tool to the surface being taken, and therefore to the workpiece, during cutting it. According to the numerical control of machines (ISO 841) shown in Figure 2.10, this force is called as the resultant cutting force R , which is a 3D vector. All the time, the cutting edge is the initial point of this axis system. Z-axis is in line with the feed motion orientation and the y-axis is in line with the prime motion orientation.

Cutting force is usually divided into three elements throughout the axis of the tool coordinate system for convenience's sake and F_c (may be called as tangential force) has its principal and strongest element throughout the y-axis. It's usually the most important element. In the z-axis, the force F_f is in line with the feed direction. F_f is called as feed force (may be called as axial force). F_p is called a radial element because it works throughout the workpiece's radial direction. As seen in Figure 2.10, the workpiece exerts a response force R to the tool (b). Figure 2.10 shows how this force is broken down into three elements (b). Besides these, the element F_{xz} should be taken into account, which functions in the xz plane and is required to increase precision.

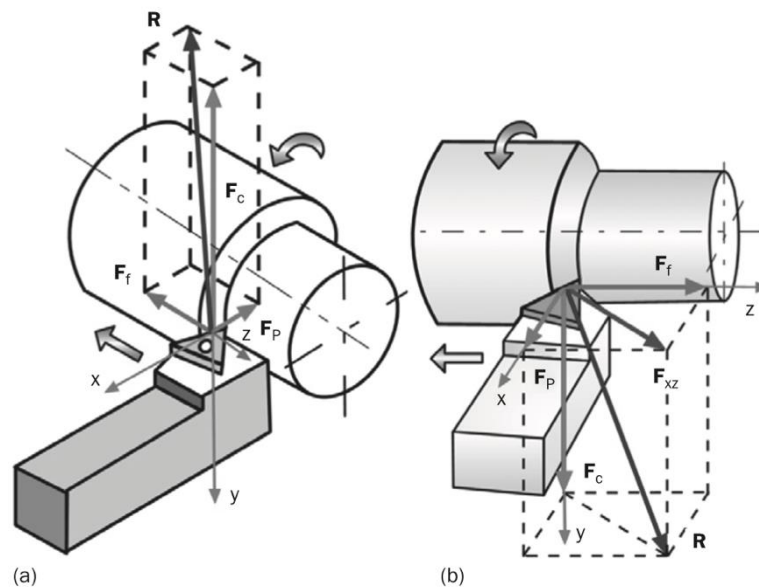


Figure 2.10: Cutting force and its elements: (a) as exerted to the workpiece, (b) as exerted to the tool (Source: [59]).

Cutting force performance is also profoundly affected by the experimental variables such as cutting speed, spindle speed, feed rate, feed per tooth, tool nose radius, depth of cut, cutting time etc.

2.5 Tool Wear

A material removal process provides dimensional accuracy and excellence of material texture. The degree of surface quality is mostly connected with the surface profile of the cutting tool. Tools wear over time because of the mechanical, thermal, chemical and abrasive loads and thus tool change operations make an unproductive production due to cutting tool cost and set-up time which is an unavailable period to produce. These instabilities create different work areas for tool users and machine manufacturers.

The tool wear is based on friction of metal cutting which is affected by the cutting power, process excellence, tool life and manufacturing cost. As tool wear reaches high, the surface quality decreases and dimension error starts appearing as seen in Figure 2.12.

Determining the life of the cutting tool is beyond the measurements of flank or crater wear because the unknown inputs also play a role for tool wear in small and even large part. With high-speed cutting operations cutting loads on cutting tools increase in proportion to cutting speed. Figure 2.11 indicates that cutting speed ranges according to different materials [60].

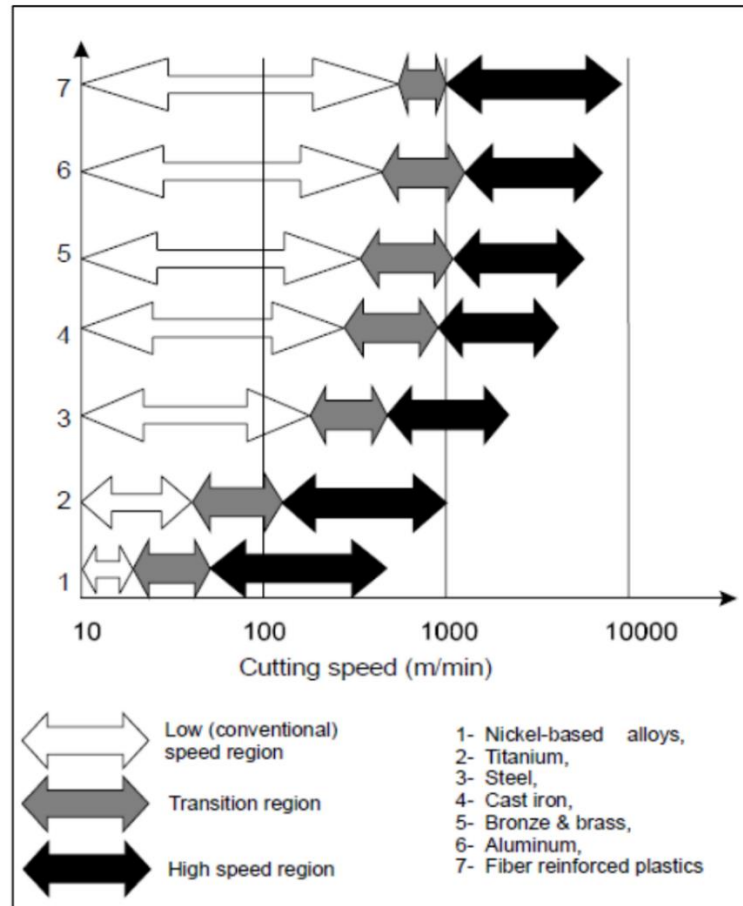


Figure 2.11: Cutting speeds in milling for different materials (Source: [60])

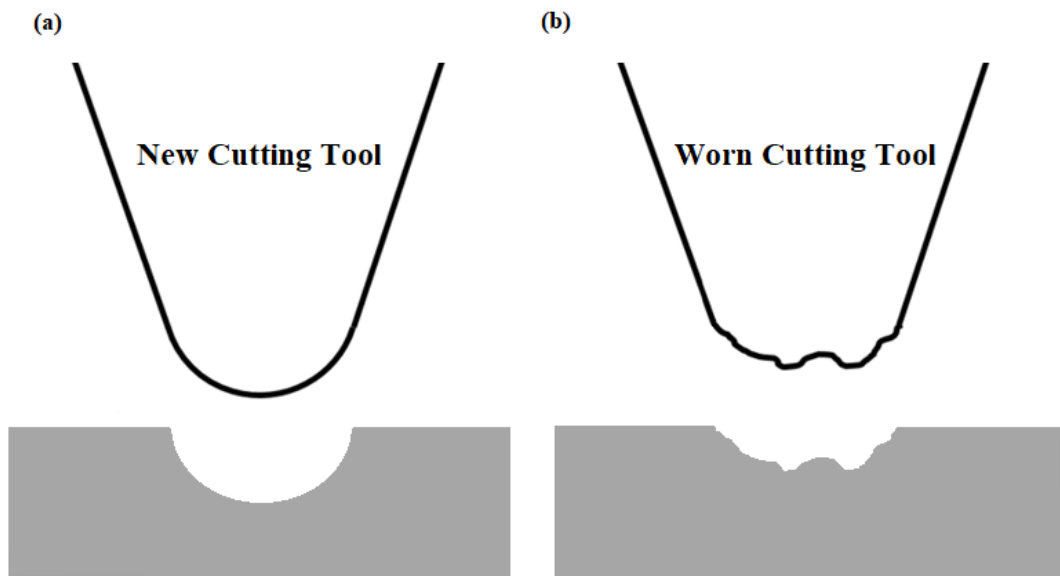


Figure 2.12: Comparison between the workpiece surfaces
(a) new cutting tool and (b) worn cutting tool

In end-mill cutters occurs mainly two different types of wear. One of them is flank wear where occurs at the cutting edges of tool. Another type is central wear where

occurs at the center of the tool. Figure 2.13 shows the wear mechanisms where is monitored by SEM and types of the wear. Comparing with the ordinary flank wear of the single point turning tool or twist drill, these types of wear are completely different [61].

Increased tool life reduces these repetitive processes at this stage. Therefore, choosing the optimal cutting parameters is a great importance for a milling process and also turning processes at the point of cost and quality.

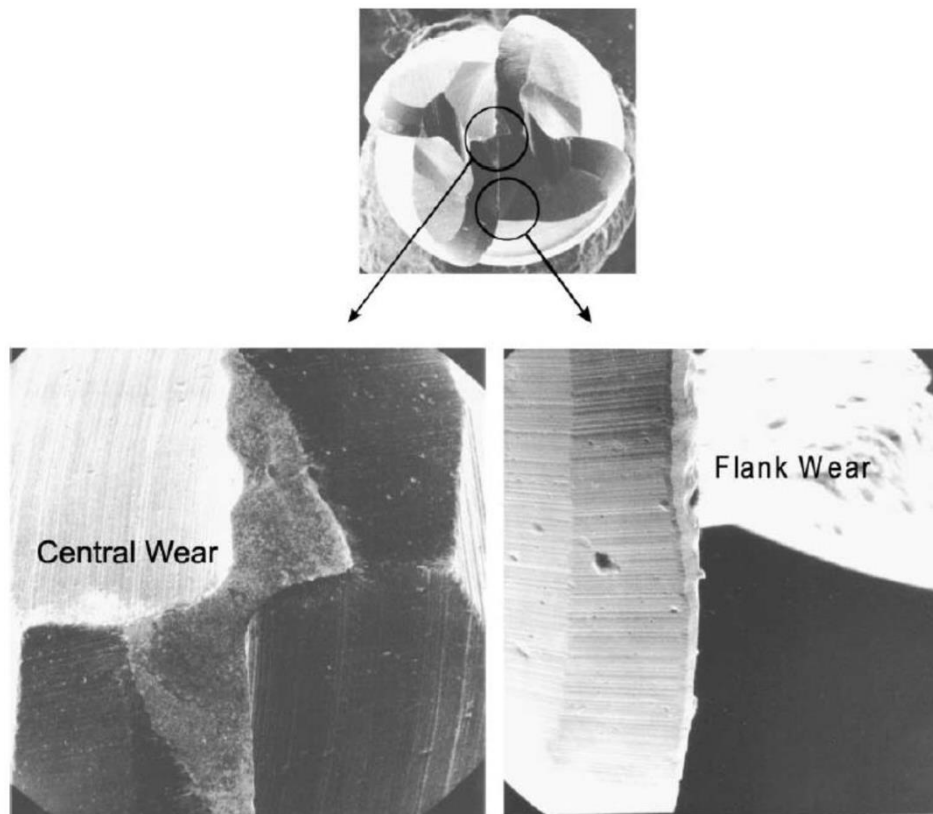


Figure 2.13: Central wear and flank wear at the cutting edges are monitored by SEM with original magnification 100 times (Source: [61])

Chapter 3

Regression Analysis

Regression analysis is utilized to simulate the correlation of the input and output of the engineering systems as a mathematical function. Statistical measurements are increased to find the strength of the relationship between dependent and independent variables. This mathematical function is named as regression equation.

Regression analysis offers a mathematical equation which is named regression equation. Gauss and Legendre used the least-squares methods which is the basic mathematical tool in order to calculate the length of the arc of the meridian from Dunkirk to Barcelona [29]. The first progress for regression is made by Francis Galton to investigate the relationship the height of children and their parents. He observed that the height of the children of short parents tended to be short and height of the children of long parents tended to be long. Also, he found that the height of his children tended to approach the mean of the mass average. This tendency is called “regression to mediocrity” by Galton. This study is the first regression analysis [30].

3.1 Regression Models

One of the basic elements of regression analysis is the regression model. A model is a mathematical function that describes the experimental system in which quantitative terms are studied. In general, a model is represented as;

$$y = f(x; a) \tag{3.1}$$

Generally, the models have three basic components: mathematical relationship or function (f), parameters (a) and variables (x). In the most common cases, they have only one or two independent variables, and are simple from real-valued continuous equations. These include exponential, hyperbolic and logistic functions. The same functions can also be used to model completely irrelevant events from existing physical processes.

Depending on how the function is derived, the models can be classified into two groups. One of them is structured or mechanistic models and the another is unstructured or empirical models.

Structured models can be obtained from the theoretical background of the mechanism. Unstructured models are chosen from empirical functions. Because they are useful in explaining measurements. A third group of semi-empirical models is classified between these two types, since they are derived from theoretical considerations and partly from observations.

Another component of the models is parameters. When the function determines the type of curve, its actual shape, position and ratio are determined by the parameter values. In mechanical and semi-empirical models, the parameters are fundamentally important as they represent proportions or diffusion coefficients. In empirical models, the parameters are necessary to define the curve precisely and more efficiently, but do not represent any fundamental feature of the system.

Depending on the mathematical expression of the parameters within the model function, we can classify the models in two categories as linear and nonlinear. This distinction is important. Since the methodology required for the operation of mathematical models generated by nonlinear functions is much more complex than linear models. Secondly, linear models are often easy to handle and understand, although they can be used to model only a few phenomenon in real life.

The functions may also be linear or non-linear according to their independent variables. Any combination of linearity or non-linearity is available according to variables and parameters.

In the context of this thesis, due to the complexity of the problem, nonlinear regression models were preferred.

3.2 Purpose of Regression Analysis

Nonlinear regression can be used for three different purposes:

- Testing the validity of the model (or comparing the hypothesis),
- Characterize the model (in other words to estimate the parameters),
- Estimating the behavior of the system (interpolation and calibration).

Model validation or comparison is an important application of regression analysis. Reaching a well-fitting curve between model and experiment data for a system is one of the best indicators of the success of the mathematical model. But a good fit is not always a proof that the model is correct. At this stage, action of the researcher is significantly important to build meaningful work.

The estimation of the parameters is a direct result of regression. Regression is useful for predicting behavior, i.e. interpolation (or prediction) and calibration (or inverse prediction). Interpolation and extrapolation can be used to predict the behavior of the system without having to perform real experiments.

3.3 Non-Linear Regression Analysis

Nonlinear regression is more flexible than linear regression. Since the function does not need to be linear or linearizable. For this reason, it provides a wide selection of nonlinear regression phenomena to fit the data. The only requirement for the function “ f ” is that it differs according to its elements. This can be calculated with the least squares method. Nonlinear regression may be more appropriate than the use of transformations and linear regression where the f function can be linearized.

For nonlinear regression, mathematical modeling processes can be carried out systematically by taking into consideration the important features.

Nonlinear regression requires knowledge of the function “f” which requires a comprehensive understanding of the process under consideration (polynomial, trigonometric, exponential, etc.). The linear regression models are suitable for process estimations, which are roughly defined, but do not require precise clarity.

The nonlinear regression model can be expressed as;

$$y_i = f(y_i; x) + \varepsilon_i \quad (3.2)$$

It is assumed that the ε error term can be taken independently and is normally distributed. Since nonlinear regression models contain the most general mathematical expressions, it is not possible to write their functionalized generalized form. However, a few basic types of the function used in the field of engineering can be expressed as below:

Polynomial type function;

$$y = a_0 + a_1x + a_2x^2 + \dots + a_nx^n \quad (3.3)$$

Exponential type function;

$$y = a_0 + a_1e^x + a_2e^{x^2} + \dots + a_ne^{x^n} \quad (3.4)$$

Trigonometric type function;

$$y = a_0 + a_1\sin x + a_2\sin x^2 + \dots + a_n\sin x^n \quad (3.5)$$

Logarithmic type function;

$$y = a_0 + a_1\ln x + a_2\ln x^2 + \dots + a_n\ln x^n \quad (3.5)$$

Rational type function:

$$y = \frac{a_0 + a_1x + a_2x^2 + \cdots + a_nx^n}{b_0 + b_1x + b_2x^2 + \cdots + b_nx^n} \quad (3.6)$$

At this stage, the multivariate states of the above model types can be derived with similar logic with more than one input. Another important point is that, for example, special functions or different combinations of elementary functions can be selected as model structures by acquiring a broader understanding of the families of mathematical functions.

Chapter 4

Neuroregression Approach

This chapter surveys the fundamental mathematical instruments. Many researchers are going to be familiar with several of the topics presented here. The reader can evaluate which areas need to be studied further. The main aim of the chapter is to present the essential and modern approaches to the modeling and design of engineering structures in a concise manner. Figure 4.1 shows all these steps without breaking the order of the optimal design process for a system.

4.1 Design of Experiments (DOE)

Design of Experiments (DOE) is a helpful method to find new processes, try to learn more about the existing processes, and optimize them for an excellent performance. In this section, we present and discuss some DOE techniques. As mentioned before, this part's goal is to establish the issue by highlighting the key approaches utilized in practice. As a result, the lineup of methods considered has a great distance from exhaustive. It is crucial to choose adequate statistical tools to analyze the data available, since the results can be significantly affected by noise. Replication, randomization, and blocking are the fundamental principles of statistical methods in DOE. Replication is the experiment's repetition to achieve a more accurate result and to reduce the experimental error. Randomization identifies the irregular array in which the experiments are to be carried out. Blocking is intended to insulate a known methodical bias influence and inhibit the main effects from being obscured [62, 63]. Due to the number of crunchers concerned and the use of complicated statistical jargon engineers generally do not like to employ DOE [63]. In manufacturing processes, experiments are being carried out to enhance our knowledge and understanding of them. The relationships

between the core factors of the inputs and the behaviors of the output can, therefore, be examined [63, 64]. One of the comprehensive strategies in engineering companies promoted by plenty of engineers is One-Variable-At-a-Time (OVAT). In this approach, it is changed one parameter at a time, with all other factors fixed throughout the experiment. The results, however, are unreliable, wasteful, and may offer the processes a misleading conclusion. If a particular attribute of a component is affected by several factors, then the best choice is DOE [63, 64, 65]. An engineer frequently makes systematic changes in the input parameters and specifies how well the output performance varies. It is known that all parameters have not the same impact on the results. The aim of a deliberate design is, therefore, to realize which process parameters tend to affect the output more and then to identify the best levels for the factors [62, 63, 66]. This approach provides high process efficiency, more stable results, low manufacturing costs, and saves time for the researchers.

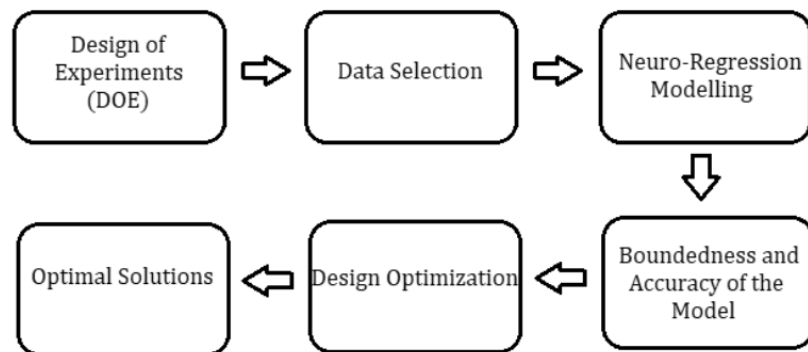


Figure 4.1: Flow diagram of design process

4.1.1 DOE Techniques

The selection of a DOE approach relies on the experiment's goals and the number of factors to be considered. In this section, the most widely used approaches have been listed and explained briefly. These approaches are Randomized Complete Block Design, Full Factorial, Fractional Factorial, Central Composite, Box-Behnken, Taguchi, Latin Hypercube, and D-Optimal Design [62].

4.1.1.1 Randomized Complete Block Design

The distribution of treatment for experimental components is not strictly limited. In practice, however, there are situations in which the experimental data varies relatively widely. In such situations, the design made in relation is called a Randomized Complete Block Design (RCBD). The main goal of blocking is to minimize the variability between experimental units within a block and to maximize the variation between blocks.

Advantages of the RCBD

1. It is possible to remove the treatments or replicates from the analysis.
2. Several treatments can be more often replicated than the others.
3. There is no strict limitation on the number of treatments or replicates.
4. Even if the experimental error is not homogeneous, there can still be valid comparisons [63, 67].

Disadvantages of the RCBD

1. There exists a smaller error on df for a small number of treatments.
2. If the number of treatments is enormous and there is a considerable variation between experimental units, it is possible to obtain a significant error term.
3. RCBD is not very good on the efficiency of the experiment when there is missing data.

4.1.1.2 Full Factorial Design

It is generally known that the DOE method most frequently used in production industries are full and fractional factorial designs at second and third levels. Factorial designs might allow a researcher to explore a response consistent on the impact of the variables. A factorial design may be separated as full or fractional factorials. An experimental design that every factor setting occurs with every other one is a full factorial design. If the amount of elements is five or higher, a full factorial design needs a significant amount of operations and is not very useful. In these cases, a fractional factorial design is a better choice [63, 64].

4.1.1.3 Fractional Factorial Design

Researchers usually cannot have sufficient time, money, and funding to conduct full factorial studies. If some higher-order relationships are not essential, the primary effects and second-order interplays can be acquired by operating only a section of the full factorial study. A fractional factorial design is defined as a form of orthogonal array layout that enables researchers to explore significant impacts and the required impacts of relationships with a minimum amount of exercises or experimental runs [63, 64, 67, 68].

4.1.1.4 Central Composite Design

The highest degree important response surface design is a central composite design, which creates a factorial design. Five factorial levels are desired for a central composite design. Among the most critical advantages is that the corner points are checked, if it is shown that curvature is not substantial, then it is accomplished. If the curvature exists, the primary task is to generate the star runs [65].

4.1.1.5 Box-Behnken Design

Box-Behnken Design is based on the cube edge midpoints rather than the corner points, lead to fewer runs; however, apart from the Central Composite Design, all runs must also be done. It should be noted that only three-factor levels are appropriate in The Box-Behnken Design. It has advantages if the curvature stated in the screening experiment is likely necessary [63].

4.1.1.6 Taguchi Design

Taguchi methods, or sometimes called robust design methods, are statistical methods. The primary purpose is to keep the output fluctuation minimal even in the appearance of noise. The technique significantly increases the efficiency of engineering. The Taguchi design helps to guarantee product quality by deliberately considering the noise factors and the amount of mistake in the area. This approach

centers on enhancing the primary function of the design process, thereby promoting flexible designs [63, 67].

Advantages

1. It is simple and easy to use in several other engineering circumstances, enabling it as a robust yet straightforward tool.
2. It underlines, within some qualification constraints, a mean production characteristic rate comparable with the final rate instead of just a rate, thus enhancing the quality of the product.
3. Without an impractically large number of testings, it enables the investigation of many distinct variables.

Disadvantages

1. Precisely that the acquired findings are only comparative and do not specify which variable has the most significant impact on the characteristic value of the product.
2. It can not be used in all interactions among all the parameters, since orthogonal arrays do not examine all parameter combinations.
3. It is hard to account for parameter interactions.
4. It is offline and hence improper for a procedure that changes dynamically, as in a computer simulation.

4.1.1.7 Latin Hypercube Design

It is a technique to produce an almost random specimen of data sets from a Multidimensional Distribution, as well as a generalization of the Latin Square Concept to a random set of measurements. In this approach the first step is, to identify how many sample points to get an address and through which row and column the sample point was drawn for each sample point. Latin Hypercube

method guarantees that collection of arbitrarily generated values represents the actual fluctuation, while standard arbitrary specimen selecting is only a set of random numbers with no ensures [62–64].

4.1.1.8 Optimal Design (D-Optimal)

It is a computer-aided design that includes the finest portion amongst all feasible experiments. Software tools may also have distinct processes to generate D-optimal designs because the final design may vary on the tool to be used [63, 68]. A selection method creates the finest design based on a chosen factor and a specified amount of test runs. This approach is especially helpful if classical design methods are not being used. These situations are:

1. If supplies or factor configurations are restricted.
2. If decreasing in the amount of design runs is required.
3. When using the operation and mixing variables in the same design.
4. When the experiments already carried out must be included.
5. If the region of the experiments is unstable [63, 65, 66].

4.2 Mathematical Modeling

When examining the literature, studies performed for the intent of engineering optimization, some inadequate approaches were recognized and listed below:

- i) Since, the interaction of all experimental and constructional variables must be taken into account while optimizing, updating in the one input with preserving the other constant is not a satisfying description, and this approach leads to disregarding the nonlinear influence of input variables.
- ii) For many test data generation investigations, the objective function is selected one or two traditional regression models. The key difficulty is to calculate the R^2 value of the model for empirical research. The fact that R^2 is high does not, by itself, reflect the entire process. It measures how well the applied model's solutions match those of the empirical data. In another saying, even if the R^2 value is so high for actual structure, it does not indicate a fine match all the time.

Besides, the model is limited to explaining the empirical data, but not the underlying reaction of events. The need for recently developed engineering modeling surveys, including a variety of regression configurations and approaches, is a result of this.

iii)The engineering model function must also be constrained. The whole engineering design variables are recognized to be limited. In order to determine which models are also constrained by the engineering design variables ranges, it is necessary to determine which models are constrained prior to the optimization phase.

iv)In certain cases, algorithms' dependability, sensibility, and stability are not considered in optimization investigations of engineering organizations. For the stochastic search techniques, anyway, it is vital.

This is why a unique approximation is proposed to the modeling, design, and optimization operation for optimizing the design variables. As a first step, a comprehensive analysis of multiple nonlinear neuro-regressions is completed, comprising linear, quadratic, trigonometric and logarithmic, as well as their rational versions for the solution problem. For the second step, models are verified for their limits to ensure that they can supply useful results. It is then followed by a variety of direct search strategies (including stochastic ones).

Optimization of engineering structures begins with defining model in mathematical way. Regression Analysis (RA), Response Surface Methodology (RSM), Finite Difference Technique (FDT) and Artificial Neural Networks (ANN) are used to identify mathematical models. An objective function of the optimization problem defined by the model is also derived.

4.2.1 Coefficient of Determination

The coefficient of determination (R^2) is simply the proportion of observed y change which is examined by the simple linear regression model. R^2 is a ratio and the higher this ratio indicates that the regression model explains the variability for the observed values better. If the value of R^2 is so small, then another model is

established to explain the variation. Usually, this model is selected as a non-linear or multiple regression model containing multiple independent variables. Although this value is not a fixed value in the literature, it is expected to be above 0.90.

The calculation of the R^2 is given below [33].

$$R^2 = 1 - \frac{SSE}{SST} \quad (4.1)$$

where SSE is the summation of squares due to error and SST is the total summation of squares.

The summation of squares owing to regression (SSR) is calculated by using the formula given in Equation 4.2. Summation of squares caused by error (SSE) is computed by Equation 4.3. The Total Summation of Squares (SST) is summation of SSR and SSE in Equation 4.4. In this notation the population mean is \bar{y} , prediction mean is \hat{y} and y is the observation value.

$$SSR = \sum(\hat{y} - \bar{y}) \quad (4.2)$$

$$SSE = \sum(\hat{y} - \bar{y})^2 \quad (4.3)$$

$$SST = SSR + SSE = \sum(y - \bar{y}) \quad (4.4)$$

SSR is the measure of explained variation, SSE (summation of the squared errors) is the measure of unexplained variation and SST (total summation of squares) is the compute of total change in y [34].

4.2.2 Training and Testing

The mathematical model should be trained with training data set. The purpose of training is to investigate the model for testing. Splitting a dataset into training and testing datasets is important for better prediction the phenomena. By comparing

the predictions to the actual response variable in the test data, it will be able to evaluate model's accuracy.

The gold standard for assessing the competence of mathematical model to estimate the phenomena is to use independent test set. The model has a probability to fit the data for selected training data set. However, model performance is determined by testing the model with an external test data which is chosen from data set [35].

The data are separated into two groups randomly and 80% of the data is utilized for training, while 20% is utilized for testing. The test stage is then used to produce the estimated outcomes by reducing the influence of regression model discrepancies, which helps to find out candidate models' estimative skills. To illustrate if the model is logical, it is also necessary to evaluate the limits of the candidate models for given values. After collecting the appropriate models in terms of R^2_{training} and R^2_{testing} , the maximum and minimum values of the models at the given interval for each model variable are calculated.

Chapter 5

Optimization Process

5.1 Introduction

Finding an approximation of an optimal solution for a function which is defined on a subset of finite-dimensional space is one of the most common problems in applied mathematics. In combinatorial optimization problems which are crucial for most machine learning approaches, there are some objective functions that are supposed to be optimized to find an approximation of an optimal solution. Fifty years ago, there were a lot of numerical optimization procedures for these optimization problems; most of them were deterministic (traditional optimization techniques). However, with the development of computer technology, stochastic methods (non-traditional optimization techniques) have become the essential tools for areas such as engineering, science, business, and statistics. These methods are relatively the latest available and popular because of the particular characteristics that aren't present in the unarbitrary algorithm [67, 68]. For instance, stochastic methods always include probability, such as according to the random distribution of rainfall and water usage, in a reservoir, predicting the water level periodically or forecasting the various of wasted interactions for a channel of interaction depending upon to the random variables appropriate steady bandwidth. On the contrary, unarbitrary methods include possibility under no circumstances; and outcomes take place based on exact input values [69].

Random-variable stochastic optimization is the method of reducing or increasing the evaluation of a statistical or mathematical function. Noise in calculations or Monte Carlo randomization in the detection method, or both, might introduce unpredictability [70, 71].

In the information technology field and message processing as well as in geography, aerospace and finance, stochastic systems may be used to model a wide range of industrial, economic, biological and technical challenges. In these systems, stochastic optimization is appropriate in order to solve decision-making problems, and many researchers have considered stochastic optimization methods in solving these problems. For instance, Yan et al. [73] suggested a qualitative and quantitative combined modeling specification depending on a progressively model configuration framework which consists of the meta-meta model, the meta-model, and the top-degree model. The results of the study showed that the suggested technique could comprehensively describe the complicated structure. Li and Zhang [74] studied the problem of uncertain probabilistic linear-quadratic optimum management under the unequal constraints for the final form. In this study, they proved the Karush-Kuhn-Tucker (KKT) argument with hybrid constraints, and then they obtained new types of Riccati equations. This equation provides the necessary conditions for an optimum linear form control process management existence which is produced by KKT argument. The development of a dynamic programming algorithm was achieved in order to solve the uncertain constrained stochastic linear quadratic subject. Aydin et al. [75] studied on the modeling of geometrically steady multilayered composites by the use of the efficient global optimization method (EGO). The optimization problem of a composite plate under good rigidity and poor thermal and poor humidity dilatation coefficients was solved. The proposed optimization algorithm in this study is experimentally verified. After the design and optimization processes were completed, failure analysis of the optimized polymers has been made using Tsai–Hill, Hoffman, Tsai–Wu and Hashin–Rotem norm. Generic steps of stochastic optimizations for renewable energy applications were extensively examined by Zakaria et al. [76]. Furthermore, the positive and negative sides of the stochastic optimization were emphasized. Significant optimization methods belong to the stochastic optimization stages are emphasized.

In their study, Niamsup and Rajchakit [77] introduced the latest improvements and significant stochastic optimization methods. It is claimed that the stochastic optimization methods are always more efficient than the deterministic optimization

techniques for social, economic, technical aspects of renewable energy systems. Niamsup and Rajchakit examined polytopic discretely timed stochastic functions in the period time-variant delays applying the parametric dependent Lyapunov-Krasovskii functional coupled with linear matrix inequality methods and fresh form for the strong stableness of the stochastic structure were proposed.

Maggioni et al. [78] studied the problem which was encountered by a bike-sharing service provider who needed to control a group of bicycles over a series of bicycle terminals, every single having a defined volume and stochastic requirement that changes over time. Multi-phase stochastic optimization methods are presented to determine the best number of bicycles to assign to each terminal at the start of the operation for unidirectional bicycle distribution systems. Finally, managerial insights are provided comparing the solution supplied in the real system with the solutions obtained by using the two-stage and the multi-stage models.

Gutierrez et al. [79] studied on how to cope with the problem of indefinite case in the optimal management of the hydrogen network of a petroleum refinery. A two-stage stochastic optimization method was used to analyze the effect of raw changes in the operation of the network, and they were analyzed on how to solve the hydrogen network problem to obtain feasible solutions with stochastic and deterministic solutions by using real plant data.

Khayyam et al. [80] proposed a stochastic optimization model for carbon fiber production in the carbonizing technique in order to minimize the amount of energy used in a proper interval of fundamental structural characteristics. They developed procedure operations, and fifty samples of fiber were analyzed for each set of operations, their tensile strength, and modulus. During the manufacturing of the specimens, the energy consumption was controlled on the procedure material, and the five distribution functions were analyzed in order to evaluate distribution functions that could the most accurate define the mechanical properties distribution of fibers. The Kolmogorov–Smirnov test was performed in order to confirm the dispersion goodness of fit and correlational statistics. The result of the study showed that the production quality could be predicted using the stochastic

optimization models in the given range, and this method minimized the amount of energy used of the procedure.

Tifkitsis et al. [81] produced a stochastic multi-objective cure optimization methodology and performed it on the thick epoxy/ carbon fiber laminates. Kriging method, which substitutes into Finite Element (FE) simulation, was used to construct a surrogate model for computational efficiency. Surrogate model and Monte Carlo were coupled and incorporated into a stochastic multi-objective optimization frame depend on Genetic Algorithms. The outcomes indicated that there exists a substantial decrease of 40% in the temperature exceeding and curing time in comparison to regular cure characteristics.

Genetic Algorithm (GA), Simulated Annealing (SA), Differential Evolution (DE), Nelder-Mead (NM), Random Search (RS), Particle Swarm Optimization (PSO), Ant Colony Optimization (ACO), Artificial Bee Colony (ABC), Markov Chain Monte Carlo (MCMC), Tabu Search (TS), Harmony Search (HS), Grenade Explosion Method (GEM), Covariance Matrix Adaption (CMA) are the examples of stochastic optimization methods [70–73]. Researchers continue to improve, and to add new stochastic methods or both to the literature. In the following subsections, some commonly used stochastic optimization methods are briefly overviewed.

5.2 Simulated Annealing

Simulation annealing (SA) method, which is one of the most effective and general optimization algorithms of stochastic algorithms, is quite useful to get the lowest limit of a function of a considerable number of independent variables. Besides, the SA method includes the analogy between the physical annealing process and finding the minimum function value in mixed-integer, discrete, or continuous minimization problems. In condensed matter physics, the physical tempering procedure is known as a thermal procedure in order to obtain the low energy states of a solid in a heat bath. Random search with regards to a Markov chain is the basis of the SA algorithm, which allows modifications that advance the objective function but also retains some non-ideal modifications.

At each iteration in the SA algorithm, a fresh random point is produced, and when any stoppage requirements are met, the process stops (Figure 5.1). The distance between the new and existing position or the scope of the search is on the strength of Boltzmann distribution with a scale in proportion to the temperature. Boltzmann Probability Distribution [71, 82–84] is defined as

$$P(E) = e^{-E/kT}$$

where,

$P(E)$: The Probability of Achieving the Energy Level (E),

k : The Constant of Boltzmann,

T : Temperature.

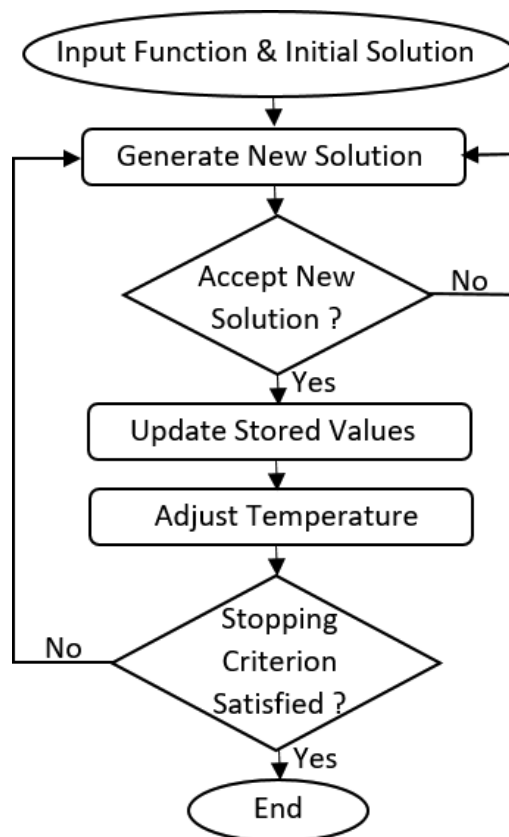


Figure 5.1: Flowchart of Simulated Annealing algorithm [82].

5.3 Differential Evolution

Differential Evolution (DE) is a search technique that was developed by Storn and Price in 1996 for optimization problems over continuous domains. DE is among the most effective techniques for real-parameter optimization methods at present. This algorithm comprises four basic stages: selection, crossover, mutation, and initialization. There exist three real management elements in this algorithm: (i) differentiation/mutation constant, (ii) crossover constant and (iii) population size. The differential evolution performance relies on the manipulation of target and difference vector to obtain a trial vector. The other control parameters in DE algorithm are (i) problem dimension that scales the difficulty of the optimization case, and (ii) the maximum number of generations known as a stopping condition, and (iii) boundary constraints [71, 84]. A flowchart summarizing the process of DE algorithm is shown in Figure 5.2.

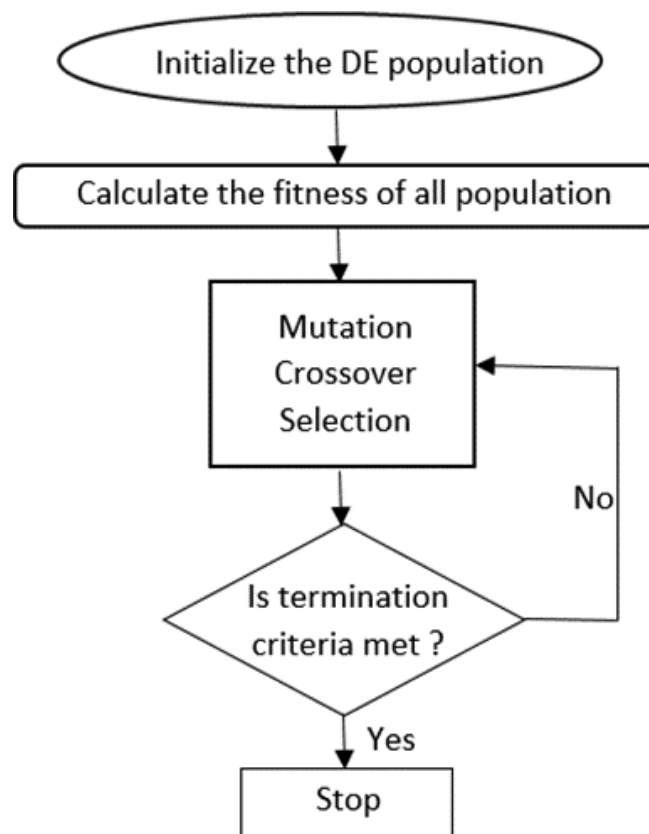


Figure 5.2: Flowchart of Differential Evolution algorithm [85].

The differential evolution algorithm is a population-based algorithm like GA that uses similar operators. The primary difference between these algorithms is that GA relies on a crossover, which is a mechanism of useful and probabilistic exchange of information among solutions in order to find better solutions. However, DE relies on mutation operation as the primary search mechanism. This main operation is based on the differences among randomly sampled pairs of solutions in the population. Even though this method is numerically uneconomical, DE is strong and efficient enough to find an optimum global value and to prevent the local minimum irrespective of initial points [86].

5.4 Nelder-Mead

Nelder-Mead (NM) is a traditional local search technique that was first introduced by Nelder and Mead in 1965 for unconstrained optimization problems. Besides that, modified versions of the Nelder-Mead method can be used for the optimization problems which contains continuous design variables, non-linear constraints and mixed integers. Even though Nelder-Mead is not a global optimization method, it is ideal for problems with a limited number of local minimums [89]. A flowchart summarizing the process of Nelder-Mead algorithm is shown in Figure 5.3.

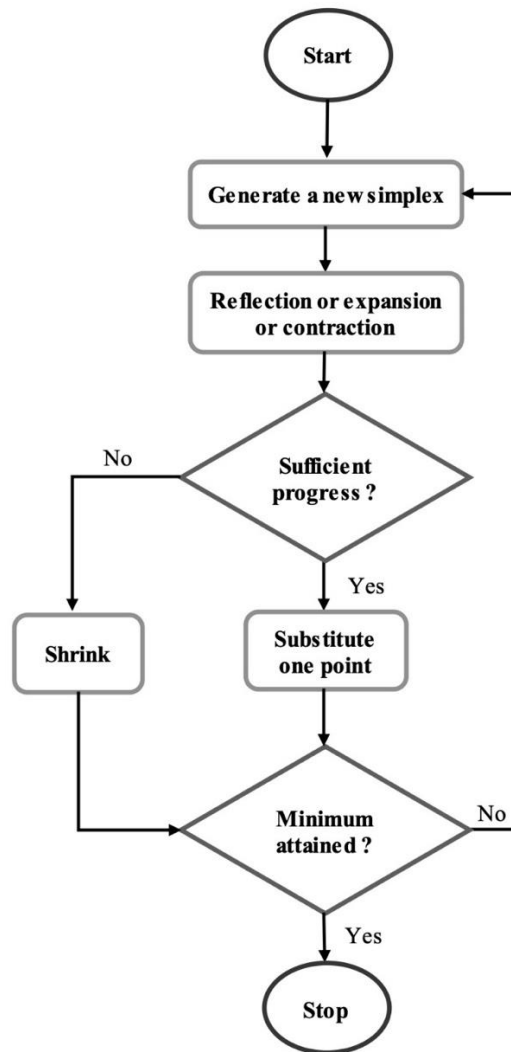


Figure 5.3: Flowchart of Nelder-Mead algorithm [89].

5.5 Random Search

The Random Search, also known as the Monte-Carlo method, is a stochastic algorithm that differs from the highest deterministic search algorithms such as Branch and Bound, Interval Analysis, and Tunneling. The RS algorithm's solution procedure has certain benefits. For example, while small step approaches can locate only the top of a local peak, some type of true search strategy should be combined when a search for the absolute maximum of a multimodal function is desired. There are several common methods and programs based on random number generator in the stochastic process. In order to get approximation to any desired distribution, the resultant data must be scaled and modified. The major benefit for the proper utilization of Random Search methods is that the method

may achieve the global optimum for non-convex, non-differentiable objective functions containing continuous, discrete regions. Another benefit of the RS technique is that it is very simple to apply for complicated problems. Generally, RS methods perform without failures and are known as robust as a consequence of quick answers for insufficiently structured global optimization problems [89]. A flowchart summarizing the process of Random Search algorithm is shown in Figure 5.4.

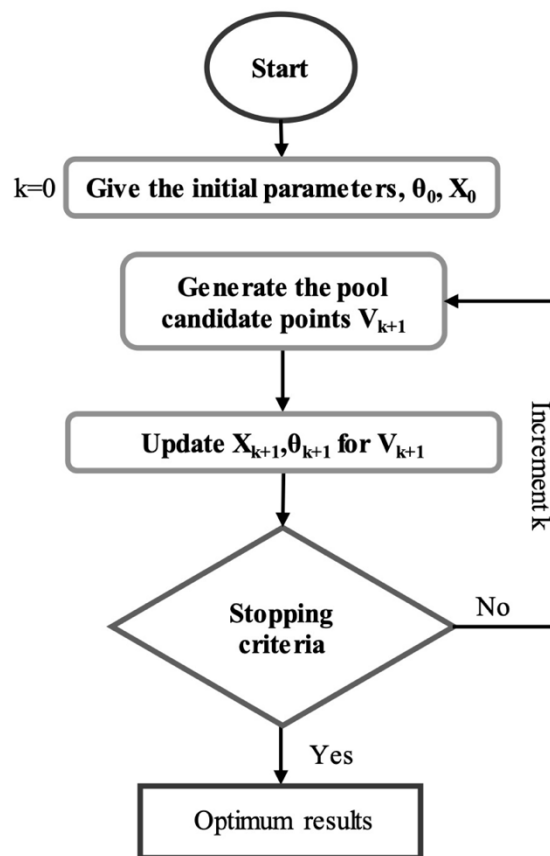


Figure 5.4: Flowchart of Random Search algorithm [89].

Chapter 6

Mathematica Implementation

6.1 Global and Local Optimization by Mathematica

The Mathematica software has a collection of commands which make exact-numeric optimization to solve linear-nonlinear and unconstrained-constrained problems. In this respect, *NMinimize* and *NMaximize* commands are used in numeric global optimization methods while *Minimize* and *Maximize* commands are only appropriate for exact global optimization. Numeric local optimization is carried out by using the *FindMinimum* command. The abovementioned commands could all be utilized for linear-nonlinear and constrained-unconstrained optimization problems [90]. Detail explanations about commands, algorithms, and which types of problems they are used to solve are given in Table 6.1 and Figure 6.1.

Numerical global optimization strategies for restricted nonlinear problems may be widely classified as gradient-based techniques and direct search techniques. Gradient-based methods make apply of first or second derivatives of objective function and constraints for calculation, while Direct search methods have a probabilistic process and do not need derivative information.

When the objective function and all constraints are linear functions of optimization variables, the problem is known as linear programming (LP) problem. An optimization issue can be solved using nonlinear programming (NLP) when certain constraints or objective functions are nonlinear. Maximum, minimum or stationary points are calculated for an objective function over unknown real variables in the presence of congruent and noncongruent, together termed constraints [90].

All four methods — *Minimize*, *Maximize*, *NMinimize* and *NMaximize* — are applicable when a global optimization is required. For the type of optimization problems comprising random multinomial issues, *Minimize* and *Maximize* could discover global optimum that are accurate. Questions involving global optimization can be handled computationally utilizing *NMinimize* or precisely utilizing *Minimize*. In addition to this, due to their asymptotic complicatedness, the methods utilized are just acceptable for situations with a limited number of variables. If the question requires a local optimum, or it can be solved utilizing only one or a few distinct points of departure, *FindMinimum* is the right tool. It simply tries to identify a local minimum. It could be worthwhile to use *NMinimize* for minor issues, also for local optimal solution. *NMinimize* utilizes only one of four direct search methods (Nelder–Mead, differential evolution, simulated annealing and random search). A mix of KKT solution, inner point, and penalty technique is utilized to perfect the solution. *NMinimize* must be stronger than *FindMinimum* if efficiency is not a concern, besides being a global optimal solver. In contrast, when the efficiency is significant, *FindMinimum* may be utilized if a local minimum is required, or an excellent point of departure is required, or the situation has just one lower point (e.g., convex), or the situation is big-budget. The similar challenge with seven parameters is answered with utilizing *FindMinimum* and *NMinimize*. The computation of the limitations is rather costly. [90].

In this chapter, the Mathematica instructions (*FindMinimum*, *NMaximize*, *Nminimize*, *RandomSearch*, *SimulatedAnnealing*, *NelderMead*, *DifferentialEvolution*) are explained and the capability of the algorithms are utilized to determine the global lower limit for distinct test functions.

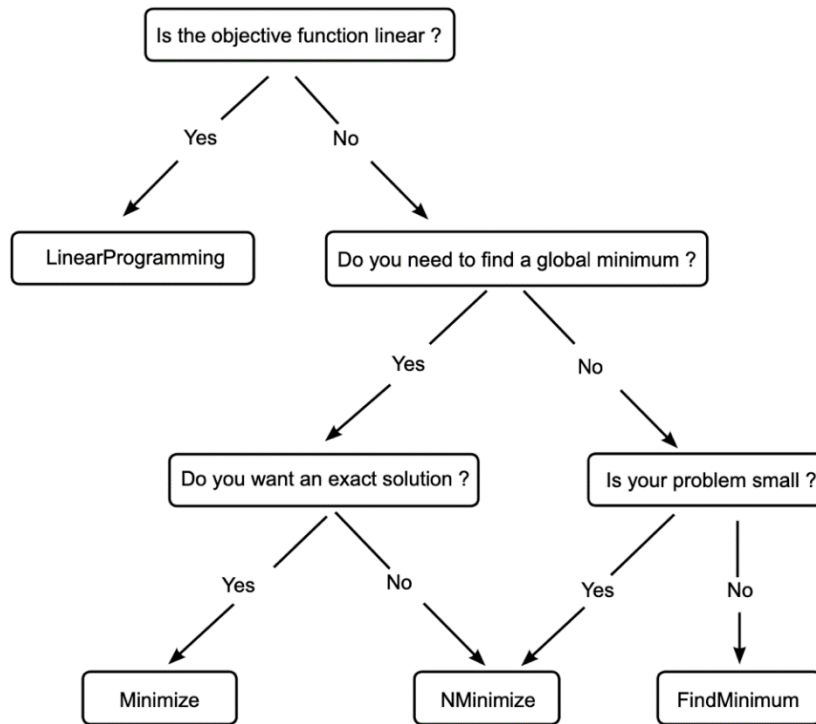


Figure 6.1: Mathematica optimization process [90].

Table 6.1: Optimization methods and instructions [90].

Optimization Types	Optimization Methods/Algorithms	Mathematica Commands
• Numerical Local Optimization	• Linear Programming Methods • Nonlinear Interior Point Algorithms	<i>FindMinimum</i> <i>FindMaximum</i>
• Numerical Global Optimization	• Linear Programming Methods • Differential Evolution • Nelder-Mead • Simulated Annealing • Random Search	<i>NMinimize</i> <i>NMaximize</i>
• Exact Global Optimization	• Linear Programming Methods, • Cylindrical Algebraic Decomposition • Lagrange Multipliers • Integer Linear Programming	<i>Minimize</i> <i>Maximize</i>
• Linear Optimization	• Linear Programming Methods (simplex, revised simplex, interior point)	<i>LinearProgramming</i>

6.1.1 FindMinimum

The *FindMinimum* command is utilized to determine the global lower limit function for unconstrained and constrained optimization problems [90].

The options of the *FindMinimum* command are *Method*, *MaxIterations*, *WorkingPrecision*, *PrecisionGoal*, and *AccuracyGoal*.

The *Method* option ventilates that the *FindMinimum* command selects which method solves problems. Hereof, unconstrained optimization problems; (i) *Newton* utilizes the exact Hessian or a finite difference approximation, (ii) *QuasiNewton* uses the quasi-Newton BFGS approximation which was composed by updates based on past steps, (iii) the *LevenbergMarquardt* method also known as the damped least- squares (DLS) method, is employed to solve non-linear least-squares problems, (iv) the *ConjugateGradient* method is appropriate for solving linear systems, (v) the *PrincipalAxis* method does not need derivatives and it requires two starting conditions in each variable. In constrained optimization problems, only *InteriorPoint* can be selected as a method.

The *MaxIterations* option indicates the maximum number of iterations which ought to be utilized. In the restricted optimization problems, the standard “*MaxIterations*->500” is utilized.

WorkingPrecision, *PrecisionGoal*, and *AccuracyGoal* are options specifying the number of digits of precision. The former controls the internal computations while the latter checks the final result. By default, *WorkingPrecision*->prec is equal to *MachinePrecision* but If *prec*>*MachinePrecision* a constant *prec* value which is used during the calculation. When *AccuracyGoal* and *PrecisionGoal* cases are selected as *Automatic*, the standard values are set to *WorkingPrecision*/3 and *Infinity*, respectively [90].

Carron table function, which is a non-separable and multimodal function, and has many local minima has taken as a test function, and the *FindMinimum* command and the effect of its options in finding the local minima are investigated [92].

```
In[1]:= f[x1_,x2_] := -(Cos[x1]Cos[x2]
Exp[Abs[1-((x1^2+x2^2)^0.5)/Pi]])^2/30
In[2]:= Plot3D[f[x1,x2],{x1,-10,10},{x2,-10,10},
AxesLabel->{x1,x2,y}]
In[3]:= FindMinimum[{f[x1,x2],-10<=x1<=10,-10<=x2<=10},{x1,x2}]
Out[3]= {-24.1568,{x1->9.64617,x2->9.64617}}
In[4]:= FindMinimum[{f[x1,x2],-10<=x1<=10,-10<=x2<=10},
{x1,x2},Method->"InteriorPoint"]
```

```

Out[4]= {-0.246302, {x1 -> -1.22418*10^-14,
x2 -> -1.29143*10^-14}}
In[5]:= Do[Print[FindMinimum[{f[x1,x2],-10<=x1<=10,
-10<=x2<=10},{x1,x2},Method->"InteriorPoint",
"MaxIterations"->i]],
{i,{1,10,100,500,1000,2000,4000,8000}}]
{-0.0105322,{x1->0.969586,x2->0.969586}}
{-0.246302,{x1->-8.74067*10^-8,x2->-8.74067*10^-8}}
{-0.246302,{x1->-8.37899*10^-15,x2->-8.38925*10^-15}}
{-0.246302,{x1->-1.22418*10^-14,x2->-1.29143*10^-14}}
{-0.246302,{x1->-1.22418*10^-14,x2->-1.29143*10^-14}}
{-0.246302,{x1->-1.22418*10^-14,x2->-1.29143*10^-14}}
{-0.246302,{x1->-1.22418*10^-14,x2->-1.29143*10^-14}}
{-0.246302,{x1->-1.22418*10^-14,x2->-1.29143*10^-14}}
In[6]:= Table[Print[FindMinimum[{f[x1,x2],-10<=x1<=10,
-10<=x2<=10},{x1,RandomReal[{-10,10}]},
{x2,RandomReal[{-10,10}]}],Method->
"InteriorPoint"]],{10}]
{-0.0368271,{x1->0.000019185,x2->-3.44978}}
{-1.42781,{x1->6.50458,x2->-6.50458}}
{-6.7549,{x1->9.68366,x2->-6.45799}}
{-0.272117,{x1->3.63079*10^-7,x2->-6.59135}}
{-1.42781,{x1->6.50458,x2->-6.50458}}
{-2.01069,{x1->-1.67999*10^-7,x2->9.73295}}
{-1.42781,{x1->-6.50458,x2->-6.50458}}
{-0.436543,{x1->6.56051,x2->3.28309}}
{-0.0843916,{x1->-3.36299,x2->3.36298}}
{-2.78243,{x1->-9.71802,x2->3.24199}}

```

6.1.2 NMinimize and NMaximize Functions

By utilizing search methods, these Mathematica functions allow us to reach optimal solution difficult issues in science and engineering and their particular characteristics. They are effective at discovering global optimum solutions, but even without restrictions and boundary conditions, it may be challenging to get optimized results. The best way to cope with this situation might be optimizing given functions with different initial conditions. The following examples are obtained again using the initial test functions; Ackley function of $f(x_1, x_2)$ and Holder Table 1 function of $g(x_3, x_4)$, respectively.

```

In[15]:= NMinimize[{f[x1,x2],-35<=x1<=35,-35<=x2<=35},{x1,x2}]
Out[15]= {0.8740,{x1->-0.9984,x2->-2.9952}}
In[4]:= NMaximize[{f[x1,x2],-35<=x1<=35,-35<=x2<=35},{x1,x2}]
Out[4]= {12.3202,{x1->34.5137,x2->34.51377}}
In[7]:= NMinimize[{g[x3,x4],-10<=x3<=10,-10<=x4<=10},{x3,x4}]

```



```

Out[7]=      {-26.9203, {x3→9.6461, x4→9.6461}}
In[8]:=      NMaximize[{g[x3, x4], -10≤x3≤10, -10≤x4≤10}, {x3, x4}]
Out[8]=      {-2.5326×[10]^(-13), {x3→-4.7498, x4→-4.7123}}

```

According to initial results, global minima and maximal values of Ackley Function might be achieved. However, it is seen that it was not valid for Holder Table 1 function. Adjustment of the parameters or changing the restriction region might be effective towards obtaining global values.

Limitations can be the shape of lists and/or logical mixtures of alternatives, equalities and inequities inside the domain. To exemplify, $\mathbf{z} \in \mathbf{Integers}$, should be added in line if it is necessary to describe outcomes as integers. Due to this limitation, the only solutions that are feasible are integers. To start optimal solution, the *NMinimize* instruction also requires a quadrilateral beginning area. There should be upper and lower boundaries for every parameter in the provided function. Utilizing the *Method* selection allow us to establish various types of search methods is a procedure to get unautomated set results as seen previous parts of this chapter performed using *SA* and *RS* algorithms. Here, it can be said that if the function being minimized or maximized (called as an objective function) and constraints are linear, the *LinearProgramming* method is the default setting in the solving process. If the central part of the objective function is not numerical and also the variables are in integer form, *DE* is the algorithm as default. In other situations, *NM* is the search algorithm to be used. If *NelderMead* does not provide desirable solutions, it switches with *DE* to obtain optimum values [90].

6.2 Random Search

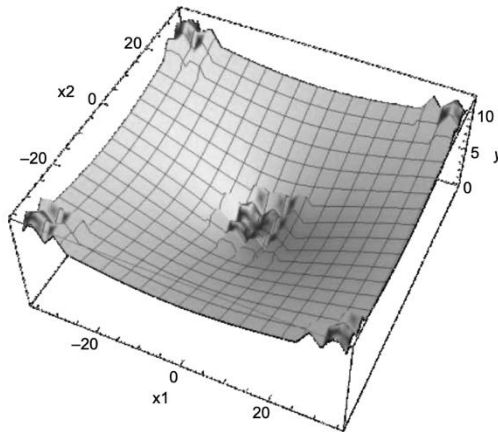
The Random Search (RS) method implemented by Mathematica has a stochastic approach. In the working process, the algorithm composes population, including random starting points, and then the algorithm evaluates the convergence behavior of the points of departure to the local lowest limit utilizing the *FindMinimum* local search method. During this process, the options: (i) *SearchPoints* determines the number of starting points as per “min(10 f,100)” expression, where f is the total amount of variables, (ii) *RandomSeed* adjusts the starting value for random

number producer, (iii) Method is defined by which method to use for minimizing the objective function by *FindMinimum*. In here, for unconstrained optimization problems, *FindMinimum* command uses Quasi-Newton as search method which does not need the second derivatives (Hessians matrix) to be calculated; instead, the Hessian is revised by examining consecutive gradient vectors. In the event that the constrained optimization problem, the nonlinear interior point is selected as a search method by the *FindMinimum* command, (iv) *PostProcess* option can be selected as Karush–Kuhn–Tucker (KKT) conditions or *FindMinimum*. At the end of these processes, the finest local lower limit is selected as result.

Mathematica automatically controls the options *InitialPoints*, *Method*, *PenaltyFunction*, *PostProcess*, and *SearchPoints* used in random search algorithm, and appropriate values of options are selected according to optimization problems [90]. The RS algorithm follows the procedure given in Figure 6.2.

In order to verify the effectiveness capacity of the Random Search algorithm in finding the global minimum, separable and non-separable multimodal test functions having more than one, few or many local minima are used. This kind of global optimization problems are quite hard when an algorithm is not designed appropriately, and it can be inserted into the local minima without finding the global minimums or not all global minimums. In this respect, the first selected test function, which has global minima is located at $f(0,0) = 0$ is Ackley [92]. The following commands give the Mathematica syntax for the definition of Ackley function and its 3D plot in an interval.

```
In[1]:= f[x1_,x2_] := -20Exp[(-0.02Sqrt[0.5(x1^2+x2^2)])]
          -Exp[(0.5(Cos[2Pix1]+Cos[2Pix2]))]+20+Exp[1];
In[2]= Plot3D[f[x1,x2],{x1,-35,35},{x2,-35,35},
             AxesLabel->{x1,x2,y}]
```



It is noted that the *RandomSearch* command may not find a global minimum without working any alteration of its options.

```
In[3]:= NMinimize[{f[x1,x2], -35<=x1<=35, -35<=x2<=35},
{x1,x2},Method->"RandomSearch"]
Out[3]= {2.83635, {x1->-5.99749,x2->8.99623}}
```

Sometimes changing the search point option that specifies the number of points to start searches can be effective in finding a global minimum.

```
In[4]:= Do[Print[NMinimize[{f[x1,x2], -35<=x1<=35, -35<=x2<=35},
{x1,x2},Method->{"RandomSearch","SearchPoints"->i}]],
{i,500,3000,500}]
{0.39531, {x1->0.996345,x2->0.996345}}
{0.280127, {x1->-5.04225*10^-24,x2->-0.9948}}
{0.280127, {x1->-5.04225*10^-24,x2->-0.9948}}
{0.280127, {x1->-5.04225*10^-24,x2->-0.9948}}
{0.280127, {x1->-5.04225*10^-24,x2->-0.9948}}
{1.2012*10^-9, {x1->-8.42728*10^-10,x2->-4.16243*10^-9}}
```

The effect of the *RandomSeed* option, which constitutes starting value for the random number generator, can be investigated below. In the previous example, while the *"Searchpoints"->500* is not sufficient to reach the global minimum, in the following example a global minimum can be obtained by setting the values of the *SearchPoints* and the *RandomSeed* to 500 and 5, respectively.

```
In[5]:= Do[Print[NMinimize[{f[x1,x2], -35<=x1<=35, -35<=x2<=35},
{x1,x2},Method->{"RandomSearch","SearchPoints"->500,
"RandomSeed"->i}]],{i,5}]
{0.280127, {x1->-7.38323*10^-25,x2->0.9948}}
{7.40815*10^-10, {x1->6.89861*10^-10,
x2->-2.52669*10^-9}}
```

```
{0.280127, {x1->5.59478*10^-24, x2->0.9948}}
{0.39531, {x1->0.996345, x2->0.996345}}
{1.37499*10^-9, {x1->-3.64123*10^-9,
x2->-3.22083*10^-9}}
```

In here, points are produced on a matrix to utilize as starting points. If the approximate solution range of the problem can be estimated, assigning the starting point makes it easier to get the solution.

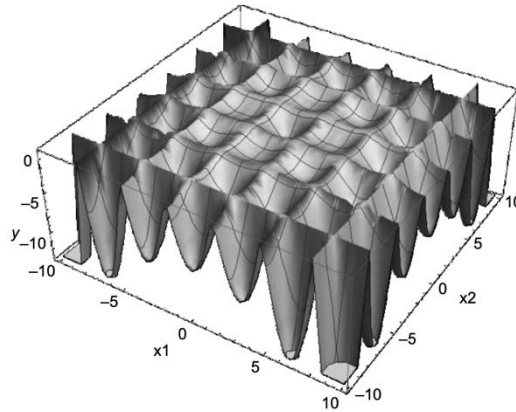
```
In[6]:= Print[NMinimize[{f[x1,x2], -35<=x1<=35, -35<=x2<=35},
{x1,x2},Method->{"RandomSearch", "InitialPoints"-
>Flatten[Table[{i,j},{i,-35,35,5},{j,-35,35,5}],1}]]]
Out[6]= {-4.44089*10^-16, {x1->-1.52703*10^-15, x2->-
1.52703*10^-15}}
```

PostProcess option is not of primary importance for this problem. *PostProcess* methods *KKT* and *FindMinimum* give the same results.

```
In[7]:= Print[NMinimize[{f[x1,x2], -35<=x1<=35, -35<=x2<=35},
{x1,x2},Method->{"RandomSearch", "SearchPoints"->3000,
"PostProcess"->KKT}]]]
Out[7]= {1.2012*10^-9, {x1->-8.42726*10^-10,
x2->-4.16243*10^-9}}
In[8]:= Print[NMinimize[{f[x1,x2], -35<=x1<=35, -35<=x2<=35},
{x1,x2},Method->{"RandomSearch", "SearchPoints"->3000,
"PostProcess"->FindMinimum}]]]
Out[8]= {1.2012*10^-9, {x1->-8.42728*10^-10,
x2->-4.16243*10^-9}}
```

Another test function Holder Table 1, which is separable and multimodal, is used to evaluate the capability of *RandomSearch* command in finding the global minimum. This test function has global minima in located at $f(\pm 9.646168, \pm 9.646168) = -26.920336$. The followings are Mathematica syntax for the definition of the "Holder Table 1" function and its 3D plot.

```
Clear[f];
In[9]:= f[x1_,x2_] := -Abs[Cos[x1]Cos[x2]Exp
[Abs[1-((x1^2+x2^2)^0.5)/Pi]]];
In[10]:= Plot3D[f[x1,x2],{x1,-10,10},{x2,-10,10}]
```



The RS algorithm finds one of the global minimum points without working any alteration of its options for this problem.

```

In[11]:= NMinimize[{f[x1,x2], -10≤x1≤10, -10≤x2≤10},
                {x1,x2},Method->"RandomSearch"]
Out[11]= {-26.9203, {x1 -> -9.64617, x2 -> -9.64617}}
In[12]:= Do[Print[NMinimize[{f[x1,x2], -10≤x1≤10, -10≤x2≤10},
                {x1,x2},Method->{"RandomSearch", "RandomSeed"->i}],
                {i,{1,6,7}}]
                {-26.9203, {x1->-9.64617, x2->9.64617}}
                {-26.9203, {x1->-9.64617, x2->-9.64617}}
                {-26.9203, {x1->9.64617, x2->9.64617}}

```

6.3 Simulated Annealing

The Simulated Annealing (SA) algorithm implemented by Mathematica is a stochastic approach having a working process based on the physical annealing procedure of solids. The SA is designed to find the largest or smallest values of functions having many variables and the smallest values of nonlinear functions having many local minimums. The algorithm is named Simulated Annealing because it exemplifies the perfect arrangement of atoms of solid bodies and minimizing the potential energy during the cooling process. The algorithm enables the system to depart from the local minimum and to investigate and to find an improved global minimum [93].

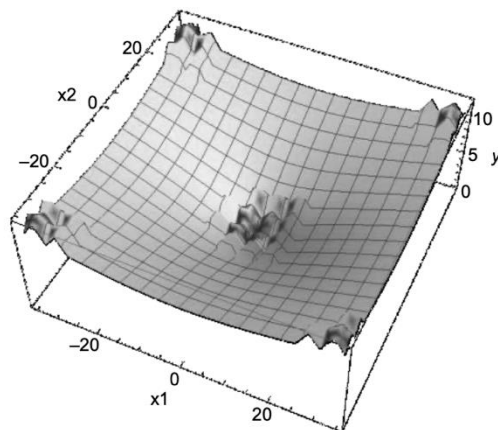
In the working process for each iteration; firstly, the startup solution “Z” is produced, Secondly, “Z_{new}” is generated in the vicinity of the present point, “Z” and then Z_{best} is defined.

If $f(Z_{\text{new}}) \leq f(Z_{\text{best}})$, Z_{new} replaces Z_{best} and Z . Otherwise, Z_{new} replaces with Z . In this loop, options *InitialPoints*, *SearchPoints*, and *RandomSeed* are capable of determining the initial guess and its number and starting value, respectively. In the SA algorithm, random movements in the search space are performed based on the Boltzmann probability distribution $e^{D(k, \Delta f, f_0)}$. In the equation, D is the function explained by option Boltzmann Exponent, k is the present iteration, Δf is the variance in the objective function. In the Mathematica, if the user does not select manually, B is defined as $\frac{-\Delta f \log(k+1)}{10}$ by *BoltzmannExponent*.

For all starting points, the working process introduced above is returned by the time either the algorithm converges to a spot, or the algorithm remains at the identical point as a result of the number of iterations assigned by the option *LevelIterations* [94]. The SA algorithm follows the procedure given in Figure 6.3.

“Ackley” and “Holder Table 1” is used to evaluate the performance capacity of the *SimulatedAnnealing* command to find the global minimum.

```
In[1]:= f[x1_,x2_] := -20 Exp[(-0.02 Sqrt[0.5 (x1^2+x2^2)])] -
Exp[(0.5 (Cos[2 Pi x1]+Cos[2 Pi x2]))]+20+Exp[1];
In[2]= Plot3D[f[x1,x2],{x1,-35,35},{x2,-35,35},
AxesLabel->{x1,x2,y}]
```



The SA algorithm may not find a global minimum by using the default value of its options.

```
In[3]:= NMinimize[{f[x1,x2], -35<=x1<=35, -35<=x2<=35},
{x1,x2},Method->{"SimulatedAnnealing"}]
```

```
Out[3]= {2.37578, {x1 -> 7.99584, x2 -> 3.99792}}
```

BoltzmannExponent includes a function which determines a new point at each iteration; thus, the **BoltzmannExponent** is a significant option that shows the way to achieve a global minimum. If this function is utilized without a default value, the obtained result can be changed. However, in the following problem, changing this option alone has not been enough to determine the global lower limit.

```
In[4]:= NMinimize[{f[x1,x2], -35<=x1<=35, -35<=x2<=35}, {x1,x2},
Method->{"SimulatedAnnealing", "BoltzmannExponent"}
->Function[{i,df,f0}, -df/(Exp[i/10])]]]
Out[4]= {0.830095, {x1 -> -2.99495, x2 -> 6.41153*10^-9}}
```

For this problem, although the **PerturbationScale** alters the result, changing this option alone has not been enough to find the global minimum. The algorithm attains to local minimum points.

```
In[5]:= Do[Print[NMinimize[{f[x1, x2], -35 <= x1 <= 35, -35 <= x2
<= 35}, {x1, x2}, Method -> {"SimulatedAnnealing",
"PerturbationScale" -> i}]], {i, 15}]
{2.37578, {x1->7.99584, x2->3.99792}}
{2.40345, {x1->0.999488, x2->8.99539}}
{1.0993, {x1->-1.04986*10^-9, x2->3.99502}}
{3.8527, {x1->-1.99944, x2->14.9958}}
{6.15308, {x1->-23.9966, x2->-9.9986}}
{4.50046, {x1->14.9966, x2->-9.99773}}
{4.26698, {x1->11.9971, x2->-11.9971}}
{4.27353, {x1->7.99805, x2->-14.9963}}
{2.63697, {x1->5.99725, x2->-7.99634}}
{6.15308, {x1->-23.9966, x2->-9.9986}}
{6.15308, {x1->-23.9966, x2->-9.9986}}
{6.15308, {x1->-23.9966, x2->-9.9986}}
{6.15308, {x1->-23.9966, x2->-9.9986}}
{6.15308, {x1->-23.9966, x2->-9.9986}}
{6.15308, {x1->-23.9966, x2->-9.9986}}
```

Using many more **SearchPoints**, a global minimum can be obtained.

```
In[6]:= Do[Print[NMinimize[{f[x1,x2], -35<=x1<=35, -35<=x2<=35},
{x1,x2}, Method-> {"SimulatedAnnealing",
"SearchPoints"->i}]], {i, 100, 500, 100}]
{0.830095, {x1->-2.99495, x2->7.32049*10^-10}}
{0.62186, {x1->1.99543, x2->-0.997715}}
{0.280127, {x1->-1.64485*10^-9, x2->-0.9948}}
{0.280127, {x1->0.9948, x2->5.25186*10^-12}}
{1.937*10^-9, {x1->-2.31279*10^-9, x2->-6.44598*10^-9}}
```

As previously seen, while changing the search points alone is sufficient to determine the global lower limit., in the case of conducting a search utilizing the *RandomSeed*, *PerturbationScale*, and *BoltzmannExponent*, the algorithm seizes the local minimums.

```
In[7]:= Do[Print[NMinimize[{f[x1,x2],-35<=x1<=35,
-35<=x2<=35},{x1,x2},Method->
{"SimulatedAnnealing","RandomSeed"->i}],{i,0,10}]
{2.37578,{x1->7.99584,x2->3.99792}}
{0.557056,{x1->-4.99634*10^-9,x2->1.99487}}
{2.15456,{x1->7.99533,x2->-0.999416}}
{0.39531,{x1->0.996345,x2->0.996345}}
{3.46466,{x1->-8.99708,x2->9.99676}}
{0.993567,{x1->2.99583,x2->1.99722}}
{1.58244,{x1->-2.9975,x2->-4.99584}}
{1.22508,{x1->-3.99557,x2->1.99779}}
{1.46596,{x1->1.99819,x2->-4.99546}}
{0.39531,{x1->-0.996345,x2->0.996345}}
{2.29034,{x1->4.99729,x2->6.9962}}
```

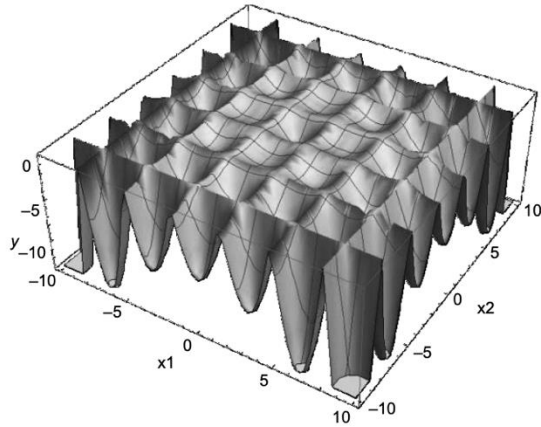
```
In[8]:= Do[Print[NMinimize[{f[x1,x2],-35<=x1<=35,-35<=x2<=35},
{x1,x2},Method-> {"SimulatedAnnealing",
"PerturbationScale"->3,"SearchPoints"->500,
"RandomSeed"->i}], {i, 0, 10, 1}]
{-4.44089*10^-16,{x1->-1.62365*10^-15,
x2->2.19073*10^-16}}
{0.39531,{x1->-0.996345,x2->0.996345}}
{0.557056,{x1->1.99487,x2->-1.44602*10^-11}}
{1.16405,{x1->-2.99649,x2->-2.99649}}
{0.557056,{x1->-1.99487,x2->-6.2523*10^-11}}
{0.62186,{x1->-1.99543,x2->-0.997715}}
{0.557056,{x1->1.99487,x2->7.97744*10^-12}}
{0.39531,{x1->0.996345,x2->0.996345}}
{0.280127,{x1->0.9948,x2->-6.58993*10^-9}}
{2.09443*10^-9,{x1->-7.39447*10^-9,
x2->-3.93044*10^-10}}
{0.993567,{x1->-1.99722,x2->-2.99583}}
```

```
Clear[f]
```

```
In[9]:= f[x1_,x2_]:=-Abs[Cos[x1]Cos[x2]
```

```
Exp[Abs[1-((x1^2+x2^2)^0.5)/Pi]]];
```

```
In[10]:= Plot3D[f[x1,x2],{x1,-10,10},{x2,-10,10}]
```

The Simulated Annealing algorithm finds one of the global minimum points without working any alteration of its options for this problem.

```
In[11]:= NMinimize[{f[x1,x2],-10<=x1<=10,-10<=x2<=10},{x1,x2},
Method->"SimulatedAnnealing"]
Out[11]= {-26.9203, {x1 -> 9.64617, x2 -> 9.64617}}
```

Unlike the Random Search algorithm, four distinct global minimum points can be found by using the Simulated Annealing algorithm.

```
In[12]:= Do[Print[NMinimize[{f[x1,x2],-10<=x1<=10,
-10<=x2<=10},{x1,x2},Method->
{"SimulatedAnnealing","RandomSeed"->i}],
{i,{1,2,3,11}}],
{-26.9203,{x1->9.64617,x2->9.64617}}
{-26.9203,{x1->-9.64617,x2->-9.64617}}
{-26.9203,{x1->-9.64617,x2->9.64617}}
{-26.9203,{x1->9.64617,x2->-9.64617}}
```

6.4 Differential Evolution

Differential evolution (DE) is among the most regular stochastic search methods in the optimization and solution of complicated and challenging design problems. The algorithm is built on four main steps which are initialization, mutation, crossover, and selection. Although *DE* is an efficient search algorithm thanks to covering a population of solutions in iterations rather than a single solution, it computationally requires more process time which makes it an expensive method. *DE* is a robust and reliable algorithm to obtain global optimum. However, there is

uncertainty finding global optimum points as also valid for other types of search methods [96].

In iterations, a fresh group of k points is produced. Then, the j^{th} fresh point is produced by taking three arbitrary points such as z_1, z_2 , and z_3 from the previously generated group. Then it builds the new formation by $z_s = z_3 + s(z_1 - z_2)$ that s is the actual scaling coefficient. A new point z_{new} is generated from z_j and z_s by picking the i^{th} coordinate or another coordinate of j^{th} from z_s with the probability of p . Then, z_{new} changes with z_j , if the function of $h(z_{\text{new}})$ is smaller than the function of $h(z_j)$ [90].

None of the modification parameters in the DifferentialEvolution command which are *CrossProbability (P)*, *InitialPoints*, *PenaltyFunction*, *PostProcess*, *RandomSeed*, *ScalingFactor*, *SearchPoints*, and *Tolerance* warranties the discovery of global optimum. The algorithm's procedure workflow is depicted in Figure 6.4 [99].

As performed with previous search algorithms, the same test functions of Ackley and Holder Table 1 are used to evaluate the capacity of the DE algorithm to determine the global lower limit.

```
In[3]:= NMinimize[{f[x1,x2], -35<=x1<=35, -35<=x2<=35}, {x1,x2},
Method->"DifferentialEvolution"]
Out[3]= {2.2587*10^-9, {x1 -> -1.63413*10^-9, x2 -> -
7.81672*10^-9}}
```

Changing *ScalingFactor* from default value of 0.6 to 0.7 obtained better results considering global optima.

```
In[5]:= NMinimize[{f[x1,x2], -35<=x1<=35, -35<=x2<=35}, {x1,x2},
Method->{"DifferentialEvolution",
"ScalingFactor"-> 0.7}]
Out[5]= {3.74914*10^-10, {x1 -> 8.68579*10^-10, x2 -> -
1.00129*10^-9}}
```

Here, adjusting *ScalingFactor*, *RandomSeed*, *CrossProbability* or *SearchPoints* didn't produce better global optima. Therefore they were kept at a default.

The global minima of other test function Holder Table 1 were tried to find by the algorithm. Initial steps are same with previously used algorithms.

```
In[10]:= NMinimize[{f[x1,x2], -10≤x1≤10, -10≤x2≤10},{x1,x2}, -
Method->"DifferentialEvolution"]
Out[10]= {-26.9203, {[x1 -> 9.64617, x2 -> -9.64617]}
```

In this example of function, all of the parameters being different than their default values did not obtain neither different results nor better global minima.

6.5 Nelder-Mead

Nelder-Mead (NM) or Simplex is one of the derivative-free optimization methods among other traditional local search algorithms. It was firstly designed for unconstrained optimization problems [97]. In m -dimensional space and given a function of m variables, this method keeps a group of $m+1$ points generating the vertices of a polytope. It should be noted that the simplex approach for linear programming should not be mistaken with this technique. Iterations have performed by forming $m+1$ points as $y_1, y_2, y_3, \dots, y_{m+1}$. These points form the functions are ordered as $h(y_1) \leq h(y_2) \leq h(y_3) \leq \dots h(y_{m+1})$. After the fresh point is constructed to improve with the previous the lowest point y_{m+1} . A polytope can be defined in terms of its centroid ($c = S^{m-1} y_i$) being the average position of all the points of an object. Here, a trial point should be defined (y_t). It is produced by reflecting the worst point until centroid, $y_t = c + \alpha(c - y_{m+1})$ where α is a variable being larger than 0. In this part, the new point need not be a new worst point or a new best point. Hence, $h(y_1) \leq h(y_t) \leq h(y_m)$, y_t replace with y_{m+1} . After obtaining a fresh point being greater than the initial highest point, it means that reflection is successfully obtained. Further, it can be continued with $y_e = c + \beta(y_t - r)$ where β being larger than 1 is a parameter to largen polytope. If $h(y_e)$ is obtained as smaller than $h(y_t)$, it means that the expansion process is achieved. Therefore, y_e changes with y_{m+1} . Alternatively, else, y_t changes as y_{m+1} . Another certain step for the algorithm process is that if the fresh point y_t underperforms to the second-lowest point, $h(y_t) \leq h(y_m)$, the polytope is thought as very large and it is required to be constricted.

Hence, a fresh test point is obtained using the following expressions [98].

$$y_c = \begin{cases} c + \gamma (y_{m+1} - c), & \text{if } h(y_t) \geq h(y_{m+1}) \\ c + \gamma (y_t - c), & \text{if } h(y_t) < h(y_{m+1}) \end{cases}$$

where γ is a parameter ranging between 0 to 1. If contraction is achieved, it means that $h(y_c)$ is smaller than $\text{Min}[h(y_{m+1}), h(y_t)]$. Reversely, more process is required to obtain strong contraction.

Nelder-Mead has specific flexible options similar to other algorithms which are *ContractRatio*, *ExpandRatio*, *InitialPoints*, *PenaltyFunction*, *PostProcess*, *RandomSeed*, *ReflectRatio*, *ShrinkRatio*, and *Tolerance*. Even though this algorithm does not provide complete specifications that an accurate global optimization method should require, it tends to work well for the problem having less local minima. As previous algorithms, Nelder-Mead is used to obtain optimum global values for Ackley and Holder Table 1 test functions [90].

```
In[5]:= NMinimize[{f[x1,x2],-35<=x1<=35,-35<=x2<=35},{x1,x2},
Method->"NelderMead"]
Out[5]= {0.87404, {x1 -> -0.998405, x2 -> -2.99522}}
```

It can be seen that results of the first trial are outperformed by DE while it gives better global optima compared to Random Search and Simulated Annealing solutions for Ackley function with the default set.

RandomSeed, which is referred to as one of the critical adjustment parameters of NM might directly affect the performance of the NM finding global minima.

```
In[6]:= Do[Print[NMinimize[{f[x1,x2],-35<=x1<=35,-35<=x2<=35},
{x1,x2},Method->{"NelderMead",
"RandomSeed"->i}]],{i,5}]
Out[6]= {0.557056, {x1->8.15872*10^-25, x2->-1.99487}}
{0.280127, {x1->0.9948, x2->-6.32493*10^-9}}
{7.12481, {x1->-20.9977, x2->-22.9975}}
{2.32486*10^-10, {x1->4.63269*10^-10,
x2->-6.78982*10^-10}}
{1.3908, {x1->-4.99519, x2->-0.999038}}
```

Adjusting *RandomSeed* parameters provided a better minimum value of 2.32486×10^{-10} , compared to trial performed with default set.

In this algorithm, other possible useful adjustment parameters are referred to as *ShrinkRatio*, *ContractRatio*, and *ReflectRatio*. However, it did not obtain global

minima in Ackley function, as indicated the following.

```
In[7]:= Do[Print[NMinimize[{f[x1,x2],-35≤x1≤35,-35≤x2≤35},
{x1,x2},Method->{"NelderMead", "ShrinkRatio"->0.95,
"ContractRatio"->0.95,"ReflectRatio"->2,
"RandomSeed"->i}],{i,5}]
Out[7]= {0.39531,{x1->-0.996345,x2->-0.996345}}
{0.783523,{x1->-1.99642,x2->1.99642}}
{7.37952,{x1->-5.99939,x2->-31.9967}}
{0.39531,{x1->-0.996345,x2->0.996345}}
{2.40704*10^-9,{x1->-2.92841*10^-9,
x2->-7.99045*10^-9}}
```

Another test function Holder Table 1 was minimized using the *NMinimize* command. As seen below, the global minima with default values were -26.9203 .

```
In[12]:= NMinimize[{f[x1,x2],-10≤x1≤10,-10≤x2≤10},{x1,x2},-
Method->"NelderMead"]
Out[12]= {-26.9203, {x1 -> 9.64617, x2 -> 9.64617}}
```

As applied for previous test function, firstly *RandomSeed* have been adjusted to find global minima.

```
In[13]:= Do[Print[NMinimize[{f[x1,x2],-10≤x1≤10,-10≤x2≤10},
{x1,x2},Method->{"NelderMead",
"RandomSeed"->i}],{i,5}]
Out[13]= {-26.9203,{x1->-9.64617,x2->-9.64617}}
{-9.13635,{x1->3.24199,x2->-9.71802}}
{-26.9203,{x1->9.64617,x2->-9.64617}}
{-7.76664,{x1->2.08542*10^-8,x2->9.73295}}
{-7.76664,{x1->-7.64705*10^-9,x2->-9.73295}}
```

Outputs of this trial showed that adjustment of *RandomSeed* as is was not sufficient to reach minimum value. Lastly, other possibly useful parameters concerning literature for *NelderMead* were adjusted to obtain global minima.

```
In[14]:= Do[Print[NMinimize[{f[x1,x2],-10≤x1≤10,-10≤x2≤10},
{x1,x2},Method->{"NelderMead", "ShrinkRatio"->0.95,
"ContractRatio"->0.95,"ReflectRatio"->2,
"RandomSeed"->i}],{i,5}]
Out[14]= {-26.9203,{x1->-9.64617,x2->-9.64617}}
{-26.9203,{x1->-9.64617,x2->-9.64617}}
{-26.9203,{x1->-9.64617,x2->-9.64617}}
{-26.9203,{x1->-9.64617,x2->-9.64617}}
{-26.9203,{x1->-9.64617,x2->-9.64617}}
```

In this example, it was seen that none of the parameters could assure that a global minimum is different from the value obtained using the default settings.

Chapter 7

Case Studies

In this chapter, an attempt is made to determine if the answer to a few optimization issues found in the previous papers may be improved by applying advanced optimization methods to them. Twelve different literature studies, like the optimization of surface roughness, cutting forces, tool life, and tool wear are examined for research. The decided problems were answered by using 13 different linear and non-linear structurally different regression models. To evaluate these literature studies other advanced optimization techniques are used such as MDE (Modified Differential Evolution), MSA (Modified Simulated Annealing), MRS (Modified Random Search) and MNM (Modified Nelder-Mead).

7.1 Mathematical Models

In this part of the thesis, it is aimed to build a mathematical model for optimum outputs as a function of the input parameters. A mathematical model of the operation was built to determine the minimum or maximum values of outputs. Non-linear multivariable regression has been used for this purpose. Then, the mathematical model obtained from analysis will be used to obtain optimum solution of the process and to determine the influence of the design variables on the outputs.

The main purpose of these analysis and optimization processes is to show whether the classical R^2 optimization studies in research studies do not provide the desired results in the full sense and whether more consistent and more optimum results can be obtained by using the same parameters.

The regression models to be used in the analysis and optimization process are listed in Table 7.1.

In order to make the model names in each study more understandable and distinctive, a coding in the form of CSX-OY-Z has been developed. Here CS; case study, X; number of case study, O; output, Y; number of outputs of that case study and Z; indicates the nomenclature of the model. If it is necessary to give an example; CS3-O4-SON; It refers to the SON model for the 4th output in the 3rd case study. Explicit expressions of these abbreviated models are given in the Appendix A section.

Table 7.1: Multiple regression model names, numbers, nomenclatures and formulas

Model Name	Model Number	Nomenclature	Formula
Multiple linear	1	L	$Y = \sum_{i=1}^t (a_i x_i) + c$
Multiple linear rational	2	LR	$Y = \frac{\sum_{i=1}^t (a_i x_i) + c_1}{\sum_{j=1}^t (\beta_j x_j)} + c_2$
Second order multiple nonlinear	3	SON	$Y = \sum_{k=1}^t \sum_{j=1}^t (a_j x_j x_k) + \sum_{i=1}^t (a_i x_i) + c$
Second order multiple nonlinear rational	4	SONR	$Y = \frac{\sum_{k=1}^t \sum_{j=1}^t (a_j x_j x_k) + \sum_{i=1}^t (a_i x_i) + c_1}{\sum_{l=1}^t \sum_{m=1}^t (\beta_m x_m x_l) + \sum_{n=1}^t (\beta_n x_n)} + c_2$
Third order multiple nonlinear	5	TON	$Y = \sum_{l=1}^t \sum_{m=1}^t \sum_{p=1}^t (\beta_l x_l x_m x_p) + \sum_{k=1}^t \sum_{j=1}^t (a_j x_j x_k) + \sum_{i=1}^t (a_i x_i) + c$
First order trigonometric multiple nonlinear	6	FOTN	$Y = \sum_{i=1}^t (a_i \sin[x_i] + a_i \cos[x_i]) + c$
First order trigonometric multiple nonlinear rational	7	FOTNR	$Y = \frac{\sum_{i=1}^t (a_i \sin[x_i] + a_i \cos[x_i]) + c_1}{\sum_{j=1}^t (\beta_j \sin[x_j] + \gamma_j \cos[x_j])} + c_2$
Second order trigonometric multiple nonlinear	8	SOTN	$Y = \sum_{i=1}^t (a_i \sin[x_i] + a_i \cos[x_i]) + \sum_{j=1}^t (\beta_j \sin^2[x_j] + \gamma_j \cos^2[x_j]) + c$

Table 7.1: Multiple regression model names, numbers, nomenclatures and formulas (continued)

Second order trigonometric multiple nonlinear rational	9	SOTNR	$Y = \frac{\sum_{i=1}^t (a_i \sin[x_i] + a_i \cos[x_i]) + \sum_{j=1}^t (\beta_j \sin^2[x_j] + \gamma_j \cos^2[x_j]) + c_1}{\sum_{k=1}^t (\theta_k \sin[x_k] + \theta_k \cos[x_k]) + \sum_{l=1}^t (\delta_l \sin^2[x_l] + \delta_l \cos^2[x_l])} + c_2$
First order logarithmic multiple nonlinear	10	FOLN	$Y = \sum_{i=1}^t (a_i \text{Log}[x_i]) + c$
First order logarithmic multiple nonlinear rational	11	FOLNR	$Y = \frac{\sum_{i=1}^t (a_i \text{Log}[x_i]) + c_1}{\sum_{j=1}^t (\beta_j \text{Log}[x_j])} + c_2$
Second order logarithmic multiple nonlinear	12	SOLN	$Y = \sum_{k=1}^t \sum_{j=1}^t (a_j \text{Log}[x_j x_k]) + \sum_{i=1}^t (a_i \text{Log}[x_i]) + c$
Second order logarithmic multiple nonlinear rational	13	SOLNR	$Y = \frac{\sum_{k=1}^t \sum_{j=1}^t (a_j \text{Log}[x_j x_k]) + \sum_{i=1}^t (a_i \text{Log}[x_i]) + c_1}{\sum_{m=1}^t \sum_{l=1}^t (a_l \text{Log}[x_l x_m]) + \sum_{n=1}^t (a_n \text{Log}[x_n])} + c_2$

7.2 Case Study #1

The first literature study which optimization process was studied taken from Aouici et al [44]. In the study, surface roughness comparison between cubic boron nitride (CBN7020) and ceramics was studied. The machining part was AISI H11 hot work steel which treated at 50 HRC. Taguchi's L18 (21×32) orthogonal matrix was used to design the study. To verify the validity of multiple linear regression model and evaluate the outcomes of machine settings and cutting parameters called as cutting speed, feed rate and depth of cut, on Ra and Rt, the response surface methodology (RSM) and analysis of variance (ANOVA) was used. As a consequence of the study, the importance of the influences of design variables on surface roughness was listed as feed rate, cutting speed and depth of cut, respectively. In the cutting tool results, CBN7020 had a better performance than ceramics. To minimize the surface roughness, conjunction of poor feed rate and strong cutting speed is required. The main purpose of our analysis and optimization processes is to show whether the classical R² optimization studies in research studies do not provide the desired results in the full sense and whether more

consistent and more optimum results can be obtained by using the same parameters.

As depicted in Table 7.2, the changes in values of these input parameters provided the obtaining of different results for the arithmetic mean roughness (R_{aCC670} , R_{aCC650} and $R_{aCBN7020}$) (μm) and total roughness (R_{tCC670} , R_{tCC650} and $R_{tCBN7020}$) (μm).

Therefore, these obtaining results depending on the change in these input parameter values are sufficient to develop an optimization strategy. Moreover, it is impossible to determine a proportional connection between measured roughness values and input parameters (cutting speed, feed rate and depth of cut), as understood from Table 7.2. Therefore, it is necessary to optimize these parameters to minimize both arithmetic mean roughness and total roughness.

Table 7.2: Experimental results of arithmetic mean and total roughness with different experimental conditions [44].

Exp. No	Cutting speed (V_c , m/min)	Feed rate (f , mm/rev)	Depth of cut (a_p , mm)	CC670 (Ra, μm)	CC670 (Rt, μm)	CC650 (Ra, μm)	CC650 (Rt, μm)	CBN7020 (Ra, μm)	CBN7020 (Rt, μm)
1	120	0.08	0.15	0.440	2.70	0.350	3.32	0.350	2.00
2	120	0.08	0.30	0.430	2.79	0.400	2.67	0.390	2.30
3	120	0.08	0.45	0.420	2.81	0.410	3.07	0.300	1.80
4	120	0.12	0.15	0.530	3.22	0.460	3.54	0.460	3.00
5	120	0.12	0.30	0.490	3.30	0.490	3.59	0.495	2.85
6	120	0.12	0.45	0.520	3.41	0.510	3.60	0.565	3.05
7	120	0.16	0.15	0.690	4.79	0.560	3.75	0.560	3.70
8	120	0.16	0.30	0.700	4.82	0.590	3.97	0.545	4.15
9	120	0.16	0.45	0.680	4.90	0.620	4.16	0.565	3.05
10	180	0.08	0.15	0.430	2.69	0.300	2.80	0.230	1.60
11	180	0.08	0.30	0.430	2.75	0.330	2.82	0.210	1.50
12	180	0.08	0.45	0.400	2.83	0.340	2.85	0.180	1.20
13	180	0.12	0.15	0.510	3.18	0.430	3.36	0.360	2.20
14	180	0.12	0.30	0.460	3.25	0.460	3.40	0.270	1.70
15	180	0.12	0.45	0.470	3.33	0.470	3.41	0.340	2.20
16	180	0.16	0.15	0.590	4.43	0.540	3.67	0.500	3.20
17	180	0.16	0.30	0.570	4.56	0.560	3.76	0.475	2.35
18	180	0.16	0.45	0.640	4.74	0.580	3.81	0.505	2.85

The behavior of the system was explained by the multiple linear regression models given below [44];

$$Ra_{CC670} = 0.0975 + 0.00115Vc + 4.6875f - 0.31388ap - 0.01667Vc \times f + 0.00037Vc \times ap + 1.875f \times ap \quad (7.5)$$

$$Rt_{CC670} = 0.11806 + 3.3796 \times 10^{-3}Vc + 31.0625f - 0.39167p - 0.0521Vc \times f + 3.5185 \times 10^{-3}Vc \times ap + 3.5416f \times ap \quad (7.6)$$

$$Ra_{CC650} = 0.27722 - 0.001259Vc + 1.70833f + 0.3ap + 0.0694Vc \times f - 0.00092Vc \times ap + 2.6577 \times 10^{-15}f \times ap \quad (7.7)$$

$$Rt_{CC650} = 2.9592 - 3.009 \times 10^{-3}Vc + 7.4792f - 1.675ap - 3.4722Vc \times f + 3.7037 \times 10^{-4}Vc \times ap + 15.625f \times ap \quad (7.8)$$

$$Ra_{CBN7020} = 0.62194 - 0.00337Vc + 0.02083f + 0.06944ap + 0.01597Vc \times f - 0.002315Vc \times ap + 2.2916f \times ap \quad (7.9)$$

$$Rt_{CBN7020} = 1.3555 - 7.5925 \times 10^{-3}Vc + 28.3333f - 2.4873 \times 10^{-14}ap - 0.0486Vc \times f + 9.2592 \times 10^{-4}Vc \times ap - 8.3333f \times ap \quad (7.10)$$

The experimental data was represented by these regression models with determination coefficients (R^2) of 0.9375, 0.9326, 0.9955, 0.9160, 0.9274 and 0.8889, respectively.

Aouici et al. [44] figured out this limited optimization issue by defining all the input parameters as discrete and proceeded in the modeling process only according to the standard R^2 results and listed the models. The R^2 values Aouici et al [44] found vary between 89% and 99%. Aouici et al [44] does not mention the R^2_{training} and R^2_{testing} distinction in the modeling process and does not mention determining models according to different scenarios. It is seen that smaller surface roughness may be calculated with the variables as a consequence of optimization.

7.2.1 Optimization Scenarios

For all scenarios, the limitations for the system inputs (design parameters) are as in the following form;

$$\begin{array}{ll}
120 \leq \text{Cutting Speed} \leq 180 & , \quad (m/min) \\
0.08 \leq \text{Feed Rate} \leq 0.16 & , \quad (mm/rev) \\
0.15 \leq \text{Depth of Cut} \leq 0.45 & , \quad (mm)
\end{array}$$

7.2.1.1 Scenario 1

Arithmetic mean roughness and total roughness are explained by the objective functions in this optimal solution problem. There are no constraints about the input parameters so they can be real numbers, and the computation domain is continuous. The primary goal is to minimize arithmetic surface roughness and total roughness. It is also technically possible to see these theory-based boundaries of the objective function this way.

7.2.1.2 Scenario 2

Scenario 1 should include additional realistic situations in addition to knowledge-based ones. A novel optimal solution is provided that implies the reduction of surface roughness for this application. Input parameters are also restricted with integers.

7.2.1.3 Scenario 3

As dissimilar from scenario 1, nonlinear constraints are added for the optimization problem. Total roughness must be smaller than $2.8 \mu\text{m}$ for arithmetic surface roughness and arithmetic surface roughness must be smaller than $0.41 \mu\text{m}$ for the total roughness. Problem solving will be more complex and difficult in this instance than in scenarios 1 and 2.

7.2.1.4 Scenario 4

In the constructed of scenario 4, more viable and more limited issue situations should be included to scenario 2. For that reason, there is a new optimum solution problem created to the minimization of the surface roughness. Unlike Scenario 2, in scenario 4 parameters can only take the values in the data table.

7.2.2 Results and Discussion

In our approach, different from the classical ones, various regression models are first tested utilizing both R^2_{training} and R^2_{testing} values (not only R^2 as in the classical approach) to reveal what is the degree of performance of the model can explain the method. Besides, the model's operational restriction (boundedness) is also checked by calculating the highest and lowest values that the related model creates. Therefore, our proposed design strategy provides producing realistic values. Also, it is necessary to check the limitedness of decided models, whether producing realistic results. Regarding of these facts, by using our proposed approach, the experimental data tables of arithmetic mean roughness (Ra_{CC670} , Ra_{CC650} and $Ra_{CBN7020}$) (μm) and total roughness (Rt_{CC670} , Rt_{CC650} and $Rt_{CBN7020}$) listed as Table 7.3, 7.4, 7.5, 7.6, 7.7 and 7.8 can be seen below. Therefore, it is necessary to optimize these parameters to minimize both arithmetic mean roughness and total roughness.

Table 7.3: Results of the Neuro-regression models for the arithmetic mean roughness for Ra_{CC670}

Models	R^2_{training}	R^2_{testing}	Max (μm)	Min (μm)
CS1-O1-L	0.92	0.81	0.659	0.392
CS1-O1-LR	0.99	0.71	0.769	0.406
CS1-O1-SON	0.98	0.91	0.716	0.406
CS1-O1-SONR	0.95	0.88	0.698	0.399
CS1-O1-TON	1.00	0.42	0.820	0.418
CS1-O1-FOTN	0.95	0.84	12.772	-16.113
CS1-O1-FOTNR	0.99	-53.02	2.285×10^7	-432472.
CS1-O1-SOTN	1.00	0.76	12.287	-1029.2
CS1-O1-SOTNR	0.98	0.58	0.706	0.328
CS1-O1-FOLN	0.87	0.79	0.648	0.391
CS1-O1-FOLNR	0.98	0.79	0.748	0.408
CS1-O1-SOLN	0.98	0.91	0.699	0.414
CS1-O1-SOLNR	0.96	0.81	0.687	0.419

Table 7.4: Results of the Neuro-regression models for the total roughness for R_{tCC670}

Models	R^2_{training}	R^2_{testing}	Max (μm)	Min (μm)
CS1-O2-L	0.92	0.94	4.621	2.529
CS1-O2-LR	0.99	0.99	4.997	2.693
CS1-O2-SON	0.99	0.99	4.951	2.705
CS1-O2-SONR	0.02	-0.13	3.583	3.497
CS1-O2-TON	1.00	0.97	5.095	2.585
CS1-O2-FOTN	0.99	0.99	148.760	-193.804
CS1-O2-FOTNR	0.99	0.97	1.844×10^7	-6.450×10^{10}
CS1-O2-SOTN	1.00	0.97	960.515	-8.924
CS1-O2-SOTNR	0.99	0.90	4.935	2.172
CS1-O2-FOLN	0.86	0.88	4.505	2.516
CS1-O2-FOLNR	0.99	0.99	4.946	2.691
CS1-O2-SOLN	0.99	0.99	4.923	2.637
CS1-O2-SOLNR	0.95	0.96	4.736	2.545

Table 7.5: Results of the Neuro-regression models for the arithmetic mean roughness for R_{aCC650}

Models	R^2_{training}	R^2_{testing}	Max (μm)	Min (μm)
CS1-O3-L	0.99	0.99	0.621	0.310
CS1-O3-LR	0.99	0.97	0.602	0.304
CS1-O3-SON	0.99	0.99	0.602	0.301
CS1-O3-SONR	0.99	0.99	0.604	0.302
CS1-O3-TON	1.00	0.99	0.620	0.300
CS1-O3-FOTN	0.99	0.99	2.165	-0.820
CS1-O3-FOTNR	0.99	0.99	1.768×10^8	-1.242×10^{11}
CS1-O3-SOTN	1.00	0.99	2.495	-207.403
CS1-O3-SOTNR	1.00	0.98	0.623	0.292
CS1-O3-FOLN	0.98	0.99	0.610	0.305
CS1-O3-FOLNR	0.99	0.97	0.595	0.301
CS1-O3-SOLN	0.99	0.99	0.603	0.301
CS1-O3-SOLNR	1.00	0.98	0.615	0.300

Table 7.6: Results of the Neuro-regression models for the total roughness for R_{tCC650}

Models	R^2_{training}	R^2_{testing}	Max (μm)	Min (μm)
CS1-O4-L	0.93	0.54	4.008	2.764
CS1-O4-LR	0.97	-0.18	3.954	2.626
CS1-O4-SON	0.97	0.24	4.109	2.749
CS1-O4-SONR	0.04	-0.71	3.401	3.339
CS1-O4-TON	1.00	-1.04	4.262	2.669
CS1-O4-FOTN	0.96	0.40	68.297	-44.407
CS1-O4-FOTNR	0.99	0.26	1.239×10^8	-7.533×10^6
CS1-O4-SOTN	1.00	-0.22	5515.130	-55.930
CS1-O4-SOTNR	1.00	-29.05	1.399×10^{12}	-2.928×10^9
CS1-O4-FOLN	0.95	0.44	3.965	2.738
CS1-O4-FOLNR	0.97	0.10	3.980	2.715
CS1-O4-SOLN	0.97	0.22	4.093	2.741
CS1-O4-SOLNR	0.99	-7.56	3.902	1.388

Table 7.7: Results of the Neuro-regression models for the arithmetic mean roughness for $R_{aCBN7020}$

Models	R^2_{training}	R^2_{testing}	Max (μm)	Min (μm)
CS1-O5-L	0.91	0.84	0.606	0.218
CS1-O5-LR	0.96	0.70	0.634	0.159
CS1-O5-SON	0.96	0.72	0.620	0.166
CS1-O5-SONR	0.96	0.70	0.632	0.159
CS1-O5-TON	1.00	-0.47	0.773	0.18
CS1-O5-FOTN	0.92	0.75	14.344	-9.852
CS1-O5-FOTNR	0.99	0.88	54311.4	-6.139×10^7
CS1-O5-SOTN	1.00	-0.27	23.244	-1712.8
CS1-O5-SOTNR	1.00	0.73	1.050×10^{11}	-11465.1
CS1-O5-FOLN	0.92	0.79	0.596	0.212
CS1-O5-FOLNR	0.95	0.74	0.619	0.167
CS1-O5-SOLN	0.95	0.74	0.610	0.171
CS1-O5-SOLNR	0.96	0.68	0.603	0.234

Table 7.8: Results of the Neuro-regression models for the total roughness for $R_{tCBN7020}$

Models	R^2_{training}	R^2_{testing}	Max (μm)	Min (μm)
CS1-O6-L	0.96	-0.28	3.909	1.297
CS1-O6-LR	0.98	-1.23	4.286	1.216
CS1-O6-SON	0.98	-0.92	4.046	1.189
CS1-O6-SONR	0.03	-0.25	2.576	2.523
CS1-O6-TON	1.00	-5.24	4.675	1.164
CS1-O6-FOTN	0.97	-0.67	10.546	-3.485
CS1-O6-FOTNR	0.98	-1.09	2.356×10^6	-1.762×10^{10}
CS1-O6-SOTN	0.99	0.97	18.922	-7.911
CS1-O6-SOTNR	0.97	-1.66	4.693	1.375
CS1-O6-FOLN	0.95	-0.19	3.831	1.284
CS1-O6-FOLNR	0.98	-1.09	4.246	1.258
CS1-O6-SOLN	0.98	-0.84	4.043	1.605
CS1-O6-SOLNR	0.93	-0.64	4.032	1.641

For the first output of the study (R_{acc670} , Aouici et al. [44]), results show that if the R^2 value was the key element considered in deciding the model, we may conclude that all models accurately describe the process. Because R^2_{training} results are nearly all close to 1.

The initial assumption would be that models 2, 3, 4 and 12 are suitable if the selection had just been based on R^2_{training} and R^2_{testing} . Based on this argument, utilizing a method that considers the desired models' capacity to provide realistic values, it is determined that only models 3 and 12 are suitable. As a result, misleading findings are unavoidable if the model building-optimum result finding analyses are not addressed as outlined in this article.

As can be seen in Table 7.4, estimation capacity (R^2_{testing}) of model 3 (SON) and model 12 (SOLN) are the same while model 3 was achieved lower arithmetic mean roughness than the model 12. With this approach, the obtained second order multiple nonlinear model 3 (CS1-O1-SON) was chosen as the objective function required in analyses to get optimum results of R_{acc670} .

Table 7.9 shows the outcomes of three specific optimization scenarios for the chosen model. In scenario 1, all of the variables were utilized with their upper and lower limits in a continuous interval. The minimum surface roughness outcomes, depending on all of the optimization techniques, were $0.406\ \mu\text{m}$, which correspond to CS1-O1-SON. The suggested (optimum) designs are; cutting speed: 180 (m/min), feed rate: 0.08 (mm/rev) and depth of cut: 0.45 (mm). $0.406\ \mu\text{m}$ is a realistic result by compared with the results of experiment [0.40, 0.70]. We could say that the minimum experimental results and the optimization results are really close to each other.

In scenario 2, feed rate and depth of cut have been handled as continuous parameters, whereas the cutting speed is discontinuous (integers). In this case, the minimum surface roughness results for the SON model were same as the scenario 1.

In the third optimization scenario, the only limitation condition in the optimization process was taken as the total roughness value smaller than 2.8 for CC670, which is the same material. The lowest surface roughness found as $0.443\ \mu\text{m}$. The suggested (optimal) designs are; the cutting speed: 180 (m/min), the feed rate: 0.08 (mm/rev) and depth of cut: 0.167533 (mm). $0.443\ \mu\text{m}$ is a realistic result by compared with the results of experiment [0.40, 0.70]. We could say that the minimum outcomes of experiment and the optimization results of the third scenario are really close to each other.

For the fourth optimization scenario, all of the input parameters are supposed to be real numbers and the design variables can only take the experimental values. The results are the same with scenario 1 and 2.

From the point of stability, gaining identical outcomes for scenarios 1, 2, 3, and 4, whose phenomenological foundation is addressed using four distinct direct search methods, enhances the chance that acquired results are global optimum. Besides that, utilizing various methods for scenario 2 produces dissimilar outcomes, although they are identical. This situation is critical for optimization issues comprising restriction types that are similar to those in scenarios 2 and 3.

Furthermore, utilizing the SON model to solve the optimization issue for scenarios 1, 2, 3 and 4, the optimal surface roughness was found to be 0.406 μm .

For the second output of the study (R_{tCC670} , Aouici et al. [44]), the initial assumption would be that models 2, 3, 11 and 12 are suitable if the selection had just been based on R^2_{training} and R^2_{testing} . Based on this argument, utilizing a method that considers the simplicity of the models and the desired models' capacity to provide realistic values, it is determined that only model 2 (LR) is suitable. As a result, misleading findings are unavoidable if the model building-optimum result finding analyses are not addressed as outlined in this article. Thus, the obtained model 2 (CS1-O2-LR) was chosen as the objective function required in analyses to get optimum results of R_{tCC670} . Outcomes of the selected model can be spotted in Table 7.5.

Table 7.10 shows the outcomes of three specific optimization scenarios for the chosen model. In scenario 1, all of the variables were utilized with their upper and lower limits in a continuous interval. The minimum surface roughness outcomes, depending on all of the optimization techniques, were 2.692 μm , which correspond to CS1-O2-LR. The suggested (optimum) designs are; cutting speed: 180 (m/min), feed rate: 0.08 (mm/rev) and depth of cut: 0.15 (mm). 2.692 μm is a realistic result by compared with the results of experiment [2.69, 4.90]. We could say that the minimum experimental results and the optimization results are really close to each other.

In scenario 2, feed rate and depth of cut have been handled as continuous parameters, whereas the cutting speed is discontinuous (integers). In this case, the minimum surface roughness results for the LR model were same as the scenario 1.

In the third optimization scenario, the only limitation condition in the optimization process was taken as the arithmetic mean roughness value smaller than 0.41 for CC670, which is the same material. The minimum surface roughness found as 2.783 μm . The suggested (optimum) designs are; the cutting speed: 180 (m/min), the feed rate: 0.08 (mm/rev) and depth of cut: 0.167533 (mm). 2.783 μm is a realistic result by compared with the results of experiment [2.69, 4.90]. We could

say that the minimum outcomes of experiment and the optimization results of the third scenario are really close to each other.

For the fourth optimization scenario, all of the input parameters are supposed to be real numbers and the design variables can only take the experimental values. The results are the same with scenario 1 and 2.

From the point of stability, gaining identical outcomes for scenarios 1, 2, 3, and 4, whose phenomenological foundation is addressed using four distinct direct search methods, enhances the chance that acquired results are global optimum. Besides that, utilizing various methods for scenario 2 produces dissimilar outcomes, although they are identical. This situation is critical for optimization issues comprising restriction types that are similar to those in scenarios 2 and 3. Furthermore, utilizing the LR model to solve the optimization issue for scenarios 1, 2, 3 and 4, the optimal surface roughness was found to be 2.692 μm .

For the third output of the study (R_{ACC650} , Aouici et al. [44]), the initial assumption would be that lots of models are suitable if the selection had just been based on R^2_{training} and R^2_{testing} . Based on this argument, utilizing a method that considers the simplicity of the models and the desired models' capacity to provide realistic values, it is determined that only model 3 (SON) is suitable. As a result, misleading findings are unavoidable if the model building-optimum result finding analyses are not addressed as outlined in this article. Thus, the obtained model 3 (CS1-O3-SON) was chosen as the objective function required in analyses to get optimum results of R_{ACC650} . Outcomes of the selected model can be spotted in Table 7.6.

Table 7.11 shows the outcomes of three specific optimization scenarios for the chosen model. In scenario 1, all of the variables were utilized with their upper and lower limits in a continuous interval. The minimum surface roughness outcomes, depending on all of the optimization techniques, were 0.301 μm , which correspond to SON. The suggested (optimum) designs are; the cutting speed: 180 (m/min), the feed rate: 0.08 (mm/rev) and depth of cut: 0.15 (mm). 0.301 μm is a realistic result by compared with the results of experiment [0.30, 0.59]. We could say that the

minimum experimental results and the optimization results are really close to each other.

In scenario 2, feed rate and depth of cut have been handled as continuous parameters, whereas the cutting speed is discontinuous (integers). In this case, the minimum surface roughness results for the SON model were same as the scenario 1.

In the third optimization scenario, the only limitation condition in the optimization process was taken as the total roughness value smaller than 2.8 for CC650, which is the same material. The results are the same with scenario 1 and 2.

For the fourth optimization scenario, all of the input parameters are supposed to be real numbers and the design variables can only take the experimental values. The results are the same with scenario 1, 2 and 3.

From the point of stability, gaining identical outcomes for scenarios 1, 2, 3, and 4, whose phenomenological foundation is addressed using four distinct direct search methods, enhances the chance that acquired results are global optimum. Besides that, utilizing various methods for scenario 2 produces dissimilar outcomes, although they are identical. This situation is critical for optimization issues comprising restriction types that are similar to those in scenarios 2 and 3. Furthermore, utilizing the SON model to solve the optimization issue for scenarios 1, 2, 3 and 4, the optimal surface roughness was found to be 0.301 μm .

For the fourth output of the study (R_{tCC650} , Aouici et al. [44]), the initial assumption would be that models 1 and 10 are suitable if the selection had just been based on R^2_{training} and R^2_{testing} . Based on this argument, utilizing a method that considers the simplicity of the models and the desired models' capacity to provide realistic values, it is determined that only model 1 (L) is suitable. As a result, misleading findings are unavoidable if the model building-optimum result finding analyses are not addressed as outlined in this article. Thus, the obtained model 1 (CS1-O4-L) was chosen as the objective function required in analyses to get optimum results of R_{tCC650} . Outcomes of the selected model can be spotted in Table 7.7.

Table 7.12 shows the outcomes of three specific optimization scenarios for the chosen model. In scenario 1, all of the variables were utilized with their upper and lower limits in a continuous interval. The minimum surface roughness outcomes, depending on all of the optimization techniques, were $2.764 \mu\text{m}$, which correspond to L. The suggested (optimum) designs are; the cutting speed: 180 (m/min), the feed rate: 0.08 (mm/rev) and depth of cut: 0.15 (mm). $2.764 \mu\text{m}$ is a realistic result by compared with the results of experiment [2.67, 4.16]. We could say that the minimum experimental results and the optimization results are really close to each other.

In scenario 2, feed rate and depth of cut have been handled as continuous parameters, whereas the cutting speed is discontinuous (integers). In this case, the minimum surface roughness results for the L model were same as the scenario 1.

In the third optimization scenario, the only limitation condition in the optimization process was taken as the total roughness value smaller than 0.41 for CC650, which is the same material. The results are the same with scenario 1 and 2.

For the fourth optimization scenario, all of the input parameters are supposed to be real numbers and the design variables can only take the experimental values. The results are the same with scenario 1 and 2.

From the point of stability, gaining identical outcomes for scenarios 1, 2, 3, and 4, whose phenomenological foundation is addressed using four distinct direct search methods, enhances the chance that acquired results are global optimum. Besides that, utilizing various methods for scenario 2 produces dissimilar outcomes, although they are identical. This situation is critical for optimization issues comprising restriction types that are similar to those in scenarios 2 and 3. Furthermore, utilizing the L model to solve the optimization issue for scenarios 1, 2, 3 and 4, the optimal surface roughness was found to be $2.764 \mu\text{m}$.

For the fifth output of the study (R_{aCBN7020} , Aouici et al. [44]), results show that if the R^2 value was the key element considered in decided the model, we may conclude that all models accurately describe the process. Because R^2_{training} results are nearly all close to 1.

The initial assumption would be that models 1, 2, 3, and 4 are suitable if the selection had just been based on R^2_{training} and R^2_{testing} . Based on this argument, utilizing a method that considers the desired models' capacity to provide realistic values, it is determined that only models 3 and 12 are suitable. As a result, misleading findings are unavoidable if the model building-optimum result finding analyses are not addressed as outlined in this article.

As can be seen in Table 7.8, estimation capacity (R^2_{testing}) of model 2 (L) and model 4 (SONR) are the same while model 2 was achieved lower arithmetic mean roughness than the model 4. With this approach, the obtained second order multiple nonlinear model 2 (CS1-O5-LR) was chosen as the objective function required in analyses to get optimum results of Ra_{CBN7020} .

Table 7.13 shows the outcomes of three specific optimization scenarios for the chosen model. In scenario 1, all of the variables were utilized with their upper and lower limits in a continuous interval. The minimum surface roughness outcomes, depending on all of the optimization techniques, were $0.159 \mu\text{m}$, which correspond to LR. The suggested (optimum) designs are; the cutting speed: 180 (m/min), the feed rate: 0.08 (mm/rev) and depth of cut: 0.45 (mm). $0.159 \mu\text{m}$ is a realistic result by compared with the results of experiment [0.180, 0.565]. We could say that the optimization results have reached smaller values than the minimum experimental results.

In scenario 2, feed rate and depth of cut have been handled as continuous parameters, whereas the cutting speed is discontinuous (integers). In this case, the minimum surface roughness results for the LR model were same as the scenario 1.

In the third optimization scenario, the only limitation condition in the optimization process was taken as the total roughness value smaller than 1 for CBN7020, which is the same material. The minimum surface roughness found as $0.159 \mu\text{m}$. The suggested (optimum) designs are; cutting speed: 179.974 (m/min), feed rate: 0.08 (mm/rev) and depth of cut: 0.45 (mm). $0.159 \mu\text{m}$ is a realistic result by compared with the results of experiment [0.180, 0.565]. We could say that the optimization results have reached smaller values than the minimum experimental results.

For the fourth optimization scenario, all of the input parameters are supposed to be real numbers and the design variables can only take the experimental values. The results are the same with scenario 1 and 2.

From the point of stability, gaining identical outcomes for scenarios 1, 2, 3, and 4, whose phenomenological foundation is addressed using four distinct direct search methods, enhances the chance that acquired results are global optimum. Besides that, utilizing various methods for scenario 2 produces dissimilar outcomes, although they are identical. This situation is critical for optimization issues comprising restriction types that are similar to those in scenarios 2 and 3. Furthermore, utilizing the LR model to solve the optimization issue for scenarios 1, 2, 3 and 4, the optimal surface roughness was found to be 0.15887 μm .

For the sixth output of the study ($R_{t_{\text{CBN7020}}}$, Aouici et al. [44]), the initial assumption would be that lots of models are suitable if the selection had just been based on R^2_{training} and R^2_{testing} . Based on this argument, utilizing a method that considers the simplicity of the models and the desired models' capacity to provide realistic values, it is determined that only model 8 (SOTN) is suitable. As a result, misleading findings are unavoidable if the model building-optimum result finding analyses are not addressed as outlined in this article. Thus, the obtained model 8 (CS1-O6-SOTN) was chosen as the objective function required in analyses to get optimum results of $R_{t_{\text{CBN7020}}}$. Outcomes of the selected model can be spotted in Table 7.9.

Table 7.14 shows the outcomes of three specific optimization scenarios for the chosen model. In scenario 1, all of the variables were utilized with their upper and lower limits in a continuous interval. There are four different results for four different optimization algorithms. The minimum surface roughness results were approximate values to zero. Thus, for the optimization scenario 1, minimum surface roughness can be taken as zero. But it is not a realistic solution.

In scenario 2, feed rate and depth of cut have been handled as continuous parameters, whereas the cutting speed is discontinuous (integers). While zero values can not be taken as realistic solution, there are two different realistic result.

In this case, the minimum surface values for the SOTN model were 0.372 μm and 0.819 μm . The suggested (optimum) designs for 0.372 μm ; cutting speed: 145 (m/min), feed rate: 0.0920285 (mm/rev) and depth of cut: 0.395611 (mm), for 0.819 μm ; cutting speed: 136 (m/min), feed rate: 0.08 (mm/rev) and depth of cut: 0.312207 (mm).

In the third optimization scenario, the only limitation condition in the optimization process was taken as the arithmetic mean roughness value smaller than 0.25 for CBN7020, which is the same material. There are four different results for four different optimization algorithms. The minimum surface roughness results were approximate values to zero. Thus, for the optimization scenario 3, minimum surface roughness can be taken as zero. But it is not a realistic solution.

For the fourth optimization scenario, all of the input parameters are supposed to be real numbers and the design variables can only take the experimental values. The minimum surface roughness had found as 1.187 μm . The suggested (optimum) designs are; cutting speed: 180 (m/min), feed rate: 0.08 (mm/rev) and depth of cut: 0.3 (mm). 1.187 μm is a realistic and better result in comparison with the experimental values [1.20, 4.15].

From the point of stability, gaining identical outcomes for only scenario 4, whose phenomenological foundation is addressed using four distinct direct search methods, enhances the chance that acquired results are global optimum. Other scenarios' outcomes are not realistic. Furthermore, utilizing the SOTN model to solve the optimization issue for scenarios 1, 2, 3 and 4, the optimal surface roughness was found to be 1.187 μm .

Table 7.9: Optimization problem results of selected model CS1-O1-SON for arithmetic mean roughness (R_{acc670})

Objective Functions	Scenario No	Constraints	Optimization Algorithm	Arithmetic Mean Roughness (μm)	Suggested Design
CS1-O1-SON	1	$120 < x_1 < 180$, $0.08 < x_2 < 0.16$, $0.15 < x_3 < 0.45$	MDE	0.406	$x_1 = 180, x_2 = 0.08, x_3 = 0.45$
			MSA	0.406	$x_1 = 180, x_2 = 0.08, x_3 = 0.45$
			MRS	0.406	$x_1 = 180, x_2 = 0.08, x_3 = 0.45$
			MNM	0.406	$x_1 = 180, x_2 = 0.08, x_3 = 0.45$
	2	$120 < x_1 < 180$, $0.08 < x_2 < 0.16$, $0.15 < x_3 < 0.45$, $\{x_1\} \in \text{Integers}$	MDE	0.406	$x_1 = 180, x_2 = 0.08, x_3 = 0.45$
			MSA	0.413	$x_1 = 132, x_2 = 0.080007, x_3 = 0.444227$
			MRS	0.406	$x_1 = 180, x_2 = 0.08, x_3 = 0.45$
			MNM	0.406	$x_1 = 2600, x_2 = 0.0800002, x_3 = 0.45$
	3	$120 < x_1 < 180$, $0.08 < x_2 < 0.16$, $0.15 < x_3 < 0.45$, Total Roughness $R_{acc670} < 2.8$	MDE	0.443	$x_1 = 180, x_2 = 0.08, x_3 = 0.167533$
			MSA	0.443	$x_1 = 180, x_2 = 0.08, x_3 = 0.167533$
			MRS	0.443	$x_1 = 180, x_2 = 0.08, x_3 = 0.167533$
			MNM	0.443	$x_1 = 180, x_2 = 0.08, x_3 = 0.167533$
4	$x_1 = \{120, 180\}$, $x_2 = \{0.08, 0.12, 0.16\}$, $x_3 = \{0.15, 0.30, 0.45\}$	MDE	0.406	$x_1 = 180, x_2 = 0.08, x_3 = 0.45$	
		MSA	0.406	$x_1 = 180, x_2 = 0.08, x_3 = 0.45$	
		MRS	0.406	$x_1 = 180, x_2 = 0.08, x_3 = 0.45$	
		MNM	0.406	$x_1 = 180, x_2 = 0.08, x_3 = 0.45$	

Table 7.10: Optimization problem results of selected model CS1-O2-LR for total roughness (R_{tcc670})

Objective Functions	Scenario No	Constraints	Optimization Algorithm	Arithmetic Mean Roughness (μm)	Suggested Design
CS1-O2-LR	1	$120 < x_1 < 180$, $0.08 < x_2 < 0.16$, $0.15 < x_3 < 0.45$	MDE	2.693	$x_1 = 180, x_2 = 0.08, x_3 = 0.15$
			MSA	2.693	$x_1 = 180, x_2 = 0.08, x_3 = 0.15$
			MRS	2.693	$x_1 = 180, x_2 = 0.08, x_3 = 0.15$
			MNM	2.693	$x_1 = 180, x_2 = 0.08, x_3 = 0.15$
	2	$120 < x_1 < 180$, $0.08 < x_2 < 0.16$, $0.15 < x_3 < 0.45$, $\{x_1\} \in \text{Integers}$	MDE	2.693	$x_1 = 180, x_2 = 0.08, x_3 = 0.15$
			MSA	2.694	$x_1 = 173, x_2 = 0.0800005, x_3 = 0.1500001$
			MRS	2.693	$x_1 = 180, x_2 = 0.08, x_3 = 0.15$
			MNM	2.693	$x_1 = 180, x_2 = 0.08, x_3 = 0.45$
	3	$120 < x_1 < 180$, $0.08 < x_2 < 0.16$, $0.15 < x_3 < 0.45$, Arithmetic Mean Roughness $R_{tcc670} < 0.41$	MDE	2.783	$x_1 = 180, x_2 = 0.08, x_3 = 0.367581$
			MSA	2.783	$x_1 = 180, x_2 = 0.08, x_3 = 0.367581$
			MRS	2.783	$x_1 = 180, x_2 = 0.08, x_3 = 0.367581$
			MNM	2.783	$x_1 = 180, x_2 = 0.08, x_3 = 0.367581$
4	$x_1 = \{120, 180\}$, $x_2 = \{0.08, 0.12, 0.16\}$, $x_3 = \{0.15, 0.30, 0.45\}$	MDE	2.693	$x_1 = 180, x_2 = 0.08, x_3 = 0.15$	
		MSA	2.693	$x_1 = 180, x_2 = 0.08, x_3 = 0.15$	
		MRS	2.693	$x_1 = 180, x_2 = 0.08, x_3 = 0.15$	
		MNM	2.693	$x_1 = 180, x_2 = 0.08, x_3 = 0.15$	

Table 7.11: Optimization problem results of selected model CS1-O3-SON for arithmetic mean roughness (Ra_{CC650})

Objective Functions	Scenario No	Constraints	Optimization Algorithm	Arithmetic Mean Roughness (µm)	Suggested Design
CS1-O3-SON	1	$120 < x_1 < 180,$ $0.08 < x_2 < 0.16,$ $0.15 < x_3 < 0.45$	MDE	0.301	$x_1 = 180, x_2 = 0.08, x_3 = 0.15$
			MSA	0.301	$x_1 = 180, x_2 = 0.08, x_3 = 0.15$
			MRS	0.301	$x_1 = 180, x_2 = 0.08, x_3 = 0.15$
			MNM	0.301	$x_1 = 180, x_2 = 0.08, x_3 = 0.15$
	2	$120 < x_1 < 180,$ $0.08 < x_2 < 0.16,$ $0.15 < x_3 < 0.45,$ $\{x_1\} \in \text{Integers}$	MDE	0.301	$x_1 = 180, x_2 = 0.08, x_3 = 0.15$
			MSA	0.330	$x_1 = 157, x_2 = 0.0800003, x_3 = 0.1500003$
			MRS	0.301	$x_1 = 180, x_2 = 0.08, x_3 = 0.15$
			MNM	0.301	$x_1 = 180, x_2 = 0.08, x_3 = 0.15$
	3	$120 < x_1 < 180,$ $0.08 < x_2 < 0.16,$ $0.15 < x_3 < 0.45,$ Total Roughness $R_{tcc650} < 2.8$	MDE	0.301	$x_1 = 180, x_2 = 0.08, x_3 = 0.15$
			MSA	0.301	$x_1 = 180, x_2 = 0.08, x_3 = 0.15$
			MRS	0.301	$x_1 = 180, x_2 = 0.08, x_3 = 0.15$
			MNM	0.301	$x_1 = 180, x_2 = 0.08, x_3 = 0.15$
4	$x_1 = \{120, 180\},$ $x_2 = \{0.08, 0.12, 0.16\},$ $x_3 = \{0.15, 0.30, 0.45\}$	MDE	0.301	$x_1 = 180, x_2 = 0.08, x_3 = 0.15$	
		MSA	0.301	$x_1 = 180, x_2 = 0.08, x_3 = 0.15$	
		MRS	0.301	$x_1 = 180, x_2 = 0.08, x_3 = 0.15$	
		MNM	0.301	$x_1 = 180, x_2 = 0.08, x_3 = 0.15$	

Table 7.12: Optimization problem results of selected model CS1-O4-L for total roughness (R_{tCC650})

Objective Functions	Scenario No	Constraints	Optimization Algorithm	Arithmetic Mean Roughness (μm)	Suggested Design
CS1-O4-L	1	$120 < x_1 < 180$, $0.08 < x_2 < 0.16$, $0.15 < x_3 < 0.45$	MDE	2.764	$x_1 = 180, x_2 = 0.08, x_3 = 0.15$
			MSA	2.764	$x_1 = 180, x_2 = 0.08, x_3 = 0.15$
			MRS	2.764	$x_1 = 180, x_2 = 0.08, x_3 = 0.15$
			MNM	2.764	$x_1 = 180, x_2 = 0.08, x_3 = 0.15$
	2	$120 < x_1 < 180$, $0.08 < x_2 < 0.16$, $0.15 < x_3 < 0.45$, $\{x_1\} \in \text{Integers}$	MDE	2.764	$x_1 = 180, x_2 = 0.08, x_3 = 0.15$
			MSA	2.801	$x_1 = 171, x_2 = 0.08, x_3 = 0.190462$
			MRS	2.764	$x_1 = 180, x_2 = 0.08, x_3 = 0.15$
			MNM	2.764	$x_1 = 180, x_2 = 0.08, x_3 = 0.45$
	3	$120 < x_1 < 180$, $0.08 < x_2 < 0.16$, $0.15 < x_3 < 0.45$, Arithmetic Mean Roughness $R_{tCC670} < 0.41$	MDE	2.764	$x_1 = 180, x_2 = 0.08, x_3 = 0.15$
			MSA	2.764	$x_1 = 180, x_2 = 0.08, x_3 = 0.15$
			MRS	2.764	$x_1 = 180, x_2 = 0.08, x_3 = 0.15$
			MNM	2.764	$x_1 = 180, x_2 = 0.08, x_3 = 0.15$
4	$x_1 = \{120, 180\}$, $x_2 = \{0.08, 0.12, 0.16\}$, $x_3 = \{0.15, 0.30, 0.45\}$	MDE	2.764	$x_1 = 180, x_2 = 0.08, x_3 = 0.15$	
		MSA	2.764	$x_1 = 180, x_2 = 0.08, x_3 = 0.15$	
		MRS	2.764	$x_1 = 180, x_2 = 0.08, x_3 = 0.15$	
		MNM	2.764	$x_1 = 180, x_2 = 0.08, x_3 = 0.15$	

Table 7.13: Optimization problem results of selected model CS1-O5-LR for arithmetic mean roughness (Ra_{CBN7020})

Objective Functions	Scenario No	Constraints	Optimization Algorithm	Arithmetic Mean Roughness (μm)	Suggested Design
CS1-O5-LR	1	$120 < x_1 < 180$, $0.08 < x_2 < 0.16$, $0.15 < x_3 < 0.45$	MDE	0.159	$x_1 = 180, x_2 = 0.08, x_3 = 0.45$
			MSA	0.159	$x_1 = 180, x_2 = 0.08, x_3 = 0.45$
			MRS	0.159	$x_1 = 180, x_2 = 0.08, x_3 = 0.45$
			MNMM	0.159	$x_1 = 180, x_2 = 0.08, x_3 = 0.45$
	2	$120 < x_1 < 180$, $0.08 < x_2 < 0.16$, $0.15 < x_3 < 0.45$, $\{x_1\} \in \text{Integers}$	MDE	0.159	$x_1 = 180, x_2 = 0.08, x_3 = 0.45$
			MSA	0.188	$x_1 = 180, x_2 = 0.08, x_3 = 0.384379$
			MRS	0.159	$x_1 = 180, x_2 = 0.08, x_3 = 0.45$
			MNMM	0.159	$x_1 = 180, x_2 = 0.08, x_3 = 0.45$
	3	$120 < x_1 < 180$, $0.08 < x_2 < 0.16$, $0.15 < x_3 < 0.45$, Total Roughness $R_{\text{tCBN7020}} < 1$	MDE	0.159	$x_1 = 179.974, x_2 = 0.08, x_3 = 0.45$
			MSA	0.159	$x_1 = 179.974, x_2 = 0.08, x_3 = 0.45$
			MRS	0.159	$x_1 = 179.974, x_2 = 0.08, x_3 = 0.45$
			MNMM	0.159	$x_1 = 179.974, x_2 = 0.08, x_3 = 0.45$
4	$x_1 = \{120, 180\}$, $x_2 = \{0.08, 0.12, 0.16\}$, $x_3 = \{0.15, 0.30, 0.45\}$	MDE	0.159	$x_1 = 180, x_2 = 0.08, x_3 = 0.45$	
		MSA	0.159	$x_1 = 180, x_2 = 0.08, x_3 = 0.45$	
		MRS	0.159	$x_1 = 180, x_2 = 0.08, x_3 = 0.45$	
		MNMM	0.159	$x_1 = 180, x_2 = 0.08, x_3 = 0.45$	

Table 7.14: Optimization problem results of selected model CS1-O6-SOTN for total roughness (Rt_{CEN7020})

Objective Functions	Scenario No	Constraints	Optimization Algorithm	Total Roughness (µm)	Suggested Design
CS1-O6-SOTN	1	$120 < x_1 < 180$, $0.08 < x_2 < 0.16$, $0.15 < x_3 < 0.45$	MDE	9.976×10^{-8}	$x_1 = 167.319, x_2 = 0.128785, x_3 = 0.15$
			MSA	7.466×10^{-8}	$x_1 = 179.904, x_2 = 0.125843, x_3 = 0.220831$
			MRS	1.013×10^{-6}	$x_1 = 138.048, x_2 = 0.0815888, x_3 = 0.150704$
			MNM	4.038×10^{-8}	$x_1 = 169.957, x_2 = 0.147278, x_3 = 0.302972$
	2	$120 < x_1 < 180$, $0.08 < x_2 < 0.16$, $0.15 < x_3 < 0.45$, $\{x_1\} \in \text{Integers}$	MDE	4.030×10^{-8}	$x_1 = 141, x_2 = 0.0843388, x_3 = 0.419426$
			MSA	0.372	$x_1 = 145, x_2 = 0.0920285, x_3 = 0.395611$
			MRS	0.819	$x_1 = 136, x_2 = 0.08, x_3 = 0.312207$
			MNM	9.702×10^{-8}	$x_1 = 141, x_2 = 0.129507, x_3 = 0.338041$
	3	$120 < x_1 < 180$, $0.08 < x_2 < 0.16$, $0.15 < x_3 < 0.45$, Arithmetic Mean Roughness $R_{\text{ACENT7020}} < 0.25$	MDE	7.360×10^{-8}	$x_1 = 179.929, x_2 = 0.0883825, x_3 = 0.404029$
			MSA	9.994×10^{-8}	$x_1 = 179.931, x_2 = 0.0816388, x_3 = 0.191194$
			MRS	9.995×10^{-8}	$x_1 = 179.933, x_2 = 0.0829057, x_3 = 0.211605$
			MNM	3.252×10^{-8}	$x_1 = 179.941, x_2 = 0.0816429, x_3 = 0.323025$
4	$x_1 = \{120, 180\}$, $x_2 = \{0.08, 0.12, 0.16\}$, $x_3 = \{0.15, 0.30, 0.45\}$	MDE	1.187	$x_1 = 180, x_2 = 0.08, x_3 = 0.3$	
		MSA	1.187	$x_1 = 180, x_2 = 0.08, x_3 = 0.3$	
		MRS	1.187	$x_1 = 180, x_2 = 0.08, x_3 = 0.3$	
		MNM	1.187	$x_1 = 180, x_2 = 0.08, x_3 = 0.3$	

Consequently, i) The regression models used for modeling have to be tested through both R^2_{training} and R^2_{testing} values. The model's operational restriction (boundedness) has also to be checked by calculating the maximum and minimum values generated by the respective model is realistic or not. ii) In our approach, the data generated by the model stay within the realistic boundaries different from the interval produced by the model given in the reference study. iii) This reveals that the prediction capability of the process was better and more accurate than the classical approach.

7.3 Case Study #2

The second literature study which optimization process was studied taken from Bouacha et al. [45]. The present work concerns an experimental study of hard turning of AISI 52100 bearing steel, with CBN tool. The combined effects of process parameters (cutting speed, feed rate, depth of cut and cutting time) on response parameters (tool wear, surface roughness, cutting forces and metal volume removed) are investigated using ANOVA analysis. The relationship between process parameters and performance characteristics through the response surface methodology (RSM) are modeled. Also, Grey-Taguchi technique, composite desirability function, and genetic algorithm are also utilized as multi-objective optimization methodologies to discover the response parameters that optimize both performance and efficiency. Tool wear is most influenced by cutting speed, according to the outcomes of the study. The cutting forces are substantially influenced by the depth of cut, while the surface roughness is only minimally influenced. On all performance metrics, the cutting time has a significant influence. GA appears to be the most beneficial option, despite the fact that the outcomes anticipated by the other optimization methods were very comparable. Eventually, the suggested experimental and embedded techniques provide valid methodology for building model, finding optimum results, and developing the process of hard turning.

Researchers report an operational investigation of hard turning of AISI 52100 using a CBN tool. Through the use of ANOVA analysis, the cumulative impacts of

design variables (cutting speed, feed rate, depth of cut, and cutting duration) are studied. Response surface methodology (RSM) is used to model the connection between design variables and system outcomes.

As depicted in Table 7.15, the changes in values of these input parameters provided the obtaining of different results for tool wear, surface roughness and cutting forces (F_a , F_c , F_p).

Therefore, these obtaining results depending on the change in these design variables are sufficient to develop an optimization strategy. Moreover, it is impossible to determine a proportional connection between measured roughness values and four input parameters (cutting speed, feed rate, depth of cut and cutting time), as understood from Table 7.15. Therefore, it is necessary to optimize these parameters to minimize both tool wear, surface roughness and cutting forces.

Table 7.15: Experimental results of tool wear, surface roughness and cutting force components with different experimental conditions [45]

Exp No	Cutting speed (V_c , m/min)	Feed rate (f , mm/rev)	Depth of cut (a_p , mm)	Cutting time (t , min)	Tool Wear (VB, mm)	Roughness (R_a , μm)	F_a (N)	F_c (N)	F_R (N)
1	130	0.08	0.2	2	0.084	0.44	82.744	123.002	176.593
2	130	0.08	0.4	8	0.117	0.49	152.597	239.540	324.300
3	130	0.08	0.6	16	0.167	0.60	276.241	384.466	489.182
4	130	0.12	0.2	8	0.135	0.57	115.106	176.829	256.964
5	130	0.12	0.4	16	0.189	0.64	221.779	343.770	422.870
6	130	0.12	0.6	2	0.145	0.52	192.287	293.685	383.130
7	130	0.16	0.2	16	0.204	0.72	207.259	289.045	376.932
8	130	0.16	0.4	2	0.159	0.60	159.270	267.728	329.497
9	130	0.16	0.6	8	0.198	0.66	234.182	370.295	442.989
10	185	0.08	0.2	8	0.143	0.40	80.191	135.725	192.594
11	185	0.08	0.4	16	0.229	0.51	196.834	289.232	390.096
12	185	0.08	0.6	2	0.125	0.37	188.788	305.305	364.599
13	185	0.12	0.2	16	0.238	0.58	152.343	252.941	322.213
14	185	0.12	0.4	2	0.137	0.43	144.326	224.610	276.195
15	185	0.12	0.6	8	0.215	0.49	215.682	354.162	423.569
16	185	0.16	0.2	2	0.165	0.48	109.806	189.885	229.928
17	185	0.16	0.4	8	0.220	0.55	169.717	302.452	365.498
18	185	0.16	0.6	16	0.311	0.72	263.419	367.407	472.337
19	260	0.08	0.2	16	0.335	0.50	123.456	169.460	250.099
20	260	0.08	0.4	2	0.157	0.24	85.409	156.239	224.892
21	260	0.08	0.6	8	0.264	0.37	187.376	294.777	392.673
22	260	0.12	0.2	2	0.168	0.32	70.918	108.529	161.465
23	260	0.12	0.4	8	0.277	0.44	140.801	224.081	304.269
24	260	0.12	0.6	16	0.395	0.58	235.473	356.022	464.571
25	260	0.16	0.2	8	0.299	0.48	136.281	209.356	264.654
26	260	0.16	0.4	16	0.415	0.69	209.982	298.312	412.839
27	260	0.16	0.6	2	0.252	0.43	171.994	256.994	335.734

The behavior of the system was explained by the multiple linear regression models given below [45];

$$VB = -0.06932 + 0.000382 \times Vc + 0.83611 \times f + 0.083611 \times ap - 0.005104 \times t + 0.000072 \times Vc \times t \quad (7.7)$$

$$Ra = 0.4393 - 0.001610 \times Vc + 1.9583 \times f + 0.06944 \times ap + 0.000146 \times t + 0.00007 \times Vc \times t \quad (7.8)$$

$$Fa = -55.44 - 0.23895 \times Vc + 1024.4 \times f + 433.69 \times ap + 5.4559 \times t - 1560.1 \times f \times ap \quad (7.9)$$

$$Fc = -76.34 - 0.36381 \times Vc + 1671.6 \times f + 681.42 \times ap + 6.5242 \times t - 2603.7 \times f \times ap \quad (7.10)$$

$$Fp = -43.15 - 0.33442 \times Vc + 1622.6 \times f + 736.57 \times ap + 8.8774 \times t - 2579.4 \times f \times ap \quad (7.11)$$

The experimental data was represented by these regression models with determination coefficients (R^2) of 0.992, 0.978, 0.980, 0.973 and 0.992, respectively.

Bouacha et al. [45] figured out this limited optimization issue by defining all the input parameters as discrete and proceeded in the modeling process only according to the standard R^2 results and listed the models. The R^2 values Bouacha et al [45] found vary between 97% and 99%. Bouacha et al [45] does not mention the R^2_{training} and R^2_{testing} distinction in the modeling process and does not mention determining models according to different scenarios. As can be clearly seen, it is seen that smaller response parameters may be calculated with the variables as a consequence of optimization.

7.3.1 Optimization Scenarios

For all scenarios, the limitations for the system inputs (design parameters) are as in the following form;

$$\begin{aligned} 130 \leq \text{Cutting speed} \leq 260 & , \quad (m/min) \\ 0.08 \leq \text{Feed rate} \leq 0.16 & , \quad (mm/rev) \\ 0.02 \leq \text{Depth of cut} \leq 0.06 & , \quad (mm) \\ 2 \leq \text{Cutting Time} \leq 16 & , \quad (min) \end{aligned}$$

7.3.1.1 Scenario 1

Tool wear, surface roughness and cutting forces are explained by the objective functions in this optimal solution problem. There are no constraints about the input parameters so they can be real numbers, and the computation area is continuous. The primary goal is to minimize the tool wear, surface roughness and cutting forces. It is also technically possible to see these theory-based boundaries of the objective function this way.

7.3.1.2 Scenario 2

Scenario 1 should include additional realistic situations in addition to knowledge-based ones. A novel optimal solution is provided that implies the reduction of the responses for this application. Input parameters are also restricted with integers.

7.3.1.3 Scenario 3

As different from scenario 1, non-linear constraints are added for the optimization problem. Surface roughness must be smaller than $0.25\ \mu\text{m}$ for tool wear. Tool wear must be smaller than $0.1\ \text{mm}$ for surface roughness. F_c and F_p must be smaller than $100\ \text{N}$ and $150\ \text{N}$ for F_a , respectively. F_a and F_p must be smaller than $50\ \text{N}$ and $150\ \text{N}$ for F_c , respectively. F_a and F_c must be smaller than $50\ \text{N}$ and $100\ \text{N}$ for F_p , respectively. Problem solving will be more complex and difficult in this instance than in scenarios 1 and 2.

7.3.1.4 Scenario 4

In the constructed of scenario 4, more viable and more limited issue situations should be included to scenario 2. For that reason, there is a new optimum solution problem created to the minimization of the response values. Unlike Scenario 2, in scenario 4 parameters can only take the values in the data table.

7.3.2 Results and Discussion

In our approach, different from the classical ones, various regression models are first tested utilizing both R^2_{training} and R^2_{testing} values (not only R^2 as in the classical

approach) to reveal what is the degree of performance of the model can explain the method. Besides, the model's operational restriction (boundedness) is also checked by calculating the highest and lowest values that the related model creates. Therefore, our proposed design strategy provides producing realistic values. Also, it is necessary to check the limitedness of decided models, whether producing realistic results. Regarding of these facts, by using our proposed approach, the experimental data tables of tool wear, surface roughness and cutting forces (F_a , F_c , F_p) listed as Table 7.16, 7.17, 7.18, 7.19 and 7.20 can be seen below. Therefore, it is necessary to optimize these parameters to minimize of all the response values.

Table 7.16: Results of the Neuro-regression models for the tool wear (VB)

Models	R^2_{training}	R^2_{testing}	Max (mm)	Min (mm)
CS2-O1-L	0.94	0.76	0.396	0.046
CS2-O1-LR	0.99	0.93	0.420	0.075
CS2-O1-SON	0.99	0.98	0.433	0.081
CS2-O1-SONR	0.15	0.10	0.270	0.180
CS2-O1-TON	1.00	0.90	0.428	0.080
CS2-O1-FOTN	0.95	0.64	1.248	-0.034
CS2-O1-FOTNR	0.99	0.92	5.466×10^{11}	-4.704×10^8
CS2-O1-SOTN	1.00	0.87	1.191	-0.590
CS2-O1-SOTNR	0.99	0.95	1.676	0.027
CS2-O1-FOLN	0.90	0.64	0.371	0.039
CS2-O1-FOLNR	0.99	0.97	0.414	0.077
CS2-O1-SOLN	0.99	0.99	0.431	0.082
CS2-O1-SOLNR	0.94	0.55	0.442	0.076

Table 7.17: Results of the Neuro-regression models for the surface roughness (Ra)

Models	R^2_{training}	R^2_{testing}	Max (μm)	Min (μm)
CS2-O2-L	0.94	0.96	0.759	0.269
CS2-O2-LR	0.96	0.96	0.749	0.256
CS2-O2-SON	0.99	0.99	0.735	0.231
CS2-O2-SONR	0.91	0.96	0.702	0.253
CS2-O2-TON	1.00	0.95	0.869	0.214
CS2-O2-FOTN	0.96	0.94	1.462	0.159
CS2-O2-FOTNR	0.99	0.78	5.756×10^7	-3.526×10^{10}
CS2-O2-SOTN	1.00	0.64	3.811	-0.783
CS2-O2-SOTNR	0.99	0.98	1.627	0.170
CS2-O2-FOLN	0.88	0.90	0.722	0.273
CS2-O2-FOLNR	0.92	0.87	0.760	0.284
CS2-O2-SOLN	0.98	0.99	0.752	0.233
CS2-O2-SOLNR	0.97	0.98	0.788	0.243

Table 7.18: Results of the Neuro-regression models for the cutting force (Fa)

Models	R^2_{training}	R^2_{testing}	Max (N)	Min (N)
CS2-O3-L	0.95	0.98	290.413	49.476
CS2-O3-LR	0.96	0.99	280.451	46.899
CS2-O3-SON	0.98	0.99	284.13	47.433
CS2-O3-SONR	0.99	0.53	1.995×10^{12}	-11901.
CS2-O3-TON	1.00	0.94	338.949	32.708
CS2-O3-FOTN	0.96	0.95	613.636	-57.965
CS2-O3-FOTNR	0.98	0.48	9.497×10^{11}	-3.790×10^8
CS2-O3-SOTN	1.00	0.54	454.233	-1806.61
CS2-O3-SOTNR	1.00	-1.19	8.338×10^9	-5.650×10^{15}
CS2-O3-FOLN	0.85	0.96	271.593	48.450
CS2-O3-FOLNR	0.88	0.96	271.04	56.222
CS2-O3-SOLN	0.98	0.99	282.323	38.127
CS2-O3-SOLNR	-3.91	-44.21	2.479×10^{12}	-1.050×10^{10}

Table 7.19: Results of the Neuro-regression models for the cutting force (Fc)

Models	R^2_{training}	R^2_{testing}	Max (N)	Min (N)
CS2-O4-L	0.93	0.95	433.037	91.025
CS2-O4-LR	0.95	0.99	404.862	67.539
CS2-O4-SON	0.99	0.81	444.091	100.076
CS2-O4-SONR	0.99	0.89	428.228	89.300
CS2-O4-TON	1.00	0.86	446.199	81.372
CS2-O4-FOTN	0.97	0.80	987.856	-197.359
CS2-O4-FOTNR	0.99	0.82	5.239×10^{13}	-8.396×10^{12}
CS2-O4-SOTN	1.00	0.60	620.481	-761.287
CS2-O4-SOTNR	0.91	-18.06	1.478×10^9	-7.947×10^{13}
CS2-O4-FOLN	0.88	0.97	410.467	85.999
CS2-O4-FOLNR	0.90	0.97	392.783	87.970
CS2-O4-SOLN	0.99	0.85	439.141	91.759
CS2-O4-SOLNR	0.93	0.55	1.029×10^8	-2.286×10^9

Table 7.20: Results of the Neuro-regression models for the cutting force (Fp)

Models	R^2_{training}	R^2_{testing}	Max (N)	Min (N)
CS2-O5-L	0.97	0.96	536.395	143.841
CS2-O5-LR	0.98	0.99	506.387	107.657
CS2-O5-SON	0.99	0.96	522.032	119.698
CS2-O5-SONR	1.00	0.94	574.984	150.046
CS2-O5-TON	1.00	0.97	500.764	133.973
CS2-O5-FOTN	0.98	0.92	1167.33	-50.001
CS2-O5-FOTNR	0.99	-17.80	9.871×10^9	-5.742×10^{10}
CS2-O5-SOTN	1.00	0.90	548.906	-354.309
CS2-O5-SOTNR	-12.89	-6.13	3.144×10^8	0.441
CS2-O5-FOLN	0.93	0.97	508.646	136.646
CS2-O5-FOLNR	0.94	0.98	491.851	126.219
CS2-O5-SOLN	0.99	0.97	515.215	108.11
CS2-O5-SOLNR	1.00	0.93	522.290	151.331

For the first output of the study (VB, Bouacha et al. [45]), the initial assumption would be that models 2, 3, 9, 11 and 12 are suitable if the selection had just been based on R^2_{training} and R^2_{testing} . Based on this argument, utilizing a method that considers the simplicity of the models and the desired models' capacity to provide

realistic values, it is determined that only model 2 (LR) is suitable. As a result, misleading findings are unavoidable if the model building-optimum result finding analyses are not addressed as outlined in this article. Thus, the obtained model 2 (CS2-O1-LR) was chosen as the objective function required in analyses to get optimum results of tool wear. Outcomes of the selected model can be spotted in Table 7.16.

Table 7.21 shows the outcomes of three specific optimization scenarios for the chosen model. In scenario 1, all of the variables were utilized with their upper and lower limits in a continuous interval. The minimum tool wear outcomes, depending on all of the optimization techniques, were 0.075 mm, which correspond to LR. The suggested (optimum) designs are; cutting speed: 130 (m/min), feed rate: 0.08 (mm/rev), depth of cut: 0.08 (mm) and cutting time: 2 (min). 0.075 mm is a realistic result by compared with the results of experiment [0.084, 0.415]. We could say that the optimization results have reached smaller values than the minimum experimental results.

In scenario 2, feed rate and depth of cut have been handled as continuous parameters, whereas the cutting speed and cutting time are discontinuous (integers). Although there are three different results, the minimum tool wear values for the LR model were same as the scenario 1.

In the third optimization scenario, the only limitation condition in the optimization process was taken as the surface roughness value smaller than 0.25 for tool wear. The minimum tool wear found as 0.117 mm. The suggested (optimum) designs are; cutting speed: 238.276 (m/min), feed rate: 0.08 (mm/rev), depth of cut: 0.2 (mm) and cutting time: 2 (min). 0.117 mm is a realistic result by compared with the results of experiment. We could say that the minimum experimental results and the optimization results of the third scenario are quite close to each other.

For the fourth optimization scenario, all of the input parameters are supposed to be real numbers and the design variables can only take the experimental values. The results are the same with scenario 1 and 2.

From the point of stability, gaining identical outcomes for scenarios 1, 2, 3, and 4, whose phenomenological foundation is addressed using four distinct direct search methods, enhances the chance that acquired results are global optimum. Besides that, utilizing various methods for scenario 2 produces dissimilar outcomes, although they are identical. This situation is critical for optimization issues comprising restriction types that are similar to those in scenarios 2 and 3. Furthermore, utilizing the LR model to solve the optimization issue for scenarios 1, 2, 3 and 4, the optimal tool wear was found to be 0.075 mm.

For the second output of the study (Ra, Bouacha et al. [45]), results show that if the R^2 value was the key element considered in decided the model, we may conclude that all models accurately describe the process. Because R^2_{training} results are nearly all close to 1.

The initial assumption would be that lots of models are suitable if the selection had just been based on R^2_{training} and R^2_{testing} . Based on this argument, utilizing a method that considers the simplicity of the models and the desired models' capacity to provide realistic values, it is determined that only model 3 (SON) is suitable. As a result, misleading findings are unavoidable if the model building-optimum result finding analyses are not addressed as outlined in this article. Thus, the obtained model 3 (CS2-O2-SON) was chosen as the objective function required in analyses to get optimum results of surface roughness. Outcomes of the selected model can be spotted in Table 7.17.

Table 7.22 shows the outcomes of three specific optimization scenarios for the chosen model. In scenario 1, all of the variables were utilized with their upper and lower limits in a continuous interval. The minimum surface roughness outcomes, depending on all of the optimization techniques, were 0.230 μm , which correspond to SON. The suggested (optimum) designs are; cutting speed: 260 (m/min), feed rate: 0.08 (mm/rev), depth of cut: 0.2 (mm) and cutting time: 2 (min). 0.230 μm is a realistic result by compared with the results of experiment [0.24, 0.72]. We could say that the optimization results reach lower surface roughness than experimental results.

In scenario 2, feed rate and depth of cut have been treated as continuous variables while the cutting speed and cutting time are discrete (integers). Although there are three different results, the minimum surface roughness results for the SON model were same as the scenario 1.

In the third optimization scenario, the only limitation condition in the optimization process was taken as the tool wear smaller than 0.1 for surface roughness. The minimum surface roughness found as 0.289 μm . The suggested (optimum) designs are; cutting speed: 207.446 (m/min), feed rate: 0.08 (mm/rev), depth of cut: 0.2 (mm) and cutting time: 2 (min). 0.289 μm is a realistic result by compared with the results of experiment. We could say that the minimum experimental results and the optimization results of the third scenario are really close to each other.

For the fourth optimization scenario, all of the input parameters are supposed to be real numbers and the design variables can only take the experimental values. The results are the same with scenario 1 and 2.

From the point of stability, gaining identical outcomes for scenarios 1, 2, 3, and 4, whose phenomenological foundation is addressed using four distinct direct search methods, enhances the chance that acquired results are global optimum. Besides that, utilizing various methods for scenario 2 produces dissimilar outcomes, although they are identical. This situation is critical for optimization issues comprising restriction types that are similar to those in scenarios 2 and 3. Furthermore, utilizing the SON model to solve the optimization issue for scenarios 1, 2, 3 and 4, the optimal surface roughness was found to be 0.230 μm .

For the third output of the study (Fa, Bouacha et al. [45]), results show that if the R^2 value was the key element considered in decided the model, we may conclude that all models accurately describe the process. Because R^2_{training} results are nearly all close to 1.

The initial assumption would be that lots of models are suitable if the selection had just been based on R^2_{training} and R^2_{testing} . Based on this argument, utilizing a method that considers the simplicity of the models and the desired models' capacity to provide realistic values, it is determined that only model 1 (L) is suitable. As a

result, misleading findings are unavoidable if the model building-optimum result finding analyses are not addressed as outlined in this article. Thus, the obtained model 1 (CS2-O3-L) was chosen as the objective function required in analyses to get optimum results of cutting force (F_a). Outcomes of the selected model can be spotted in Table 7.18.

Table 7.23 shows the outcomes of three specific optimization scenarios for the chosen model. In scenario 1, all of the variables were utilized with their upper and lower limits in a continuous interval. The minimum cutting force (F_a) outcomes, depending on all of the optimization techniques, were 49.476 N, which correspond to L. The suggested (optimum) designs are; cutting speed: 260 (m/min), feed rate: 0.08 (mm/rev), depth of cut: 0.2 (mm) and cutting time: 2 (min). 49.476 N is a realistic result by compared with the results of experiment [70.918, 276.241]. We could say that the optimization results reach lower cutting force than experimental results.

In scenario 2, feed rate and depth of cut have been treated as continuous variables while the cutting speed and cutting time are discrete (integers). The minimum cutting force results for the L model were same as the scenario 1.

In the third optimization scenario, the only limitation condition in the optimization process was taken as the tangential cutting force (F_c) smaller than 100 N and thrust force (F_p) smaller than 150 N for feed force (F_a). The results are the same with scenario 1 and 2.

For the fourth optimization scenario, all of the input parameters are supposed to be real numbers and the design variables can only take the experimental values. The results are the same with scenario 1 and 2.

From the point of stability, gaining identical outcomes for scenarios 1, 2, 3, and 4, whose phenomenological foundation is addressed using four distinct direct search methods, enhances the chance that acquired results are global optimum. Besides that, utilizing various methods for scenario 2 produces dissimilar outcomes, although they are identical. This situation is critical for optimization issues comprising restriction types that are similar to those in scenarios 2 and 3.

Furthermore, utilizing the L model to solve the optimization issue for scenarios 1, 2, 3 and 4, the optimal cutting force was found to be 49.4757 N. We could say that the optimization results reach lower cutting force than experimental results.

For the fourth output of the first study (Fc, Bouacha et al. [45]), results show that if the R^2 value was the key element considered in decided the model, we may conclude that all models accurately describe the process. Because R^2_{training} results are nearly all close to 1.

The initial assumption would be that lots of models are suitable if the selection had just been based on R^2_{training} and R^2_{testing} . Based on this argument, utilizing a method that considers the simplicity of the models and the desired models' capacity to provide realistic values, it is determined that only model 4 (SONR) is suitable. As a result, misleading findings are unavoidable if the model building-optimum result finding analyses are not addressed as outlined in this article. Thus, the obtained model 4 (CS2-O4-SONR) was chosen as the objective function required in analyses to get optimum results of tangential cutting force (Fc). Outcomes of the selected model can be spotted in Table 7.19.

Table 7.24 shows the outcomes of three specific optimization scenarios for the chosen model. In scenario 1, all of the variables were utilized with their upper and lower limits in a continuous interval. The minimum tangential cutting force (Fc) outcomes, depending on all of the optimization techniques, were 89.301 N, which correspond to SONR. The suggested (optimum) designs are; cutting speed: 260 (m/min), feed rate: 0.08 (mm/rev), depth of cut: 0.2 (mm) and cutting time: 2 (min). 89.301 N is a realistic result by compared with the results of experiment [108.529, 384.466]. We could say that the scenario 1 results reach lower cutting force than experimental results.

In scenario 2, feed rate and depth of cut have been treated as continuous variables while the cutting speed and cutting time are discrete (integers). Although, there are three different results but the minimum tangential cutting force results for the SONR model were same as the scenario 1.

In the third optimization scenario, the only limitation condition in the optimization process was taken as the feed force (F_a) smaller than 50 N and thrust force (F_p) smaller than 150 N for tangential cutting force (F_c). The results are the same with scenario 1 and 2.

For the fourth optimization scenario, all of the input parameters are supposed to be real numbers and the design variables can only take the experimental values. The results are the same with scenario 1 and 2.

From the point of stability, gaining identical outcomes for scenarios 1, 2, 3, and 4, whose phenomenological foundation is addressed using four distinct direct search methods, enhances the chance that acquired results are global optimum. Besides that, utilizing various methods for scenario 2 produces dissimilar outcomes, although they are identical. This situation is critical for optimization issues comprising restriction types that are similar to those in scenarios 2 and 3. Furthermore, utilizing the SONR model to solve the optimization issue for scenarios 1, 2, 3 and 4, the optimal tangential cutting force was found to be 89.301 N. We could say that the optimization results reach lower cutting force than experimental results.

For the fifth output of the first study (F_p , Bouacha et al. [45]), results show that if the R^2 value was the key element considered in deciding the model, we may conclude that all models accurately describe the process. Because R^2_{training} results are nearly all close to 1.

The initial assumption would be that lots of models are suitable if the selection had just been based on R^2_{training} and R^2_{testing} . Based on this argument, utilizing a method that considers the simplicity of the models and the desired models' capacity to provide realistic values, it is determined that only model 3 (SON) is suitable. As a result, misleading findings are unavoidable if the model building-optimum result finding analyses are not addressed as outlined in this article. Thus, the obtained model 3 (CS2-O5-SON) was chosen as the objective function required in analyses to get optimum results of thrust cutting force (F_p). Outcomes of the selected model can be spotted in Table 7.20.

Table 7.25 shows the outcomes of three specific optimization scenarios for the chosen model. In scenario 1, all of the variables were utilized with their upper and lower limits in a continuous interval. The minimum thrust force (F_p) outcomes, depending on all of the optimization techniques, were 119.698 N, which correspond to SON. The suggested (optimum) designs are; cutting speed: 260 (m/min), feed rate: 0.08 (mm/rev), depth of cut: 0.2 (mm) and cutting time: 2 (min). 119.698 N is a realistic result by compared with the results of experiment [161.465, 189.182].

In scenario 2, feed rate and depth of cut have been treated as continuous variables while the cutting speed and cutting time are discrete (integers). The minimum thrust force values for the SON model were same as the scenario 1.

In the third optimization scenario, the only limitation condition in the optimization process was taken as the feed force (F_a) smaller than 50 N and tangential force (F_c) smaller than 100 N for thrust force (F_p). The results are the same with scenario 1 and 2.

For the fourth optimization scenario, all of the input parameters are supposed to be real numbers and the design variables can only take the experimental values. The results are the same with scenario 1 and 2.

From the point of stability, gaining identical outcomes for scenarios 1, 2, 3, and 4, whose phenomenological foundation is addressed using four distinct direct search methods, enhances the chance that acquired results are global optimum. Besides that, utilizing various methods for scenario 2 produces dissimilar outcomes, although they are identical. This situation is critical for optimization issues comprising restriction types that are similar to those in scenarios 2 and 3. Furthermore, utilizing the SON model to solve the optimization issue for scenarios 1, 2, 3 and 4, the optimal thrust force was found to be 119.698 N. We could say that the optimization results reach lower cutting force than experimental results.

Table 7.21: Optimization problem results of selected model CS2-O1-LR for tool wear (VB)

Objective Functions	Scenario No	Constraints	Optimization Algorithm	Tool Wear (mm)	Suggested Design
CS2-O1-LR	1	130 < x1 < 260,	MDE	0.075	x1 = 130, x2 = 0.08, x3 = 0.2, x4 = 2
		0.08 < x2 < 0.16,	MSA	0.075	x1 = 130, x2 = 0.08, x3 = 0.2, x4 = 2
		0.2 < x3 < 0.6,	MRS	0.075	x1 = 130, x2 = 0.08, x3 = 0.2, x4 = 2
		2 < x4 < 16	MNM	0.075	x1 = 130, x2 = 0.08, x3 = 0.2, x4 = 2
	2	130 < x1 < 260,	MDE	0.075	x1 = 130, x2 = 0.08, x3 = 0.2, x4 = 2
		0.08 < x2 < 0.16,	MSA	0.097	x1 = 172, x2 = 0.0800525, x3 = 0.307319, x4 = 2
		0.2 < x3 < 0.6,	MRS	0.085	x1 = 168, x2 = 0.08, x3 = 0.2, x4 = 2
		2 < x4 < 16 {x1, x4} ∈ Integers	MNM	0.075	x1 = 130, x2 = 0.08, x3 = 0.2, x4 = 2
	3	130 < x1 < 260,	MDE	0.117	x1 = 238.276, x2 = 0.08, x3 = 0.2, x4 = 2
		0.08 < x2 < 0.16,	MSA	0.117	x1 = 238.276, x2 = 0.08, x3 = 0.2, x4 = 2
		0.2 < x3 < 0.6,	MRS	0.117	x1 = 238.276, x2 = 0.08, x3 = 0.2, x4 = 2
		2 < x4 < 16 Surface Roughness < 0.25	MNM	0.117	x1 = 238.276, x2 = 0.08, x3 = 0.2, x4 = 2
4	x1 = {130, 185, 260},	MDE	0.075	x1 = 130, x2 = 0.08, x3 = 0.2, x4 = 2	
	x2 = {0.08, 0.12, 0.16},	MSA	0.075	x1 = 130, x2 = 0.08, x3 = 0.2, x4 = 2	
	x3 = {0.2, 0.4, 0.6},	MRS	0.075	x1 = 130, x2 = 0.08, x3 = 0.2, x4 = 2	
	x4 = {2, 8, 16}	MNM	0.075	x1 = 130, x2 = 0.08, x3 = 0.2, x4 = 2	

Table 7.22: Optimization problem results of selected model CS2-O2-SON for surface roughness (Ra)

Objective Functions	Scenario No	Constraints	Optimization Algorithm	Surface Roughness (μm)	Suggested Design
CS2-O2-SON	1	$130 < x_1 < 260$, $0.08 < x_2 < 0.16$, $0.2 < x_3 < 0.6$, $2 < x_4 < 16$	MDE	0.230	$x_1 = 260, x_2 = 0.08, x_3 = 0.2, x_4 = 2$
			MSA	0.230	$x_1 = 260, x_2 = 0.08, x_3 = 0.2, x_4 = 2$
			MRS	0.230	$x_1 = 260, x_2 = 0.08, x_3 = 0.2, x_4 = 2$
			MINM	0.230	$x_1 = 260, x_2 = 0.08, x_3 = 0.2, x_4 = 2$
	2	$130 < x_1 < 260$, $0.08 < x_2 < 0.16$, $0.2 < x_3 < 0.6$, $2 < x_4 < 16$ $\{x_1, x_4\} \in \text{Integers}$	MDE	0.230	$x_1 = 260, x_2 = 0.08, x_3 = 0.2, x_4 = 2$
			MSA	0.286	$x_1 = 212, x_2 = 0.0800012, x_3 = 0.238621, x_4 = 2$
			MRS	0.264	$x_1 = 257, x_2 = 0.08, x_3 = 0.2, x_4 = 4$
			MINM	0.231	$x_1 = 259, x_2 = 0.08, x_3 = 0.2, x_4 = 2$
	3	$130 < x_1 < 260$, $0.08 < x_2 < 0.16$, $0.2 < x_3 < 0.6$, $2 < x_4 < 16$ Tool wear < 0.1	MDE	0.289	$x_1 = 207.446, x_2 = 0.08, x_3 = 0.2, x_4 = 2$
			MSA	0.289	$x_1 = 207.446, x_2 = 0.08, x_3 = 0.2, x_4 = 2$
			MRS	0.289	$x_1 = 207.446, x_2 = 0.08, x_3 = 0.2, x_4 = 2$
			MINM	0.289	$x_1 = 207.446, x_2 = 0.08, x_3 = 0.2, x_4 = 2$
4	$x_1 = \{130, 185, 260\}$, $x_2 = \{0.08, 0.12, 0.16\}$, $x_3 = \{0.2, 0.4, 0.6\}$, $x_4 = \{2, 8, 16\}$	MDE	0.230	$x_1 = 260, x_2 = 0.08, x_3 = 0.2, x_4 = 2$	
		MSA	0.230	$x_1 = 260, x_2 = 0.08, x_3 = 0.2, x_4 = 2$	
		MRS	0.230	$x_1 = 260, x_2 = 0.08, x_3 = 0.2, x_4 = 2$	
		MINM	0.230	$x_1 = 260, x_2 = 0.08, x_3 = 0.2, x_4 = 2$	

Table 7.23: Optimization problem results of selected model CS2-O3-L for cutting force (Fa)

Objective Functions	Scenario No	Constraints	Optimization Algorithm	Fa (N)	Suggested Design
CS2-O3-L	1	130 < x1 < 260,	MDE	49.476	x1 = 260, x2 = 0.08, x3 = 0.2, x4 = 2
		0.08 < x2 < 0.16,	MSA	49.476	x1 = 260, x2 = 0.08, x3 = 0.2, x4 = 2
		0.2 < x3 < 0.6,	MRS	49.476	x1 = 260, x2 = 0.08, x3 = 0.2, x4 = 2
		2 < x4 < 16	MNM	49.476	x1 = 260, x2 = 0.08, x3 = 0.2, x4 = 2
	2	130 < x1 < 260,	MDE	49.476	x1 = 260, x2 = 0.08, x3 = 0.2, x4 = 2
		0.08 < x2 < 0.16,	MSA	49.476	x1 = 260, x2 = 0.08, x3 = 0.2, x4 = 2
		0.2 < x3 < 0.6,	MRS	61.422	x1 = 257, x2 = 0.08, x3 = 0.2, x4 = 4
		2 < x4 < 16	MNM	82.377	x1 = 130, x2 = 0.08, x3 = 0.2, x4 = 2
	3	{x1, x4} ∈ Integers	MDE	49.476	x1 = 260, x2 = 0.08, x3 = 0.2, x4 = 2
		130 < x1 < 260,	MSA	49.476	x1 = 260, x2 = 0.08, x3 = 0.2, x4 = 2
		0.08 < x2 < 0.16,	MRS	49.476	x1 = 260, x2 = 0.08, x3 = 0.2, x4 = 2
		0.2 < x3 < 0.6,	MNM	49.476	x1 = 260, x2 = 0.08, x3 = 0.2, x4 = 2
4	2 < x4 < 16,	MDE	49.476	x1 = 260, x2 = 0.08, x3 = 0.2, x4 = 2	
	Fc < 100	MSA	49.476	x1 = 260, x2 = 0.08, x3 = 0.2, x4 = 2	
	Fp < 150	MRS	49.476	x1 = 260, x2 = 0.08, x3 = 0.2, x4 = 2	
	x1 = {130, 185, 260},	MNM	49.476	x1 = 260, x2 = 0.08, x3 = 0.2, x4 = 2	
x2 = {0.08, 0.12, 0.16},	MSA	49.476	x1 = 260, x2 = 0.08, x3 = 0.2, x4 = 2		
x3 = {0.2, 0.4, 0.6},	MRS	49.476	x1 = 260, x2 = 0.08, x3 = 0.2, x4 = 2		
x4 = {2, 8, 16}	MNM	49.476	x1 = 260, x2 = 0.08, x3 = 0.2, x4 = 2		

Table 7.24: Optimization problem results of selected model CS2-O4-SONR for cutting force (Fc)

Objective Functions	Scenario No	Constraints	Optimization Algorithm	Fc (N)	Suggested Design
CS2-O4-SONR	1	$130 < x1 < 260,$ $0.08 < x2 < 0.16,$ $0.2 < x3 < 0.6,$ $2 < x4 < 16$	MDE	89.301	$x1 = 260, x2 = 0.08, x3 = 0.2, x4 = 2$
			MSA	89.301	$x1 = 260, x2 = 0.08, x3 = 0.2, x4 = 2$
			MRS	89.301	$x1 = 260, x2 = 0.08, x3 = 0.2, x4 = 2$
			MNM	120.774	$x1 = 130, x2 = 0.08, x3 = 0.2, x4 = 2$
	2	$130 < x1 < 260,$ $0.08 < x2 < 0.16,$ $0.2 < x3 < 0.6,$ $2 < x4 < 16$ $\{x1, x4\} \in \text{Integers}$	MDE	89.301	$x1 = 260, x2 = 0.08, x3 = 0.2, x4 = 2$
			MSA	89.301	$x1 = 260, x2 = 0.08, x3 = 0.2, x4 = 2$
			MRS	97.707	$x1 = 257, x2 = 0.08, x3 = 0.2, x4 = 4$
			MNM	120.774	$x1 = 130, x2 = 0.08, x3 = 0.2, x4 = 2$
	3	$130 < x1 < 260,$ $0.08 < x2 < 0.16,$ $0.2 < x3 < 0.6,$ $2 < x4 < 16$ $Fa < 50$ $Fp < 150$	MDE	89.301	$x1 = 260, x2 = 0.08, x3 = 0.2, x4 = 2$
			MSA	89.301	$x1 = 260, x2 = 0.08, x3 = 0.2, x4 = 2$
			MRS	89.301	$x1 = 260, x2 = 0.08, x3 = 0.2, x4 = 2$
			MNM	89.301	$x1 = 260, x2 = 0.08, x3 = 0.2, x4 = 2$
4	$x1 = \{130, 185, 260\},$ $x2 = \{0.08, 0.12, 0.16\},$ $x3 = \{0.2, 0.4, 0.6\},$ $x4 = \{2, 8, 16\}$	MDE	89.301	$x1 = 260, x2 = 0.08, x3 = 0.2, x4 = 2$	
		MSA	89.301	$x1 = 260, x2 = 0.08, x3 = 0.2, x4 = 2$	
		MRS	89.301	$x1 = 260, x2 = 0.08, x3 = 0.2, x4 = 2$	
		MNM	89.301	$x1 = 260, x2 = 0.08, x3 = 0.2, x4 = 2$	

Table 7.25: Optimization problem results of selected model CS2-O5-SON for cutting force (Fp)

Objective Functions	Scenario No	Constraints	Optimization Algorithm	Fp (N)	Suggested Design
CS2-O5-SON	1	130 < x1 < 260,	MDE	119.698	x1 = 260, x2 = 0.08, x3 = 0.2, x4 = 2
		0.08 < x2 < 0.16,	MSA	119.698	x1 = 260, x2 = 0.08, x3 = 0.2, x4 = 2
		0.2 < x3 < 0.6,	MRS	119.698	x1 = 260, x2 = 0.08, x3 = 0.2, x4 = 2
		2 < x4 < 16	MNM	119.698	x1 = 260, x2 = 0.08, x3 = 0.2, x4 = 2
	2	130 < x1 < 260,	MDE	119.698	x1 = 260, x2 = 0.08, x3 = 0.2, x4 = 2
		0.08 < x2 < 0.16,	MSA	119.698	x1 = 260, x2 = 0.08, x3 = 0.2, x4 = 2
		0.2 < x3 < 0.6,	MRS	142.971	x1 = 257, x2 = 0.08, x3 = 0.2, x4 = 4
		2 < x4 < 16	MNM	173.052	x1 = 131, x2 = 0.08, x3 = 0.2, x4 = 2
	3	130 < x1 < 260,	MDE	119.698	x1 = 260, x2 = 0.08, x3 = 0.2, x4 = 2
		0.08 < x2 < 0.16,	MSA	119.698	x1 = 260, x2 = 0.08, x3 = 0.2, x4 = 2
		0.2 < x3 < 0.6,	MRS	119.698	x1 = 260, x2 = 0.08, x3 = 0.2, x4 = 2
		2 < x4 < 16 Fa < 50 Fc < 100	MNM	119.698	x1 = 260, x2 = 0.08, x3 = 0.2, x4 = 2
4	x1 = {130, 185, 260},	MDE	119.698	x1 = 260, x2 = 0.08, x3 = 0.2, x4 = 2	
	x2 = {0.08, 0.12, 0.16},	MSA	119.698	x1 = 260, x2 = 0.08, x3 = 0.2, x4 = 2	
	x3 = {0.2, 0.4, 0.6},	MRS	119.698	x1 = 260, x2 = 0.08, x3 = 0.2, x4 = 2	
	x4 = {2, 8, 16}	MNM	119.698	x1 = 260, x2 = 0.08, x3 = 0.2, x4 = 2	

Consequently, i) The regression models used for modeling have to be tested through both R^2_{training} and R^2_{testing} values. The model's operational restriction (boundedness) has also to be checked by calculating the maximum and minimum values generated by the respective model is realistic or not. ii) In our approach, the data generated by the model stay within the realistic boundaries different from the interval produced by the model given in the reference study. iii) This reveals that the prediction capability of the process was better and more accurate than the classical approach.

7.4 Case Study #3

The third literature study which optimization process was studied taken from Davoodi et al. [46]. On N-155, an iron-nickel-base superalloy, are examined the influences of cutting settings on tool life for PVD TiAlN-coated carbide tools and on the volume of machining process extracted during machining. Each of the design parameters, cutting speed and feed rate, was set at five levels. In order to simulate the connections between design variables and response parameters, response surface approach was applied (RSM). ANOVA was used to determine the suitability of the mathematical model and its associated variables. Models used to estimate tool life and material removal yielded successful outcomes. Cutting tool inserts were inspected under a scanning electron microscope and wear processes were investigated at different cutting speeds, as well. Desirability function-based optimization was used to evaluate optimal results of tool life and material removal in order to reach the highest possible level of production efficiency.

As depicted in Table 7.26, the changes in values of these input parameters provided the obtaining of different results for the tool life (cutting time) (min) and volume removed (mm^3).

Therefore, these obtaining results depending on the change in these input parameter values are sufficient to develop an optimization strategy. Moreover, it is impossible to establish a proportional connection between measured tool life, volume removed values and two design variables (cutting speed and feed rate) as understood from

Table 7.26. Therefore, it is necessary to optimize these parameters to achieve maximum amount of material volume removed (mm^3) in minimum tool life (cutting time) (min).

Table 7.26: Experimental results of tool life and volume removed with different experimental conditions [46]

Exp No	Cutting speed (V_c , m/min)	Feed rate (f , mm/rev)	Tool life (T , min)	Volume Removed (V , mm^3)
1	70	0.200	5.20	78162.5
2	80	0.175	4.30	80119.4
3	70	0.150	7.60	74003.9
4	70	0.150	7.43	74007.5
5	70	0.150	7.50	74011.6
6	70	0.100	10.50	73537.4
7	80	0.125	7.36	74001.3
8	60	0.125	12.20	77841.6
9	70	0.150	7.52	74015.3
10	70	0.150	7.51	74020.1
11	90	0.150	6.40	81032.3
12	60	0.175	8.40	78953.5
13	50	0.150	13.50	86933.6

The behavior of the system was explained by the multiple linear regression models given below [46];

$$T = 70.172 - 1.153 \times V_c - 149.393 \times f + 0.006 \times V_c^2 + 131.310 \times f^2 + 0.740 \times V_c \times f \quad (7.12)$$

$$V = 266806 - 4379.98 \times V_c - 522422 \times f + 25.06 \times V_c^2 + 756408 \times f^2 + 5006.20 \times V_c \times f \quad (7.13)$$

The experimental data was represented by these regression models with determination coefficients (R^2) of 0.9773 and 0.9772, respectively.

Davoodi et al. [46] figured out this limited optimization issue by defining all the input parameters as discrete and proceeded in the modeling process only according to the standard R^2 results and listed the models. The R^2 values Davoodi et al [46] found as 97.73% and 97.72%. Davoodi et al [46] does not mention the R^2_{training} and R^2_{testing} distinction in the modeling process and does not mention determining

models according to different scenarios. As can be clearly seen, it is seen that smaller tool life (cutting time) may be calculated with the variables as a consequence of optimization. For the volume removed, the given regression model does not work properly and correctly. The results are very different when compared with the experimental results.

7.4.1 Optimization Scenarios

For all scenarios, the limitations for the system inputs (design parameters) as in the following form;

$$\begin{aligned} 50 \leq \text{Cutting speed} \leq 90 & \quad , \quad (m/min) \\ 0.125 \leq \text{Feed rate} \leq 0.2 & \quad , \quad (mm/rev) \end{aligned}$$

7.4.1.1 Scenario 1

Tool life is explained by the objective function in this optimal solution problem. There are no constraints about the input parameters so they can be real numbers, and the computation area is continuous. The primary goal is to minimize the tool life (cutting time). It is also technically possible to see these theory-based boundaries of the objective function this way.

7.4.1.2 Scenario 2

Scenario 2 should include additional realistic situations in addition to knowledge-based ones. A novel optimal solution is provided that implies the reduction of the responses for this application. Input parameters are also restricted with integers.

7.4.1.3 Scenario 3

In the constructed of scenario 3, more viable and more limited issue situations should be included to scenario 2. For that reason, there is a new optimum solution problem created to the minimization of the response values. Unlike Scenario 2, in scenario 3 parameters can only take the values in the data table.

7.4.2 Results and Discussion

In our approach, different from the classical ones, various regression models are first tested utilizing both R^2_{training} and R^2_{testing} values (not only R^2 as in the classical approach) to reveal what is the degree of performance of the model can explain the method. Besides, the model's operational restriction (boundedness) is also checked by calculating the highest and lowest values that the related model creates. Therefore, our proposed design strategy provides producing realistic values. Also, it is necessary to check the limitedness of decided models, whether producing realistic results. Regarding of these facts, by using our proposed approach, the experimental data tables of tool life and volume removed listed as Table 7.27 and 7.28 can be seen below. As can be seen in Table 7.28, there are no realistic and logical results for the volume removed. Also, a realistic connection between design parameters and volume removed could not be established. Thus, optimization process has been studied only for tool life.

Table 7.27: Results of the Neuro-regression models for the tool life (cutting time)

Models	R^2_{training}	R^2_{testing}	Max (min)	Min (min)
CS3-O1-L	0.86	0.80	13.469	1.4379
CS3-O1-LR	0.97	0.45	15.625	2.661
CS3-O1-SON	0.99	0.04	15.528	2.180
CS3-O1-SONR	0.17	-3.00	9.315	8.189
CS3-O1-TON	0.99	0.88	15.675	2.835
CS3-O1-FOTN	0.59	-42.79	14.919	-5.167
CS3-O1-FOTNR	0.99	-22.99	3.681×10^{11}	-2.615×10^{13}
CS3-O1-SOTN	0.99	0.24	14.909	0.422
CS3-O1-SOTNR	0.99	-0.68	19.049	3.989
CS3-O1-FOLN	0.90	0.86	13.967	2.261
CS3-O1-FOLNR	0.97	0.12	14.815	1.986
CS3-O1-SOLN	0.99	-0.06	15.560	1.976
CS3-O1-SOLNR	0.97	0.64	15.211	2.929

Table 7.28: Results of the Neuro-regression models for the volume removed

Models	R^2_{training}	R^2_{testing}	Max (mm ³)	Min (mm ³)
CS3-O2-L	0.19	-0.88	83506.1	73352.3
CS3-O2-LR	0.86	-0.27	∞	$-\infty$
CS3-O2-SON	0.99	-0.76	15.528	2.180
CS3-O2-SONR	-301.17	-1451.2	9.315	8.189
CS3-O2-TON	1.00	0.30	15.675	2.835
CS3-O2-FOTN	0.45	-17.85	14.919	-5.167
CS3-O2-FOTNR	1.00	-3.02	3.681×10^{11}	-2.615×10^{13}
CS3-O2-SOTN	1.00	-1.75	14.909	0.422
CS3-O2-SOTNR	-311.59	-1482.1	19.049	3.989
CS3-O2-FOLN	0.25	-0.43	13.967	2.261
CS3-O2-FOLNR	0.73	-10.02	14.815	1.986
CS3-O2-SOLN	0.99	0.11	15.560	1.976
CS3-O2-SOLNR	-299.10	-1483.67	15.211	2.929

For the output of the study (T, Davoodi et al. [46]), results show that if the R^2 value was the key element considered in deciding the model, we may conclude that all models accurately describe the process. Because R^2_{training} results are nearly all close to 1.

The initial assumption would be that lots of models are suitable if the selection had just been based on R^2_{training} and R^2_{testing} . Based on this argument, utilizing a method that considers the simplicity of the models and the desired models' capacity to provide realistic values, it is determined that only model 5 (TON) is suitable. As a result, misleading findings are unavoidable if the model building-optimum result finding analyses are not addressed as outlined in this article. Thus, the obtained model 5 (CS3-O1-TON) was chosen as the objective function required in analyses to get optimum results of tool life. Outcomes of the selected model can be spotted in Table 7.27.

Table 7.29 shows the outcomes of three specific optimization scenarios for the chosen model. In scenario 1, all of the variables were utilized with their upper and lower limits in a continuous interval. The minimum tool life (cutting time) outcomes, depending on all of the optimization techniques, were 2.834 min, which

correspond to TON. The suggested (optimum) designs are; cutting speed: 83.8916 (m/min) and feed rate: 0.2 (mm/rev). 2.834 min is a realistic result by compared with the results of experiment [4.30 13.50]. We could say that the optimization results reach lower tool life (cutting time) than experimental results.

In scenario 2, feed rate has been treated as continuous variables while the cutting speed is discrete (integers). The minimum tool life (cutting time) found as 2.835 min for the TON model.

For the third optimization scenario, all of the input parameters are supposed to be real numbers and the design variables can only take the experimental values. The results are the same with scenario 1 and 2.

From the point of stability, gaining identical outcomes for scenarios 1, 2 and 3 whose phenomenological foundation is addressed using four distinct direct search methods, enhances the chance that acquired results are global optimum. Besides that, utilizing various methods for scenario 2 produces dissimilar outcomes, although they are identical. This situation is critical for optimization issues comprising restriction types that are similar to those in scenarios 2 and 3. Furthermore, utilizing the TON model to solve the optimization issue for scenarios 1, 2 and 3 the optimal tool life (cutting time) was found to be 2.83436 min. We could say that the optimization results reach lower cutting force than experimental results.

Table 7.29: Optimization problem results of selected model CS3-O1-TON for tool life (cutting time)

Objective Functions	Scenario No	Constraints	Optimization Algorithm	Tool Life (min)	Suggested Design
CS3-O1-TON	1	$50 < x_1 < 90,$ $0.125 < x_2 < 0.2$	MDE	2.834	$x_1 = 83.8921, x_2 = 0.2$
			MSA	2.834	$x_1 = 83.8917, x_2 = 0.2$
			MRS	2.834	$x_1 = 83.8916, x_2 = 0.2$
			MNM	2.834	$x_1 = 83.8916, x_2 = 0.2$
	2	$50 < x_1 < 90,$ $0.125 < x_2 < 0.2,$ $\{x_1\} \in \text{Integers}$	MDE	2.835	$x_1 = 84, x_2 = 0.2$
			MSA	2.835	$x_1 = 84, x_2 = 0.199878$
			MRS	2.835	$x_1 = 84, x_2 = 0.2$
			MNM	2.835	$x_1 = 89, x_2 = 0.2$
	3	$x_1 = \{50, 60, 70, 80, 90\},$ $x_2 = \{0.125, 0.15, 0.175, 0.2\}$	MDE	2.898	$x_1 = 80, x_2 = 0.2$
			MSA	2.988	$x_1 = 80, x_2 = 0.2$
			MRS	2.988	$x_1 = 80, x_2 = 0.2$
			MNM	2.988	$x_1 = 80, x_2 = 0.2$

Consequently, i) The regression models used for modeling have to be tested through both R^2_{training} and R^2_{testing} values. The model's operational restriction (boundedness) has also to be checked by calculating the maximum and minimum values generated by the respective model is realistic or not. ii) In our approach, the data generated by the model stay within the realistic boundaries different from the interval produced by the model given in the reference study. iii) This reveals that the prediction capability of the process was better and more accurate than the classical approach.

7.5 Case Study #4

The third literature study which optimization process was studied taken from Hanief et al [47]. The pressures applied on a cutting tool during a cutting process have a significant impact on its lifespan. In terms of complexity, the machining procedure is rather difficult. Developing a complete model that incorporates all factors is quite challenging. With the use of a high-speed steel (HSS) machining tool, this study intends to create a model to explore the impacts of design variables (speed, depth, and feed rate) on cutting forces during process. A full factorial design was used to enhance the data's dependability and reliability degree. On the basis of design variables, artificial neural networks and multiple regression techniques were utilized to simulate cutting forces. Analysis of variance (ANOVA) was performed to test the regression model's suitability. The ANOVA showed that the regression model could determine the cutting forces. The ANN model, on the other hand, was shown to be more precise than the regression model.

As depicted in Table 7.30, the changes in values of these input parameters provided the obtaining of different results for the resultant force.

Therefore, these obtaining results depending on the change in these input parameter values are sufficient to develop an optimization strategy. Moreover, it is impossible to determine a proportional connection of measured cutting force values and three input parameters (cutting speed, feed rate and depth of cut) as understood from Table 7.30. Therefore, it is necessary to optimize these parameters to achieve minimum cutting force (N).

Table 7.30: Experimental results of resultant force with different experimental conditions [47]

Exp No	Cutting speed (v , m/min)	Feed rate (f , mm/rev)	Depth of cut (d , mm)	Resultant Force (f_R , N)
1	840	0.40	0.10	5.1266
2	840	0.40	0.13	5.8563
3	840	0.40	0.16	7.3708
4	1280	0.40	0.10	6.2632
5	1280	0.40	0.13	7.8619
6	1280	0.40	0.16	9.0650
7	1000	0.40	0.10	6.6832
8	1000	0.40	0.13	6.9717
9	1000	0.40	0.16	7.7756
10	840	0.80	0.10	8.0678
11	840	0.80	0.13	8.4087
12	840	0.80	0.16	10.0298
13	1280	0.80	0.10	8.5716
14	1280	0.80	0.13	8.5161
15	1280	0.80	0.16	9.9617
16	1000	0.80	0.10	8.9073
17	1000	0.80	0.13	8.9073
18	1000	0.80	0.16	8.2918
19	840	0.12	0.10	4.0710
20	840	0.12	0.13	3.3434
21	840	0.12	0.16	4.0590
22	1280	0.12	0.10	5.3841
23	1280	0.12	0.13	2.4105
24	1280	0.12	0.16	4.8550
25	1000	0.12	0.10	3.9355
26	1000	0.12	0.13	3.9558
27	1000	0.12	0.16	5.3155

The behavior of the system was explained by the multiple linear regression models given below [47];

$$f_R = 3.9093 \times v^{0.2226} \times f^{0.4145} \times d^{0.3008} \quad (7.14)$$

Hanief et al. [47] figured out this limited optimization issue by defining all the input parameters as discrete and proceeded in the modeling process only according to the standard R^2 results and listed the models. Hanief et al. [47] does not mention the R^2_{training} and R^2_{testing} distinction in the modeling process and does not mention determining models according to different scenarios. As can be clearly seen, it is seen that smaller cutting force (resultant force) may be calculated with the variables as a consequence of optimization.

7.5.1 Optimization Scenarios

For all scenarios, the limitations for the system inputs (design parameters) as in the following form;

$$\begin{aligned} 840 \leq \text{Cutting speed} \leq 1280 & , \quad (m/min) \\ 0.12 \leq \text{Feed rate} \leq 0.8 & , \quad (mm/rev) \\ 0.1 \leq \text{Depth of cut} \leq 0.16 & , \quad (mm) \end{aligned}$$

7.5.1.1 Scenario 1

Cutting force is explained by the objective function in this optimal solution problem. There are no constraints about the input parameters so they can be real numbers, and the computation area is continuous. The primary goal is to minimize the cutting force. It is also technically possible to see these theory-based boundaries of the objective function this way.

7.5.1.2 Scenario 2

Scenario 2 should include additional realistic situations in addition to knowledge-based ones. A novel optimal solution is provided that implies the reduction of the responses for this application. Input parameters are also restricted with integers.

7.5.1.3 Scenario 3

In the constructed of scenario 3, more viable and more limited issue situations should be included to scenario 2. For that reason, there is a new optimum solution problem created to the minimization of the response values. Unlike Scenario 2, in scenario 3 parameters can only take the values in the data table.

7.5.2 Results and Discussion

In our approach, different from the classical ones, various regression models are first tested utilizing both R^2_{training} and R^2_{testing} values (not only R^2 as in the classical approach) to reveal what is the degree of performance of the model can explain the method. Besides, the model's operational restriction (boundedness) is also checked by calculating the highest and lowest values that the related model creates. Therefore, our proposed design strategy provides producing realistic values. Also, it is necessary to check the limitedness of decided models, whether producing realistic results. Regarding of these facts, by using our proposed approach, the experimental data table of cutting force (resultant force) listed as Table 7.31 can be seen below.

Table 7.31: Results of the Neuro-regression models for the cutting force

Models	R^2_{training}	R^2_{testing}	Max (N)	Min (N)
CS4-O-L	0.84	0.79	9.629	3.965
CS4-O-LR	0.89	0.91	9.738	3.859
CS4-O-SON	0.91	0.82	9.689	3.537
CS4-O-SONR	0.99	0.61	1.832×10^9	1.552
CS4-O-TON	0.97	0.64	9.995	2.981
CS4-O-FOTN	0.91	0.82	11.134	1.386
CS4-O-FOTNR	0.96	0.69	5.013×10^8	-1.483×10^{10}
CS4-O-SOTN	0.99	0.23	24702.1	-9583.14
CS4-O-SOTNR	0.99	-0.86	1.057×10^9	-7.058×10^{11}
CS4-O-FOLN	0.87	0.85	9.354	3.539
CS4-O-FOLNR	0.88	0.86	9.576	3.777
CS4-O-SOLN	0.91	0.83	9.744	3.511
CS4-O-SOLNR	0.99	0.54	7.097×10^9	-0.117

For the fourth study (f_R , Hanief et al [47]) the initial assumption would be that models 2, 3, 6 and 12 are suitable if the selection had just been based on R^2_{training} and R^2_{testing} . Based on this argument, utilizing a method that considers the simplicity of the models and the desired models' capacity to provide realistic values, it is determined that only model 6 (FOTN) is suitable. Because model 6 has lower value than the other models. As a result, misleading findings are unavoidable

if the model building-optimum result finding analyses are not addressed as outlined in this article. Thus, the obtained model 6 (CS4-O-FOTN) was chosen as the objective function required in analyses to get optimum results of cutting force. Outcomes of the selected model can be spotted in Table 7.31.

Table 7.32 shows the outcomes of three specific optimization scenarios for the chosen model. In scenario 1, all of the variables were utilized with their upper and lower limits in a continuous interval. The minimum cutting force outcomes, depending on all of the optimization techniques, were 1.384 N, which correspond to FOTN. The suggested (optimum) design variables are change with optimization algorithms so there are four different cutting speed values. However, feed rate: 0.12 (mm/rev) and depth of cut: 0.121838 (mm). 1.384 N is a realistic result by compared with the results of experiment [2.4105, 10.0298]. We could say that the optimization results reach lower cutting force than experimental results, but it should be noted that the design parameters are not equal the experimental ones.

In scenario 2, feed rate and depth of cut have been treated as continuous variables while the cutting speed is discrete (integers). Although, there are 4 dissimilar outcomes but the minimum cutting force found as 1.384 N for the FOTN model. The suggested (optimum) design variables are; cutting speed: 1008 (m/min), feed rate: 0.12 (mm/rev) and depth of cut: 0.121838 (mm).

For the third optimization scenario, all of the input parameters are supposed to be real numbers and the design variables can only take the experimental values. The minimum cutting force had found as 3.551 N. The suggested (optimum) design variables are; cutting speed: 840 (m/min), feed rate: 0.12 (mm/rev) and depth of cut: 0.13 (mm). 3.55051 N is a realistic result. We could say that as a result of the optimization process a better and lower cutting force result was obtained. As can be seen from the results, the FOTN model chosen for the optimization process has achieved lower results in scenarios 1 and 2 than the experimental results. However, in scenario 3, when design variables are accepted as experimental values, bigger result has been obtained than experimental results.

Table 7.32: Optimization problem results of selected model CS4-O-FOTN for cutting force (resultant force)

Objective Functions	Scenario No	Constraints	Optimization Algorithm	Resultant Force (N)	Suggested Design
CS4-O-FOTN	1	$840 < x_1 < 1280$, $0.12 < x_2 < 0.8$, $0.1 < x_3 < 0.16$	MDE	1.384	$x_1 = 976.596, x_2 = 0.12, x_3 = 0.121838$
			MSA	1.384	$x_1 = 1265.62, x_2 = 0.12, x_3 = 0.121838$
			MRS	1.384	$x_1 = 1215.36, x_2 = 0.12, x_3 = 0.121838$
			MNM	1.384	$x_1 = 1127.39, x_2 = 0.12, x_3 = 0.121838$
	2	$840 < x_1 < 1280$, $0.12 < x_2 < 0.8$, $0.1 < x_3 < 0.16$, $\{x_1\} \in \text{Integers}$	MDE	1.384	$x_1 = 1008, x_2 = 0.12, x_3 = 0.121838$
			MSA	1.421	$x_1 = 1184, x_2 = 0.12, x_3 = 0.115474$
			MRS	1.387	$x_1 = 1184, x_2 = 0.12, x_3 = 0.121838$
			MNM	1.434	$x_1 = 1247, x_2 = 0.12, x_3 = 0.121836$
	3	$x_1 = \{840, 1000, 1280\}$, $x_2 = \{0.12, 0.4, 0.8\}$, $x_3 = \{0.1, 0.13, 0.16\}$	MDE	3.551	$x_1 = 840, x_2 = 0.12, x_3 = 0.13$
			MSA	3.551	$x_1 = 840, x_2 = 0.12, x_3 = 0.13$
			MRS	3.551	$x_1 = 840, x_2 = 0.12, x_3 = 0.13$
			MNM	3.551	$x_1 = 840, x_2 = 0.12, x_3 = 0.13$

7.6 Case Study #5

The fifth literature study which optimization process was studied taken from Jena et al [48]. The goal is creating an avenue, beneficial for machining industries' point of view to achieve their goals. Thus, this work focuses on create a regression model and reach optimal outcomes of response (here, surface roughness) in FDHT of AISI grade 4340 steel cut by coated ceramic tool using statistical approaches such as response surface methodology followed by desirability function analysis.

As depicted in Table 7.33, the changes in values of these input parameters provided the obtaining of different results for the surface roughness.

Therefore, these obtaining results depending on the change in these input parameter values are sufficient to develop an optimization strategy. Moreover, it is impossible to determine a proportional connection of measured surface roughness and three input parameters (cutting speed, axial feed and depth of cut) as understood from Table 7.33. Therefore, it is necessary to optimize these parameters to achieve minimum surface roughness.

Table 7.33: Experimental results of resultant force with different experimental conditions [48]

Exp No	Cutting speed (v , m/min)	Axial feed (f , mm/rev)	Depth of cut (d , mm)	Surface Roughness (Ra , μm)
1	110	0.06	0.2	0.41
2	110	0.10	0.3	0.55
3	110	0.14	0.4	0.77
4	110	0.18	0.5	0.96
5	160	0.06	0.3	0.38
6	160	0.10	0.2	0.52
7	160	0.14	0.5	0.61
8	160	0.18	0.4	0.74
9	210	0.06	0.4	0.34
10	210	0.10	0.5	0.49
11	210	0.14	0.2	0.56
12	210	0.18	0.3	0.65
13	260	0.06	0.5	0.38
14	260	0.10	0.4	0.46
15	260	0.14	0.3	0.66
16	260	0.18	0.2	0.72

The behavior of the system was explained by the multiple linear regression models given below [48];

$$\begin{aligned}
 Ra &= 0.41829 - 0.00319 \times v + 4.175 \times f + 0.26773 \times d \\
 &+ 0.00002 \times v^2 - 1.5625 \times f^2 + 0.625 \times d^2 - 0.01068 \times v \times f \\
 &- 0.00541 \times v \times d + 2.44318 \times f \times d
 \end{aligned} \tag{7.15}$$

The experimental data was represented by this regression model with determination coefficient (R^2) of 0.978.

Jena et al. [48] figured out this limited optimization issue by defining all the input parameters as discrete and proceeded in the modeling process only according to the standard R^2 results and listed the models. The R^2 value Jena et al [48] found as 97.8%. Jena et al [48]] does not mention the R^2_{training} and R^2_{testing} distinction in the modeling process and does not mention determining models according to different scenarios. As can be clearly seen, it is seen that smaller surface roughness may be calculated with the variables as a consequence of optimization.

7.6.1 Optimization Scenarios

For all scenarios, the limitations for the system inputs (design parameters) as in the following form;

$$\begin{aligned} 110 \leq \text{Cutting speed} \leq 260 & , \quad (m/min) \\ 0.06 \leq \text{Axial feed} \leq 0.18 & , \quad (mm/rev) \\ 0.2 \leq \text{Depth of cut} \leq 0.5 & , \quad (mm) \end{aligned}$$

7.6.1.1 Scenario 1

Surface roughness is explained by the objective function in this optimal solution problem. There are no constraints about the input parameters so they can be real numbers, and the computation area is continuous. The primary goal is to minimize the surface roughness. It is also technically possible to see these theory-based boundaries of the objective function this way.

7.6.1.2 Scenario 2

Scenario 2 should include additional realistic situations in addition to knowledge-based ones. A novel optimal solution is provided that implies the reduction of the responses for this application. Input parameters are also restricted with integers.

7.6.1.3 Scenario 3

In the constructed of scenario 3, more viable and more limited issue situations should be included to scenario 2. For that reason, there is a new optimum solution problem created to the minimization of the response values. Unlike Scenario 2, in scenario 3 parameters can only take the values in the data table.

7.6.2 Results and Discussion

In our approach, different from the classical ones, various regression models are first tested utilizing both R^2_{training} and R^2_{testing} values (not only R^2 as in the classical approach) to reveal what is the degree of performance of the model can explain the method. Besides, the model's operational restriction (boundedness) is also checked by calculating the highest and lowest values that the related model creates.

Therefore, our proposed design strategy provides producing realistic values. Also, it is necessary to check the limitedness of decided models, whether producing realistic results. Regarding of these facts, by using our proposed approach, the experimental data table of surface roughness listed as Table 7.34 can be seen below.

Table 7.34: Results of the Neuro-regression models for the surface roughness

Models	R²_{training}	R²_{testing}	Max (µm)	Min (µm)
CS5-O-L	0.89	0.86	0.885	0.267
CS5-O-LR	0.94	0.95	0.962	-0.110
CS5-O-SON	0.97	0.96	0.725	0.321
CS5-O-SONR	0.50	0.44	0.896	0.452
CS5-O-TON	1.00	0.96	1.026	0.293
CS5-O-FOTN	0.96	0.74	3.719	0.320
CS5-O-FOTNR	0.97	0.94	1.259x10 ⁹	-2.653x10 ¹²
CS5-O-SOTN	1.00	0.25	17.509	-1.142
CS5-O-SOTNR	0.98	0.95	6.311x10 ⁹	-5.528x10 ¹²
CS5-O-FOLN	0.88	0.86	0.860	0.241
CS5-O-FOLNR	0.95	0.95	0.963	0.270
CS5-O-SOLN	0.98	0.80	0.720	0.292
CS5-O-SOLNR	0.93	0.85	0.930	0.292

For the fifth study (Ra, Jena et al [48]), results show that if the R² value was the key element considered in decided the model, we may conclude that all models accurately describe the process. Because R²_{training} results are nearly all close to 1.

The initial assumption would be that models 3 and 5 are suitable if the selection had just been based on R²_{training} and R²_{testing}. Based on this argument, utilizing a method that considers the simplicity of the models and the desired models' capacity to provide realistic values, it is determined that only model 3 (SON) is suitable. As a result, misleading findings are unavoidable if the model building-optimum result finding analyses are not addressed as outlined in this article. Thus, the obtained model 3 (CS5-O-SON) was chosen as the objective function required in analyses to get optimum results of surface roughness. Outcomes of the selected model can be spotted in Table 7.34.

Table 7.35 shows the outcomes of three specific optimization scenarios for the chosen model. In scenario 1, all of the variables were utilized with their upper and lower limits in a continuous interval. The minimum surface roughness outcomes, depending on all of the optimization techniques, were $0.321\ \mu\text{m}$, which correspond to SON. The suggested (optimum) design variables are change with optimization algorithms so there are four different surface roughness values. However, cutting speed: 216 (m/min), feed rate: 0.06 (mm/rev) and depth of cut: 0.5 (mm). $0.321\ \mu\text{m}$ is a realistic result by compared with the results of experiment [0.34, 0.96]. We could say that the optimization results reach lower surface roughness than experimental results.

In scenario 2, feed rate and depth of cut have been treated as continuous variables while the cutting speed is discrete (integers). Although, there are 3 dissimilar outcomes but the minimum surface roughness for the SON model were same as the scenario 1.

For the third optimization scenario, all of the input parameters are supposed to be real numbers and the design variables can only take the experimental values. The minimum surface roughness had found as $0.321\ \mu\text{m}$. The suggested (optimum) design variables are; cutting speed: 210 (m/min), feed rate: 0.06 (mm/rev) and depth of cut: 0.5 (mm). $0.321\ \mu\text{m}$ is a realistic result. We could say that the optimization results reach lower surface roughness than experimental results.

In this study, the results of scenario 3 had lower surface roughness than the experimental results, even if the greater surface roughness value had reached in scenario 3 compared to scenarios 1 and 2. It can be seen clearly understood that the optimization work had been carried out in a healthy way and its purpose has been achieved.

Table 7.35: Optimization problem results of selected model CS5-O-SON for surface roughness

Objective Functions	Scenario No	Constraints	Optimization Algorithm	Surface Roughness (μm)	Suggested Design
CS5-O-SON	1	$110 < x_1 < 260,$ $0.06 < x_2 < 0.18,$ $0.2 < x_3 < 0.5$	MDE	0.321	$x_1 = 215.972, x_2 = 0.06, x_3 = 0.5$
			MSA	0.321	$x_1 = 215.963, x_2 = 0.06, x_3 = 0.5$
			MRS	0.321	$x_1 = 215.963, x_2 = 0.06, x_3 = 0.5$
			MNM	0.321	$x_1 = 215.963, x_2 = 0.06, x_3 = 0.5$
	2	$110 < x_1 < 260,$ $0.06 < x_2 < 0.18,$ $0.2 < x_3 < 0.5$ $\{x_1\} \in \text{Integers}$	MDE	0.321	$x_1 = 216, x_2 = 0.06, x_3 = 0.5$
			MSA	0.345	$x_1 = 207, x_2 = 0.0631414, x_3 = 0.424542$
			MRS	0.321	$x_1 = 215, x_2 = 0.06, x_3 = 0.5$
			MNM	0.321	$x_1 = 216, x_2 = 0.06, x_3 = 0.5$
	3	$x_1 = \{110, 160, 210, 260\},$ $x_2 = \{0.06, 0.1, 0.14, 0.18\},$ $x_3 = \{0.2, 0.3, 0.4, 0.5\}$	MDE	0.321	$x_1 = 210, x_2 = 0.06, x_3 = 0.5$
			MSA	0.321	$x_1 = 210, x_2 = 0.06, x_3 = 0.5$
			MRS	0.321	$x_1 = 210, x_2 = 0.06, x_3 = 0.5$
			MNM	0.321	$x_1 = 210, x_2 = 0.06, x_3 = 0.5$

7.7 Case Study #6

The sixth literature study which optimization process was studied taken from Kovac et al [49]. Surface quality in face milling is examined as a function of machining settings in this research. This study describes a new technique to simulating surface roughness that makes use of artificial intelligence technologies. An experimental model is developed utilizing fuzzy logic and regression analysis in this study. After that, the surface roughness values estimated from those models are compared to the actual surface roughness. In comparison to standard techniques, such as regression analysis, the findings revealed that the suggested system could considerably improve the performance of product profiles. Surface roughness may be accurately predicted by using fuzzy logic modeling, depending on the outcomes.

As depicted in Table 7.36, the changes in values of these input parameters provided the obtaining of different results for the surface roughness.

Therefore, these obtaining results depending on the change in these input parameter values are sufficient to develop an optimization strategy. Moreover, it is impossible to determine a proportional connection between measured surface roughness and four input parameters (cutting speed, feed per tooth, depth of cut and flank wear land) as understood from Table 7.36. Therefore, it is necessary to optimize these parameters to achieve minimum surface roughness.

Table 7.36: Experimental results of resultant force with different experimental conditions [49]

Exp No	Cutting speed (v , m/s)	Feed per tooth (f , mm/tooth)	Depth of cut (a , mm)	Width of flank wear (VB , mm)	Surface Roughness (Ra , μm)
1	2.32	0.178	1	0.12	2
2	3.67	0.178	1	0.12	1.45
3	2.32	0.280	1	0.12	2
4	3.67	0.280	1	0.12	1.3
5	2.32	0.178	2.25	0.12	2.1
6	3.67	0.178	2.25	0.12	1.4
7	2.32	0.280	2.25	0.12	2
8	3.67	0.280	2.25	0.28	1.45
9	2.32	0.178	1	0.28	3.05
10	3.67	0.178	1	0.28	2.2
11	2.32	0.280	1	0.28	3.1
12	3.67	0.280	1	0.28	2.7
13	2.32	0.178	2.25	0.28	3.5
14	3.67	0.178	2.25	0.28	2.45
15	2.32	0.280	2.25	0.28	2.4
16	3.67	0.280	2.25	0.28	1.75
17	2.95	0.223	1.5	0.18	1.6
18	2.95	0.223	1.5	0.18	1.6
19	2.95	0.223	1.5	0.18	2.2
20	2.95	0.223	1.5	0.18	1.85
21	2.95	0.223	1.5	0.18	2.3
22	2.95	0.223	1.5	0.18	2.7
23	1.83	0.223	1.5	0.18	3.3
24	4.65	0.223	1.5	0.18	1.05
25	2.95	0.142	1.5	0.18	2.1
26	2.95	0.351	1.5	0.18	2.5
27	2.95	0.223	0.67	0.18	2
28	2.95	0.223	3.37	0.18	2.2
29	2.95	0.223	1.5	0.08	1.45
30	2.95	0.223	1.5	0.40	2.6

The behavior of the system was explained by the multiple linear regression models given below [49];

$$Ra = 10.9163 \times v^{-0.8945} \times f^{-0.0462} \times a^{-0.0151} \times VB^{0.4556} \quad (7.16)$$

Kovac et al. [49] figured out this limited optimization issue by defining all the input parameters as discrete and proceeded in the modeling process only according to the standard R^2 results and listed the models. Kovac et al [49] does not mention the R^2_{training} and R^2_{testing} distinction in the modeling process and does not mention determining models according to different scenarios. As can be clearly seen, it is seen that smaller surface roughness may be calculated with the variables as a consequence of optimization.

7.7.1 Optimization Scenarios

For all scenarios, the limitations for the system inputs (design parameters) as in the following form;

$$\begin{aligned}
 1.83 \leq \text{Cutting speed} &\leq 4.65 && , \quad (m/s) \\
 0.142 \leq \text{Feed per tooth} &\leq 0.351 && , \quad (mm/t) \\
 0.67 \leq \text{Depth of cut} &\leq 3.37 && , \quad (mm) \\
 0.08 \leq \text{Width of flank wear land} &\leq 0.40 && , \quad (mm)
 \end{aligned}$$

Since there is no input value that can be integer and there is no other output which can restrict the system, some of the scenarios can not be applied.

7.7.1.1 Scenario 1

Surface roughness is explained by the objective function in this optimal solution problem. There are no constraints about the input parameters so they can be real numbers, and the computation area is continuous. The primary goal is to minimize the surface roughness. It is also technically possible to see these theory-based boundaries of the objective function this way.

7.7.1.2 Scenario 2

In the constructed of scenario 2, more viable and more limited issue situations should be included to scenario 1. For that reason, there is a new optimum solution problem created to the minimization of the response values. Unlike Scenario 1, in scenario 2 parameters can only take the values in the data table.

7.7.2 Results and Discussion

In our approach, different from the classical ones, various regression models are first tested utilizing both R^2_{training} and R^2_{testing} values (not only R^2 as in the classical approach) to reveal what is the degree of performance of the model can explain the method. Besides, the model's operational restriction (boundedness) is also checked by calculating the highest and lowest values that the related model creates. Therefore, our proposed design strategy provides producing realistic values. Also, it is necessary to check the limitedness of decided models, whether producing realistic results. Regarding of these facts, by using our proposed approach, the experimental data table of surface roughness listed as Table 7.37 can be seen below.

Table 7.37: Results of the Neuro-regression models for the surface roughness

Models	R^2_{training}	R^2_{testing}	Max (μm)	Min (μm)
CS6-O-L	0.62	0.69	4.269	0.176
CS6-O-LR	0.72	-17.72	∞	$-\infty$
CS6-O-SON	0.83	-0.45	6.263	0.489
CS6-O-SONR	0.79	-0.46	3.014×10^{12}	0.182
CS6-O-TON	0.88	-1.22	7.419	-3.362
CS6-O-FOTN	0.67	0.45	3.881	0.797
CS6-O-FOTNR	0.75	-29.64	1.291×10^{11}	-7.849×10^6
CS6-O-SOTN	0.85	-0.39	6.002	-2.926
CS6-O-SOTNR	0.79	-0.75	20.596	0.393
CS6-O-FOLN	0.65	0.85	4.026	0.276
CS6-O-FOLNR	0.71	0.33	4.542×10^7	-1.412×10^7
CS6-O-SOLN	0.81	0.07	6.727	-0.159
CS6-O-SOLNR	0.86	0.85	5.559	-2.879×10^7

For the sixth study (Ra, Kovac et al [49]), the initial assumption would be that only one model is suitable if the selection had just been based on R^2_{training} and R^2_{testing} . Based on this argument, utilizing a method that considers the desired models' capacity to provide realistic values, it is determined that only model 13 (SOLNR) is suitable. Model 13 appears having a negative minimum result. As it is a very small amount that result can be taken as zero. As a result, misleading findings are

unavoidable if the model building-optimum result finding analyses are not addressed as outlined in this article. Thus, the obtained model 13 (CS6-O-SOLNR) was chosen as the objective function required in analyses to get optimum results of surface roughness. Outcomes of the selected model can be spotted in Table 7.37.

Table 7.38 shows the outcomes of two specific optimization scenarios for the chosen model. Optimization scenario 2 is not applicable for this study, because there are not any design variable that can be integer. In the optimization scenarios, minimum surface roughness had found as 0.188 μm with the following parameters; cutting speed: 4.65 (m/s), feed: 0.351 (mm/tooth), depth of cut: 1 (mm) and flank wear: 0.4 (mm). 0.188 μm is a better result in comparison with the experimental values [1.05, 3.5]. We could say that as a result of the optimization process better and lower surface roughness result was obtained. One of the most important reasons to reach this minimum result is that the design of experiment has not been done systematically. If we look at the experimental table, there is only an experiment where the cutting speed is 4.65 m/s.

Table 7.38: Optimization problem results of selected model CS6-O-SOLNR for surface roughness

Objective Functions	Scenario No	Constraints	Optimization Algorithm	Surface Roughness (μm)	Suggested Design
CS6-O-SOLNR	1	$1.83 < x_1 < 4.65,$	MDE	3.803×10^{-7}	$x_1 = 4.65, x_2 = 0.333664, x_3 = 3.16892, x_4 = 0.0800064$
		$0.142 < x_2 < 0.351,$	MSA	8.149×10^{-8}	$x_1 = 4.27824, x_2 = 0.302776, x_3 = 2.23787, x_4 = 0.153542$
		$0.67 < x_3 < 3.37,$	MRS	5.712×10^{-8}	$x_1 = 4.27519, x_2 = 0.297941, x_3 = 2.17235, x_4 = 0.169962$
		$0.08 < x_4 < 0.40$	MNM	6.990×10^{-8}	$x_1 = 4.56062, x_2 = 0.327534, x_3 = 3.21847, x_4 = 0.140127$
	2	$x_1 = \{183, 2.32, 2.95, 3.67, 4.65\},$	MDE	0.188	$x_1 = 4.65, x_2 = 0.351, x_3 = 1, x_4 = 0.4$
		$x_2 = \{0.142, 0.178, 0.223, 0.280, 0.351\},$	MSA	0.188	$x_1 = 4.65, x_2 = 0.351, x_3 = 1, x_4 = 0.4$
		$x_3 = \{0.67, 1, 1.5, 2.25, 3.37\},$	MRS	0.188	$x_1 = 4.65, x_2 = 0.351, x_3 = 1, x_4 = 0.4$
		$x_4 = \{0.08, 0.12, 0.18, 0.28, 0.40\}$	MNM	0.188	$x_1 = 4.65, x_2 = 0.351, x_3 = 1, x_4 = 0.4$

Regarding of these facts, by using our proposed approach, for surface roughness the design variables were fitted to the given multiple linear rational function with $R^2_{\text{training}} = 0.86$ and $R^2_{\text{testing}} = 0.85$ values: $(0.876953 + 0.515023 \text{ Log}[x1] + 0.502096 \text{ Log}[x1]^2 + 0.767089 \text{ Log}[x2] + 1.93999 \text{ Log}[x1] \text{ Log}[x2] + 1.89879 \text{ Log}[x2]^2 + 0.326182 \text{ Log}[x3] + 0.759354 \text{ Log}[x1] \text{ Log}[x3] + 1.00894 \text{ Log}[x2] \text{ Log}[x3] + 1.7903 \text{ Log}[x3]^2 + 0.160736 \text{ Log}[x4] + 1.80025 \text{ Log}[x1] \text{ Log}[x4] + 0.9205 \text{ Log}[x2] \text{ Log}[x4] + 1.55392 \text{ Log}[x3] \text{ Log}[x4] + 0.864499 \text{ Log}[x4]^2) / (1.51101 + 1.3603 \text{ Log}[x1] - 1.00906 \text{ Log}[x1]^2 + 0.942904 \text{ Log}[x2] - 0.420822 \text{ Log}[x1] \text{ Log}[x2] + 0.323479 \text{ Log}[x2]^2 + 2.08135 \text{ Log}[x3] + 0.341663 \text{ Log}[x1] \text{ Log}[x3] + 1.48955 \text{ Log}[x2] \text{ Log}[x3] + 0.90751 \text{ Log}[x3]^2 + 3.1366 \text{ Log}[x4] + 0.523403 \text{ Log}[x1] \text{ Log}[x4] + 1.12312 \text{ Log}[x2] \text{ Log}[x4] + 1.03579 \text{ Log}[x3] \text{ Log}[x4] + 1.11833 \text{ Log}[x4]^2)$. According to scenario 1, minimum surface roughness can be taken as zero. In scenario 2, minimum surface roughness has found as 0.188122 with the following conditions; cutting speed: 4.65m/s, feed per tooth: 0.351mm/tooth, depth of cut: 1mm and and width of flank wear land: 0.4mm. 0.188 μm could be a realistic and better result in comparison with the experimental results [1.05, 3.5]. Both optimization results and the experimental results have minimum surface roughness value at the highest cutting speed (4.65m/s). One of the reasons why smaller values could not be obtained in the experimental results, single experiment was made with a cutting speed value of 4.65 can be showed.

7.8 Case Study #7

The seventh literature study which optimization process was studied taken from Meddour et al [50]. To simulate the surface roughness and cutting force in the finish turning of AISI 4140 hard materials using a ceramic tool, this work is presented in this article. Artificial Neural Networks (ANN) are being utilized to enhance estimation in this case. According to the response surface methodology (RSM), cutting speed, depth of cut and feed rate affect the response parameters. Increased cutting speed reduces the undesirable effects of feed rate. Bigger nose radius processing provides surfaces with higher physical qualities. Various multi-objective optimization tasks can be accomplished utilizing the Desirability Function Approach (DF) and the Non-dominated Sorting Genetic Algorithm

(NSGA-II) combined with ANN models. This approach is shown to be significantly successful than DF technique and to give a variety of non-dominated solutions that meets the demands of components condition, productivity, and cutting force, all of which lead to improved productivity and increased profitability. A further benefit of using the NSGA-II and ANN models together was the ability to forecast a low degree of surface roughness well below the measured result.

As depicted in Table 7.38, the changes in values of these input parameters provided the obtaining of different results for the surface roughness and cutting forces.

Therefore, these obtaining results depending on the change in these input parameter values are sufficient to develop an optimization strategy. Moreover, it is impossible to establish a proportional connection between measured response values and four design variables (cutting speed, feed per tooth, depth of cut and flank wear land) as understood from Table 7.38. Therefore, it is necessary to optimize these parameters to achieve minimum response values.

Table 7.39: Experimental results of surface roughness and cutting forces with different experimental conditions [50]

Exp. No	Cutting speed (V_c , m/min)	Depth of cut (a_p , mm)	Feed rate (f , mm/rev)	Tool nose radius (r , mm)	Surface Roughness (R_a , μm)	Feed (F_x , N)	Thrust (F_y , N)	Tangential (F_z , N)
1	182	0.3	0.11	1.6	0.33	60.10	147.64	124.80
2	182	0.2	0.11	1.2	0.29	36.94	114.76	92.60
3	182	0.2	0.14	1.6	0.38	38.41	127.70	110.53
4	182	0.2	0.08	1.6	0.24	32.02	112.15	80.54
5	244	0.2	0.11	1.6	0.26	31.11	120.44	95.90
6	182	0.1	0.08	1.2	0.27	20.71	67.63	56.09
7	244	0.1	0.11	1.2	0.34	26.69	91.95	56.47
8	182	0.2	0.08	0.8	0.37	50.57	108.92	72.81
9	244	0.2	0.08	1.2	0.32	39.45	96.53	52.64
10	182	0.3	0.08	1.2	0.28	48.71	135.45	106.64
11	182	0.2	0.11	1.2	0.3	32.06	119.02	79.04
12	182	0.2	0.14	0.8	0.42	35.65	109.77	107.85
13	182	0.2	0.11	1.2	0.32	37.69	118.21	94.51
14	120	0.2	0.14	1.2	0.43	34.57	107.84	100.93
15	182	0.2	0.11	1.2	0.33	40.84	88.87	90.79
16	120	0.2	0.11	0.8	0.43	42.99	116.32	86.67
17	120	0.1	0.11	1.2	0.37	26.07	71.52	59.24
18	120	0.3	0.11	1.2	0.38	61.93	151.92	130.04
19	182	0.1	0.11	0.8	0.4	17.94	79.82	50.33
20	182	0.2	0.11	1.2	0.29	37.46	100.68	80.76
21	120	0.2	0.08	1.2	0.25	37.92	92.67	97.92
22	244	0.3	0.11	1.2	0.32	55.67	130.85	116.22
23	182	0.3	0.11	0.8	0.43	59.30	122.81	117.51
24	182	0.1	0.14	1.2	0.31	27.38	97.77	62.44
25	244	0.2	0.14	1.2	0.37	53.49	148.85	104.54
26	182	0.1	0.11	1.6	0.25	22.59	87.66	67.54
27	244	0.2	0.11	0.8	0.5	44.69	100.24	85.56
28	120	0.2	0.11	1.6	0.35	28.87	95.73	99.62
29	182	0.3	0.14	1.2	0.34	59.53	171.31	153.56

The behavior of the system was explained by the multiple linear regression models given below [50];

$$\begin{aligned}
 Ra &= 0.6548 + 2.246 E - 004 \times Vc - 0.3015 \times ap + 2.774 \times f & (7.17) \\
 &- 0.7968 \times r - 1.2096 E003 \times Vc \times ap - 0.01747 \times Vc \times f \\
 &- 1.61295 E - 003 \times Vc \times r + 1.666 \times ap \times f + 0.3125 \times ap \times r \\
 &+ 1.8749 \times f \times r + 1.0275 E - 005 \times Vc^2 + 0.199 \times ap^2 \\
 &- 3.333 \times f^2 + 0.2781 \times r^2
 \end{aligned}$$

$$\begin{aligned}
 Fx &= 144.83 - 0.380 \times Vc + 112 \times ap - 1328.135 \times f - 48.178 \times f & (7.18) \\
 &- 48.178 \times r - 0.277 \times Vc \times ap + 2.337 \times Vc \times f \\
 &+ 5.443 E - 003 \times Vc \times r + 345.833 \times ap \times f - 24.0625 \times ap \times r \\
 &+ 443.958 \times f \times r + 5.421 E - 004 \times Vc^2 + 248.016 \times ap^2 \\
 &+ 1615.462 \times f^2 - 1.983 \times r^2
 \end{aligned}$$

$$\begin{aligned}
 Fy &= 261.238 - 0.563 \times Vc + 301.383 \times ap - 2346.382 \times f & (7.19) \\
 &- 115.136 \times r - 1.673 \times Vc \times ap + 4.993 \times Vc \times f + 0.411 \times Vc \times r \\
 &+ 476.666 \times ap \times f + 106.187 \times ap \times r + 306.249 \times f \times r \\
 &- 2.106 E - 004 \times Vc^2 + 315.85 \times ap^2 + 6323.333 \times f^2 - 1.454 \times r^2
 \end{aligned}$$

$$\begin{aligned}
 Fz &= 197.822 - 0.727 \times Vc + 21.201 \times ap - 2004.187 \times f + 8.317 \times r & (7.20) \\
 &- 0.445 \times Vc \times ap + 6.571 \times Vc \times f - 0.026 \times Vc \times r \\
 &+ 3380.833 \times ap \times f - 62 \times ap \times r - 105.208 \times f \times r \\
 &+ 1.1251 E - 004 \times Vc^2 + 232.375 \times ap^2 + 3361.111 \times f^2 \\
 &+ 13.570 \times r^2
 \end{aligned}$$

The experimental data was represented by these regression models with determination coefficients (R^2) of 0.91, 0.90, 0.89 and 0.97, respectively.

Meddour et al. [50] figured out this limited optimization issue by defining all the input parameters as discrete and proceeded in the modeling process only according to the standard R^2 results and listed the models. The R^2 values Meddour et al [50] found vary between 89% and 97%. Meddour et al [50] does not mention the R^2_{training} and R^2_{testing} distinction in the modeling process and does not mention determining models according to different scenarios. As can be clearly seen that the smaller surface roughness and cutting forces may be calculated with the variables as a consequence of optimization.

7.8.1 Optimization Scenarios

For all scenarios, the limit values for the system inputs (design parameters) as in the following form;

$$\begin{array}{ll}
120 \leq \text{Cutting speed} \leq 244 & , \quad (m/min) \\
0.1 \leq \text{Depth of cut} \leq 0.3 & , \quad (mm) \\
0.08 \leq \text{Feed rate} \leq 0.14 & , \quad (mm/rev) \\
0.8 \leq \text{Tool nose radius} \leq 1.6 & , \quad (mm)
\end{array}$$

7.8.1.1 Scenario 1

Surface roughness and cutting forces are explained by the objective functions in this optimal solution problem. There are no constraints about the input parameters so they can be real numbers, and the computation area is continuous. The primary goal is to minimize the response parameters. It is also technically possible to see these theory-based boundaries of the objective function this way.

7.8.1.2 Scenario 2

Scenario 1 should include additional realistic situations in addition to knowledge-based ones. A novel optimal solution is provided that implies the reduction of the responses for this application. Input parameters are also restricted with integers. There is only one design variable that can be integer number.

7.8.1.3 Scenario 3

As different from scenario 1, non-linear constraints are added for the optimization problem. For the first output, surface roughness (Ra) there is no scenario 3. For feed force (Fx), thrust force should be smaller than 70 and tangential force should be smaller than 50. For thrust force (Fy), feed force should be smaller than 25 and tangential force should be smaller than 50. For tangential force (Fz), feed force should be smaller than 25 and thrust force should be smaller than 70. Problem solving will be more complex and difficult in this instance than in scenarios 1 and 2.

7.8.1.4 Scenario 4

In the constructed of scenario 4, more viable and more limited issue situations should be included to scenario 2. For that reason, there is a new optimum solution problem created to the minimization of the response values. Unlike Scenario 2, in scenario 4 parameters can only take the values in the data table.

7.8.2 Results and Discussion

In our approach, different from the classical ones, various regression models are first tested utilizing both R^2_{training} and R^2_{testing} values (not only R^2 as in the classical approach) to reveal what is the degree of performance of the model can explain the method. Besides, the model's operational restriction (boundedness) is also checked by calculating the highest and lowest values that the related model creates. Therefore, our proposed design strategy provides producing realistic values. Also, it is necessary to check the limitedness of decided models, whether producing realistic results. Regarding of these facts, by using our proposed approach, the experimental data tables of surface roughness and cutting forces (F_x , F_y and F_z) listed as Table 7.39, 7.40, 7.41 and 7.42 can be seen below. Therefore, it is necessary to optimize these parameters to minimize of all the response values.

Table 7.40: Results of the Neuro-regression models for the surface roughness

Models	R^2_{training}	R^2_{testing}	Max (μm)	Min (μm)
CS7-O1-L	0.70	-6.64	0.468	0.2075
CS7-O1-LR	0.80	-15.12	∞	$-\infty$
CS7-O1-SON	0.94	-2.63	0.528	0.201
CS7-O1-SONR	0.09	-2.72	0.360	0.317
CS7-O1-TON	0.99	-1.17	0.561	0.172
CS7-O1-FOTN	0.82	-1.48	0.707	0.219
CS7-O1-FOTNR	0.95	-6.67	6.584×10^6	-1.691×10^8
CS7-O1-SOTN	1.00	1.00	5.097	5.006×10^{-9}
CS7-O1-SOTNR	0.99	-6614.43	2.941×10^6	-3.895×10^{10}
CS7-O1-FOLN	0.74	-4.91	0.478	0.202
CS7-O1-FOLNR	0.79	-12.71	61.498	-47.059
CS7-O1-SOLN	0.93	-1.66	0.512	0.218
CS7-O1-SOLNR	0.99	-289.99	1.392×10^8	-7.738×10^6

Table 7.41: Results of the Neuro-regression models for the cutting force (Fx, feed force)

Models	R^2_{training}	R^2_{testing}	Max (N)	Min (N)
CS7-O2-L	0.82	0.85	62.035	16.921
CS7-O2-LR	0.82	0.83	65.780	19.325
CS7-O2-SON	0.93	0.50	70.161	10.967
CS7-O2-SONR	0.27	-0.54	62.829	30.254
CS7-O2-TON	0.98	-0.13	81.747	5.688
CS7-O2-FOTN	0.85	0.78	84.849	17.181
CS7-O2-FOTNR	0.96	0.33	2.249×10^8	-3.906×10^8
CS7-O2-SOTN	0.98	-17.49	831.029	-1301.14
CS7-O2-SOTNR	0.99	-1.38	3.035×10^8	-4.811×10^8
CS7-O2-FOLN	0.77	0.68	57.449	17.036
CS7-O2-FOLNR	0.53	-0.02	1.304×10^9	-6.991×10^7
CS7-O2-SOLN	0.92	0.67	67.663	11.978
CS7-O2-SOLNR	0.95	0.12	60.889	16.646

Table 7.42: Results of the Neuro-regression models for the cutting force (Fy, thrust force)

Models	R^2_{training}	R^2_{testing}	Max (N)	Min (N)
CS7-O3-L	0.82	0.49	169.773	57.808
CS7-O3-LR	0.55	-0.55	∞	$-\infty$
CS7-O3-SON	0.89	0.77	198.564	58.642
CS7-O3-SONR	0.37	0.09	160.96	89.796
CS7-O3-TON	0.96	0.83	191.548	63.564
CS7-O3-FOTN	0.84	0.43	195.57	65.208
CS7-O3-FOTNR	0.81	0.00	5.004×10^8	-43652
CS7-O3-SOTN	0.96	-14.05	1377.85	-2113.1
CS7-O3-SOTNR	-0.18	-11.92	2.341×10^9	-1.089×10^9
CS7-O3-FOLN	0.78	0.46	159.616	54.773
CS7-O3-FOLNR	0.77	-0.46	5.666×10^8	-1.314×10^7
CS7-O3-SOLN	0.89	0.66	195.288	53.231
CS7-O3-SOLNR	0.94	0.60	1.131×10^{10}	64.048

Table 7.43: Results of the Neuro-regression models for the cutting force (Fz, tangential force)

Models	R^2_{training}	R^2_{testing}	Max (N)	Min (N)
CS7-O4-L	0.92	0.73	147.559	37.711
CS7-O4-LR	0.96	0.72	155.604	47.253
CS7-O4-SON	0.97	0.89	156.69	43.897
CS7-O4-SONR	0.23	0.16	119.894	77.882
CS7-O4-TON	0.99	0.69	180.635	43.216
CS7-O4-FOTN	0.94	0.68	168.588	43.83
CS7-O4-FOTNR	0.98	0.43	4.016×10^{10}	-8.648×10^7
CS7-O4-SOTN	0.99	0.61	161.902	-268.552
CS7-O4-SOTNR	0.99	0.32	2.729×10^9	-1.545×10^{16}
CS7-O4-FOLN	0.89	0.66	139.254	33.988
CS7-O4-FOLNR	0.28	-0.79	1.641×10^8	-3.363×10^7
CS7-O4-SOLN	0.98	0.90	158.211	43.985
CS7-O4-SOLNR	0.99	0.60	208.708	-4.534×10^8

For the first output of the study (Ra, Meddour et al [50]), the initial assumption would be that only one model is suitable if the selection had just been based on R^2_{training} and R^2_{testing} . Based on this argument, utilizing a method that considers the desired models' capacity to provide realistic values, it is determined that only model 8 (SOTN) is suitable. As a result, misleading findings are unavoidable if the model building-optimum result finding analyses are not addressed as outlined in this article. Thus, the obtained model 8 (CS7-O1-SOTN) was chosen as the objective function required in analyses to get optimum results of surface roughness. Outcomes of the selected model can be spotted in Table 7.39.

Table 7.43 shows the outcomes of three specific optimization scenarios for the chosen model. In scenario 1, all of the variables were utilized with their upper and lower limits in a continuous interval. There are four different results for the four different optimization algorithms but the minimum surface roughness results can be taken as zero. But, it could not be a realistic result.

In scenario 2, feed rate, depth of cut and tool nose radius have been handled as continuous parameters, whereas the cutting speed is discontinuous (integers). In this case, there are 4 different results but the minimum surface roughness value for

the SON model can be taken as 0.108668 μm . That is the only realistic result of the scenario 2.

There is no scenario 3 for surface roughness.

For the fourth optimization scenario, all of the input parameters are supposed to be real numbers and the design variables can only take the experimental values. The minimum surface roughness had found as 0.155 μm . The suggested (optimum) design variables are; cutting speed: 244 (m/min), depth of cut: 0.1 (mm/rev), feed rate: 0.08 (mm) and tool nose radius: 1.6 (mm). 0.155 μm is a realistic and better result by compared with the results of experiment [0.24, 0.5]. We could say that as a result of the optimization process a better and lower surface roughness result was obtained.

For the second output of the study (Fx, Meddour et al [50]), the initial assumption would be that models 1 and 2 are suitable if the selection had just been based on R^2_{training} and R^2_{testing} . Based on this argument, utilizing a method that considers the desired models' capacity to provide realistic values, it is determined that only models 1 and 2 are suitable. As a result, misleading findings are unavoidable if the model building-optimum result finding analyses are not addressed as outlined in this article. As can be seen in Table 7.40, estimation capacity (R^2_{testing}) of model 1 (L) and model 2 (LR) are the same while model 1 was achieved lower cutting force than the model 2. With this approach, the obtained model 1 (L) is appropriate. Because model 1 has lower value than the model 2. Thus, the obtained model 1 (CS7-O2-L) was chosen as the objective function required in analyses to get optimum results of Fx.

Table 7.44 shows the outcomes of four specific optimization scenarios for the chosen model. In scenario 1, all of the variables were utilized with their upper and lower limits in a continuous interval. The minimum cutting force (Fx) outcomes, depending on all of the optimization techniques, were 16.921 N, which correspond to L. The suggested (optimum) designs are; cutting speed: 120 (m/min), depth of cut: 0.1 (mm), feed rate: 0.08 (mm/rev) and tool nose radius: 1.6 (mm). 16.921 N is a realistic result by compared with the results of experiment [17.94, 60.10]. We

could say that the optimization scenario 1 reach lower cutting force than experimental results.

In scenario 2, feed rate, depth of cut and tool nose radius have been handled as continuous parameters, whereas the cutting speed is discontinuous (integers). In this case, there are 3 different results but the minimum cutting force value for the L model were same as the scenario 1.

In the third optimization scenario, the only limitation condition in the optimization process was taken as the thrust force (F_y) smaller than 70 N and tangential force (F_z) smaller than 50 N for feed force (F_x). The minimum cutting force has found as 21.688 N based on all optimization algorithms. The suggested (optimum) design variables are; cutting speed: 244 (m/min), depth of cut: 0.1 (mm), feed rate: 0.08 (mm/rev) and tool nose radius: 1.28994 (mm). 21.688 N is a realistic result by compared with the results of experiment.

For the fourth optimization scenario, all of the input parameters are supposed to be real numbers and the design variables can only take the experimental values. The results are the same with scenario 1 and 2.

From the point of stability, gaining identical outcomes for scenarios 1, 2, 3, and 4, whose phenomenological foundation is addressed using four distinct direct search methods, enhances the chance that acquired results are global optimum. Besides that, utilizing various methods for scenario 2 produces dissimilar outcomes, although they are identical. This situation is critical for optimization issues comprising restriction types that are similar to those in scenarios 2 and 3. Furthermore, utilizing the L model to solve the optimization issue for scenarios 1, 2, 3 and 4, the best cutting force was found to be 16.9207 N.

For the third output of the study (F_y , Meddour et al [50]), the initial assumption would be that only one model is suitable if the selection had just been based on R^2_{training} and R^2_{testing} . Based on this argument, utilizing a method that considers the desired models' capacity to provide realistic values, it is determined that only model 5 (TON) is suitable. As a result, misleading findings are unavoidable if the model building-optimum result finding analyses are not addressed as outlined in this

article. Thus, the obtained model 5 (CS7-O3-TON) was chosen as the objective function required in analyses to get optimum results of F_y . Outcomes of the selected model can be spotted in Table 7.41.

Table 7.45 shows the outcomes of four specific optimization scenarios for the chosen model. In scenario 1, all of the variables were utilized with their upper and lower limits in a continuous interval. There are three different results for the scenario 1. The minimum cutting force (F_y) outcomes, depending only the MRS algorithm, were 60.120 N, which correspond to TON. The suggested (optimum) designs are; cutting speed: 244 (m/min), depth of cut: 0.3 (mm), feed rate: 0.08 (mm/rev) and tool nose radius: 0.8 (mm). 60.120 N is a realistic result by compared with the results of experiment [67.63, 171.31]. We could say that the optimization scenario 1 reach lower cutting force than experimental results.

In scenario 2, feed rate, depth of cut and tool nose radius have been treated as continuous variables while the cutting speed is discrete (integers). In this case, there are 4 different results, but the minimum cutting force value based on the MSA optimization algorithm for the TON model can be taken as 61.129 N. The suggested (optimum) design variables for 61.129 N are; cutting speed: 243 (m/min), depth of cut: 0.3 (mm), feed rate: 0.08 (mm/rev) and tool nose radius: 0.8 (mm). As in the optimization scenario 1, results are smaller than experimental results in scenario 2.

In the third optimization scenario, the only limitation condition in the optimization process was taken as the feed force (F_x) smaller than 25 N and tangential force (F_z) smaller than 50 N for thrust force (F_y). The results are the same with scenario 1 and 2. The minimum cutting force has found as 66.190 N based on all optimization algorithms. The suggested (optimum) design variables are; cutting speed: 244 (m/min), depth of cut: 0.1 (mm), feed rate: 0.08 (mm/rev) and tool nose radius: 1.28994 (mm). 66.190 N is a realistic and better result in comparison with the experimental values.

For the fourth optimization scenario, all of the input parameters are supposed to be real numbers and the design variables can only take the experimental values. The

minimum cutting force results are the same with scenario 1. Minimum cutting force for all the optimization algorithms had found as 61.129 N.

From the point of stability, gaining identical outcomes for scenarios 1, 2, 3, and 4, whose phenomenological foundation is addressed using four distinct direct search methods, enhances the chance that acquired results are global optimum. Besides that, utilizing various methods for scenario 2 produces dissimilar outcomes, although they are identical. This situation is critical for optimization issues comprising restriction types that are similar to those in scenarios 2 and 3. Furthermore, utilizing the TON model to solve the optimization issue for scenarios 1, 2, 3 and 4, the best cutting force can be taken as 61.129 N.

For the fourth output of the study (Fz, Meddour et al [50]), the initial assumption would be that models 3 and 12 are suitable if the selection had just been based on R^2_{training} and R^2_{testing} . Based on this argument, utilizing a method that considers the simplicity of the model and the desired models' capacity to provide realistic values, it is determined that only models 3 and 12 are suitable. As a result, misleading findings are unavoidable if the model building-optimum result finding analyses are not addressed as outlined in this article. As can be seen in Table 7.42, simplicity of model 3 is better than model 12. With this approach, the obtained model 3 (SON) is appropriate. Thus, the obtained model 3 (CS7-O4-SON) was chosen as the objective function required in analyses to get optimum results of Fz.

Table 7.46 shows the outcomes of four specific optimization scenarios for the chosen model. In scenario 1, all of the variables were utilized with their upper and lower limits in a continuous interval. There are three different results for the scenario 1. The minimum cutting force (Fz) outcomes were 43.8962 N, which correspond to SON. The suggested (optimum) designs are; cutting speed: 244 (m/min), depth of cut: 0.1 (mm), feed rate: 0.08 (mm/rev) and tool nose radius: 0.8 (mm). 43.896 N is a realistic result by compared with the results of experiment [50.33, 153.56]. We could say that the optimization scenario 1 reach lower cutting force than experimental results.

In scenario 2, feed rate, depth of cut and tool nose radius have been handled as continuous parameters, whereas the cutting speed is discontinuous (integers). The minimum cutting force for the SON model was same as the scenario 1.

In the third optimization scenario, the only limitation condition in the optimization process was taken as the feed force (F_x) smaller than 25 N and thrust force (F_y) smaller than 70 N for tangential force (F_z). The results are the same with scenario 1 and 2. The minimum cutting force has found as 47.576 N based on all optimization algorithms. The suggested (optimum) design variables are; cutting speed: 244 (m/min), depth of cut: 0.1 (mm), feed rate: 0.08 (mm/rev) and tool nose radius: 1.14716 (mm). 47.576 N is a realistic and better result in comparison with the experimental values.

For the fourth optimization scenario, all of the input parameters are supposed to be real numbers and the design variables can only take the experimental values. The minimum cutting force results are the same with scenarios 1 and 2.

From the point of stability, gaining identical outcomes for scenarios 1, 2, 3, and 4, whose phenomenological foundation is addressed using four distinct direct search methods, enhances the chance that acquired results are global optimum. Besides that, utilizing various methods for scenario 2 produces dissimilar outcomes, although they are identical. This situation is critical for optimization issues comprising restriction types that are similar to those in scenarios 2 and 3. Furthermore, utilizing the SON model to solve the optimization issue for scenarios 1, 2, 3 and 4, the best cutting force can be taken as 43.896 N. Due to the optimization results, the model chosen for the optimization procedure has achieved lower results than the experimental results.

Table 7.44: Optimization problem results of selected model CS7-O1-SOTN for surface roughness (Ra)

Objective Functions	Scenario No	Constraints	Optimization Algorithm	Feed Force (N)	Suggested Design
CS7-O1-SOTN	1	$120 < x1 < 244,$	MDE	6.062×10^{-9}	$x1 = 170.507, x2 = 0.1332226, x3 = 0.0812488, x4 = 1.17342$
		$0.1 < x2 < 0.3,$	MSA	1.733×10^{-8}	$x1 = 136.686, x2 = 0.12729, x3 = 0.0814472, x4 = 1.59995$
		$0.08 < x3 < 0.14,$	MRS	6.522×10^{-9}	$x1 = 205.605, x2 = 0.3, x3 = 0.0800003, x4 = 1.12592$
		$0.8 < x4 < 1.6$	MNMI	1.880×10^{-8}	$x1 = 189.446, x2 = 0.254518, x3 = 0.116577, x4 = 1.08584$
	2	$120 < x1 < 244,$	MDE	1.995×10^{-12}	$x1 = 237, x2 = 0.281563, x3 = 0.0847264, x4 = 1.10575$
		$0.1 < x2 < 0.3,$	MSA	0.001	$x1 = 177, x2 = 0.299956, x3 = 0.139946, x4 = 0.800487$
		$0.08 < x3 < 0.14,$	MRS	0.001	$x1 = 177, x2 = 0.3, x3 = 0.14, x4 = 0.8$
		$0.8 < x4 < 1.6$ $\{x1\} \in \text{Integers}$	MNMI	0.109	$x1 = 243, x2 = 0.1, x3 = 0.14, x4 = 0.8$
	4	$x1 = \{120, 182, 244\},$	MDE	0.155	$x1 = 244, x2 = 0.1, x3 = 0.08, x4 = 1.6$
		$x2 = \{0.1, 0.2, 0.3\},$	MSA	0.155	$x1 = 244, x2 = 0.1, x3 = 0.08, x4 = 1.6$
		$x3 = \{0.08, 0.11, 0.14\},$	MRS	0.155	$x1 = 244, x2 = 0.1, x3 = 0.08, x4 = 1.6$
		$x4 = \{0.8, 1.2, 1.6\}$	MNMI	0.155	$x1 = 244, x2 = 0.1, x3 = 0.08, x4 = 1.6$

Table 7.45: Optimization problem results of selected model CS7-O2-L for feed force (Fx)

Objective Functions	Scenario No	Constraints	Optimization Algorithm	Feed Force (N)	Suggested Design
CS7-O2-L	1	120 < x1 < 244,	MDE	16.921	x1 = 120, x2 = 0.1, x3 = 0.08, x4 = 1.6
		0.1 < x2 < 0.3,	MSA	16.921	x1 = 120, x2 = 0.1, x3 = 0.08, x4 = 1.6
		0.08 < x3 < 0.14,	MRS	16.921	x1 = 120, x2 = 0.1, x3 = 0.08, x4 = 1.6
		0.8 < x4 < 1.6	MNM	16.921	x1 = 120, x2 = 0.1, x3 = 0.08, x4 = 1.6
	2	120 < x1 < 244,	MDE	16.921	x1 = 120, x2 = 0.1, x3 = 0.08, x4 = 1.6
		0.1 < x2 < 0.3,	MSA	17.019	x1 = 120, x2 = 0.100034, x3 = 0.0815639, x4 = 1.59939
		0.08 < x3 < 0.14,	MRS	17.173	x1 = 134, x2 = 0.1, x3 = 0.08, x4 = 1.6
		0.8 < x4 < 1.6 {x1} ∈ Integers	MNM	16.921	x1 = 120, x2 = 0.1, x3 = 0.08, x4 = 1.6
	3	120 < x1 < 244,	MDE	21.688	x1 = 244, x2 = 0.1, x3 = 0.08, x4 = 1.28994
		0.1 < x2 < 0.3,	MSA	21.688	x1 = 244, x2 = 0.1, x3 = 0.08, x4 = 1.28994
		0.08 < x3 < 0.14,	MRS	21.688	x1 = 244, x2 = 0.1, x3 = 0.08, x4 = 1.28994
		0.8 < x4 < 1.6, Tangential Force < 50, Thrust Force < 70	MNM	21.688	x1 = 244, x2 = 0.1, x3 = 0.08, x4 = 1.28994
4	x1 = {120, 182, 244},	MDE	16.921	x1 = 120, x2 = 0.1, x3 = 0.08, x4 = 1.6	
	x2 = {0.1, 0.2, 0.3},	MSA	16.921	x1 = 120, x2 = 0.1, x3 = 0.08, x4 = 1.6	
	x3 = {0.08, 0.11, 0.14},	MRS	16.921	x1 = 120, x2 = 0.1, x3 = 0.08, x4 = 1.6	
	x4 = {0.8, 1.2, 1.6}	MNM	16.921	x1 = 120, x2 = 0.1, x3 = 0.08, x4 = 1.6	

Table 7.46: Optimization problem results of selected model CS7-O3-TON for thrust force (Fy)

Objective Functions	Scenario No	Constraints	Optimization Algorithm	Thrust Force (N)	Suggested Design
CS7-O3-TON	1	$120 < x1 < 244$,	MDE	65.271	$x1 = 244, x2 = 0.1, x3 = 0.08, x4 = 1.38679$
		$0.1 < x2 < 0.3$,	MSA	65.271	$x1 = 244, x2 = 0.1, x3 = 0.08, x4 = 1.38569$
		$0.08 < x3 < 0.14$,	MRS	60.120	$x1 = 244, x2 = 0.3, x3 = 0.08, x4 = 0.8$
		$0.8 < x4 < 1.6$	MNM	65.271	$x1 = 244, x2 = 0.1, x3 = 0.08, x4 = 1.38653$
	2	$120 < x1 < 244$,	MDE	65.271	$x1 = 244, x2 = 0.1, x3 = 0.08, x4 = 1.38679$
		$0.1 < x2 < 0.3$,	MSA	61.129	$x1 = 243, x2 = 0.3, x3 = 0.08, x4 = 0.8$
		$0.08 < x3 < 0.14$,	MRS	63.135	$x1 = 241, x2 = 0.3, x3 = 0.08, x4 = 0.8$
		$0.8 < x4 < 1.6$, $\{x1\} \in \text{Integers}$	MNM	67.770	$x1 = 120, x2 = 0.1, x3 = 0.0849117, x4 = 1.20602$
	3	$120 < x1 < 244$,	MDE	66.190	$x1 = 244, x2 = 0.1, x3 = 0.08, x4 = 1.28994$
		$0.1 < x2 < 0.3$,	MSA	66.190	$x1 = 244, x2 = 0.1, x3 = 0.08, x4 = 1.28994$
		$0.08 < x3 < 0.14$,	MRS	66.190	$x1 = 244, x2 = 0.1, x3 = 0.08, x4 = 1.28994$
		$0.8 < x4 < 1.6$, Feed Force < 25, Tangential Force < 50	MNM	66.190	$x1 = 244, x2 = 0.1, x3 = 0.08, x4 = 1.28994$
4	$x1 = \{120, 182, 244\}$,	MDE	60.120	$x1 = 244, x2 = 0.3, x3 = 0.08, x4 = 0.8$	
	$x2 = \{0.1, 0.2, 0.3\}$,	MSA	60.120	$x1 = 244, x2 = 0.3, x3 = 0.08, x4 = 0.8$	
	$x3 = \{0.08, 0.11, 0.14\}$,	MRS	60.120	$x1 = 244, x2 = 0.3, x3 = 0.08, x4 = 0.8$	
	$x4 = \{0.8, 1.2, 1.6\}$	MNM	60.120	$x1 = 244, x2 = 0.3, x3 = 0.08, x4 = 0.8$	

Table 7.47: Optimization problem results of selected model CS7-O4-SON for tangential force (Fz)

Objective Functions	Scenario No	Constraints	Optimization Algorithm	Thrust Force (N)	Suggested Design
CS7-O4-SON	1	120 < x1 < 244,	MDE	43.896	x1 = 244, x2 = 0.1, x3 = 0.08, x4 = 0.8
		0.1 < x2 < 0.3,	MSA	43.896	x1 = 244, x2 = 0.1, x3 = 0.08, x4 = 0.8
		0.08 < x3 < 0.14,	MRS	43.896	x1 = 244, x2 = 0.1, x3 = 0.08, x4 = 0.8
		0.8 < x4 < 1.6	MNM	43.896	x1 = 244, x2 = 0.1, x3 = 0.08, x4 = 0.8
	2	120 < x1 < 244,	MDE	43.896	x1 = 244, x2 = 0.1, x3 = 0.08, x4 = 0.8
		0.1 < x2 < 0.3,	MSA	43.896	x1 = 244, x2 = 0.1, x3 = 0.08, x4 = 0.8
		0.08 < x3 < 0.14,	MRS	43.896	x1 = 244, x2 = 0.1, x3 = 0.08, x4 = 0.8
		0.8 < x4 < 1.6, {x1} ∈ Integers	MNM	43.896	x1 = 244, x2 = 0.1, x3 = 0.08, x4 = 0.8
	3	120 < x1 < 244,	MDE	47.576	x1 = 244, x2 = 0.1, x3 = 0.08, x4 = 1.14716
		0.1 < x2 < 0.3,	MSA	47.576	x1 = 244, x2 = 0.1, x3 = 0.08, x4 = 1.14716
		0.08 < x3 < 0.14,	MRS	---	NO LOGICAL SOLUTION
		0.8 < x4 < 1.6, Feed Force < 25, Thrust Force < 70	MNM	47.576	x1 = 244, x2 = 0.1, x3 = 0.08, x4 = 1.14716
4	x1 = {120, 182, 244},	MDE	43.896	x1 = 244, x2 = 0.1, x3 = 0.08, x4 = 0.8	
	x2 = {0.1, 0.2, 0.3},	MSA	43.896	x1 = 244, x2 = 0.1, x3 = 0.08, x4 = 0.8	
	x3 = {0.08, 0.11, 0.14},	MRS	43.896	x1 = 244, x2 = 0.1, x3 = 0.08, x4 = 0.8	
	x4 = {0.8, 1.2, 1.6}	MNM	43.896	x1 = 244, x2 = 0.1, x3 = 0.08, x4 = 0.8	

For first output surface roughness (Ra) the design variables were fitted to the model with $R^2_{\text{training}} = 1.00$ and $R^2_{\text{testing}} = 1.00$ values: $\text{Abs}[-0.428198 - 0.789724 \text{Cos}[x1] + 0.419809 \text{Cos}[x1]^2 - 1.14756 \text{Cos}[x2] - 4.20092 \text{Cos}[x1] \text{Cos}[x2] + 0.973106 \text{Cos}[x2]^2 + 0.0618098 \text{Cos}[x3] + 2.21932 \text{Cos}[x1] \text{Cos}[x3] + 2.36543 \text{Cos}[x2] \text{Cos}[x3] + 1.51433 \text{Cos}[x3]^2 - 4.12479 \text{Cos}[x4] + 0.44785 \text{Cos}[x1] \text{Cos}[x4] + 9.40322 \text{Cos}[x2] \text{Cos}[x4] - 4.77729 \text{Cos}[x3] \text{Cos}[x4] - 1.13648 \text{Cos}[x4]^2 - 1.67836 \text{Sin}[x1] - 1.36064 \text{Cos}[x1] \text{Sin}[x1] + 7.30472 \text{Cos}[x2] \text{Sin}[x1] - 4.48619 \text{Cos}[x3] \text{Sin}[x1] + 0.0744336 \text{Cos}[x4] \text{Sin}[x1] - 0.596695 \text{Sin}[x1]^2 - 1.1232 \text{Sin}[x2] - 1.25851 \text{Cos}[x1] \text{Sin}[x2] + 0.453946 \text{Cos}[x2] \text{Sin}[x2] + 0.0018139 \text{Cos}[x3] \text{Sin}[x2] + 3.0389 \text{Cos}[x4] \text{Sin}[x2] + 1.46066 \text{Sin}[x1] \text{Sin}[x2] - 1.18069 \text{Sin}[x2]^2 - 4.25857 \text{Sin}[x3] + 3.10668 \text{Cos}[x1] \text{Sin}[x3] - 4.48172 \text{Cos}[x2] \text{Sin}[x3] - 3.1809 \text{Cos}[x3] \text{Sin}[x3] + 4.6226 \text{Cos}[x4] \text{Sin}[x3] - 2.62635 \text{Sin}[x1] \text{Sin}[x3] - 2.70701 \text{Sin}[x2] \text{Sin}[x3] - 1.97363 \text{Sin}[x3]^2 - 1.21038 \text{Sin}[x4] + 0.295984 \text{Cos}[x1] \text{Sin}[x4] - 1.8804 \text{Cos}[x2] \text{Sin}[x4] + 1.26921 \text{Cos}[x3] \text{Sin}[x4] - 1.45892 \text{Cos}[x4] \text{Sin}[x4] - 0.0163039 \text{Sin}[x1] \text{Sin}[x4] + 1.62642 \text{Sin}[x2] \text{Sin}[x4] + 8.03857 \text{Sin}[x3] \text{Sin}[x4] + 0.431409 \text{Sin}[x4]^2$. According to scenarios, minimum surface roughness has found as $0.155 \mu\text{m}$. The suggested (optimum) design variables are; cutting speed: 244 (m/min), depth of cut: 0.1 (mm/rev), feed rate: 0.08 (mm) and tool nose radius: 1.6 (mm). $0.155 \mu\text{m}$ could be a realistic and better result in comparison with the experimental results [0.24, 0.5].

For second output feed force (Fx) the design variables were fitted to the model with $R^2_{\text{training}} = 0.82$ and $R^2_{\text{testing}} = 0.85$ values: $6.85614 + 0.0180162 [x1] + 164.894 [x2] + 56.0767 [x3] - 8.17055 [x4]$. According to scenarios, minimum feed force has found as 16.921 N with the following conditions; cutting speed: 120m/min, depth of cut: 0.1mm, feed rate: 0.08mm/rev and and tool nose radius: 1.6mm. 16.921 N could be a realistic and better result in comparison with the experimental results [17.94, 61.93].

For third output thrust force (Fy) the design variables were fitted to the model with $R^2_{\text{training}} = 0.96$ and $R^2_{\text{testing}} = 0.83$ values: $122.983 - 0.0806463 [x1] - 0.00110289 [x1]^2 + 1.91791 \times 10^{-6} [x1]^3 + 388.008 [x2] + 5.61377 [x1] [x2] - 0.0126331 [x1]^2 [x2] + 453.431 [x2]^2 - 19.6677 [x1] [x2]^2 - 2267.35 [x2]^3 + 319.979 [x3] - 13.1523$

$[x1] [x3] + 0.0249281 [x1]^2 [x3] - 1650.55 [x2] [x3] - 23.5131 [x1] [x2] [x3] + 12889.3 [x2]^2 [x3] - 3494.05 [x3]^2 + 40.8215 [x1] [x3]^2 + 26539.5 [x2] [x3]^2 - 70469.4 [x3]^3 - 79.7281 [x4] + 0.571859 [x1] [x4] - 0.000449922 [x1]^2 [x4] - 943.099 [x2] [x4] + 6.23819 [x1] [x2] [x4] + 2869.03 [x2]^2 [x4] + 778.269 [x3] [x4] + 3.38332 [x1] [x3] [x4] - 3823.16 [x2] [x3] [x4] + 17924.8 [x3]^2 [x4] - 17.0813 [x4]^2 - 0.644103 [x1] [x4]^2 - 316.453 [x2] [x4]^2 - 1777.75 [x3] [x4]^2 + 109.793 [x4]^3$. According to scenarios, minimum thrust force has found as 60.120 N with the following conditions; cutting speed: 244m/min, depth of cut: 0.3mm, feed rate: 0.08mm/rev and and tool nose radius: 0.8mm. 60.120 N could be a realistic and better result in comparison with the experimental results [67.63, 171.31].

For forth output tangential force (Fz) the design variables were fitted to the model with $R^2_{\text{training}} = 0.97$ and $R^2_{\text{testing}} = 0.89$ values: $185.476 - 0.631289 [x1] + 0.000535502 [x1]^2 - 39.8502 [x2] - 0.294205 [x1] [x2] + 235.804 [x2]^2 - 1871.6 [x3] + 4.52075 [x1] [x3] + 3380.83 [x2] [x3] + 4262.12 [x3]^2 + 9.79693 [x4] - 0.0542013 [x1] [x4] - 28.9436 [x2] [x4] - 105.208 [x3] [x4] + 13.0136 [x4]^2$. According to scenarios, minimum tangential force has found as 43.896 N with the following conditions; cutting speed: 244m/min, depth of cut: 0.1mm, feed rate: 0.08mm/rev and and tool nose radius: 0.8mm. 43.896 N could be a realistic and better result in comparison with the experimental results [50.33, 153.56].

7.9 Case Study #8

The eighth literature study which optimization process was studied taken from Qu et al [51]. Deflection, quality, and productivity of formed parts are affected by the machining parameters selected when milling thin-walled plates. To find and evaluate the optimal design variables for thin-walled plates, this study proposes an optimization technique. Based on the experimental data, regression models for cutting force and surface roughness have been constructed as objective functions. It is also examined how design variables impact response parameters. In this work, cutting force, surface roughness, and material removal rate are investigated under constraint-induced restrictions.

As depicted in Table 7.47, the changes in values of these input parameters provided the obtaining of different outcomes for the surface roughness and cutting force.

Therefore, these obtaining results depending on the change in these input parameter values are sufficient to develop an optimization strategy. Moreover, it is impossible to establish a proportional connection between measured surface roughness, cutting forces values and three input variables (spindle speed, feed per tooth and axial depth of cut) as understood from Table 7.47. Therefore, it is necessary to optimize these parameters to reach minimum response parameters.

Table 7.48: Experimental results of surface roughness and cutting force with different experimental conditions [51]

Exp No	Spindle speed (n , r/min)	Feed per tooth (f , mm)	Axial depth of cut (ap , mm)	Cutting Force (Fa , N)	Surface Roughness (Ra , μm)
1	1600	0.15	0.4	27.3	0.532
2	1600	0.15	0.55	42.7	0.853
3	1600	0.15	0.7	58.5	1.215
4	1600	0.2	0.4	33.2	0.587
5	1600	0.2	0.55	52.8	0.912
6	1600	0.2	0.7	70.2	1.316
7	1600	0.25	0.4	39.2	0.671
8	1600	0.25	0.55	54.6	1.030
9	1600	0.25	0.7	69.8	1.487
10	2100	0.15	0.4	35.3	0.498
11	2100	0.15	0.55	49.6	0.834
12	2100	0.15	0.7	68.5	1.042
13	2100	0.2	0.4	39.7	0.566
14	2100	0.2	0.55	56.5	0.878
15	2100	0.2	0.7	73.4	1.195
16	2100	0.25	0.4	43.9	0.627
17	2100	0.25	0.55	58.3	0.902
18	2100	0.25	0.7	73.6	1.268
19	2600	0.15	0.4	38.5	0.468
20	2600	0.15	0.55	52.7	0.815
21	2600	0.15	0.7	72.3	0.926
22	2600	0.2	0.4	43.6	0.487
23	2600	0.2	0.55	61.3	0.773
24	2600	0.2	0.7	82.3	1.026
25	2600	0.25	0.4	48.9	0.568
26	2600	0.25	0.55	71.4	0.869
27	2600	0.25	0.7	85.6	1.056

The behavior of the system was explained by the regression models given below [51];

$$Fa = -52.07 - 0.006 \times n + 381.01 \times f + 80.35 \times ap + 0.0243 \times n \times f - 13.333 \times f \times ap + 0.0116 \times n \times ap - 784.44 \times f^2 + 9.8765 \times ap^2 \quad (7.21)$$

$$Ra = -1.2445 + 0.0005 \times n + 0.3691 \times f + 3.738 \times ap - 0.01 \times n \times f + 2.8889 \times f \times ap - 0.0008 \times n \times ap + 4.0222 \times f^2 - 0.4864 \times ap^2 \quad (7.22)$$

The experimental data was represented by these regression models with determination coefficients (R^2) of 0.9864 and 0.9882, respectively.

Qu et al. [51] figured out this limited optimization issue by defining all the input parameters as discrete and proceeded in the modeling process only according to the standard R^2 results and listed the models. The R^2 values Qu et al. [51] found about 98%. Qu et al. [51] does not mention the R^2_{training} and R^2_{testing} distinction in the modeling process and does not mention determining models according to different scenarios. As can be clearly seen that smaller surface roughness and cutting forces may be calculated with the variables as a consequence of optimization.

7.9.1 Optimization Scenarios

For all scenarios, the limitations for the system inputs (design parameters) as in the following form;

$$\begin{aligned} 1600 \leq \text{Spindle speed} \leq 2600 & \quad , \quad (r/min) \\ 0.15 \leq \text{Feed per tooth} \leq 0.25 & \quad , \quad (mm) \\ 0.4 \leq \text{Axial depth of cut} \leq 0.7 & \quad , \quad (mm) \end{aligned}$$

7.9.1.1 Scenario 1

Surface roughness and cutting forces are explained by the objective functions in this optimal solution problem. There are no constraints about the input parameters so they can be real numbers, and the computation area is continuous. The primary goal is to minimize the response parameters. It is also technically possible to see these theory-based boundaries of the objective function this way.

7.9.1.2 Scenario 2

Scenario 1 should include additional realistic situations in addition to knowledge-based ones. A novel optimal solution is provided that implies the reduction of the responses for this application. Input parameters are also restricted with integers.

7.9.1.3 Scenario 3

As different from scenario 1, non-linear constraints are added for the optimization problem. For cutting force, surface roughness should be smaller than 20 N and for surface roughness, cutting force should be smaller than 0.43 μm . Problem solving will be more complex and difficult in this instance than in scenarios 1 and 2.

7.9.1.4 Scenario 4

In the constructed of scenario 4, more viable and more limited issue situations should be included to scenario 2. For that reason, there is a new optimum solution problem created to the minimization of the response values. Unlike Scenario 2, in scenario 4 parameters can only take the values in the data table.

7.9.2 Results and Discussion

In our approach, different from the classical ones, various regression models are first tested utilizing both R^2_{training} and R^2_{testing} values (not only R^2 as in the classical approach) to reveal what is the degree of performance of the model can explain the method. Besides, the model's operational restriction (boundedness) is also checked by calculating the highest and lowest values that the related model creates. Therefore, our proposed design strategy provides producing realistic values. Also, it is necessary to check the limitedness of decided models, whether producing realistic results. Regarding of these facts, by using our proposed approach, the experimental data tables of surface roughness and cutting forces listed as Table 7.48 and 7.49 can be seen below. Therefore, it is necessary to optimize these parameters to minimize of all the response values.

Table 7.49: Results of the Neuro-regression models for the cutting force

Models	R^2_{training}	R^2_{testing}	Max (N)	Min (N)
CS8-O1-L	0.98	0.98	84.199	26.822
CS8-O1-LR	0.98	0.96	86.012	28.958
CS8-O1-SON	0.99	0.97	85.413	28.870
CS8-O1-SONR	1.00	0.87	85.616	-2.782×10^{10}
CS8-O1-TON	1.00	0.97	86.582	27.845
CS8-O1-FOTN	0.98	0.99	90.391	19.691
CS8-O1-FOTNR	0.99	0.97	94.896	26.314
CS8-O1-SOTN	1.00	0.97	5520.05	-999.647
CS8-O1-SOTNR	1.00	0.37	2.327×10^{10}	-6.118×10^9
CS8-O1-FOLN	0.97	0.98	82.658	25.645
CS8-O1-FOLNR	0.98	0.96	85.101	28.813
CS8-O1-SOLN	0.99	0.97	85.153	28.914
CS8-O1-SOLNR	1.00	0.92	85.623	-2.546×10^{11}

Table 7.50: Results of the Neuro-regression models for the surface roughness

Models	R^2_{training}	R^2_{testing}	Max (μm)	Min (μm)
CS8-O2-L	0.96	0.95	1.328	0.414
CS8-O2-LR	0.99	0.98	1.468	0.495
CS8-O2-SON	0.99	0.98	1.445	0.498
CS8-O2-SONR	1.00	0.91	1.508	0.460
CS8-O2-TON	1.00	0.97	1.494	0.465
CS8-O2-FOTN	0.96	0.95	1.421	0.419
CS8-O2-FOTNR	0.99	0.94	0.509	-2.173×10^7
CS8-O2-SOTN	1.00	0.97	547.542	-117.88
CS8-O2-SOTNR	0.99	0.91	1.943×10^8	-1.797×10^{14}
CS8-O2-FOLN	0.95	0.96	1.310	0.399
CS8-O2-FOLNR	0.98	0.98	1.475	0.492
CS8-O2-SOLN	0.98	0.97	1.438	0.497
CS8-O2-SOLNR	1.00	0.99	8.75×10^9	0.459

For the first output of the study (Fa, Qu et al. [51]), results show that if the R^2 value was the key element considered in decided the model, we may conclude that all models accurately describe the process. Because R^2_{training} results are nearly all close to 1.

The initial assumption would be that lots of models are suitable if the selection had just been based on R^2_{training} and R^2_{testing} . Based on this argument, utilizing a method that considers the simplicity of the models and the desired models' capacity to provide realistic values, it is determined that only model 6 (FOTN) is suitable. As a result, misleading findings are unavoidable if the model building-optimum result finding analyses are not addressed as outlined in this article. Thus, the obtained model 6 (CS8-O1-FOTN) was chosen as the objective function required in analyses to get optimum results of cutting force. Outcomes of the selected model can be spotted in Table 7.48.

Table 7.50 shows the outcomes of four specific optimization scenarios for the chosen model. In scenario 1, all of the variables were utilized with their upper and lower limits in a continuous interval. The minimum cutting force outcomes, depending on all of the optimization techniques, were 19.693 N, which correspond to FOTN. The suggested (optimum) design variables are change with optimization algorithms so there are four different spindle speed values. However, feed per tooth: 0.15 (mm) and axial depth of cut: 0.4 (mm). 19.693 N is a realistic and better result by compared with the results of experiment [27.3, 85.6]. We could say that the optimization scenario 1 reach lower cutting force than experimental results.

In the second optimization scenario, feed per tooth and axial depth of cut have been treated as continuous parameters while the spindle speed is discrete (integers). In this case, there are three different results but the minimum cutting force value for the FOTN model can be taken as 19.695 N. The suggested (optimum) design variables are; spindle speed: 2378 (r/min), feed per tooth: 0.15 (mm) and axial depth of cut: 0.4 (mm). In the scenario 2, minimum cutting force results are smaller than experimental results as in scenario 1.

In the third optimization scenario, the only limitation condition in the optimization process was taken as the surface roughness (R_a) smaller than 0.43 μm for the cutting force (F_a). The results are the same with scenario 1 and 2.

For the fourth optimization scenario, all of the input parameters are supposed to be real numbers and the design variables can only take the experimental values. The

minimum cutting force had found as 26.813 N. The suggested (optimum) design variables are; spindle speed: 1600 (r/min), feed per tooth: 0.15 (mm) and axial depth of cut: 0.4 (mm). Optimization scenario 4 results are better by compared with the results of experiment.

Although the outcomes of scenario 4 are bigger compared to scenarios 1, 2 and 3, it can be seen that it shows better results when compared to the reference study. It is clearly stated that the created model according to the reference study and optimization process provides efficient and robust results.

For the second output of the study (Ra, Qu et al [51]), results show that if the R^2 value was the key element considered in decided the model, we may conclude that all models accurately describe the process. Because R^2_{training} results are nearly all close to 1.

The initial assumption would be that lots of models are suitable if the selection had just been based on R^2_{training} and R^2_{testing} . Based on this argument, utilizing a method that considers the simplicity of the models and the desired models' capacity to provide realistic values, it is determined that only model 1 (L) is suitable. As a result, misleading findings are unavoidable if the model building-optimum result finding analyses are not addressed as outlined in this article. Thus, the obtained model 1 (CS8-O2-L) was chosen as the objective function required in analyses to get optimum results of surface roughness. Outcomes of the selected model can be spotted in Table 7.49.

Table 7.51 shows the outcomes of four specific optimization scenarios for the chosen model. In scenario 1, all of the variables were utilized with their upper and lower limits in a continuous interval. The minimum cutting force outcomes, depending on all of the optimization techniques, were 0.414 μm , which correspond to FOTN. The suggested (optimum) design variables are; cutting speed: 2600 (r/min), feed per tooth: 0.15 (mm/rev) and axial depth of cut: 0.4 (mm). 0.414 μm is a realistic and better result by compared with the results of experiment [0.468, 1.487]. We could say that the optimization scenario 1 reach lower cutting force than experimental results.

In the second optimization scenario, feed per tooth and axial depth of cut have been treated as continuous variables while the cutting speed is discrete (integers). The minimum surface roughness outcomes for the L model were same as the scenario 1.

In the third optimization scenario, the only limitation condition in the optimization process was taken as the cutting force (F_a) smaller than 20 N for the surface roughness (R_a). Although there are three different results, the minimum surface roughness is 0.414 μm .

For the fourth optimization scenario, all of the input parameters are supposed to be real numbers and the design variables can only take the experimental values. The results are the same with scenario 1 and 2.

From the point of stability, gaining identical outcomes for scenarios 1, 2, 3, and 4, whose phenomenological foundation is addressed using four distinct direct search methods, enhances the chance that acquired results are global optimum. Besides that, utilizing various methods for scenario 3 produces dissimilar outcomes, although they are identical. This situation is critical for optimization issues comprising restriction types that are similar to those in scenarios 2 and 3. Furthermore, utilizing the L model to solve the optimization issue for scenarios 1, 2, 3 and 4, the best surface roughness can be taken as 0.414 μm . Due to the optimization results, the model chosen for the optimization procedure has achieved lower results than the experimental results.

Table 7.51: Optimization problem results of selected model CS8-O1-FOTN for cutting force

Objective Functions	Scenario No	Constraints	Optimization Algorithm	Cutting Force (N)	Suggested Design
CS8-O1-FOTN	1	$1600 < x1 < 2600,$ $0.15 < x2 < 0.25,$ $0.4 < x3 < 0.7,$	MDE	19.693	$x1 = 1755.98, x2 = 0.15, x3 = 0.4$
			MSA	19.693	$x1 = 2082.71, x2 = 0.15, x3 = 0.4$
			MRS	19.693	$x1 = 1931.91, x2 = 0.15, x3 = 0.4$
			MNM	19.693	$x1 = 2591.65, x2 = 0.15, x3 = 0.4$
	2	$1600 < x1 < 2600,$ $0.15 < x2 < 0.25,$ $0.4 < x3 < 0.7,$ $\{x1\} \in \text{Integers}$	MDE	19.695	$x1 = 2378, x2 = 0.15, x3 = 0.4$
			MSA	19.701	$x1 = 2001, x2 = 0.150014, x3 = 0.400005$
			MRS	19.695	$x1 = 2378, x2 = 0.15, x3 = 0.4$
			MNM	19.726	$x1 = 2598, x2 = 0.15, x3 = 0.4$
	3	$1600 < x1 < 2600,$ $0.15 < x2 < 0.25,$ $0.4 < x3 < 0.7,$ Surface Roughness < 0.43	MDE	19.693	$x1 = 2597.93, x2 = 0.15, x3 = 0.4$
			MSA	19.693	$x1 = 2579.08, x2 = 0.15, x3 = 0.4$
			MRS	19.693	$x1 = 2597.93, x2 = 0.15, x3 = 0.4$
			MNM	19.693	$x1 = 2597.93, x2 = 0.15, x3 = 0.4$
4	$x1 = \{1600, 2100, 2600\},$ $x2 = \{0.15, 0.20, 0.25\},$ $x3 = \{0.4, 0.55, 0.7\}$	MDE	26.813	$x1 = 1600, x2 = 0.15, x3 = 0.4$	
		MSA	26.813	$x1 = 1600, x2 = 0.15, x3 = 0.4$	
		MRS	26.813	$x1 = 1600, x2 = 0.15, x3 = 0.4$	
		MNM	26.813	$x1 = 1600, x2 = 0.15, x3 = 0.4$	

Table 7.52: Optimization problem results of selected model CS8-O2-L for surface roughness

Objective Functions	Scenario No	Constraints	Optimization Algorithm	Surface Roughness (μm)	Suggested Design
CS8-O2-L	1	$1600 < x_1 < 2600,$ $0.15 < x_2 < 0.25,$ $0.4 < x_3 < 0.7,$	MDE	0.414	$x_1 = 2600, x_2 = 0.15, x_3 = 0.4$
			MSA	0.414	$x_1 = 2600, x_2 = 0.15, x_3 = 0.4$
			MRS	0.414	$x_1 = 2600, x_2 = 0.15, x_3 = 0.4$
			MNM	0.414	$x_1 = 2600, x_2 = 0.15, x_3 = 0.4$
	2	$1600 < x_1 < 2600,$ $0.15 < x_2 < 0.25,$ $0.4 < x_3 < 0.7,$ $\{x_1\} \in \text{Integers}$	MDE	0.414	$x_1 = 2600, x_2 = 0.15, x_3 = 0.4$
			MSA	0.414	$x_1 = 2600, x_2 = 0.15, x_3 = 0.4$
			MRS	0.414	$x_1 = 2600, x_2 = 0.15, x_3 = 0.4$
			MNM	0.414	$x_1 = 2600, x_2 = 0.15, x_3 = 0.4$
	3	$1600 < x_1 < 2600,$ $0.15 < x_2 < 0.25,$ $0.4 < x_3 < 0.7,$ Cutting Force < 20	MDE	0.414	$x_1 = 2598.15, x_2 = 0.15, x_3 = 0.4$
			MSA	0.459	$x_1 = 2334.25, x_2 = 0.15, x_3 = 0.4$
			MRS	0.414	$x_1 = 2598.15, x_2 = 0.15, x_3 = 0.4$
			MNM	0.559	$x_1 = 1743.63, x_2 = 0.15, x_3 = 0.4$
4	$x_1 = \{1600, 2100, 2600\},$ $x_2 = \{0.15, 0.20, 0.25\},$ $x_3 = \{0.4, 0.55, 0.7\}$	MDE	0.414	$x_1 = 2600, x_2 = 0.15, x_3 = 0.4$	
		MSA	0.414	$x_1 = 2600, x_2 = 0.15, x_3 = 0.4$	
		MRS	0.414	$x_1 = 2600, x_2 = 0.15, x_3 = 0.4$	
		MNM	0.414	$x_1 = 2600, x_2 = 0.15, x_3 = 0.4$	

Regarding of these facts, by using our proposed approach, for cutting force the design variables were fitted to the model with $R^2_{\text{training}} = 0.98$ and $R^2_{\text{testing}} = 0.99$ values: $-1375.27 + 12.9017 \text{ Cos}[x1] + 1393.95 \text{ Cos}[x2] - 69.4043 \text{ Cos}[x3] - 2.18913 \text{ Sin}[x1] + 395.32 \text{ Sin}[x2] + 88.8538 \text{ Sin}[x3]$. Minimum cutting force has found as 19.693 N according to scenarios 1, 2 and 3. In scenario 4, minimum cutting force has found as 26.813 N with the following conditions; spindle speed: 1600r/min, feed per tooth: 0.15m and axial depth of cut: 0.4mm. 26.813 N is a realistic and better result in comparison with the experimental results [27.3, 85.6].

For surface roughness the design variables were fitted to the model with $R^2_{\text{training}} = 0.96$ and $R^2_{\text{testing}} = 0.95$ values: $-0.161913 - 0.000169284 [x1] + 1.33365 [x2] + 2.03907 [x3]$. According to scenarios, minimum surface roughness has found as 0.414 μm with the following conditions; spindle speed: 2600r/min, feed per tooth: 0.15m and axial depth of cut: 0.4mm. 0.414 μm is a realistic and better result in comparison with the experimental results [0.468, 1.316].

7.10 Case Study #9

The ninth literature study which optimization process was studied taken from Paturi et al. [52]. This study provides a regression analysis and artificial neural network (ANN) technique for forecasting surface roughness during hard turning of AISI 52100. Real-time Taguchi L27 orthogonal array tests provided the surface roughness data necessary to develop and assess RA and ANN models. Design variables such as cutting speed, feed rate, and depth of cut were evaluated as inputs in the construction of RA and ANN models. The accuracy of the RA model was checked using the analysis of variance (ANOVA), Anderson–Darling test, and standard normal plots. In order to practice and validate the neural network model, the MATLAB tool was used. Models RA and ANN were used to estimate surface roughness degree. There is a correlation both projected and empirical values when employing RA or ANN models.

As depicted in Table 7.52, the changes in values of these input parameters provided the obtaining of different results for the surface roughness.

Therefore, these obtaining results depending on the change in these input parameter values are sufficient to develop an optimization strategy. Moreover, it is impossible to establish a proportional connection between measured surface roughness and three design variables (cutting speed, feed and depth of cut) as understood from Table 7.52. Therefore, it is necessary to optimize these parameters to achieve minimum surface roughness.

Table 7.53: Experimental results of surface roughness with different experimental conditions [52]

Exp No	Cutting speed (V_c, m/min)	Feed (f, mm/rev)	Depth of cut (ap, mm)	Surface Roughness (R_a, μm)
1	100	0.1	0.05	3.25
2	100	0.1	0.10	3.5
3	100	0.1	0.15	3.83
4	100	0.2	0.05	4.81
5	100	0.2	0.10	5.36
6	100	0.2	0.15	5.52
7	100	0.3	0.05	6.77
8	100	0.3	0.10	7.11
9	100	0.3	0.15	7.39
10	150	0.1	0.05	2.47
11	150	0.1	0.10	2.85
12	150	0.1	0.15	3.23
13	150	0.2	0.05	4.06
14	150	0.2	0.10	4.45
15	150	0.2	0.15	5.02
16	150	0.3	0.05	6.39
17	150	0.3	0.10	7.08
18	150	0.3	0.15	7.53
19	200	0.1	0.05	1.95
20	200	0.1	0.10	2.38
21	200	0.1	0.15	2.95
22	200	0.2	0.05	3.38
23	200	0.2	0.10	4.03
24	200	0.2	0.15	4.37
25	200	0.3	0.05	5.51
26	200	0.3	0.10	5.89
27	200	0.3	0.15	6.51

The behavior of the system was explained by the regression models given below [52];

$$Ra = 2.5422 - 0.0041 \times Vc + 8.0111 \times f + 3.4222 \times ap + 25.5 \times f^2 - 8 \times ap^2 - 0.001 \times Vc \times f + 0.036 \times Vc \times ap + 7 \times f \times ap \quad (7.23)$$

The experimental data was represented by these regression model with determination coefficient (R^2) of 0.978.

Paturi et al. [52] figured out this limited optimization issue by defining all the input parameters as discrete and proceeded in the modeling process only according to the standard R^2 results and listed the models. The R^2 value Paturi et al [52] found about 97.8%. Paturi et al. [52] does not mention the R^2_{training} and R^2_{testing} distinction in the modeling process and does not mention determining model according to different scenarios. As can be clearly seen that smaller surface roughness may be calculated with the variables as a consequence of optimization.

7.10.1 Optimization Scenarios

For all scenarios, the limitations for the system inputs (design parameters) as in the following form;

$$\begin{aligned} 100 \leq \text{Cutting speed} \leq 200 & , \quad (m/min) \\ 0.1 \leq \text{Feed} \leq 0.3 & , \quad (mm/rev) \\ 0.05 \leq \text{Depth of cut} \leq 0.15 & , \quad (mm) \end{aligned}$$

7.10.1.1 Scenario 1

Surface roughness is explained by the objective function in this optimal solution problem. There are no constraints about the input parameters so they can be real numbers, and the computation area is continuous. The primary goal is to minimize the surface roughness. It is also technically possible to see these theory-based boundaries of the objective function this way.

7.10.1.2 Scenario 2

Scenario 2 should include additional realistic situations in addition to knowledge-based ones. A novel optimal solution is provided that implies the reduction of the

responses for this application. Input parameters are also restricted with integers. There is only one design variable that can be integer number.

7.10.1.3 Scenario 3

In the constructed of scenario 3, more viable and more limited issue situations should be included to scenario 2. For that reason, there is a new optimum solution problem created to the minimization of the response values. Unlike Scenario 2, in scenario 3 parameters can only take the values in the data table.

7.10.2 Results and Discussion

In our approach, different from the classical ones, various regression models are first tested utilizing both R^2_{training} and R^2_{testing} values (not only R^2 as in the classical approach) to reveal what is the degree of performance of the model can explain the method. Besides, the model's operational restriction (boundedness) is also checked by calculating the highest and lowest values that the related model creates. Therefore, our proposed design strategy provides producing realistic values. Also, it is necessary to check the limitedness of decided models, whether producing realistic results. Regarding of these facts, by using our proposed approach, the experimental data table of surface roughness listed as Table 7.53 can be seen below.

Table 7.54: Results of the Neuro-regression models for the surface roughness

Models	R^2_{training}	R^2_{testing}	Max (μm)	Min (μm)
CS9-O-L	0.98	0.97	7.617	1.871
CS9-O-LR	0.99	0.99	7.639	1.917
CS9-O-SON	0.99	0.98	7.588	1.812
CS9-O-SONR	0.99	-3.36	8.524×10^9	1.935
CS9-O-TON	0.99	0.97	7.592	1.978
CS9-O-FOTN	0.99	0.98	7.984	-3.127
CS9-O-FOTNR	0.99	0.96	7.565	1.997
CS9-O-SOTN	0.99	0.97	18036.	1.943
CS9-O-SOTNR	0.99	0.99	9.301×10^{11}	-2.714×10^{11}
CS9-O-FOLN	0.95	0.88	7.418	1.734
CS9-O-FOLNR	0.99	0.96	7.582	1.928
CS9-O-SOLN	0.99	0.97	7.581	1.809
CS9-O-SOLNR	0.99	-2.34	7.389	1.959

For the ninth study (Ra, Paturi et al. [52]), results show that if the R^2 value was the key element considered in deciding the model, we may conclude that all models accurately describe the process. Because R^2_{training} results are nearly all close to 1.

The initial assumption would be that lots of models are suitable if the selection had just been based on R^2_{training} and R^2_{testing} . Based on this argument, utilizing a method that considers the simplicity of the models and the desired models' capacity to provide realistic values, it is determined that only model 1 (L) is suitable. As a result, misleading findings are unavoidable if the model building-optimum result finding analyses are not addressed as outlined in this article. Thus, the obtained model 1 (CS9-O-L) was chosen as the objective function required in analyses to get optimum results of surface roughness. Outcomes of the selected model can be spotted in Table 7.53.

Table 7.54 shows the outcomes of three specific optimization scenarios for the chosen model. In scenario 1, all of the variables were utilized with their upper and lower limits in a continuous interval. The minimum surface roughness outcomes, depending on all of the optimization techniques, were $1.871 \mu\text{m}$, which correspond to L. The suggested (optimum) design variables are; cutting speed: 200 (m/min),

feed rate: 0.1 (mm/rev) and depth of cut: 0.05 (mm). 1.871 μm is a realistic result by compared with the results of experiment [1.95, 7.53]. We could say that the optimization results reach lower surface roughness than experimental results.

In scenario 2, feed rate and depth of cut have been treated as continuous variables while the cutting speed is discrete (integers). The minimum surface roughness outcomes for the L model were same as scenario 1.

For the third optimization scenario, all of the input parameters are supposed to be real numbers and the design variables can only take the experimental values. The results are the same with scenario 1 and 2.

From the point of stability, gaining identical outcomes for scenarios 1, 2 and 3, whose phenomenological foundation is addressed using four distinct direct search methods, enhances the chance that acquired results are global optimum. This situation is critical for optimization issues comprising restriction types that are similar to those in scenarios 1, 2 and 3. Furthermore, utilizing the L model to solve the optimization issue for scenarios 1, 2 and 3, the best surface roughness can be taken as 1.87138 μm . Due to the optimization results, the model chosen for the optimization procedure has achieved lower results than the experimental results.

Table 7.55: Optimization problem results of selected model CS9-O-L for surface roughness

Objective Functions	Scenario No	Constraints	Optimization Algorithm	Surface Roughness (μm)	Suggested Design
CS9-O-L	1	$100 < x_1 < 200,$ $0.1 < x_2 < 0.3,$ $0.05 < x_3 < 0.15$	MDE	1.871	$x_1 = 200, x_2 = 0.1, x_3 = 0.05$
			MSA	1.871	$x_1 = 200, x_2 = 0.1, x_3 = 0.05$
			MRS	1.871	$x_1 = 200, x_2 = 0.1, x_3 = 0.05$
			MNM	1.871	$x_1 = 200, x_2 = 0.1, x_3 = 0.05$
	2	$100 < x_1 < 200,$ $0.1 < x_2 < 0.3,$ $0.05 < x_3 < 0.15,$ $\{x_1\} \in \text{Integers}$	MDE	1.871	$x_1 = 200, x_2 = 0.1, x_3 = 0.05$
			MSA	2.038	$x_1 = 196, x_2 = 0.100167, x_3 = 0.0636804$
			MRS	1.871	$x_1 = 200, x_2 = 0.1, x_3 = 0.05$
			MNM	1.871	$x_1 = 200, x_2 = 0.1, x_3 = 0.05$
	3	$x_1 = \{100, 150, 200\},$ $x_2 = \{0.1, 0.2, 0.3\},$ $x_3 = \{0.05, 0.1, 0.15\}$	MDE	1.871	$x_1 = 200, x_2 = 0.1, x_3 = 0.05$
			MSA	1.871	$x_1 = 200, x_2 = 0.1, x_3 = 0.05$
			MRS	1.871	$x_1 = 200, x_2 = 0.1, x_3 = 0.05$
			MNM	1.871	$x_1 = 200, x_2 = 0.1, x_3 = 0.05$

Regarding of these facts, by using our proposed approach, for surface roughness the design variables were fitted to the model with $R^2_{\text{training}} = 0.98$ and $R^2_{\text{testing}} = 0.97$ values: $1.87061 - 0.0114886 [x1] + 18.6868 [x2] + 8.59617 [x3]$. According to scenarios, minimum surface roughness has found as $1.871 \mu\text{m}$ with the following conditions; cutting speed: 200m/min, feed: 0.1mm/rev and depth of cut: 0.05mm. $1.871 \mu\text{m}$ is a realistic and better result in comparison with the experimental results [1.95, 7.53].

As a consequence, it can be seen that when feed value rises, the grade of surface finish on the workpiece improves dramatically in the operation. With an increment in cutting speed, surface roughness tends to decrease. Smaller cutting forces and reduced heat transfer to the workpiece during the operation lead to reduced surface roughness or greater surface finish on the machined workpiece.

7.11 Case Study #10

The tenth literature study which optimization process was studied taken from Sahoo et al [53]. In this work, the Taguchi design of experiments is used to monitor the effectiveness of a multilayer-coated carbide cutting tool in the processing of toughened AISI D2 steel. To estimate surface roughness, an orthogonal Taguchi L27 array was used in the investigation. Analysis is performed on the S/N ratio and the optimal parametric situation. Besides, a variance analysis was performed in order to identify the major components that impact surface roughness. For surface roughness, feed is the greatest influential variable depending on Taguchi S/N ratio and ANOVA while the depth of cut is the poorest component. The outcomes show that the model explains 98 percent of the total variations.

As depicted in Table 7.55, the changes in values of these input parameters provided the obtaining of different results for the surface roughness.

Therefore, these obtaining results depending on the change in these input parameter values are sufficient to develop an optimization strategy. Moreover, it is impossible to establish a proportional connection between measured surface roughness and three design variables (cutting speed, feed and depth of cut) as understood from

Table 7.55. Therefore, it is necessary to optimize these parameters to achieve minimum surface roughness.

Table 7.56: Experimental results of surface roughness with different experimental conditions [53]

Exp No	Cutting speed (v , m/min)	Feed (f , mm/rev)	Depth of cut (t , mm)	Surface Roughness (Ra , μm)
1	80	0.05	0.1	0.55
2	80	0.05	0.2	0.58
3	80	0.05	0.3	0.62
4	80	0.1	0.1	0.81
5	80	0.1	0.2	0.85
6	80	0.1	0.3	0.88
7	80	0.15	0.1	1.17
8	80	0.15	0.2	1.22
9	80	0.15	0.3	1.29
10	150	0.05	0.1	0.44
11	150	0.05	0.2	0.48
12	150	0.05	0.3	0.51
13	150	0.1	0.1	0.72
14	150	0.1	0.2	0.76
15	150	0.1	0.3	0.8
16	150	0.15	0.1	1.1
17	150	0.15	0.2	1.15
18	150	0.15	0.3	1.21
19	220	0.05	0.1	0.31
20	220	0.05	0.2	0.38
21	220	0.05	0.3	0.42
22	220	0.1	0.1	0.6
23	220	0.1	0.2	0.64
24	220	0.1	0.3	0.68
25	220	0.15	0.1	0.97
26	220	0.15	0.2	1.05
27	220	0.15	0.3	1.11

The behavior of the system was explained by the regression models given below [53];

$$Ra = 0.2454 - 0.0014 \times v + 6.6444 \times f + 0.4722 \times t \quad (7.24)$$

The experimental data was represented by these regression model with determination coefficient (R^2) of 0.98.

Sahoo et al. 2013 [53] figured out this limited optimization issue by defining all the input parameters as discrete and proceeded in the modeling process only according to the standard R^2 results and listed the models. The R^2 value Sahoo et al. 2013 [53] found as 98%. Sahoo et al. 2013 [53] does not mention the R^2_{training} and R^2_{testing} distinction in the modeling process and does not mention determining model according to different scenarios. As can be clearly seen that smaller surface roughness may be calculated with the variables as a consequence of optimization.

7.11.1 Optimization Scenarios

For all scenarios, the limitations for the system inputs (design parameters) as in the following form;

$$\begin{aligned} 80 \leq \text{Cutting speed} \leq 220 & , \quad (m/min) \\ 0.05 \leq \text{Feed} \leq 0.15 & , \quad (mm/rev) \\ 0.1 \leq \text{Depth of cut} \leq 0.3 & , \quad (mm) \end{aligned}$$

7.11.1.1 Scenario 1

Surface roughness is explained by the objective function in this optimal solution problem. There are no constraints about the input parameters so they can be real numbers, and the computation area is continuous. The primary goal is to minimize the surface roughness. It is also technically possible to see these theory-based boundaries of the objective function this way.

7.11.1.2 Scenario 2

Scenario 2 should include additional realistic situations in addition to knowledge-based ones. A novel optimal solution is provided that implies the reduction of the responses for this application. Input parameters are also restricted with integers. There is only one design variable that can be integer number.

7.11.1.3 Scenario 3

In the constructed of scenario 3, more viable and more limited issue situations should be included to scenario 2. For that reason, there is a new optimum solution problem created to the minimization of the response values. Unlike Scenario 2, in scenario 3 parameters can only take the values in the data table.

7.11.2 Results and Discussion

In our approach, different from the classical ones, various regression models are first tested utilizing both R^2_{training} and R^2_{testing} values (not only R^2 as in the classical approach) to reveal what is the degree of performance of the model can explain the method. Besides, the model's operational restriction (boundedness) is also checked by calculating the highest and lowest values that the related model creates. Therefore, our proposed design strategy provides producing realistic values. Also, it is necessary to check the limitedness of decided models, whether producing realistic results. Regarding of these facts, by using our proposed approach, the experimental data table of surface roughness listed as Table 7.56 can be seen below.

Table 7.57: Results of the Neuro-regression models for the surface roughness

Models	R^2_{training}	R^2_{testing}	Max (μm)	Min (μm)
CS10-O-L	0.99	0.99	1.260	0.309
CS10-O-LR	0.99	0.99	1.278	0.325
CS10-O-SON	0.99	0.99	1.272	0.317
CS10-O-SONR	0.99	0.99	1.260	-4.631x10 ⁸
CS10-O-TON	0.99	0.99	1.279	0.315
CS10-O-FOTN	0.99	0.99	1.279	0.247
CS10-O-FOTNR	0.99	0.99	1.269	0.284
CS10-O-SOTN	0.99	0.99	4.762	-339.17
CS10-O-SOTNR	0.99	0.99	1.270	0.317
CS10-O-FOLN	0.93	0.96	1.211	0.309
CS10-O-FOLNR	0.99	0.99	1.250	0.340
CS10-O-SOLN	0.99	0.99	1.265	0.315
CS10-O-SOLNR	0.99	0.99	1.262	0.214

For the tenth study (Ra, Sahoo et al [53]), results show that if the R^2 value was the key element considered in deciding the model, we may conclude that all models accurately describe the process. Because R^2_{training} results are nearly all close to 1.

The initial assumption would be that lots of models are suitable if the selection had just been based on R^2_{training} and R^2_{testing} . Based on this argument, utilizing a method that considers the simplicity of the models and the desired models' capacity to provide realistic values, it is determined that only model 1 (L) is suitable. As a result, misleading findings are unavoidable if the model building-optimum result finding analyses are not addressed as outlined in this article. Thus, the obtained model 1 (CS10-O-L) was chosen as the objective function required in analyses to get optimum results of surface roughness. Outcomes of the selected model can be spotted in Table 7.56.

Table 7.57 shows the outcomes of three specific optimization scenarios for the chosen model. In scenario 1, all of the variables were utilized with their upper and lower limits in a continuous interval. The minimum surface roughness outcomes, depending on all of the optimization techniques, were $0.309 \mu\text{m}$, which correspond to L. The suggested (optimum) design variables are; cutting speed: 220 (m/min), feed rate: 0.05 (mm/rev) and depth of cut: 0.1 (mm). $0.309 \mu\text{m}$ is a realistic result by compared with the results of experiment [0.31, 1.29]. We could say that the optimization results reach lower surface roughness than experimental results.

In scenario 2, feed rate and depth of cut have been treated as continuous variables while the cutting speed is discrete (integers). The minimum surface roughness outcomes for the L model were same as the scenario 1.

For the third optimization scenario, all of the input parameters are supposed to be real numbers and the design variables can only take the experimental values. The results are the same with scenario 1 and 2.

From the point of stability, gaining identical outcomes for scenarios 1, 2 and 3, whose phenomenological foundation is addressed using four distinct direct search methods, enhances the chance that acquired results are global optimum. This situation is critical for optimization issues comprising restriction types that are

similar to those in scenarios 1, 2 and 3. Furthermore, utilizing the L model to solve the optimization issue for scenarios 1, 2 and 3, the best surface roughness can be taken as 0.308738 μm . Due to the optimization results, the model chosen for the optimization procedure has achieved lower results than the experimental results.

Table 7.58: Optimization problem results of selected model CS10-O-L for surface roughness

Objective Functions	Scenario No	Constraints	Optimization Algorithm	Surface Roughness (μm)	Suggested Design
CS10-O-L	1	$80 < x_1 < 220,$ $0.05 < x_2 < 0.15,$ $0.1 < x_3 < 0.3$	MDE	0.309	$x_1 = 220, x_2 = 0.05, x_3 = 0.1$
			MSA	0.309	$x_1 = 220, x_2 = 0.05, x_3 = 0.1$
			MRS	0.309	$x_1 = 220, x_2 = 0.05, x_3 = 0.1$
			MNM	0.309	$x_1 = 220, x_2 = 0.05, x_3 = 0.1$
	2	$80 < x_1 < 220,$ $0.05 < x_2 < 0.15,$ $0.1 < x_3 < 0.3,$ $\{x_1\} \in \text{Integers}$	MDE	0.309	$x_1 = 220, x_2 = 0.05, x_3 = 0.1$
			MSA	0.309	$x_1 = 220, x_2 = 0.05, x_3 = 0.1$
			MRS	0.309	$x_1 = 220, x_2 = 0.05, x_3 = 0.1$
			MNM	0.309	$x_1 = 220, x_2 = 0.05, x_3 = 0.1$
	3	$x_1 = \{80, 150, 220\},$ $x_2 = \{0.05, 0.1, 0.15\},$ $x_3 = \{0.1, 0.2, 0.3\}$	MDE	0.309	$x_1 = 220, x_2 = 0.05, x_3 = 0.1$
			MSA	0.309	$x_1 = 220, x_2 = 0.05, x_3 = 0.1$
			MRS	0.309	$x_1 = 220, x_2 = 0.05, x_3 = 0.1$
			MNM	0.309	$x_1 = 220, x_2 = 0.05, x_3 = 0.1$

Regarding of these facts, by using our proposed approach, for surface roughness the design variables were fitted to the model with $R^2_{\text{training}} = 0.99$ and $R^2_{\text{testing}} = 0.99$ values: $0.251182 - 0.00144178 [x1] + 6.62437 [x2] + 0.435294 [x3]$. According to scenarios, minimum surface roughness has found as $0.309 \mu\text{m}$ with the following conditions; cutting speed: 220m/min , feed: 0.05mm/rev and depth of cut: 0.1mm . $0.309 \mu\text{m}$ is a realistic and better result in comparison with the experimental results [0.31, 1.29].

As a consequence, at greater cutting speeds, surface roughness is minimal on average, whereas it is quite high at lower cutting speeds, according to the results of the experiment. Low feed results in lower surface roughness than other feed levels. The outcomes of the operations demonstrate that the average surface roughness increases with cutting depth and decreases with cutting depth. Surface quality worsened due to the greater feed rate. This raises chatter and causes unfinished processing of the workpiece, which results in higher surface roughness as a result of the increased feed rate. The findings show that feed has a significant impact on the roughness of the workpiece.

7.12 Case Study #11

The eleventh literature study which optimization process was studied taken from Sahoo et al. [54]. A response surface methodology and artificial neural network are used to build a prediction model, which is then optimized using a 3D surface plot. AISI 1040 steel was machined using coated carbide. The RSM model has a high coefficient of determination ($R^2 = 0.99$, which is near to unity). It suggests that the model fits well and that it is highly significant. According to the RSM model, the error percentage ranges from -2.63 to 2.47 . Operational and ANN model error ranges from -1.27 to 0.02 percent, which is substantially smaller than the RSM model. As a result, both the RSM and ANN statistical methods are able to properly forecast surface roughness. In contrast, the ANN predictive algorithm appears to perform better than the RSM model.

As depicted in Table 7.58, the changes in values of these input parameters provided the obtaining of different results for the surface roughness.

Therefore, these obtaining results depending on the change in these input parameter values are sufficient to develop an optimization strategy. Moreover, it is impossible to establish a proportional connection between measured surface roughness and three design variables (cutting speed, feed and depth of cut) as understood from Table 7.58. Therefore, it is necessary to optimize these parameters to achieve minimum surface roughness.

Table 7.59: Experimental results of surface roughness with different experimental conditions [54]

Exp No	Cutting speed (v, m/min)	Feed (f, mm/rev)	Depth of cut (d, mm)	Surface Roughness (Ra, μm)
1	60	0.04	0.1	1.40
2	60	0.04	0.3	1.57
3	60	0.04	0.5	1.75
4	60	0.08	0.1	1.80
5	60	0.08	0.3	1.98
6	60	0.08	0.5	2.10
7	60	0.12	0.1	2.30
8	60	0.12	0.3	2.35
9	60	0.12	0.5	2.42
10	160	0.04	0.1	1.44
11	160	0.04	0.3	1.61
12	160	0.04	0.5	1.65
13	160	0.08	0.1	1.85
14	160	0.08	0.3	1.89
15	160	0.08	0.5	1.92
16	160	0.12	0.1	2.23
17	160	0.12	0.3	2.28
18	160	0.12	0.5	2.33
19	260	0.04	0.1	1.46
20	260	0.04	0.3	1.52
21	260	0.04	0.5	1.55
22	260	0.08	0.1	1.73
23	260	0.08	0.3	1.78
24	260	0.08	0.5	1.81
25	260	0.12	0.1	2.05
26	260	0.12	0.3	2.18
27	260	0.12	0.5	2.10

The behavior of the system was explained by the regression models given below [54];

$$Ra = 0.8498 + 0.0018 \times v + 9.1458 \times f + 1.4222 \times d + 16.3194 \times f^2 - 0.5972 \times d^2 - 0.0115 \times v \times f - 0.0023 \times v \times d - 3.9583 \times f \times d \quad (7.25)$$

The experimental data was represented by these regression model with determination coefficient (R^2) of 0.992.

Sahoo et al. 2014 [54] figured out this limited optimization issue by defining all the input parameters as discrete and proceeded in the modeling process only according to the standard R^2 results and listed the models. The R^2 value Sahoo et al. 2014 [54] found as 98%. Sahoo et al. 2014 [54] does not mention the R^2_{training} and R^2_{testing} distinction in the modeling process and does not mention determining model according to different scenarios. As can be clearly seen that smaller surface roughness may be calculated with the variables as a consequence of optimization.

7.12.1 Optimization Scenarios

For all scenarios, the limitations for the system inputs (design parameters) as in the following form;

$$\begin{aligned} 60 \leq \text{Cutting speed} \leq 260 & , \quad (m/min) \\ 0.04 \leq \text{Feed} \leq 0.12 & , \quad (mm/rev) \\ 0.1 \leq \text{Depth of cut} \leq 0.5 & , \quad (mm) \end{aligned}$$

7.12.1.1 Scenario 1

Surface roughness is explained by the objective function in this optimal solution problem. There are no constraints about the input parameters so they can be real numbers, and the computation area is continuous. The primary goal is to minimize the surface roughness. It is also technically possible to see these theory-based boundaries of the objective function this way.

7.12.1.2 Scenario 2

Scenario 2 should include additional realistic situations in addition to knowledge-based ones. A novel optimal solution is provided that implies the reduction of the responses for this application. Input parameters are also restricted with integers. There is only one design variable that can be integer number.

7.12.1.3 Scenario 3

In the constructed of scenario 3, more viable and more limited issue situations should be included to scenario 2. For that reason, there is a new optimum solution problem created to the minimization of the response values. Unlike Scenario 2, in scenario 3 parameters can only take the values in the data table.

7.12.2 Results and Discussion

In our approach, different from the classical ones, various regression models are first tested utilizing both R^2_{training} and R^2_{testing} values (not only R^2 as in the classical approach) to reveal what is the degree of performance of the model can explain the method. Besides, the model's operational restriction (boundedness) is also checked by calculating the highest and lowest values that the related model creates. Therefore, our proposed design strategy provides producing realistic values. Also, it is necessary to check the limitedness of decided models, whether producing realistic results. Regarding of these facts, by using our proposed approach, the experimental data table of surface roughness listed as Table 7.59 can be seen below.

Table 7.60: Results of the Neuro-regression models for the surface roughness

Models	R^2_{training}	R^2_{testing}	Max (μm)	Min (μm)
CS11-O-L	0.95	0.97	2.406	1.379
CS11-O-LR	0.97	0.99	2.426	1.419
CS11-O-SON	0.99	0.95	2.445	1.411
CS11-O-SONR	0.99	-5.57	1.505×10^{12}	-5.170×10^8
CS11-O-TON	0.99	0.96	2.434	1.404
CS11-O-FOTN	0.96	0.95	2.394	0.759
CS11-O-FOTNR	0.99	0.98	2.417	1.284
CS11-O-SOTN	0.99	0.81	10.867	-2671.01
CS11-O-SOTNR	0.99	0.90	4.698×10^8	-6.088×10^{11}
CS11-O-FOLN	0.92	0.94	2.376	1.350
CS11-O-FOLNR	0.96	0.99	2.402	1.423
CS11-O-SOLN	0.99	0.95	2.452	1.437
CS11-O-SOLNR	0.99	0.47	2.177	1.400

For the eleventh study (Ra, Sahoo et al. [54]), results show that if the R^2 value was the key element considered in deciding the model, we may conclude that all models accurately describe the process. Because R^2_{training} results are nearly all close to 1.

The initial assumption would be that lots of models are suitable if the selection had just been based on R^2_{training} and R^2_{testing} . Based on this argument, utilizing a method that considers the simplicity of the models and the desired models' capacity to provide realistic values, it is determined that only model 7 (FOTNR) is suitable. As a result, misleading findings are unavoidable if the model building-optimum result finding analyses are not addressed as outlined in this article. Thus, the obtained model 7 (CS11-O-FOTNR) was chosen as the objective function required in analyses to get optimum results of surface roughness. Outcomes of the selected model can be spotted in Table 7.59.

Table 7.60 shows the outcomes of three specific optimization scenarios for the chosen model. In scenario 1, all of the variables were utilized with their upper and lower limits in a continuous interval. The minimum surface roughness outcomes, depending on all of the optimization techniques, were 1.294 μm , which correspond to FOTNR. The suggested (optimum) design variables show change. 1.294 μm is a realistic result by compared with the results of experiment [1.40, 2.42]. We could

say that the optimization scenario 1 results reach lower surface roughness than experimental results.

In scenario 2, feed rate and depth of cut have been treated as continuous variables while the cutting speed is discrete (integers). In this case, there are four different results for four different optimization algorithms. The minimum surface roughness of the scenario 2 for the MDE algorithm is 1.294 μm . The suggested (optimum) designs are; cutting speed: 224 (m/min), feed: 0.0413488 (mm/rev) and depth of cut: 0.1 (mm). We could say that the optimization scenario 2 results reach lower surface roughness than experimental results.

For the third optimization scenario, all of the input parameters are supposed to be real numbers and the design variables can only take the experimental values. The minimum surface roughness value of the scenario 3 for the FOTNR model is 1.407 μm . The suggested (optimum) designs are; cutting speed: 60 (m/min), feed: 0.04 (mm/rev) and depth of cut: 0.1 (mm). We could say that the optimization scenario 3 results are incredibly close with experimental results.

As a consequence of optimization process, if we take scenarios 1 and 2 as a reference, it can be said that the optimization process works efficiently.

Table 7.61: Optimization problem results of selected model CS11-O-FOTNR for surface roughness

Objective Functions	Scenario No	Constraints	Optimization Algorithm	Surface Roughness (μm)	Suggested Design
CS11-O-FOTNR	1	$60 < x_1 < 260,$ $0.04 < x_2 < 0.12,$ $0.1 < x_3 < 0.5$	MDE	1.294	$x_1 = 148.652, x_2 = 0.041344, x_3 = 0.1$
			MSA	1.294	$x_1 = 110.953, x_2 = 0.0413441, x_3 = 0.1$
			MRS	1.294	$x_1 = 79.5365, x_2 = 0.0413441, x_3 = 0.1$
			MNM	1.294	$x_1 = 186.351, x_2 = 0.041344, x_3 = 0.1$
	2	$60 < x_1 < 260,$ $0.04 < x_2 < 0.12,$ $0.1 < x_3 < 0.5,$ $\{x_1\} \in \text{Integers}$	MDE	1.294	$x_1 = 224, x_2 = 0.0413488, x_3 = 0.1$
			MSA	1.299	$x_1 = 130, x_2 = 0.04178, x_3 = 0.1$
			MRS	1.324	$x_1 = 142, x_2 = 0.0416938, x_3 = 0.1$
			MNM	1.295	$x_1 = 155, x_2 = 0.0412525, x_3 = 0.100354$
	3	$x_1 = \{60, 160, 260\},$ $x_2 = \{0.04, 0.08, 0.12\},$ $x_3 = \{0.1, 0.3, 0.5\}$	MDE	1.407	$x_1 = 60, x_2 = 0.04, x_3 = 0.1$
			MSA	1.407	$x_1 = 60, x_2 = 0.04, x_3 = 0.1$
			MRS	1.407	$x_1 = 60, x_2 = 0.04, x_3 = 0.1$
			MNM	1.407	$x_1 = 60, x_2 = 0.04, x_3 = 0.1$

Regarding of these facts, by using our proposed approach, for surface roughness the design variables were fitted to the model with $R^2_{\text{training}} = 0.99$ and $R^2_{\text{testing}} = 0.98$ values: $(120.894 + 0.162011 \text{ Cos}[x1] - 120.665 \text{ Cos}[x2] + 0.0701416 \text{ Cos}[x3] + 0.0798184 \text{ Sin}[x1] - 3.94732 \text{ Sin}[x2] - 0.0678742 \text{ Sin}[x3]) / (39.5546 + 0.117583 \text{ Cos}[x1] - 39.3533 \text{ Cos}[x2] - 0.0279373 \text{ Cos}[x3] + 0.0499025 \text{ Sin}[x1] - 0.820916 \text{ Sin}[x2] - 0.079732 \text{ Sin}[x3])$. Minimum surface roughness has found as 1.29441 μm according to scenario 1. In scenario 3, minimum surface roughness has found as 1.40704 μm while input parameters can only take the values in the data table. But in scenario 1, minimum surface roughness has found as 1.294 μm with four different conditions. 1.294 μm could be a realistic and better result in comparison with the experimental results [1.40, 2.42].

The experimental results show the findings demonstrate that the surface roughness increases with cutting depth and decreases with cutting depth.

7.13 Case Study #12

The twelfth literature study which optimization process was studied taken from Subramanian et al. [55]. To estimate cutting force from design variables such as speed, feed rate, and axial depth, this study will construct a predictive method. Experiments were conducted utilizing response surface methodology. Al 7075-T6 was used for the procedure, and the tool was a shoulder mill with two carbide inserts. Three-axis tool dynamometer was utilized to evaluate cutting forces. For the estimation of cutting force, a second-degree mathematical model based on design variables was created. Analysis of variance was used to assess the prediction models' suitability and found them to be sufficient. To achieve the lowest cutting force, the shoulder mill design variables were optimized using genetic algorithms (GA).

As depicted in Table 7.61, the changes in values of these input parameters provided the obtaining of different results for the cutting forces.

Therefore, these obtaining results depending on the change in these input parameter values are sufficient to develop an optimization strategy. Moreover, it is impossible

to establish a proportional connection between measured cutting forces values and three input parameters (cutting speed, cutting feed and depth of cut) as understood from Table 7.61. Therefore, it is necessary to optimize these parameters to achieve minimum cutting forces.

Table 7.62: Experimental results of surface roughness and cutting forces with different experimental conditions [55]

Exp. No	Cutting speed (V_c , m/min)	Cutting feed (f_z , mm/tooth)	Depth of cut (a_p , mm)	Infeed Force (F_x , N)	Crossfeed Force (F_y , N)	Thrust Force (F_z , N)
1	-1	-1	-1	328.604	385.23	55.993
2	1	-1	-1	240.372	356.342	47.707
3	-1	1	-1	430.682	669.992	68.255
4	1	1	-1	152.094	392.184	35.445
5	-1	-1	1	417.094	637.13	74.188
6	1	-1	1	328.862	608.242	40.377
7	-1	1	1	787.216	1200.41	86.451
8	1	1	1	508.628	922.604	28.115
9	-1.682	0	0	619.207	775.482	89.107
10	1.682	0	0	310.711	517.551	33.078
11	0	1.682	0	265.081	394.585	57.188
12	0	1.682	0	502.112	898.448	57.188
13	0	0	1.682	173.132	317.551	38.963
14	0	0	1.682	547.397	975.482	48.100
15	0	0	0	464.959	646.517	43.532
16	0	0	0	464.959	646.517	43.532
17	0	0	0	464.959	646.517	43.532
18	0	0	0	464.959	646.517	43.532
19	0	0	0	464.959	646.517	43.532
20	0	0	0	464.959	646.517	43.532

The behavior of the system was explained by the multiple linear regression models given below [55];

$$F_x = 464.959 - 91.705 \times V_c + 70.461 \times f_z + 111.256 \times a_p - 28.759 \times f_z^2 - 37.006 \times a_p^2 - 47.58 \times V_c \times f_z + 67.011 \times f_z \times a_p \quad (7.26)$$

$$F_y = 646.517 - 76.674 \times V_c + 149.781 \times f_z + 195.58 \times a_p - 62.23 \times V_c \times f_z + 69.63 \times f_z \times a_p \quad (7.27)$$

$$F_z = 43.5316 - 16.6556 \times V_c + 2.7161 \times a_p + 6.2074 \times V_c^2 + 482717 \times f_z^2 - 6.131 \times V_c \times f_z - 6.3813 \times V_c \times a_p \quad (7.28)$$

Subramanian et al. [55] figured out this limited optimization issue by defining all the input parameters as discrete and proceeded in the modeling process only according to the standard R^2 results and listed the models. Subramanian et al [55] does not mention the R^2_{training} and R^2_{testing} distinction in the modeling process and does not mention determining models according to different scenarios. As can be clearly seen that smaller cutting forces may be calculated with the variables as a consequence of optimization.

7.13.1 Optimization Scenarios

For all scenarios, the limitations for the system inputs (design parameters) as in the following form;

$$\begin{aligned} -1.682 \leq \text{Cutting speed} \leq 1.682 & \quad , \quad (m/min) \\ -1.682 \leq \text{Cutting feed} \leq 1.682 & \quad , \quad (mm) \\ -1.682 \leq \text{Depth of cut} \leq 1.682 & \quad , \quad (mm/rev) \end{aligned}$$

7.13.1.1 Scenario 1

Cutting forces are explained by the objective function in this optimal solution problem. There are no constraints about the input parameters so they can be real numbers, and the computation area is continuous. The primary goal is to minimize the surface roughness. It is also technically possible to see these theory-based boundaries of the objective function this way.

7.13.1.2 Scenario 2

In scenario 2, nonlinear constraints are added for the optimization problem. For infeed force, crossfeed force should be smaller than 300 N and thrust force should

be smaller than 30 N. For crossfeed force, infeed force should be smaller than 100 N and thrust force should be smaller than 30 N. For thrust force, infeed force should be smaller than 100 N and crossfeed force should be smaller than 300 N. The method will be harder in this situation than in first scenario.

7.13.1.3 Scenario 3

In the constructed of scenario 3, more viable and more limited issue situations should be included to scenario 2. For that reason, there is a new optimum solution problem created to the minimization of the response values. Unlike Scenario 1, in scenario 3 parameters can only take the values in the data table.

7.13.2 Results and Discussion

In our approach, different from the classical ones, various regression models are first tested utilizing both R^2_{training} and R^2_{testing} values (not only R^2 as in the classical approach) to reveal what is the degree of performance of the model can explain the method. Besides, the model's operational restriction (boundedness) is also checked by calculating the highest and lowest values that the related model creates. Therefore, our proposed design strategy provides producing realistic values. Also, it is necessary to check the limitedness of decided models, whether producing realistic results. Regarding of these facts, by using our proposed approach, the experimental data tables of cutting forces (F_x as infeed force, F_y as crossfeed force and F_z as thrust force) listed as Table 7.62, 7.63 and 7.64 can be seen below.

Table 7.63: Results of the Neuro-regression models for the cutting force (Fx, infeed force)

Models	R^2_{training}	R^2_{testing}	Max (N)	Min (N)
CS12-O1-L	0.38	0.06	801.365	102.557
CS12-O1-LR	0.94	0.65	1035.39	-207.37
CS12-O1-SON	0.99	0.91	1057.89	-203.121
CS12-O1-SONR	0.99	0.99	2.198×10^{13}	-6.391×10^{10}
CS12-O1-TON	0.99	0.22	1245.02	-650.707
CS12-O1-FOTN	0.92	0.20	729.262	82.710
CS12-O1-FOTNR	0.99	0.65	1.580×10^{12}	-4556.32
CS12-O1-SOTN	0.99	0.99	725.351	37.320
CS12-O1-SOTNR	-2.57	-2.05	1.137×10^{14}	-4.605×10^{12}
CS12-O1-FOLN	0.91	0.41	845.708	-38.273
CS12-O1-FOLNR	0.95	0.75	969.735	-231.734
CS12-O1-SOLN	0.99	0.97	988.815	-210.743
CS12-O1-SOLNR	0.99	0.65	3.140×10^{12}	-6.115×10^{10}

Table 7.64: Results of the Neuro-regression models for the cutting force (Fy, crossfeed force)

Models	R^2_{training}	R^2_{testing}	Max (N)	Min (N)
CS12-O2-L	0.96	0.74	1377.01	-66.225
CS12-O2-LR	0.69	-0.85	∞	$-\infty$
CS12-O2-SON	0.99	0.97	1692.7	124.779
CS12-O2-SONR	0.74	-8.21	1.549×10^{13}	-1.424×10^{10}
CS12-O2-TON	0.99	0.76	2559.83	-593.452
CS12-O2-FOTN	0.95	0.39	1207.05	118.73
CS12-O2-FOTNR	0.99	0.29	4.372×10^{13}	-558.639
CS12-O2-SOTN	0.99	0.12	1216.06	193.252
CS12-O2-SOTNR	-2.75	-8.19	4.357×10^{10}	-2.588×10^{12}
CS12-O2-FOLN	0.94	0.74	1245.03	-144.354
CS12-O2-FOLNR	0.99	0.83	2170.14	174.458
CS12-O2-SOLN	0.99	0.98	1655.88	104.878
CS12-O2-SOLNR	-3.93	-10.25	1.794×10^{12}	-1.776×10^{14}

Table 7.65: Results of the Neuro-regression models for the cutting force (Fz, thrust force)

Models	R ² _{training}	R ² _{testing}	Max (N)	Min (N)
CS12-O3-L	0.70	0.63	90.882	10.447
CS12-O3-LR	0.61	-0.03	∞	-∞
CS12-O3-SON	0.99	0.78	147.735	17.989
CS12-O3-SONR	0.99	-0.42	120.459	26.200
CS12-O3-TON	0.99	0.89	184.51	21.055
CS12-O3-FOTN	0.84	0.66	98.398	28.313
CS12-O3-FOTNR	0.99	-2.80	84.420	-8.937x10 ¹¹
CS12-O3-SOTN	0.99	-0.32	103.914	5.550
CS12-O3-SOTNR	-0.13	-11.22	1.793x10 ¹⁰	-5.757x10 ¹³
CS12-O3-FOLN	0.75	0.92	95.7248	18.348
CS12-O3-FOLNR	0.90	0.77	832.771	6.825
CS12-O3-SOLN	0.98	-0.18	148.759	-12.492
CS12-O3-SOLNR	0.96	-0.23	3.277x10 ¹⁴	26.711

For the first output of the study (F_x, Subramanian et al. [55]), the initial assumption would be that only one model is suitable if the selection had just been based on R²_{training} and R²_{testing}. Based on this argument, utilizing a method that considers the desired models' capacity to provide realistic values, it is determined that only model 8 (SOTN) is suitable. As a result, misleading findings are unavoidable if the model building-optimum result finding analyses are not addressed as outlined in this article. Thus, the obtained model 8 (CS12-O1-SOTN) was chosen as the objective function required in analyses to get optimum results of F_x. Outcomes of the selected model can be spotted in Table 7.62.

There is no design variable that can be integer. Thus, Table 7.65 shows the outcomes of three specific optimization scenarios for the chosen model. In scenario 1, all of the variables were utilized with their upper and lower limits in a continuous interval. The minimum cutting force (F_x) found as 37.321 N, which correspond to SOTN. The suggested (optimum) designs are; cutting speed: 1.682 (220 m/min), cutting feed: 0.93889 and depth of cut: -1.682 (0.5 mm). 37.321 N is a realistic result by compared with the results of experiment [161.19, 794.61]. We could say that the optimization scenario 1 reach lower cutting force than experimental results.

In the second optimization scenario, the only limitation condition in the optimization process was taken as the crossfeed force (F_y) smaller than 300 N and thrust force (F_z) smaller than 30 N for the infeed force (F_x). The minimum infeed force had found as 60.6562 N. We could say that the optimization scenario 2 reach lower cutting force than experimental results.

For the third optimization scenario, all of the input parameters are supposed to be real numbers and the design variables can only take the experimental values. The minimum cutting force had found as 37.896 N. The suggested (optimum) design variables are; cutting speed: 1.682 (220 m/min), cutting feed: 1 (0.09 mm/tooth) and depth of cut: -1.682 (0.5 mm). 37.896 N is a better result in comparison with the experimental values [161.19, 794.61].

We could say that the optimization scenarios results can be realistic. The main reason for the difference between the optimized results and the outcomes of the experiment is that the experimental data set is not designed in such a way that the results can be followed in a healthy and proportional way. As a result of the optimization process a better and lower cutting force value was obtained.

For the second output of the study (F_y , Subramanian et al. [55]), the initial assumption would be that models 3 and 12 are suitable if the selection had just been based on R^2_{training} and R^2_{testing} . Based on this argument, utilizing a method that considers the simplicity of the models and the desired models' capacity to provide realistic values, it is determined that only model 3 (SON) is suitable. As a result, misleading findings are unavoidable if the model building-optimum result finding analyses are not addressed as outlined in this article. Thus, the obtained model 3 (CS12-O2-SON) was chosen as the objective function required in analyses to get optimum results of F_y . Outcomes of the selected model can be spotted in Table 7.63.

There is no design variable that can be integer. Thus, Table 7.66 shows the outcomes of three specific optimization scenarios for the chosen model. In scenario 1, all of the variables were utilized with their upper and lower limits in a continuous interval. The minimum cutting force (F_y) found as 124.779 N, which correspond

to SOTN. The suggested (optimum) designs are; cutting speed: 1.682 (220 m/min), cutting feed: 1.682 (0.1 mm/tooth) and depth of cut: -1.682 (0.5 mm). 124.779 N is a realistic result by compared with the results of experiment [307.01, 1187]. We could say that the optimization scenario 1 reach lower cutting force than experimental results.

In the second optimization scenario, the only limitation condition in the optimization process was taken as the infeed force (F_x) smaller than 100 N and thrust force (F_z) smaller than 30 N for the crossfeed force (F_y). The minimum crossfeed force had found as 129.23 N.

For the third optimization scenario, all of the input parameters are supposed to be real numbers and the design variables can only take the experimental values. The minimum cutting force had found as same as in the scenario 1.

We could say that the optimization scenarios results can be realistic. The main reason for the difference between the optimized results and the outcomes of the experiment is that the experimental data set is not designed in such a way that the results can be followed in a healthy and proportional way. As a result of the optimization process a better and lower cutting force value was obtained.

For the third output of the study (F_z , Subramanian et al. [55]) the initial assumption would be that models 3 and 5 are suitable if the selection had just been based on R^2_{training} and R^2_{testing} . Based on this argument, utilizing a method that considers the simplicity of the models and the desired models' capacity to provide realistic values, it is determined that only model 3 (SON) is suitable. As a result, misleading findings are unavoidable if the model building-optimum result finding analyses are not addressed as outlined in this article. Thus, the obtained model 3 (CS12-O3-SON) was chosen as the objective function required in analyses to get optimum results of F_z . Outcomes of the selected model can be spotted in Table 7.64.

There is no design variable that can be integer. Thus, Table 7.67 shows the outcomes of three specific optimization scenarios for the chosen model. In scenario 1, all of the variables were utilized with their upper and lower limits in a continuous interval. The minimum cutting force (F_z) found as 17.989 N which correspond to

SON. The suggested (optimum) designs are; cutting speed: 1.682 (220 m/min), cutting feed: 1.682 (0.1 mm/tooth) and depth of cut: -1.682 (0.5 mm). 17.989 N is a realistic result by compared with the results of experiment [29.43, 88.29]. We could say that the optimization scenario 1 reach lower cutting force than experimental results.

In the second optimization scenario, the only limitation condition in the optimization process was taken as the infeed force (F_x) smaller than 100 N and crossfeed force (F_y) smaller than 300 N for the thrust force (F_z). The minimum thrust force had found as 18.298 N.

For the third optimization scenario, all of the input parameters are supposed to be real numbers and the design variables can only take the experimental values. The minimum cutting force had found as same as in the scenario 1. For the third output of the fifth study, it can be said clearly that as a result of the optimization process a better and smaller F_z values had obtained.

We could say that the optimization scenarios results can be realistic. The main reason for the difference between the optimized results and the outcomes of the experiment is that the experimental data set is not designed in such a way that the results can be followed in a healthy and proportional way. As a result of the optimization process a better and lower cutting force value was obtained.

Table 7.66: Optimization problem results of selected model CS12-O1-SOTN for infeed force (Fx)

Objective Functions	Scenario No	Constraints	Optimization Algorithm	Infeed Force (N)	Suggested Design
CS12-O1-SOTN	1	$-1.682 < x1 < 1.682,$ $-1.682 < x2 < 1.682,$ $-1.682 < x3 < 1.682$	MDE	37.321	$x1 = 1.682, x2 = 0.93889, x3 = -1.682$
			MSA	37.321	$x1 = 1.682, x2 = 0.93889, x3 = -1.682$
			MRS	37.321	$x1 = 1.682, x2 = 0.93889, x3 = -1.682$
			MNMM	37.321	$x1 = 1.682, x2 = 0.93889, x3 = -1.682$
	2	$-1.682 < x1 < 1.682,$ $-1.682 < x2 < 1.682,$ $-1.682 < x3 < 1.682,$ Crossfeed Force < 300, Thrust Force < 30	MDE	60.656	$x1 = 1.42278, x2 = 0.759306, x3 = -1.55971$
			MSA	60.656	$x1 = 1.42278, x2 = 0.759306, x3 = -1.55971$
			MRS	60.656	$x1 = 1.42278, x2 = 0.759306, x3 = -1.55971$
			MNMM	60.656	$x1 = 1.42278, x2 = 0.759306, x3 = -1.55971$
	3	$x1 = \{-1.682, -1, 0, 1, 1.682\},$ $x2 = \{-1.682, -1, 0, 1, 1.682\},$ $x3 = \{-1.682, -1, 0, 1, 1.682\}$	MDE	37.896	$x1 = 1.682, x2 = 1, x3 = -1.682$
			MSA	37.896	$x1 = 1.682, x2 = 1, x3 = -1.682$
			MRS	37.896	$x1 = 1.682, x2 = 1, x3 = -1.682$
			MNMM	37.896	$x1 = 1.682, x2 = 1, x3 = -1.682$

Table 7.67: Optimization problem results of selected model CS12-O2-SON for crossfeed force (Fy)

Objective Functions	Scenario No	Constraints	Optimization Algorithm	Crossfeed Force (N)	Suggested Design
CS12-O2-SON	1	$-1.682 < x1 < 1.682,$ $-1.682 < x2 < 1.682,$ $-1.682 < x3 < 1.682$	MDE	124.779	$x1 = 1.682, x2 = 1.682, x3 = -1.682$
			MSA	124.779	$x1 = 1.682, x2 = 1.682, x3 = -1.682$
			MRS	124.779	$x1 = 1.682, x2 = 1.682, x3 = -1.682$
			MNM	124.779	$x1 = 1.682, x2 = 1.682, x3 = -1.682$
	2	$-1.682 < x1 < 1.682,$ $-1.682 < x2 < 1.682,$ $-1.682 < x3 < 1.682,$ Infeed Force $< 100,$ Thrust Force < 30	MDE	129.23	$x1 = 1.682, x2 = 1.61394, x3 = -1.682$
			MSA	129.23	$x1 = 1.682, x2 = 1.61394, x3 = -1.682$
			MRS	129.23	$x1 = 1.682, x2 = 1.61394, x3 = -1.682$
			MNM	129.23	$x1 = 1.682, x2 = 1.61394, x3 = -1.682$
	3	$x1 = \{-1.682, -1, 0, 1, 1.682\},$ $x2 = \{-1.682, -1, 0, 1, 1.682\},$ $x3 = \{-1.682, -1, 0, 1, 1.682\}$	MDE	124.779	$x1 = 1.682, x2 = 1.682, x3 = -1.682$
			MSA	124.779	$x1 = 1.682, x2 = 1.682, x3 = -1.682$
			MRS	124.779	$x1 = 1.682, x2 = 1.682, x3 = -1.682$
			MNM	124.779	$x1 = 1.682, x2 = 1.682, x3 = -1.682$

Table 7.68: Optimization problem results of selected model CS12-O3-SON for thrust force (Fz)

Objective Functions	Scenario No	Constraints	Optimization Algorithm	Thrust Force (N)	Suggested Design
CS12-O3-SON	1	-1.682 < x1 < 1.682,	MDE	17.989	x1 = 1.682, x2 = 1.682, x3 = -1.682
		-1.682 < x2 < 1.682,	MSA	17.989	x1 = 1.682, x2 = 1.682, x3 = -1.682
		-1.682 < x3 < 1.682	MRS	17.989	x1 = 1.682, x2 = 1.682, x3 = -1.682
			MNIM	17.989	x1 = 1.682, x2 = 1.682, x3 = -1.682
	2	-1.682 < x1 < 1.682,	MDE	18.298	x1 = 1.682, x2 = 1.61394, x3 = -1.682
		-1.682 < x2 < 1.682,	MSA	18.298	x1 = 1.682, x2 = 1.61394, x3 = -1.682
		-1.682 < x3 < 1.682,	MRS	18.298	x1 = 1.682, x2 = 1.61394, x3 = -1.682
		Infeed Force < 100, Crossfeed Force < 300	MNIM	18.298	x1 = 1.682, x2 = 1.61394, x3 = -1.682
	3	x1 = {-1.682, -1, 0, 1, 1.682},	MDE	17.989	x1 = 1.682, x2 = 1.682, x3 = -1.682
		x2 = {-1.682, -1, 0, 1, 1.682},	MSA	17.989	x1 = 1.682, x2 = 1.682, x3 = -1.682
		x3 = {-1.682, -1, 0, 1, 1.682}	MRS	17.989	x1 = 1.682, x2 = 1.682, x3 = -1.682
			MNIM	17.989	x1 = 1.682, x2 = 1.682, x3 = -1.682

Regarding of these facts, by using our proposed approach, for infeed force (F_x) the design variables were fitted to the model with $R^2_{\text{training}} = 0.99$ and $R^2_{\text{testing}} = 0.99$ values: $60.7754 + 37.3454 \cos[x_1] + 51.0848 \cos[x_1]^2 + 64.9164 \cos[x_2] + 11.897 \cos[x_1] \cos[x_2] + 76.9012 \cos[x_2]^2 + 58.4406 \cos[x_3] - 5.73472 \cos[x_1] \cos[x_3] + 39.2186 \cos[x_2] \cos[x_3] + 72.6253 \cos[x_3]^2 - 34.1501 \sin[x_1] + 10.269 \cos[x_1] \sin[x_1] - 63.7706 \cos[x_2] \sin[x_1] - 63.7706 \cos[x_3] \sin[x_1] + 108.402 \sin[x_1]^2 + 21.9792 \sin[x_2] + 79.0787 \cos[x_1] \sin[x_2] - 79.3105 \cos[x_2] \sin[x_2] + 79.0787 \cos[x_3] \sin[x_2] - 50.874 \sin[x_1] \sin[x_2] + 60.4866 \sin[x_2]^2 + 41.8277 \sin[x_3] + 76.7693 \cos[x_1] \sin[x_3] + 76.7693 \cos[x_2] \sin[x_3] - 7.75658 \cos[x_3] \sin[x_3] + 10.922 \sin[x_1] \sin[x_3] + 78.304 \sin[x_2] \sin[x_3] + 71.4314 \sin[x_3]^2$. Minimum infeed force has found as 37.896 N in scenario 3 with the following conditions; cutting speed: 1.682, cutting feed: 1 and depth of cut: -1.682. 37.896 N could be a realistic and better result in comparison with the experimental results because the experiment had not done in full combination of all input parameters.

For second output crossfeed force (F_y) the design variables were fitted to the model with $R^2_{\text{training}} = 0.99$ and $R^2_{\text{testing}} = 0.97$ values: $645.983 - 82.5137 [x_1] + 6.60931 [x_1]^2 + 145.528 [x_2] - 52.7183 [x_1] [x_2] - 6.41306 [x_2]^2 + 193.784 [x_3] - 10.7642 [x_1] [x_3] + 60.1183 [x_2] [x_3] - 4.60535 [x_3]^2$. Minimum crossfeed force has found as 129.23 N in scenario 2. According to scenarios 1 and 3, minimum crossfeed force has found as 124.779 N with the following conditions; cutting speed: 1.682, cutting feed: 1.682 and depth of cut: -1.682. 124.779 N could be a realistic and better result in comparison with the experimental results because the experiment had not done in full combination of all input parameters.

For third output thrust force (F_z) the design variables were fitted to the model with $R^2_{\text{training}} = 0.99$ and $R^2_{\text{testing}} = 0.97$ values: $43.74 - 16.5126 [x_1] + 5.92969 [x_1]^2 + 0.857342 [x_2] - 8.4844 [x_1] [x_2] + 4.49432 [x_2]^2 + 1.84508 [x_3] - 4.0281 [x_1] [x_3] + 3.5319 [x_2] [x_3] - 1.13342 [x_3]^2$. Minimum thrust force has found as 18.298 N in scenario 2. According to scenarios 1 and 3, minimum thrust force has found as 17.989 N with the following conditions; cutting speed: 1.682, cutting feed: 1.682 and depth of cut: -1.682. 17.989 N could be a realistic and better result in

comparison with the experimental results because the experiment had not done in full combination of all input parameters.

Chapter 8

Conclusion

Surface roughness is crucial when it comes to how a machine reacts with its surroundings. The friction coefficients of rough surfaces are greater than those of smooth surfaces, thus they tend to wear down faster. Hence, surface roughness is a frequent surface quality criterion. However, reducing a machined surface's roughness will increase its production costs enormously. Sometimes, the production costs of a product is sacrificed for its effectiveness in use. The industry places a high value on reducing surface roughness.

Cutting force is the resistance of the workpiece against the intrusion of the cutting tool. These forces determine the manufacturing requirements and loads. The high amount of cutting forces cause high temperatures, vibrations, fails the structure of workpiece-tool. Measured forces may be used to determine the machinability of the workpiece, especially limited material resources and time. Therefore, detecting and minimizing cutting forces is critical in terms of material resources, manufacturing cost and time.

Machine effectiveness and expenses are heavily influenced by tool performance. In addition to the roughness left on the workpiece surface, tool performance may be evaluated by the forces produced throughout the procedure. When surfaces are processed, tensions and temperatures are generated as a result of processing forces. Tension and temperatures along tool-chip and tool-work contacts are also influenced by these factors. If the operating circumstances are not appropriately set, all of these factors contribute to a deterioration of the surface integrity. There are a number of processing factors that must be understood in order to get the best

surface qualities while minimizing the cutting pressures, tool wear, and tool life (cutting life).

The design factors (structural and empirical variables) must be tuned in order to achieve this. Inadequate techniques include (i) using traditional optimization strategies, (ii) changing one input while holding the others constant, (iii) using one or two regression models as the objective function, (iv) failing to verify the limitedness of the selected models, and (v) excluding some candidates from consideration. Mathematical optimization issues cannot be solved using these design processes.

For that reason, a unique modeling-designing-optimizing approach has been developed to reduce surface roughness, cutting forces, tool wear, and tool life (cutting life). In the process of deciding on these outcomes; literature review has been made and the determined 12 studies has been selected in order to carry out the proposed approach. Evaluations and comparisons of the outcomes has been made according to the results of the optimization technique carried out on these studies.

This study began with an in-depth examination of the use of nonlinear multiple regression analysis. It also included logical versions for linear and quadratic equations, as well as trigonometric and logarithmic problems. Furthermore, it was determined if potential models were limited in order to provide accurate values. A final direct search strategy was employed throughout the optimization stage, which included stochastic techniques. Applying more than one stochastic technique with distinct phenomenological bases increases the robustness of the solution of the optimization problem. In order to solve the optimization problem, four different optimization algorithms (MDE, MNM, MSA, MRS) have been utilized.

Results of this investigation include:

(1) R^2_{training} is compatible with all 13 models. A meaningful operational structure cannot be obtained if models are not evaluated for stability. By verifying each potential model's durability, the optimization step has been conducted with functions that generate value only within the technical constraints, in an effort to

address this disadvantage. A model with high R^2 values and a limitedness characteristic was sought.

(2) When the optimization issue becomes complex, the choice of objective function and restrictions for input parameters becomes important.

(3) When the models selected for 12 different studies were examined in the optimization study, it was observed that response values (surface roughness, cutting forces, tool wear and tool life (cutting time)) were reached lower or very close than the results of the studies.

(4) In spite of the fact that the innovative modeling-design-optimization technique proposed in this work was only utilized to minimize outputs, it may be utilized to optimize other variables in the manufacturing industry by changing objective functions, input parameters, and restrictions of the issue.

(5) This study is shown that the importance of R^2_{testing} calculation, to show the deficiencies of the approaches that are used only R^2 calculated optimization problems and to improve existing regression models.

References

- [1] Childs THC, Maekawa K, Obikawa T, Yamane Y (2000) Metal machining. Theory and application. Arnold, London.
- [2] Davim, J.P., Machining of Hard Materials. London: Springer; 2011.
- [3] Tönshoff HK, Arendt C, Ben Amor R. Cutting of hardened steel. Ann CIRP 2000;49
- [4] Kalpakjian, S., Schmid, S. R., & In Sekar, K. S. V. (2014). Manufacturing engineering and technology.
- [5] Asiltürk I, Akkus H (2011) Determining the effect of cutting parameters on surface roughness in hard turning using the Taguchi method. Measurement 44:1697–1704
- [6] Hasçalık A, Çaydaş U. Optimization of turning parameters for surface roughness and tool life based on the Taguchi method. Int J Adv Manuf Technol 2008;38: 896–903.
- [7] Ghani, J.A., Choudhury, I.A., Hassan, H.H., 2004, Application of Taguchi method in the optimization of end milling parameters. Journal of Materials Processing Technology 145, pp84 92.
- [8] Reddy, B.S., Kumar, J.S., Reddy, K.V.K., 2011, Optimization of surface roughness in CNC end milling using response surface methodology and genetic algorithm. International Journal of Engineering, Vol. 3, No. 8, pp. 102-109.
- [9] Mahapatra SS, Patnaik A. Optimization of wire electrical discharge machining (WEDM) process parameters using Taguchi method. Int J Adv Manuf Technol 2007;34:911–25.

- [10] Nalbant M, Gokkaya H, Sur G. Application of Taguchi Method in the Optimization of Cutting Parameters for Surface Roughness in Turning. *Mater Des* 2007;28:1379–85.
- [11] Davim J.P, Figueira L, Comparative evaluation of conventional and wiper ceramic tools on cutting forces, surface roughness, and tool wear in hard turning AISI D2 steel, *Proceedings of IMechE Part B: J. Engineering Manufacture*, 221 (2007), 625 – 633.
- [12] Yi, J., Jiao, L., Wang, X., Xiang, J., Yuan, M., Gao, S., 2015. Surface Roughness Models and Their Experimental Validation in Micro Milling of 6061-T6 Al Alloy by Response Surface Methodology. *Mathematical Problems in Engineering*, 2015, 1-9.
- [13] Kyratsis, P., Markopoulos, A., Efkolidis, N., Maliagkas, V., Kakoulis, K., 2018. Prediction of Thrust Force and Cutting Torque in Drilling Based on the Response Surface Methodology. *Machines*, 6(2), 24.
- [14] Hossein, A.E.; Kadirgama, K.; Hamdi, M.; and Benyounis, K.Y. (2007). Prediction of cutting force in end-milling operation of modified AISI P20 tool steel. *Journal of Materials Processing Technology*, 182(1-3), 241-247.
- [15] Neşeli S, Yıldız S, Türkeş E. Optimization of tool geometry parameters for turning operations based on the response surface methodology. *Measurement* 2011;44:580–7.
- [16] Horng JT, Liu NM, Chiang KT. Investigating the machinability evaluation of Hadfield steel in the hard turning with Al₂O₃/TiC mixed ceramic tool based on the response surface methodology. *J Mater Process Technol* 2008;208:532–41.
- [17] B. H. M. Sadeghi, ABP-neural network predict or model for plastic injection molding process, *J. Mater. Process. Technol.* 103 (3) (2000) 411–416.
- [18] T.T. Chow, G.Q. Zhang, Z. Lin, C.L. Song, Global optimization of absorption chiller system by genetic algorithm and neural network, *Energy Build.* 34 (1) (2002) 103–109.

- [19] D.F. Cook, C.T. Ragsdale, R.L. Major, Combining a neural network with a genetic algorithm for process parameter optimisation, *Eng. Appl. Artif. Intell.* 13 (4) (2000) 391–396.
- [20] S.L.B. Woll, D.J. Cooper, Pattern-based closed-loop quality control for the injection molding process, *Polym. Eng. Sci.* 37 (5) (1997) 801– 812.
- [21] C. R. Chen, H. S. Ramaswamy, Modeling and optimization of variable retort temperature (VRT) thermal processing using coupled neural networks and genetic algorithms, *J. Food Eng.* 53 (3) (2002) 209–220.
- [22] B. Ozcelik, T. Erzurumlu, Determination of effecting dimensional parameters on warpage of thin shell plastic parts using integrated response surface method and genetic algorithm, *Int. Commun. Heat Mass Transfer* 32 (2005) 1085–1094.
- [23] Zain AM, Haron H, Sharif S (2012) Integrated ANN–GA for estimating the minimum value for machining performance. *Int J Prod Res* 50(1):191–213.
- [24] Dikshit MK, Puri AB, Maity A (2014) Analysis of cutting forces and optimization of cutting parameters in high speed ball-end milling using response surface methodology and genetic algorithm. *Procedia Mater Sci* 5:1623–1632.
- [25] Sardiñas RQ, Santana MR, Brindis EA. Genetic algorithm-based multi-objective optimization of cutting parameters in turning processes. *Eng Appl Artif Intel* 2006;19: 127–33.
- [26] Gupta, Amit & Guntuku, Sharath Chandra & Desu, Raghuram & Balu, Aditya. (2014). Optimisation of turning parameters by integrating genetic algorithm with support vector regression and artificial neural networks. *The International Journal of Advanced Manufacturing Technology.* 77.
- [27] Gopan V. Wins K. L. D. Surendran A. 2018. Integrated ANN-GA Approach for Predictive Modeling and Optimization of Grinding Parameters with Surface Roughness as the Response, *Materials Today: Proceedings*, 5(5), 12133-12141.

- [28] Suresh PVS, Venkatehwarra rao K, Desmukh SG. A genetic algorithmic approach for optimization of the surface roughness prediction model. *Int J Mach Tools Manuf* 2002;42:675–80.
- [29] Cus F, Balic J. Optimization of cutting process by GA approach, *Robot. Cim-Int Manuf* 2003;19:113–21.
- [30] Tsai YH, Chen JC, Lou SJ (1999) An in-process surface recognition system based on neural networks in end milling cutting operations. *Int J Mach Tools Manuf* 39(4):583–605.
- [31] Mia M, Razi MH, Ahmad I, Mostafa R, Rahman SMS, Ahmed DH, Dey PR, Dhar NR (2017) Effect of time-controlled MQL pulsing on surface roughness in hard turning by statistical analysis and artificial neural network. *Int J Adv Manuf Technol* 91(9–12):3211–3223.
- [32] Subramanian M, Sakthivel M, Sooryaprakash K, Sudhakaran R (2013) Optimization of cutting parameters for cutting force in shoulder milling of Al7075-T6 using response surface methodology and genetic algorithm. *Procedia Eng* 64:690–700.
- [33] Feng, C. X., & Wang, X. (2002). Development of empirical models for surface roughness prediction in finish turning. *International Journal of Manufacturing Technology*, 20, 348–356.
- [34] Durakbasa, M. N., Akdogan, A., Vanli A. S. and Bulutsuz, A. G., Optimization of End Milling Parameters and Determination of The Effects of Edge Profile for High Surface Quality of AISI H13, (2014).
- [35] Polatoglu, Ilker & Aydin, Levent & Nevruz, Bilgehan & Özer, Sibel. (2020). A Novel Approach for the Optimal Design of a Biosensor. *Analytical Letters*. 53. 1-18. 10.1080/00032719.2019.1709075.
- [36] Güngör, Şahin & Aydin, Murat. (2020). Heat Transfer Optimization by Multiple Nonlinear Neuro-regression Approach for Ground Source Heat Exchanger. 10.1201/9780429289576.

- [37] Choudhary, A., Harding, J., & Tiwari, M. (2009). Data mining in manufacturing: A review based on the kind of knowledge. *Journal of Intelligent Manufacturing*, 20(5), 501–521.
- [38] Grzenda, M., Bustillo, A., & Zawistowski, P. (2010). A soft computing system using intelligent imputation strategies for roughness prediction in deep drilling. *Journal of Intelligent Manufacturing*.
- [39] Rajasekaran, T., Palanikumar, K., & Vinayagam, B. K., (2011). Application of fuzzy logic for modeling surface roughness in turning CFRP composites using CBN tool. *Production Process*.
- [40] Manisha Priyadarshini, Ajit Behera, Chandan Kumar Biswas, Biswajit Swain, Swadhin Patel, Multi-objective optimization of WEDM process by hybrid methodology, *Materials Today: Proceedings Volume 33, Part 8, 2020, Pages 5511-5513*.
- [41] Yildiz, A., Hybrid Taguchi-differential Evolution Algorithm for Optimization of Multi-pass Turning Operations, (2012).
- [42] Wang, Z. G., Wong, Y. S., and Rahman, M., Optimization of Multi-pass Milling Using Genetic Algorithm and Genetic Simulated Annealing, (2004).
- [43] Rao, S. S., *Engineering Optimization Theory and Practice*, 4th Edition, (2009), p.35-36.
- [44] Aouici, H., Fnides, B., Elbah, M., Benlahmidi, S., Bensouilah, H., & Yallese, M. (2016). Surface roughness evaluation of various cutting materials in hard turning of AISI H11. *International Journal of Industrial Engineering Computations*, 7(2), 339-352.
- [45] Bouacha, K., Yallese, M. A., Khmel, S., & Belhadi, S. (2014). Analysis and optimization of hard turning operation using cubic boron nitride tool. *International Journal of Refractory Metals and Hard Materials*, 45, 160-178.

- [46] Davoodi, B., & Eskandari, B. (2015). Tool wear mechanisms and multi-response optimization of tool life and volume of material removed in turning of N-155 iron–nickel-base superalloy using RSM. *Measurement*, 68, 286-294.
- [47] Hanief, M., Wani, M. F., & Charoo, M. S. (2017). Modeling and prediction of cutting forces during the turning of red brass (C23000) using ANN and regression analysis. *Engineering science and technology, an international journal*, 20(3), 1220-1226.
- [48] Jena, J., Panda, A., Behera, A. K., Jena, P. C., Das, S. R., & Dhupal, D. (2019). Modeling and optimization of surface roughness in hard turning of AISI 4340 steel with coated ceramic tool. In *Innovation in Materials Science and Engineering* (pp. 151-160). Springer, Singapore.
- [49] Kovac, P., Rodic, D., Pucovsky, V., Savkovic, B., & Gostimirovic, M. (2013). Application of fuzzy logic and regression analysis for modeling surface roughness in face milling. *Journal of Intelligent manufacturing*, 24(4), 755-762.
- [50] Ikhlas, M., Athmane, Y. M., Hamza, B., Ahmed, K., & Mohamed, E. (2018). Prediction of surface roughness and cutting forces using RSM, ANN, and NSGA-II in finish turning of AISI 4140 hardened steel with mixed ceramic tool. *The International Journal of Advanced Manufacturing Technology*, 97(5-8), 1931-1949.
- [51] Qu, S., Zhao, J., & Wang, T. (2017). Experimental study and machining parameter optimization in milling thin-walled plates based on NSGA-II. *The International Journal of Advanced Manufacturing Technology*, 89(5-8), 2399-2409.
- [52] Paturi, U. M. R., Devarasetti, H., & Narala, S. K. R. (2018). Application of regression and artificial neural network analysis in modelling of surface roughness in hard turning of AISI 52100 steel. *Materials Today: Proceedings*, 5(2), 4766-4777.

- [53] Sahoo, A. (2014). Application of Taguchi and regression analysis on surface roughness in machining hardened AISI D2 steel. *International Journal of Industrial Engineering Computations*, 5(2), 295-304.
- [54] Sahoo, A., Rout, A., & Das, D. (2015). Response surface and artificial neural network prediction model and optimization for surface roughness in machining. *International Journal of Industrial Engineering Computations*, 6(2), 229-240.
- [55] Subramanian, M., Sakthivel, M., Sooryaprakash, K., & Sudhakaran, R. (2013). Optimization of cutting parameters for cutting force in shoulder milling of Al7075-T6 using response surface methodology and genetic algorithm. *Procedia Engineering*, 64, 690-700.
- [56] Groover, M. P., *Fundamentals of Modern Manufacturing Materials, Processes, and Systems*, 4th Edition, (2010), p486-524.
- [57] Davim, J. P., *Modern Machining Technology*, (2011), p213-217.
- [58] Courtesy of Sandvik Coromant, <https://www.sandvik.coromant.com>
- [59] Davim, J. P., *Modern Machining Technology*, (2011), p1-61.
- [60] Dolinsek, S., Kopac, J., *Mechanism and Types of Tool Wear Particularities in Advanced Cutting Materials*, (2006).
- [61] Dolinsek, S., Sustarsic, B., Kopac, J., *Wear Mechanisms of Cutting Tools in High Speed Cutting Processes*, (2001), p351.
- [62] Cavazzuti, M. 2013. *Optimization Methods From Theory to Design: Scientific and Technological Aspects in Mechanics*. Springer, Berlin.
- [63] Antony, J. 2014. *Design of Experiments for Engineers and Scientists*. 2nd Edition. Elsevier, London.
- [64] Vecchio, R.J. 1997. *Understanding Design of Experiments*. Gardner Publications, USA.

- [65] Montgomery, D.C., Runger, G.C. and Hubele, N.F. 2010. Engineering Statistics. 5th Edition. John Wiley and Sons, USA. [62]
- [66] Antony, J. (1998). Some key things industrial engineers should know about experimental design. *Logistics Information Management*, 11(6), 386-392.
- [67] Gunst, R.F. and Mason, R.L. (2009). Fractional factorial design. *Wiley Interdisciplinary Reviews: Computational Statistics*. 1. 234 - 244. 10.1002/wics.27.
- [68] Montgomery, D.C. 2001. Design and Analysis of Experiments. John Wiley and Sons, USA.
- [69] Turhan, F. 2017. 1100 serisi alüminyum malzemelerde tig kaynağı ile oluşan kaynak dikiş geometrisinin optimizasyonu. M.S. Thesis, İzmir Katip Çelebi University, İzmir.
- [70] Ombach, J. 2014. A short introduction to stochastic optimization. *Schedae Informaticae*. 23: 9–20.
- [71] Rao, R.V. and Savsani, V.J. 2012. Mechanical Design Optimization using Advanced Optimization Techniques. Springer. London.
- [72] Tech Target, whatis.techtarget.com/definition/stochastic-optimization.
- [73] Yan, X., Zhou, Y., Wen, Y. and Chai, X. 2013. Qualitative and quantitative integrated modeling for stochastic simulation and optimization. *J. Appl. Math.* Volume 2013, Article ID 831273.1–12.
- [74] Li, G. and Zhang, W. 2013. Study on Indefinite stochastic linear quadratic optimal control with inequality constraint. *J. Appl. Math.* Volume 2013, Article ID 805829, 1–9.
- [75] Aydin, L., Aydin, O., Artem, H.S. and Mert, A. 2016. Design of dimensionally stable composites using efficient global optimization method. *J. Mater. Des. Appl.* 1–13.

- [76] Zakaria, A., Firas, B.I., Hossain-Lipu, M.S. and Hannan, M.A. 2019. Uncertainty models for stochastic optimization in renewable energy applications. *Renew. Energy*. 145: 1543–1571.
- [77] Niamsup, P. and Rajchakit, G. 2013. New results on robust stability and stabilization of linear discrete-time stochastic systems with convex polytopic uncertainties. *J. Appl. Math.* Vol. 2013, Article ID 368259.1–10.
- [78] Maggioni, F., Cagnolari, M., Bertazzi, L. and Wallace, S.W. 2019. Stochastic optimization models for a bike-sharing problem with transshipment. *Eur. J. Oper. Res.* 276(1): 272–283.
- [79] Gutierrez, G., Galan, A., Sarabia, A. and De-Prada, C. 2018. Two-stage stochastic optimization of a hydrogen network. *IFAC 18*: 263–268.
- [80] Khayyam, H., Naebe, M., Bab-Hadiashar, A., Jamshidi, F., Li, Q., Atkiss, S., Buckmaster, D. and Fox, B. 2015. Stochastic optimization models for energy management in carbonization process of carbon fiber production. *Appl. Energy*. 158: 643–655.
- [81] Tifkitsis, K.I., Mesogitis, T.S., Struzziero, G. and Skordos, A.A. 2018. Stochastic multi- objective optimisation of the cure process of thick laminates. *Compos. Part A* 112: 383–394.
- [82] Ozturk, S., Aydin, L. and Celik, E. 2018. A comprehensive study on slicing processes optimization of silicon ingot for photovoltaic applications. *J. Sol. Energy*. 161: 109–124.
- [83] Grabusts, P., Musatovs, J. and Golenkov, V. 2018. The application of simulated annealing method for optimal route detection between objects. *Procedia Comput. Sci.* 149: 95–101.
- [84] Aydin, L. and Artem, H.S. 2017. Design and optimization of fiber composites, Turkey. pp. 299–315. In: Seydibeyoglu, M.O., Mohanty, A.K. and Misra, M. [eds.]. *Woodhead Publishing Series in Composites Science and Engineering*.

- [85] Huang, Z. and Chen, Y. 2013. An improved differential evolution algorithm based on adaptive parameter. *Journal of Control Science and Engineering* Volume 2013, Article ID 462706, 1–5.
- [86] Das, S. and Suganthan, P.N. 2011. Differential evolution: A survey of the state-of-the-art. *IEEE T. Evolut. Comput.* 15(1): 4–35.
- [87] Jujjavarapu, S. and Chimmiri, V. 2016. Dynamic modeling and metabolic flux analysis for optimized production of rhamnolipids. *Chem. Eng. Commun.* 203: 326–338.
- [88] Arunachalam, V. 2008. Optimization using Differential Evolution. M.S. Thesis, The University of Western Ontario, London.
- [89] Ozturk S., Aydin L., and Celik, E., A Comprehensive Study on Slicing Processes Optimization of Silicon Ingot for Photovoltaic Applications, (2017).
- [90] Wolfram Mathematica software 11.3.
- [91] Ozturk, S., Aydin, L., Kucukdogan, N. and Celik, E. 2018. Optimization of lapping processes of silicon wafer for photovoltaic applications. *Sol. Energy* 164: 1–11.
- [92] Momin, J., Xin-She, Y. and Hans-Jürgen, Z. 2013. Test functions for global optimization: A comprehensive survey. pp. 193–222. In: Xin-She, Y., Zhihua, C., Renbin, X., Amir Hossein, G. and Mehmet, K. [eds.]. *Swarm Intelligence and Bio-Inspired Computation*, Elsevier.
- [93] Karaboğa, D. 2018. Yapay zeka optimizasyon algoritmaları. Nobel akademik yayıncılık, Ankara.
- [94] Ingber, L. 1993. Simulated annealing: Practice versus theory. *Math. Comput. Model.* 18(11): 29–57.

- [95] Savran, M. and Aydin, L. 2018. Stochastic optimization of graphite-flax/epoxy hybrid laminated composite for maximum fundamental frequency and minimum cost. *Eng. Struct.* 174: 675–687.
- [96] Storn, R., Price, K. Differential Evolution – A Simple and Efficient Heuristic for global Optimization over Continuous Spaces. *Journal of Global Optimization* 11, 341–359 (1997). <https://doi.org/10.1023/A:1008202821328>
- [97] Vo-Duy, T., Ho-Huu, V., Do-Thi, T.D., Dang-Trung, H. and Nguyen-Thoi, T. 2017. A global numerical approach for lightweight design optimization of laminated composite plates subjected to frequency constraints. *Composite Structures* 159: 646–655.
- [98] Nelder, J.A. and Mead, R. 1965. A simplex-method for function minimization. *Computer Journal* 7(4): 308–313. <https://doi.org/10.1093/comjnl/7.4.308>.

Appendices

Appendix A

Explicit Model Expressions of the Case Studies

NOTATION	CSI-O1
CSI-O1-L	$0.205985 - 0.000764479 [x1] + 2.72297 [x2] + 0.158559 [x3]$
CSI-O1-LN	$(70760.7 - 379.413 [x1] + 488635. [x2] + 14283.8 [x3]) / (236253. - 556.769 [x1] + 127446. [x2] - 16376.1 [x3])$
CSI-O1-SON	$0.170931 + 3.21796*10^{-6} [x1] - 5.83797*10^{-6} [x1]^2 + 1.8119 [x2] + 0.00979476 [x1] [x2] - 2.2425 [x2]^2 + 0.448936 [x3] - 0.00037037 [x1] [x3] - 0.107995 [x2] [x3] - 0.393295 [x3]^2$
CSI-O1-SONR	$(54262.9 + 3.90678*10^6 [x1] - 23374. [x1]^2 - 1.80442*10^7 [x2] + 3.82892*10^7 [x1] [x2] + 7.9117*10^6 [x2]^2 + 4.62388*10^8 [x3] + 441040. [x1] [x3] + 8.61705*10^7 [x2] [x3] - 4.89955*10^8 [x3]^2) / (241183. + 1.73649*10^7 [x1] - 43601. [x1]^2 - 1.5465*10^7 [x2] + 1.26744*10^7 [x1] [x2] - 1.00757*10^7 [x2]^2 - 2.39816*10^8 [x3] + 710906. [x1] [x3] - 4.88481*10^7 [x2] [x3] + 1.92096*10^8 [x3]^2)$
CSI-O1-TON	$0.199737 + 0.000260806 [x1] - 3.95103*10^{-6} [x1]^2 - 4.74001*10^{-8} [x1]^3 + 0.631643 [x2] + 0.0129166 [x1] [x2] + 0.000123611 [x1]^2 [x2] + 3.81757 [x2]^2 - 0.15625 [x1] [x2]^2 + 50.1595 [x2]^3 + 0.250407 [x3] + 0.000842471 [x1] [x3] + 8.95468*10^{-7} [x1]^2 [x3] - 0.833333 [x2] [x3] - 0.0138889 [x1] [x2] [x3] + 2.49363*10^{-14} [x2]^2 [x3] - 0.0321549 [x3]^2 + 4.29556*10^{-16} [x1] [x3]^2 + 5.55556 [x2] [x3]^2 - 0.951927 [x3]^3$
CSI-O1-FOTN	$-4.40062 - 0.934211 \text{Cos}[x1] + 4.27282 \text{Cos}[x2] + 0.381275 \text{Cos}[x3] + 0.986819 \text{Sin}[x1] + 3.26834 \text{Sin}[x2] + 0.285077 \text{Sin}[x3]$
CSI-O1-FOTNR	$(49060.3 + 15085. \text{Cos}[x1] - 52677.8 \text{Cos}[x2] + 261.804 \text{Cos}[x3] - 15388.9 \text{Sin}[x1] + 897.173 \text{Sin}[x2] - 5.77293 \text{Sin}[x3]) / (7684.95 + 10180.4 \text{Cos}[x1] - 8839.52 \text{Cos}[x2] - 1102.36 \text{Cos}[x3] - 10386.9 \text{Sin}[x1] + 8988.05 \text{Sin}[x2] - 838.893 \text{Sin}[x3])$
CSI-O1-SOTN	$62.4619 + 18.0849 \text{Cos}[x1] + 114.239 \text{Cos}[x1]^2 + 63.4121 \text{Cos}[x2] + 9.30835 \text{Cos}[x1] \text{Cos}[x2] + 64.3788 \text{Cos}[x2]^2 + 70.8335 \text{Cos}[x3] + 15.4348 \text{Cos}[x1] \text{Cos}[x3] - 526.712 \text{Cos}[x2] \text{Cos}[x3] + 79.3187 \text{Cos}[x3]^2 - 9.0846 \text{Sin}[x1] + 131.139 \text{Cos}[x1] \text{Sin}[x1] - 18.4556 \text{Cos}[x2] \text{Sin}[x1] - 15.479 \text{Cos}[x3] \text{Sin}[x1] + 114.288 \text{Sin}[x1]^2 + 39.7925 \text{Sin}[x2] + 7.89244 \text{Cos}[x1] \text{Sin}[x2] + 38.6217 \text{Cos}[x2] \text{Sin}[x2] - 74.2252 \text{Cos}[x3] \text{Sin}[x2] - 9.51127 \text{Sin}[x1] \text{Sin}[x2] - 176.29 \text{Sin}[x2]^2 + 67.5611 \text{Sin}[x3] + 14.637 \text{Cos}[x1] \text{Sin}[x3] - 162.931 \text{Cos}[x2] \text{Sin}[x3] + 94.0363 \text{Cos}[x3] \text{Sin}[x3] - 14.8457 \text{Sin}[x1] \text{Sin}[x3] - 22.9606 \text{Sin}[x2] \text{Sin}[x3] - 139.695 \text{Sin}[x3]^2$
CSI-O1-SOTNR	$(-2.17216 - 1.66863 \text{Cos}[x1] - 1.12133 \text{Cos}[x1]^2 - 4.77665 \text{Cos}[x2] - 6.06832 \text{Cos}[x1] \text{Cos}[x2] - 7.31485 \text{Cos}[x2]^2 + 4.36681 \text{Cos}[x3] + 8.96984 \text{Cos}[x1] \text{Cos}[x3] + 2.48865 \text{Cos}[x2] \text{Cos}[x3] + 9.03569 \text{Cos}[x3]^2 - 0.925832 \text{Sin}[x1] - 0.499141 \text{Cos}[x1] \text{Sin}[x1] - 4.66738 \text{Cos}[x2] \text{Sin}[x1] + 8.06917 \text{Cos}[x3] \text{Sin}[x1] - 0.0508293 \text{Sin}[x1]^2 + 15.0671 \text{Sin}[x2] - 0.053991 \text{Cos}[x1] \text{Sin}[x2] + 14.4313 \text{Cos}[x2] \text{Sin}[x2] + 6.93308 \text{Cos}[x3] \text{Sin}[x2] - 3.06626 \text{Sin}[x1] \text{Sin}[x2] + 6.1427 \text{Sin}[x2]^2 + 3.29695 \text{Sin}[x3] + 2.80989 \text{Cos}[x1] \text{Sin}[x3] + 3.30338 \text{Cos}[x2] \text{Sin}[x3] + 9.01951 \text{Cos}[x3] \text{Sin}[x3] + 2.27471 \text{Sin}[x1] \text{Sin}[x3] + 7.23901 \text{Sin}[x2] \text{Sin}[x3] - 10.2078 \text{Sin}[x3]^2) / (-5.76623 - 2.9194 \text{Cos}[x1] - 3.14237 \text{Cos}[x1]^2 - 5.05442 \text{Cos}[x2] + 1.09716 \text{Cos}[x1] \text{Cos}[x2] - 4.36441 \text{Cos}[x2]^2 + 7.35466 \text{Cos}[x3] + 7.2169 \text{Cos}[x1] \text{Cos}[x3] + 7.70531 \text{Cos}[x2] \text{Cos}[x3] + 16.7301 \text{Cos}[x3]^2 - 1.37376 \text{Sin}[x1] - 2.20613 \text{Cos}[x1] \text{Sin}[x1] + 2.40142 \text{Cos}[x2] \text{Sin}[x1] + 5.70984 \text{Cos}[x3] \text{Sin}[x1] - 1.62385 \text{Sin}[x1]^2 - 2.05518 \text{Sin}[x2] - 17.4883 \text{Cos}[x1] \text{Sin}[x2] - 1.8595 \text{Cos}[x2] \text{Sin}[x2] + 2.95296 \text{Cos}[x3] \text{Sin}[x2] - 16.4249 \text{Sin}[x1] \text{Sin}[x2] - 0.401815 \text{Sin}[x2]^2 + 5.42742 \text{Sin}[x3] + 0.707276 \text{Cos}[x1] \text{Sin}[x3] + 4.96443 \text{Cos}[x2] \text{Sin}[x3] + 16.8935 \text{Cos}[x3] \text{Sin}[x3] - 0.241646 \text{Sin}[x1] \text{Sin}[x3] + 1.66535 \text{Sin}[x2] \text{Sin}[x3] - 21.4963 \text{Sin}[x3]^2)$
CSI-O1-FOLN	$1.70676 - 0.102586 \text{Log}[x1] + 0.311766 \text{Log}[x2] + 0.0431853 \text{Log}[x3]$
CSI-O1-FOLNR	$(12.0558 - 1.72039 \text{Log}[x1] + 0.615334 \text{Log}[x2] - 0.2016 \text{Log}[x3]) / (15.0451 - 2.7507 \text{Log}[x1] - 1.35073 \text{Log}[x2] + 0.124604 \text{Log}[x3])$
CSI-O1-SOLN	$0.855693 + 0.117369 \text{Log}[x1] + 0.0126861 \text{Log}[x1]^2 + 0.0168698 \text{Log}[x2] + 0.168778 \text{Log}[x1] \text{Log}[x2] + 0.126137 \text{Log}[x2]^2 + 0.077547 \text{Log}[x3] - 0.014333 \text{Log}[x1] \text{Log}[x3] - 0.00230302 \text{Log}[x2] \text{Log}[x3] - 0.0105161 \text{Log}[x3]^2$
CSI-O1-SOLNR	$(21.1549 + 53.1589 \text{Log}[x1] + 20.4941 \text{Log}[x1]^2 + 39.0589 \text{Log}[x2] + 85.9191 \text{Log}[x1] \text{Log}[x2] + 71.2468 \text{Log}[x2]^2 - 22.6562 \text{Log}[x3] + 9.61074 \text{Log}[x1] \text{Log}[x3] + 14.8128 \text{Log}[x2] \text{Log}[x3] - 11.6124 \text{Log}[x3]^2) / (-25.9122 - 62.8707 \text{Log}[x1] + 32.6127 \text{Log}[x1]^2 - 34.15 \text{Log}[x2] + 25.9693 \text{Log}[x1] \text{Log}[x2] - 7.63437 \text{Log}[x2]^2 - 175.408 \text{Log}[x3] + 22.5698 \text{Log}[x1] \text{Log}[x3] - 9.07876 \text{Log}[x2] \text{Log}[x3] - 28.6993 \text{Log}[x3]^2)$
NOTATION	CSI-O2
CSI-O2-L	$2.13887 - 0.00232891 [x1] + 12.2965 [x2] + 0.402477 [x3]$
CSI-O2-LN	$(-44106.2 + 161.167 [x1] + 475389. [x2] + 6962.7 [x3]) / (-9453.29 + 55.5901 [x1] + 102063. [x2] + 443.234 [x3])$
CSI-O2-SON	$0.107458 + 0.00160045 [x1] + 0.0000141818 [x1]^2 + 41.2631 [x2] - 0.0451778 [x1] [x2] - 94.6869 [x2]^2 + 0.516312 [x3] - 0.00925926 [x1] [x3] + 2.66602 [x2] [x3] + 1.8285 [x3]^2$
CSI-O2-SONR	$(3.99212*10^7 + 2.8967*10^9 [x1] + 6.71317*10^9 [x1]^2 + 1.54814*10^7 [x2] + 1.85527*10^9 [x1] [x2] + 3.10133*10^6 [x2]^2 + 5.64172*10^6 [x3] + 2.03271*10^8 [x1] [x3] + 3.82976*10^6 [x2] [x3] + 754334. [x3]^2) / (-1.32595*10^8 - 9.53993*10^9 [x1] + 2.07199*10^9 [x1]^2 - 5.16935*10^7 [x2] - 6.19382*10^9 [x1] [x2] - 1.03645*10^7 [x2]^2 - 1.86136*10^7 [x3] - 6.39768*10^8 [x1] [x3] - 1.2783*10^7 [x2] [x3] - 2.44609*10^6 [x3]^2)$
CSI-O2-TON	$0.728697 + 0.00443636 [x1] + 0.0000245059 [x1]^2 + 1.28585*10^{-7} [x1]^3 + 20.4222 [x2] - 0.0651536 [x1] [x2] - 0.00145643 [x1]^2 [x2] + 40.452 [x2]^2 + 1.74479 [x1] [x2]^2 - 1240.84 [x2]^3 - 5.02437 [x3] + 0.00181493 [x1] [x3] + 0.000189321 [x1]^2 [x3] + 86.6667 [x2] [x3] + 0.368056 [x1] [x2] [x3] + 93.75 [x2]^2 [x3] + 2.34274 [x3]^2 - 0.172222 [x1] [x3]^2 - 286.111 [x2] [x3]^2 + 57.5204 [x3]^3$
CSI-O2-FOTN	$-180.813 - 38.979 \text{Cos}[x1] + 192.071 \text{Cos}[x2] - 2.0574 \text{Cos}[x3] + 39.9406 \text{Sin}[x1] + 35.3577 \text{Sin}[x2] - 0.224169 \text{Sin}[x3]$
CSI-O2-FOTNR	$(-11.7978 - 10.7541 \text{Cos}[x1] + 14.2786 \text{Cos}[x2] - 0.226774 \text{Cos}[x3] + 10.9901 \text{Sin}[x1] + 2.27668 \text{Sin}[x2] - 0.085881 \text{Sin}[x3]) / (-3.84049 - 3.42829 \text{Cos}[x1] + 4.64217 \text{Cos}[x2] - 0.080072 \text{Cos}[x3] + 3.50337 \text{Sin}[x1] + 0.699556 \text{Sin}[x2] - 0.0304874 \text{Sin}[x3])$
CSI-O2-SOTN	$-1657.32 - 378.974 \text{Cos}[x1] - 2992. \text{Cos}[x1]^2 - 1682.51 \text{Cos}[x2] - 347.656 \text{Cos}[x1] \text{Cos}[x2] - 1708.13 \text{Cos}[x2]^2 - 1879.75 \text{Cos}[x3] - 416.695 \text{Cos}[x1] \text{Cos}[x3] + 13981.4 \text{Cos}[x2] \text{Cos}[x3] - 2105.64 \text{Cos}[x3]^2 + 343.961 \text{Sin}[x1] - 3480.63 \text{Cos}[x1] \text{Sin}[x1] + 387.005 \text{Cos}[x2] \text{Sin}[x1] + 403.526 \text{Cos}[x3] \text{Sin}[x1] - 3074.72 \text{Sin}[x1]^2 - 1126.96 \text{Sin}[x2] - 242.017 \text{Cos}[x1] \text{Sin}[x2] - 1098.1 \text{Cos}[x2] \text{Sin}[x2] + 2236.55 \text{Cos}[x3] \text{Sin}[x2] + 250.048 \text{Sin}[x1] \text{Sin}[x2] + 4483.22 \text{Sin}[x2]^2 - 1714.07 \text{Sin}[x3] - 373.287 \text{Cos}[x1] \text{Sin}[x3] + 4128.86 \text{Cos}[x2] \text{Sin}[x3] - 2394.95 \text{Cos}[x3] \text{Sin}[x3] + 374.7 \text{Sin}[x1] \text{Sin}[x3] + 672.172 \text{Sin}[x2] \text{Sin}[x3] + 3762.82 \text{Sin}[x3]^2$
CSI-O2-SOTNR	$(2.30952 + 1.38988 \text{Cos}[x1] + 1.72217 \text{Cos}[x1]^2 + 2.83679 \text{Cos}[x2] + 1.4597 \text{Cos}[x1] \text{Cos}[x2] + 3.30231 \text{Cos}[x2]^2 - 2.91764 \text{Cos}[x3] - 4.64941 \text{Cos}[x1] \text{Cos}[x3] - 2.47755 \text{Cos}[x2] \text{Cos}[x3] - 6.7996 \text{Cos}[x3]^2 + 1.0988 \text{Sin}[x1] + 1.62226 \text{Cos}[x1] \text{Sin}[x1] +$

	$1.05332 \cos(x_2) \sin(x_1) - 3.6806 \cos(x_3) \sin(x_1) + 1.58734 \sin(x_1)^2 + 12.6702 \sin(x_2) - 10.8974 \cos(x_1) \sin(x_2) + 13.0956 \cos(x_2) \sin(x_2) + 12.0752 \cos(x_3) \sin(x_2) - 13.1554 \sin(x_1) \sin(x_2) + 0.0072061 \sin(x_2)^2 + 2.15353 \sin(x_3) + 2.40983 \cos(x_1) \sin(x_3) + 1.77518 \cos(x_2) \sin(x_3) - 2.07671 \cos(x_3) \sin(x_3) + 2.13011 \sin(x_1) \sin(x_3) + 8.8285 \sin(x_2) \sin(x_3) + 10.1091 \sin(x_3)^2 / (4.89263 - 2.57427 \cos(x_1) + 2.12566 \cos(x_1)^2 - 1.28182 \cos(x_2) + 2.65103 \cos(x_1) \cos(x_2) - 7.19292 \cos(x_2)^2 + 2.26898 \cos(x_3) - 0.390924 \cos(x_1) \cos(x_3) - 3.11705 \cos(x_2) \cos(x_3) + 0.34224 \cos(x_3)^2 - 3.33607 \sin(x_1) + 2.87228 \cos(x_1) \sin(x_1) + 3.10729 \cos(x_2) \sin(x_1) - 0.634333 \cos(x_3) \sin(x_1) + 3.76697 \sin(x_1)^2 - 2.97978 \sin(x_2) - 1.02764 \cos(x_1) \sin(x_2) + 0.821684 \cos(x_2) \sin(x_2) - 0.589061 \cos(x_3) \sin(x_2) - 1.41051 \sin(x_1) \sin(x_2) + 13.0855 \sin(x_2)^2 + 1.42047 \sin(x_3) + 0.864041 \cos(x_1) \sin(x_3) + 1.31179 \cos(x_2) \sin(x_3) - 0.749579 \cos(x_3) \sin(x_3) + 0.776287 \sin(x_1) \sin(x_3) - 11.7364 \sin(x_2) \sin(x_3) + 5.55039 \sin(x_3)^2)$
CS1-O2-FOLN	$8.11724 - 0.30341 \log(x_1) + 1.42728 \log(x_2) + 0.104747 \log(x_3)$
CS1-O2-FOLNR	$(2.02273 + 1.43 \log(x_1) + 2.82437 \log(x_2) + 0.0429613 \log(x_3)) / (-0.63111 + 0.504732 \log(x_1) + 0.481796 \log(x_2) - 0.0214248 \log(x_3))$
CS1-O2-SOLN	$10.1707 + 0.304156 \log(x_1) - 0.282847 \log(x_1)^2 + 3.05101 \log(x_2) - 0.795428 \log(x_1) \log(x_2) - 0.563741 \log(x_2)^2 + 2.66424 \log(x_3) - 0.347423 \log(x_1) \log(x_3) + 0.0724472 \log(x_2) \log(x_3) + 0.232699 \log(x_3)^2$
CS1-O2-SOLNR	$(4.43134*10^8 + 1.75383*10^9 \log(x_1) + 6.48712*10^9 \log(x_1)^2 + 1.10296*10^9 \log(x_2) + 7.59694*10^9 \log(x_1) \log(x_2) - 7.02112*10^9 \log(x_2)^2 + 1.47786*10^9 \log(x_3) + 3.47159*10^8 \log(x_1) \log(x_3) - 6.3174*10^9 \log(x_2) \log(x_3) + 5.26674*10^9 \log(x_3)^2) / (-9.88651*10^8 - 2.32388*10^9 \log(x_1) + 1.38571*10^9 \log(x_1)^2 + 2.08989*10^9 \log(x_2) - 2.32992*10^9 \log(x_1) \log(x_2) - 5.78296*10^9 \log(x_2)^2 - 3.46984*10^9 \log(x_3) + 6.57709*10^8 \log(x_1) \log(x_3) - 2.45876*10^9 \log(x_2) \log(x_3) + 1.69758*10^9 \log(x_3)^2)$
NOTATION	CS1-O3
CS1-O3-L	$0.276419 - 0.000471847 [x_1] + 2.79561 [x_2] - 0.0509009 [x_3]$
CS1-O3-LN	$(431298 + 589.142 [x_1] - 1.16197*10^6 [x_2] - 320915. [x_3]) / (1.09975*10^6 + 1732.53 [x_1] - 5.15022*10^6 [x_2] - 578679. [x_3])$
CS1-O3-SON	$0.505895 + 0.00144745 [x_1] - 1.21908*10^6 [x_1]^2 - 2.37814 [x_2] - 0.0151784 [x_1] [x_2] + 27.714 [x_2]^2 - 0.614421 [x_3] + 9.91831*10^18 [x_1] [x_3] + 2.93843 [x_2] [x_3] + 0.399312 [x_3]^2$
CS1-O3-SONR	$(199883 + 1.43922*10^7 [x_1] + 194551. [x_1]^2 - 1.23473*10^6 [x_2] + 2.09211*10^8 [x_1] [x_2] + 570421. [x_2]^2 - 19763.6 [x_3] - 3.70988*10^7 [x_1] [x_3] + 614532. [x_2] [x_3] - 310473. [x_3]^2) / (1.14267*10^6 + 8.22735*10^7 [x_1] + 485430. [x_1]^2 - 1.33807*10^6 [x_2] - 2.04815*10^8 [x_1] [x_2] - 482936. [x_2]^2 + 26421.6 [x_3] - 6.58176*10^7 [x_1] [x_3] - 586839. [x_2] [x_3] + 60560. [x_3]^2)$
CS1-O3-TON	$0.389272 + 0.000438874 [x_1] - 8.47553*10^6 [x_1]^2 - 9.83852*10^8 [x_1]^3 - 0.115387 [x_2] + 0.02773 [x_1] [x_2] + 0.000317289 [x_1]^2 [x_2] + 5.37926 [x_2]^2 - 0.520833 [x_1] [x_2]^2 + 202.071 [x_2]^3 + 0.259891 [x_3] + 0.00523494 [x_1] [x_3] + 0.0000492169 [x_1]^2 [x_3] - 22.5 [x_2] [x_3] - 0.0694444 [x_1] [x_2] [x_3] + 104.167 [x_2]^2 [x_3] + 0.233836 [x_3]^2 - 0.0222222 [x_1] [x_3]^2 + 2.22222 [x_2] [x_3]^2 + 1.46858 [x_3]^3$
CS1-O3-FOTN	$46.402 + 10.0261 \cos(x_1) - 48.4258 \cos(x_2) + 0.32668 \cos(x_3) - 10.2266 \sin(x_1) - 2.9802 \sin(x_2) + 0.0499277 \sin(x_3)$
CS1-O3-FOTNR	$(146.33 + 795.703 \cos(x_1) - 318.017 \cos(x_2) - 0.0863525 \cos(x_3) - 813.549 \sin(x_1) - 47.4211 \sin(x_2) - 0.715777 \sin(x_3)) / (119.79 - 1548.76 \cos(x_1) - 771.981 \cos(x_2) + 3.18282 \cos(x_3) + 1583.2 \sin(x_1) - 116.753 \sin(x_2) - 0.360149 \sin(x_3))$
CS1-O3-SOTN	$305.471 + 79.5052 \cos(x_1) + 555.217 \cos(x_1)^2 + 310.117 \cos(x_2) + 55.8749 \cos(x_1) \cos(x_2) + 4.89569*10^8 \sin(x_2)^2 + 346.138 \cos(x_3) + 74.5443 \cos(x_1) \cos(x_3) - 2573.35 \cos(x_2) \cos(x_3) + 386.869 \cos(x_3)^2 - 53.548 \sin(x_1) + 641.431 \cos(x_1) \sin(x_1) - 79.6991 \cos(x_2) \sin(x_1) - 76.5394 \cos(x_3) \sin(x_1) + 562.673 \sin(x_1)^2 + 184.194 \sin(x_2) + 38.9314 \cos(x_1) \sin(x_2) + 178.029 \cos(x_2) \sin(x_2) - 354.148 \cos(x_3) \sin(x_2) - 41.521 \sin(x_1) \sin(x_2) - 856.653 \sin(x_2)^2 + 416.647 \sin(x_3) + 89.8926 \cos(x_1) \sin(x_3) - 1013.8 \cos(x_2) \sin(x_3) + 570.333 \cos(x_3) \sin(x_3) - 91.9272 \sin(x_1) \sin(x_3) - 132.28 \sin(x_2) \sin(x_3) - 627.266 \sin(x_3)^2$
CS1-O3-SOTNR	$(1.74862*10^8 + 1.17576*10^8 \cos(x_1) + 1.10566*10^8 \cos(x_1)^2 - 7.47712*10^7 \cos(x_2) + 5.12317*10^7 \cos(x_1) \cos(x_2) - 3.14707*10^8 \cos(x_2)^2 + 2.76831*10^8 \cos(x_3) - 3.22329*10^8 \cos(x_1) \cos(x_3) + 4.69195*10^8 \cos(x_1) \cos(x_3) + 3.5154*10^8 \cos(x_3)^2 + 7.72757*10^7 \sin(x_1) + 8.27793*10^7 \cos(x_1) \sin(x_1) + 6.62455*10^7 \cos(x_2) \sin(x_1) - 3.75016*10^8 \cos(x_3) \sin(x_1) + 6.42958*10^7 \sin(x_1)^2 + 3.65561*10^8 \sin(x_2) - 1.92369*10^7 \cos(x_1) \sin(x_2) + 2.84141*10^8 \cos(x_2) \sin(x_2) + 3.24638*10^8 \cos(x_3) \sin(x_2) - 9.7695*10^7 \sin(x_1) \sin(x_2) + 4.89569*10^8 \sin(x_2)^2 + 1.6612*10^7 \sin(x_3) + 4.79062*10^8 \cos(x_1) \sin(x_3) - 8.16931*10^7 \cos(x_2) \sin(x_3) + 1.0169*10^8 \cos(x_3) \sin(x_3) + 4.65006*10^8 \sin(x_1) \sin(x_3) + 2.08513*10^8 \sin(x_3) - 1.76678*10^8 \sin(x_3)^2) / (1.30315*10^8 - 6.18732*10^7 \cos(x_1) + 5.01494*10^7 \cos(x_1)^2 + 4.12405*10^8 \cos(x_2) + 3.6563*10^7 \cos(x_1) \cos(x_2) + 6.86987*10^8 \cos(x_2)^2 + 1.32768*10^8 \cos(x_3) - 2.67172*10^8 \cos(x_1) \cos(x_3) + 3.94386*10^8 \cos(x_2) \cos(x_3) + 1.43453*10^8 \cos(x_3)^2 - 8.86394*10^7 \sin(x_1) + 6.24038*10^7 \cos(x_1) \sin(x_1) - 5.32224*10^7 \cos(x_2) \sin(x_1) - 2.8998*10^8 \cos(x_3) \sin(x_1) + 8.01659*10^7 \sin(x_1)^2 - 1.43362*10^9 \sin(x_2) - 4.97145*10^8 \cos(x_1) \sin(x_2) - 1.36275*10^9 \cos(x_2) \sin(x_2) - 1.32431*10^9 \cos(x_3) \sin(x_2) - 1.76941*10^8 \sin(x_1) \sin(x_2) - 5.56671*10^8 \sin(x_2)^2 - 1.72278*10^8 \sin(x_3) + 1.01469*10^9 \sin(x_1) \sin(x_3) - 6.72675*10^7 \cos(x_2) \sin(x_3) - 1.90615*10^8 \cos(x_3) \sin(x_3) + 1.02969*10^9 \sin(x_1) \sin(x_3) - 5.63845*10^8 \sin(x_2) \sin(x_3) - 1.31378*10^7 \sin(x_3)^2)$
CS1-O3-FOLN	$1.5087 - 0.0662141 \log(x_1) + 0.310579 \log(x_2) - 0.0134232 \log(x_3)$
CS1-O3-FOLNR	$(-16.2488 + 1.09984 \log(x_1) - 7.33263 \log(x_2) - 2.22268 \log(x_3)) / (-61.9348 + 4.35639 \log(x_1) - 23.8121 \log(x_2) - 3.87638 \log(x_3))$
CS1-O3-SOLN	$4.69245 + 0.265614 \log(x_1) - 0.0806943 \log(x_1)^2 + 3.86249 \log(x_2) - 0.214465 \log(x_1) \log(x_2) + 0.541419 \log(x_2)^2 + 0.106279 \log(x_3) + 0.0205994 \log(x_1) \log(x_3) + 0.0794431 \log(x_2) \log(x_3) + 0.0173299 \log(x_3)^2$
CS1-O3-SOLNR	$(2.70427*10^9 + 6.5892*10^9 \log(x_1) - 1.46827*10^9 \log(x_1)^2 - 2.1006*10^9 \log(x_2) + 2.34314*10^8 \log(x_1) \log(x_2) + 4.33787*10^9 \log(x_2)^2 - 2.51516*10^9 \log(x_3) + 1.4802*10^8 \log(x_1) \log(x_3) + 2.22393*10^9 \log(x_2) \log(x_3) - 1.37097*10^9 \log(x_3)^2) / (-2.0947*10^9 - 5.42603*10^9 \log(x_1) - 2.07748*10^9 \log(x_1)^2 - 2.17506*10^8 \log(x_2) - 9.38828*10^9 \log(x_1) \log(x_2) + 6.4813*10^9 \log(x_2)^2 + 1.79616*10^9 \log(x_3) - 2.65637*10^8 \log(x_1) \log(x_3) + 1.32813*10^9 \log(x_2) \log(x_3) + 6.52281*10^8 \log(x_3)^2)$
NOTATION	CS1-O4
CS1-O4-L	$0.642225 - 0.000554778 [x_1] + 23.9248 [x_2] + 0.482658 [x_3]$
CS1-O4-LN	$(87808.6 + 43.4881 [x_1] - 343658. [x_2] + 15194.3 [x_3]) / (39145.6 + 18.3972 [x_1] - 206732. [x_2] + 1568.12 [x_3])$
CS1-O4-SON	$3.70994 + 0.00953964 [x_1] - 0.0000209468 [x_1]^2 - 39.8474 [x_2] - 0.0517798 [x_1] [x_2] + 293.508 [x_2]^2 - 1.02482 [x_3] + 0.00314815 [x_1] [x_3] + 5.2579 [x_2] [x_3] + 0.823125 [x_3]^2$
CS1-O4-SONR	$(770625 + 5.59562*10^7 [x_1] + 1.41378*10^8 [x_1]^2 + 577201. [x_2] + 7.45149*10^7 [x_1] [x_2] + 131218. [x_2]^2 - 219405. [x_3] - 3.21532*10^7 [x_1] [x_3] + 112504. [x_2] [x_3] - 187346. [x_3]^2) / (-2.68203*10^6 - 1.92969*10^8 [x_1] + 4.14151*10^7 [x_1]^2 - 2.01935*10^6 [x_2] - 2.60732*10^8 [x_1] [x_2] - 459258. [x_2]^2 + 768310. [x_3] + 1.12821*10^8 [x_1] [x_3] - 393840. [x_2] [x_3] + 654367. [x_3]^2)$
CS1-O4-TON	$1.34314 + 0.00491253 [x_1] + 8.70909*10^6 [x_1]^2 - 4.54472*10^8 [x_1]^3 + 1.6216 [x_2] + 0.0295456 [x_1] [x_2] + 0.000276515 [x_1]^2 [x_2] + 44.7452 [x_2]^2 - 0.911458 [x_1] [x_2]^2 + 926.055 [x_2]^3 + 6.16785 [x_3] + 0.00162949 [x_1] [x_3] - 0.000189691 [x_1]^2 [x_3] - 113.333 [x_2] [x_3] + 0.0625 [x_1] [x_2] [x_3] + 156.25 [x_2]^2 [x_3] + 2.864 [x_3]^2 + 0.0759259 [x_1] [x_3]^2 + 119.444 [x_2] [x_3]^2 - 28.4909 [x_3]^3$
CS1-O4-FOTN	$551.546 + 119.068 \cos(x_1) - 574.535 \cos(x_2) + 1.03946 \cos(x_3) - 121.662 \sin(x_1) - 44.7449 \sin(x_2) + 0.852445 \sin(x_3)$
CS1-O4-FOTNR	$(-35.504 + 9.99726 \cos(x_1) + 32.1197 \cos(x_2) + 1.40632 \cos(x_3) - 10.2441 \sin(x_1) + 2.59855 \sin(x_2) + 0.486 \sin(x_3)) / (-14.2187 + 4.13999 \cos(x_1) + 12.9764 \cos(x_2) + 0.457618 \cos(x_3) - 4.24116 \sin(x_1) + 0.528454 \sin(x_2) + 0.136421 \sin(x_3))$
CS1-O4-SOTN	$-295.067 - 24.2663 \cos(x_1) - 515.927 \cos(x_1)^2 - 299.59 \cos(x_2) - 113.264 \cos(x_1) \cos(x_2) - 304.197 \cos(x_2)^2 - 334.866 \cos(x_3) - 69.8771 \cos(x_1) \cos(x_3) + 2495.61 \cos(x_2) \cos(x_3) - 375.979 \cos(x_3)^2 + 105.317 \sin(x_1) - 620.15 \cos(x_1) \sin(x_1) + 16.532 \cos(x_2) \sin(x_1) + 76.3357 \cos(x_3) \sin(x_1) - 565.523 \sin(x_1)^2 - 58.8462 \sin(x_2) - 16.6423 \cos(x_1) \sin(x_2) - 49.0159 \cos(x_2) \sin(x_2) + 68.4365 \cos(x_3) \sin(x_2) + 8.87313 \sin(x_1) \sin(x_2) + 1099.36 \sin(x_2)^2 - 184.991 \sin(x_3) - 39.1204 \cos(x_1) \sin(x_3) + 445.069 \cos(x_2) \sin(x_3) - 270.851 \cos(x_3) \sin(x_3) + 41.6108 \sin(x_1) \sin(x_3) - 10.7508 \sin(x_2) \sin(x_3) + 728.777 \sin(x_3)^2$
CS1-O4-SOTNR	$(7.85242*10^8 - 2.40636*10^7 \cos(x_1) + 3.77422*10^8 \cos(x_1)^2 + 7.88958*10^8 \cos(x_2) + 1.05469*10^7 \cos(x_1) \cos(x_2) + 7.98479*10^8 \cos(x_2)^2 + 6.41976*10^8 \cos(x_3) - 8.66233*10^8 \cos(x_1) \cos(x_3) + 6.43384*10^8 \cos(x_2) \cos(x_3) + 4.8465*10^8 \cos(x_3)^2 - 1.92972*10^8 \sin(x_1) + 3.74365*10^8 \cos(x_1) \sin(x_1) - 1.5992*10^8 \cos(x_2) \sin(x_1) - 9.8582*10^8 \cos(x_3) \sin(x_1) + 4.0782*10^8 \sin(x_1)^2 - 1.75687*10^9 \sin(x_2) - 5.83536*10^8 \cos(x_1) \sin(x_2) - 1.79211*10^9 \cos(x_2) \sin(x_2) - 1.64889*10^9 \cos(x_3) \sin(x_2) - 1.91695*10^8 \sin(x_1) \sin(x_2) - 1.32374*10^7 \sin(x_1) \sin(x_2) + 1.15353*10^9 \sin(x_3) + 2.54871*10^9 \cos(x_1) \sin(x_3) + 1.16098*10^9 \cos(x_2) \sin(x_3) + 1.15591*10^9 \cos(x_3) \sin(x_3) + 2.2441*10^9 \sin(x_1) \sin(x_3) - 5.33446*10^8 \sin(x_2) \sin(x_3) + 3.00592*10^8 \sin(x_3)^2) / (-4.61499*10^7 - 1.28907*10^8 \cos(x_1) - 5.02948*10^7 \cos(x_1)^2 + 1.10543*10^9 \cos(x_2) - 2.58444*10^7 \cos(x_1) \cos(x_2) + 2.21842*10^9 \cos(x_2)^2 - 4.43732*10^8 \cos(x_3) - 1.86015*10^8 \cos(x_1) \cos(x_3) + 6.58876*10^8 \cos(x_2) \cos(x_3) - 7.30382*10^8 \cos(x_3)^2 - 1.16132*10^8 \sin(x_1) - 2.13807*10^7 \cos(x_1) \sin(x_1) - 2.63803*10^8 \cos(x_2) \sin(x_1) - 8.62814*10^7 \cos(x_3) \sin(x_1) + 4.14485*10^6 \sin(x_1)^2 - 3.49311*10^9 \sin(x_2) +$

	$1.77132*10^8 \cos[x1] \sin[x2] - 3.15506*10^9 \cos[x2] \sin[x2] - 3.43973*10^9 \cos[x3] \sin[x2] + 9.2698*10^8 \sin[x1] \sin[x2] - 2.26457*10^9 \sin[x2]^2 - 9.08375*10^7 \sin[x3] + 7.41999*10^8 \cos[x1] \sin[x3] + 2.11956*10^8 \cos[x2] \sin[x3] - 4.30888*10^8 \cos[x3] \sin[x3] + 7.45381*10^8 \sin[x1] \sin[x3] - 6.75657*10^8 \sin[x2] \sin[x3] + 6.84233*10^8 \sin[x3]^2$
CS1-O4-FOLN	$9.59269 - 0.0280409 \log[x1] + 2.64562 \log[x2] + 0.131064 \log[x3]$
CS1-O4-FOLNR	$(-1028.95 + 39.7301 \log[x1] - 705.372 \log[x2] + 58.8942 \log[x3]) / (-623.22 + 19.2536 \log[x1] - 338.646 \log[x2] + 9.11852 \log[x3])$
CS1-O4-SOLN	$34.3476 + 2.38373 \log[x1] - 0.41596 \log[x1]^2 + 30.6077 \log[x2] - 0.77785 \log[x1] \log[x2] + 5.4429 \log[x2]^2 + 0.034653 \log[x3] + 0.151129 \log[x1] \log[x3] + 0.146375 \log[x2] \log[x3] + 0.119439 \log[x3]^2$
CS1-O4-SOLNR	$(4.23633*10^{10} + 1.19603*10^{11} \log[x1] + 1.40488*10^{11} \log[x1]^2 - 4.97878*10^{10} \log[x2] - 6.18295*10^{10} \log[x1] \log[x2] + 4.45798*10^{10} \log[x2]^2 - 3.07053*10^{10} \log[x3] - 1.30064*10^{10} \log[x1] \log[x3] - 3.91387*10^9 \log[x2] \log[x3] - 8.95827*10^9 \log[x3]^2) / (-1.4109*10^{11} - 3.47319*10^{11} \log[x1] + 4.12717*10^{10} \log[x1]^2 + 1.04533*10^{11} \log[x2] - 1.88844*10^{11} \log[x1] \log[x2] + 1.10015*10^{11} \log[x2]^2 + 1.12436*10^{11} \log[x3] + 6.37761*10^8 \log[x1] \log[x3] + 6.30689*10^{10} \log[x2] \log[x3] + 1.79725*10^{10} \log[x3]^2)$
NOTATION	CS1-O5
CS1-O5-L	$0.326204 - 0.0020508 [x1] + 3.21664 [x2] + 0.0248874 [x3]$
CS1-O5-LN	$(441.159 - 6.46636 [x1] + 42219.7 [x2] - 4221.31 [x3]) / (2249.69 + 21.4004 [x1] + 45758.5 [x2] - 11130.8 [x3])$
CS1-O5-SON	$0.175096 - 0.000230645 [x1] - 8.59298*10^{-6} [x1]^2 + 3.63794 [x2] + 0.0142811 [x1] [x2] - 15.1354 [x2]^2 + 0.140544 [x3] - 0.00314815 [x1] [x3] + 3.64442 [x2] [x3] - 0.13905 [x3]^2$
CS1-O5-SONR	$(154070. + 1.10924*10^7 [x1] - 189887. [x1]^2 - 3.92605*10^8 [x2] + 1.24604*10^9 [x1] [x2] - 9.65328*10^7 [x2]^2 - 6.55578*10^8 [x3] - 1.15658*10^8 [x1] [x3] - 1.00498*10^8 [x2] [x3] - 8.99939*10^8 [x3]^2) / (766007. + 5.51546*10^7 [x1] + 653946. [x1]^2 + 2.58973*10^8 [x2] + 1.37963*10^9 [x1] [x2] + 7.22644*10^7 [x2]^2 - 2.67665*10^8 [x3] - 3.24609*10^8 [x1] [x3] - 2.39358*10^6 [x2] [x3] - 1.69525*10^8 [x3]^2)$
CS1-O5-TON	$-0.246232 - 0.000273955 [x1] + 5.40196*10^{-6} [x1]^2 + 6.25492*10^{-8} [x1]^3 + 6.2779 [x2] + 0.00208604 [x1] [x2] - 0.000197926 [x1]^2 [x2] + 28.6872 [x2]^2 + 0.325521 [x1] [x2]^2 - 231.596 [x2]^3 + 2.7713 [x3] - 0.00301715 [x1] [x3] - 0.0000966795 [x1]^2 [x3] - 45. [x2] [x3] - 0.114583 [x1] [x2] [x3] - 5.20833 [x2]^2 [x3] + 0.323757 [x3]^2 + 0.0601852 [x1] [x3]^2 + 115.278 [x2] [x3]^2 - 22.8906 [x3]^3$
CS1-O5-FOTN	$-38.7599 - 8.32383 \cos[x1] + 39.8297 \cos[x2] + 0.506567 \cos[x3] + 8.59434 \sin[x1] + 8.03129 \sin[x2] + 0.182172 \sin[x3]$
CS1-O5-FOTNR	$(301.734 + 95.5493 \cos[x1] - 321.506 \cos[x2] + 0.0905315 \cos[x3] - 97.7192 \sin[x1] - 29.684 \sin[x2] - 0.0922322 \sin[x3]) / (413.356 + 633.956 \cos[x1] - 551.363 \cos[x2] + 0.583618 \cos[x3] - 648.29 \sin[x1] - 50.1215 \sin[x2] - 0.186675 \sin[x3])$
CS1-O5-SOTN	$513.544 + 83.2737 \cos[x1] + 913.858 \cos[x1]^2 + 521.356 \cos[x2] + 144.374 \cos[x1] \cos[x2] + 529.3 \cos[x2]^2 + 582.436 \cos[x3] + 129.35 \cos[x1] \cos[x3] - 4332.44 \cos[x2] \cos[x3] + 652.279 \cos[x3]^2 - 141.427 \sin[x1] + 1078.89 \cos[x1] \sin[x1] - 82.547 \cos[x2] \sin[x1] - 124.788 \cos[x3] \sin[x1] + 967.056 \sin[x1]^2 + 383.692 \sin[x2] + 86.9121 \cos[x1] \sin[x2] + 376.296 \cos[x2] \sin[x2] - 745.417 \cos[x3] \sin[x2] - 80.4177 \sin[x1] \sin[x2] - 1434.02 \sin[x2]^2 + 551.779 \sin[x3] + 120.359 \cos[x1] \sin[x3] - 1329.6 \cos[x2] \sin[x3] + 768.863 \cos[x3] \sin[x3] - 120.426 \sin[x1] \sin[x3] - 226.883 \sin[x2] \sin[x3] - 1156.19 \sin[x3]^2$
CS1-O5-SOTNR	$(0.53409 - 4.59787 \cos[x1] - 0.434595 \cos[x1]^2 - 3.05597 \cos[x2] - 2.83025 \cos[x1] \cos[x2] - 6.52608 \cos[x2]^2 + 3.33747 \cos[x3] + 6.70137 \cos[x1] \cos[x3] - 1.60527 \cos[x2] \cos[x3] + 5.51382 \cos[x3]^2 - 4.37498 \sin[x1] + 0.804635 \cos[x1] \sin[x1] - 1.87136 \cos[x2] \sin[x1] + 6.07239 \cos[x3] \sin[x1] + 1.96868 \sin[x1]^2 + 11.9858 \sin[x2] - 8.40844 \cos[x1] \sin[x2] + 10.9343 \cos[x2] \sin[x2] + 16.6257 \cos[x3] \sin[x2] - 10.5732 \sin[x1] \sin[x2] + 8.06017 \sin[x2]^2 - 1.55236 \sin[x3] + 2.77483 \cos[x1] \sin[x3] + 4.14558 \cos[x2] \sin[x3] + 0.498677 \cos[x3] \sin[x3] + 3.28677 \sin[x1] \sin[x3] - 25.271 \sin[x2] \sin[x3] - 3.97973 \sin[x3]^2) / (-3.3156 - 2.50183 \cos[x1] - 1.85822 \cos[x1]^2 - 2.68036 \cos[x2] - 4.53466 \cos[x1] \cos[x2] - 2.08151 \cos[x2]^2 + 4.32726 \cos[x3] - 0.103821 \cos[x1] \cos[x3] + 6.24063 \cos[x2] \cos[x3] + 10.0382 \cos[x3]^2 - 1.4941 \sin[x1] - 1.04014 \cos[x1] \sin[x1] - 3.61956 \cos[x2] \sin[x1] - 0.79763 \cos[x3] \sin[x1] - 0.457386 \sin[x1]^2 + 3.42359 \sin[x2] + 14.9415 \sin[x1] \sin[x2] + 3.70236 \cos[x2] \sin[x2] - 4.13786 \cos[x3] \sin[x2] + 14.1138 \sin[x1] \sin[x2] - 0.234089 \sin[x2]^2 - 1.62688 \sin[x3] + 2.69989 \cos[x1] \sin[x3] - 6.81887 \cos[x2] \sin[x3] + 4.47513 \cos[x3] \sin[x3] + 3.22954 \sin[x1] \sin[x3] + 35.5966 \sin[x2] \sin[x3] - 12.3538 \sin[x3]^2)$
CS1-O5-FOLN	$2.695 - 0.295039 \log[x1] + 0.371295 \log[x2] + 0.00714925 \log[x3]$
CS1-O5-FOLNR	$(66.1281 - 8.72996 \log[x1] + 8.12545 \log[x2] - 2.74204 \log[x3]) / (47.6673 - 6.41947 \log[x1] + 2.03775 \log[x2] - 7.00973 \log[x3])$
CS1-O5-SOLN	$0.962995 + 0.0904384 \log[x1] - 0.00227843 \log[x1]^2 - 0.80895 \log[x2] + 0.238105 \log[x1] \log[x2] - 0.0284825 \log[x2]^2 + 0.758175 \log[x3] - 0.112872 \log[x1] \log[x3] + 0.102049 \log[x2] \log[x3] - 0.0110022 \log[x3]^2$
CS1-O5-SOLNR	$(3.10754*10^8 + 7.79913*10^8 \log[x1] + 5.81593*10^7 \log[x1]^2 - 3.94321*10^8 \log[x2] + 6.7881*10^8 \log[x1] \log[x2] + 2.38227*10^8 \log[x2]^2 - 3.0252*10^8 \log[x3] - 1.51125*10^8 \log[x1] \log[x3] + 5.13562*10^7 \log[x2] \log[x3] - 3.15315*10^8 \log[x3]^2) / (-6.65847*10^7 - 1.46758*10^8 \log[x1] + 1.90667*10^8 \log[x1]^2 + 2.20028*10^8 \log[x2] + 4.68906*10^7 \log[x1] \log[x2] - 4.09414*10^8 \log[x2]^2 - 7.78554*10^7 \log[x3] - 3.65458*10^8 \log[x1] \log[x3] + 1.00446*10^8 \log[x2] \log[x3] - 4.72071*10^8 \log[x3]^2)$
NOTATION	CS1-O6
CS1-O6-L	$2.15278 - 0.0125286 [x1] + 20.9502 [x2] - 0.615991 [x3]$
CS1-O6-LN	$(133423. - 308.042 [x1] + 1.02942*10^6 [x2] - 202684. [x3]) / (61490.3 + 180.01 [x1] - 79692.9 [x2] - 68196. [x3])$
CS1-O6-SON	$0.303561 + 0.000303947 [x1] - 7.03705*10^{-6} [x1]^2 + 22.9969 [x2] - 0.0499006 [x1] [x2] + 12.089 [x2]^2 + 4.4078 [x3] - 0.0148148 [x1] [x3] + 12.1051 [x2] [x3] - 6.7118 [x3]^2$
CS1-O6-SONR	$(3.72094*10^8 + 2.68919*10^{10} [x1] + 3.03346*10^{10} [x1]^2 + 9.3461*10^7 [x2] + 1.0078*10^{10} [x1] [x2] + 1.7329*10^7 [x2]^2 + 4.16184*10^7 [x3] - 9.69093*10^8 [x1] [x3] + 1.9105*10^7 [x2] [x3] - 6.07307*10^6 [x3]^2) / (-9.41096*10^8 - 6.77174*10^{10} [x1] + 1.24627*10^{10} [x1]^2 - 2.36859*10^8 [x2] - 2.5528*10^{10} [x1] [x2] - 4.3942*10^7 [x2]^2 - 1.04645*10^8 [x3] + 2.62078*10^9 [x1] [x3] - 4.8376*10^7 [x2] [x3] + 1.57344*10^7 [x3]^2)$
CS1-O6-TON	$8.72843 + 0.0142374 [x1] - 0.000140937 [x1]^2 - 1.82563*10^{-6} [x1]^3 - 69.5614 [x2] + 0.162163 [x1] [x2] + 0.00428584 [x1]^2 [x2] - 352.312 [x2]^2 - 3.77604 [x1] [x2]^2 + 3539.41 [x2]^3 - 31.3412 [x3] + 0.0176722 [x1] [x3] + 0.00125128 [x1]^2 [x3] + 600. [x2] [x3] - 1.77083 [x1] [x2] [x3] - 781.25 [x2]^2 [x3] - 41.0327 [x3]^2 - 0.305556 [x1] [x3]^2 - 152.778 [x2] [x3]^2 + 115.345 [x3]^3$
CS1-O6-FOTN	$-19.4244 - 3.94655 \cos[x1] + 3.35143 \cos[x2] + 16.5439 \cos[x3] + 4.53649 \sin[x1] + 21.9988 \sin[x2] + 4.49749 \sin[x3]$
CS1-O6-FOTNR	$(406.041 - 2669.85 \cos[x1] + 184.761 \cos[x2] - 4.75205 \cos[x3] + 2729.12 \sin[x1] + 67.879 \sin[x2] - 4.25165 \sin[x3]) / (-485.556 + 1057.92 \cos[x1] + 253.59 \cos[x2] - 2.87077 \cos[x3] - 1081.95 \sin[x1] + 40.2756 \sin[x2] - 1.89254 \sin[x3])$
CS1-O6-SOTN	$0.492401 - 151.692 \cos[x1] - 9.57279 \cos[x1]^2 - 4.55098 \cos[x2] + 127.39 \cos[x1] \cos[x2] + 0.924079 \cos[x2]^2 + 5.90507 \cos[x3] + 25.5555 \cos[x1] \cos[x3] + 8.27464 \cos[x2] \cos[x3] - 8.13858 \cos[x3]^2 - 146.326 \sin[x1] - 7.00083 \cos[x1] \sin[x1] + 123.499 \cos[x2] \sin[x1] + 22.5273 \cos[x3] \sin[x1] + 9.46867 \sin[x1]^2 + 49.3571 \sin[x2] + 19.5253 \cos[x1] \sin[x2] + 55.7936 \cos[x2] \sin[x2] - 77.6803 \cos[x3] \sin[x2] + 12.5283 \sin[x1] \sin[x2] - 5.52318 \sin[x2]^2 - 33.9938 \sin[x3] + 4.00579 \cos[x1] \sin[x3] + 56.2516 \cos[x2] \sin[x3] - 16.9261 \cos[x3] \sin[x3] + 10.7168 \sin[x1] \sin[x3] - 31.2229 \sin[x2] \sin[x3] - 12.1494 \sin[x3]^2$
CS1-O6-SOTNR	$(4.7149*10^9 + 1.1797*10^9 \cos[x1] + 2.55184*10^9 \cos[x1]^2 + 2.9888*10^9 \cos[x2] + 1.37356*10^9 \cos[x1] \cos[x2] + 1.28585*10^9 \cos[x2]^2 + 7.76666*10^9 \cos[x3] + 3.64943*10^9 \cos[x1] \cos[x3] + 6.15448*10^9 \cos[x2] \cos[x3] + 2.03233 [x3] + 1.03704*10^{10} \cos[x3]^2 + 1.36562*10^8 \sin[x1] + 2.24152*10^9 \cos[x1] \sin[x1] + 6.98637*10^8 \cos[x2] \sin[x1] + 1.89382*10^9 \cos[x3] \sin[x1] + 2.16306*10^9 \sin[x1]^2 + 1.58334*10^{10} \sin[x2] - 1.34628*10^9 \cos[x1] \sin[x2] + 1.55402*10^{10} \cos[x2] \sin[x2] + 1.49593*10^{10} \cos[x3] \sin[x2] - 4.73329*10^9 \sin[x1] \sin[x2] + 3.42905*10^9 \sin[x2]^2 - 7.16513*10^9 \sin[x3] - 4.15045*10^9 \cos[x1] \sin[x3] - 7.76711*10^9 \cos[x2] \sin[x3] - 5.46835*10^9 \cos[x3] \sin[x3] - 2.51369*10^9 \sin[x1] \sin[x3] + 5.05052*10^9 \sin[x2] \sin[x3] - 5.65551*10^9 \sin[x3]^2) / (3.00164*10^9 + 1.1627*10^9 \cos[x1] + 1.71338*10^9 \cos[x1]^2 + 6.34182*10^9 \cos[x2] + 9.52832*10^8 \cos[x1] \cos[x2] + 9.6383*10^9 \cos[x2]^2 + 1.62333*10^9 \cos[x3] - 1.16919*10^9 \cos[x1] \cos[x3] + 4.68214*10^9 \cos[x2] \cos[x3] + 7.966*10^8 \cos[x3]^2 + 4.8961*10^8 \sin[x1] + 1.42505*10^9 \cos[x1] \sin[x1] - 4.36392*10^8 \cos[x2] \sin[x1] - 1.49391*10^9 \cos[x3] \sin[x1] + 1.28826*10^9 \sin[x1]^2 - 3.04677*10^{10} \sin[x2] + 1.02232*10^9 \cos[x1] \sin[x2] - 2.99059*10^{10} \cos[x2] \sin[x2] - 2.79962*10^{10} \cos[x3] \sin[x2] + 7.57411*10^9 \sin[x1] \sin[x2] - 6.63666*10^9 \sin[x2]^2 - 3.53306*10^9 \sin[x3] - 3.04209*10^9 \cos[x1] \sin[x3] - 2.11032*10^9 \cos[x2] \sin[x3] - 5.10015*10^9 \cos[x3] \sin[x3] - 2.21326*10^9 \sin[x1] \sin[x3] - 1.29998*10^{10} \sin[x2] \sin[x3] + 2.20504*10^9 \sin[x3]^2)$
CS1-O6-FOLN	$16.6472 - 1.82421 \log[x1] + 2.37774 \log[x2] - 0.144824 \log[x3]$
CS1-O6-FOLNR	$(22.4245 - 3.25033 \log[x1] + 1.70781 \log[x2] - 1.81553 \log[x3]) / (-2.34502 + 0.182617 \log[x1] - 1.20708 \log[x2] - 0.600333 \log[x3])$
CS1-O6-SOLN	$22.8828 + 0.986701 \log[x1] - 0.516166 \log[x1]^2 + 13.2071 \log[x2] - 0.755969 \log[x1] \log[x2] + 1.46694 \log[x2]^2 + 1.90529 \log[x3] - 0.55362 \log[x1] \log[x3] + 0.393908 \log[x2] \log[x3] - 0.590491 \log[x3]^2$

CS1-O6-SOLNR	$(1.74261 \cdot 10^9 + 4.47539 \cdot 10^9 \text{Log}[x1] + 1.34295 \cdot 10^9 \text{Log}[x1]^2 - 1.55776 \cdot 10^9 \text{Log}[x2] + 1.12216 \cdot 10^9 \text{Log}[x1] \text{Log}[x2] - 1.47239 \cdot 10^9 \text{Log}[x2]^2 - 1.47723 \cdot 10^9 \text{Log}[x3] - 1.64705 \cdot 10^9 \text{Log}[x1] \text{Log}[x3] + 3.71575 \cdot 10^8 \text{Log}[x2] \text{Log}[x3] - 6.35387 \cdot 10^7 \text{Log}[x3]^2) / (-4.43895 \cdot 10^9 - 1.08226 \cdot 10^{10} \text{Log}[x1] + 2.34325 \cdot 10^9 \text{Log}[x1]^2 + 4.28296 \cdot 10^9 \text{Log}[x2] - 1.96566 \cdot 10^9 \text{Log}[x1] \text{Log}[x2] + 2.21892 \cdot 10^9 \text{Log}[x2]^2 + 3.163 \cdot 10^9 \text{Log}[x3] - 7.91529 \cdot 10^6 \text{Log}[x1] \text{Log}[x3] - 1.23052 \cdot 10^8 \text{Log}[x2] \text{Log}[x3] + 2.18054 \cdot 10^9 \text{Log}[x3]^2)$
NOTATION	CS2-O1
CS2-O1-L	$-0.183893 + 0.00105277 [x1] + 0.773401 [x2] + 0.0686068 [x3] + 0.00883792 [x4]$
CS2-O1-LN	$(-207.933 - 0.484284 [x1] + 8014.88 [x2] + 797.351 [x3] + 34.6674 [x4]) / (10716.1 - 30.6456 [x1] + 13783.6 [x2] + 1471.9 [x3] - 70.196 [x4])$
CS2-O1-SON	$0.0845922 - 0.000905821 [x1] + 2.96677 \cdot 10^{-6} [x1]^2 + 0.408622 [x2] + 0.000768021 [x1] [x2] + 1.3977 [x2]^2 - 0.0108546 [x3] + 0.00011509 [x1] [x3] - 0.0475026 [x2] [x3] + 0.0993455 [x3]^2 - 0.0035025 [x4] + 0.0000720227 [x1] [x4] - 0.00668952 [x2] [x4] - 0.000918482 [x3] [x4] - 0.0000387693 [x4]^2$
CS2-O1-SONR	$(-1.19882 \cdot 10^9 - 1.06311 \cdot 10^{11} [x1] + 6.74774 \cdot 10^9 [x1]^2 - 1.0978 \cdot 10^8 [x2] - 7.42699 \cdot 10^9 [x1] [x2] - 1.04977 \cdot 10^7 [x2]^2 - 4.33448 \cdot 10^8 [x3] - 3.57692 \cdot 10^{10} [x1] [x3] - 3.73276 \cdot 10^7 [x2] [x3] - 1.93822 \cdot 10^8 [x3]^2 - 5.81317 \cdot 10^9 [x4] + 3.9762 \cdot 10^{10} [x1] [x4] - 4.79075 \cdot 10^8 [x2] [x4] - 2.23296 \cdot 10^9 [x3] [x4] - 4.47476 \cdot 10^{10} [x4]^2) / (2.67546 \cdot 10^8 + 2.37638 \cdot 10^{10} [x1] + 3.48292 \cdot 10^{10} [x1]^2 + 2.47689 \cdot 10^7 [x2] + 1.71031 \cdot 10^9 [x1] [x2] + 2.4142 \cdot 10^6 [x2]^2 + 9.7964 \cdot 10^7 [x3] + 8.15878 \cdot 10^9 [x1] [x3] + 8.45817 \cdot 10^6 [x2] [x3] + 4.42961 \cdot 10^7 [x3]^2 + 1.48719 \cdot 10^9 [x4] + 1.77256 \cdot 10^{10} [x1] [x4] + 1.28372 \cdot 10^8 [x2] [x4] + 5.85132 \cdot 10^8 [x3] [x4] + 1.32567 \cdot 10^{10} [x4]^2)$
CS2-O1-TON	$0.029852 + 0.000087258 [x1] + 4.52704 \cdot 10^{-7} [x1]^2 + 2.86079 \cdot 10^{-9} [x1]^3 + 0.431188 [x2] - 0.000172987 [x1] [x2] - 3.67469 \cdot 10^{-6} [x1]^2 [x2] + 1.8543 [x2]^2 + 0.00363942 [x1] [x2]^2 - 4.85637 [x2]^3 - 0.126444 [x3] + 0.0000178814 [x1] [x3] - 2.38869 \cdot 10^{-7} [x1]^2 [x3] + 0.206417 [x2] [x3] + 0.00275623 [x1] [x2] [x3] - 4.26737 [x2]^2 [x3] [x2] - 0.079225 [x3]^2 - 0.000757864 [x1] [x3]^2 + 1.52931 [x2] [x3]^2 + 0.38018 [x3]^3 - 0.00176941 [x4] + 0.00001586 [x1] [x4] + 9.23659 \cdot 10^{-8} [x1]^2 [x4] - 0.0432765 [x2] [x4] + 0.0000644144 [x1] [x2] [x4] + 0.24402 [x2]^2 [x4] + 0.0294389 [x3] [x4] + 0.0000453353 [x1] [x3] [x4] - 0.084651 [x2] [x3] [x4] - 0.0267302 [x3]^2 [x4] - 6.21219 \cdot 10^{-6} [x4]^2 - 4.01228 \cdot 10^{-7} [x1] [x4]^2 - 0.000174642 [x2] [x4]^2 - 0.000415714 [x3] [x4]^2 + 6.81741 \cdot 10^{-6} [x4]^3$
CS2-O1-FOTN	$-12.0483 + 0.230635 \text{Cos}[x1] + 12.7926 \text{Cos}[x2] - 0.317999 \text{Cos}[x3] + 0.250328 \text{Cos}[x4] + 0.136795 \text{Sin}[x1] + 2.31615 \text{Sin}[x2] - 0.0652909 \text{Sin}[x3] - 0.214575 \text{Sin}[x4]$
CS2-O1-FOTNR	$(-0.386738 + 0.396512 \text{Cos}[x1] + 2.30943 \text{Cos}[x2] - 1.57883 \text{Cos}[x3] + 0.0558798 \text{Cos}[x4] + 0.050419 \text{Sin}[x1] + 4.39469 \text{Sin}[x2] - 0.24221 \text{Sin}[x3] - 0.113801 \text{Sin}[x4]) / (-54.4657 + 0.223911 \text{Cos}[x1] + 59.1247 \text{Cos}[x2] - 5.74641 \text{Cos}[x3] - 3.2137 \text{Cos}[x4] - 1.20913 \text{Sin}[x1] + 15.5224 \text{Sin}[x2] - 1.7243 \text{Sin}[x3] + 2.25147 \text{Sin}[x4])$
CS2-O1-SOTN	$0.0157512 - 0.00593974 \text{Cos}[x1] - 0.0123339 \text{Cos}[x1]^2 + 0.0158292 \text{Cos}[x2] - 0.0047374 \text{Cos}[x1] \text{Cos}[x2] + 0.0159031 \text{Cos}[x2]^2 + 0.0160358 \text{Cos}[x3] + 0.12561 \text{Cos}[x1] \text{Cos}[x3] + 0.0159036 \text{Cos}[x2] \text{Cos}[x3] + 0.0151482 \text{Cos}[x3]^2 - 0.0520612 \text{Cos}[x4] + 0.117321 \text{Cos}[x1] \text{Cos}[x4] - 0.0437815 \text{Cos}[x2] \text{Cos}[x4] + 0.18064 \text{Cos}[x3] \text{Cos}[x4] + 0.0846731 \text{Cos}[x4]^2 + 0.0223067 \text{Sin}[x1] - 0.0484857 \text{Cos}[x1] \text{Sin}[x1] + 0.0320584 \text{Cos}[x2] \text{Sin}[x1] + 0.199263 \text{Cos}[x3] \text{Sin}[x1] + 0.209076 \text{Cos}[x4] \text{Sin}[x1] + 0.0625409 \text{Sin}[x1]^2 + 0.217166 \text{Sin}[x2] + 1.21346 \text{Cos}[x1] \text{Sin}[x2] + 0.22126 \text{Cos}[x2] \text{Sin}[x2] + 0.299218 \text{Cos}[x3] \text{Sin}[x2] - 0.968639 \text{Cos}[x4] \text{Sin}[x2] + 0.343576 \text{Sin}[x1] \text{Sin}[x2] + 1.11987 \text{Sin}[x2]^2 + 0.0794924 \text{Sin}[x3] + 0.0527824 \text{Cos}[x1] \text{Sin}[x3] + 0.0835951 \text{Cos}[x2] \text{Sin}[x3] + 0.103397 \text{Cos}[x3] \text{Sin}[x3] + 0.275553 \text{Cos}[x4] \text{Sin}[x3] + 0.0918246 \text{Sin}[x1] \text{Sin}[x3] - 0.548222 \text{Sin}[x2] \text{Sin}[x3] + 0.117911 \text{Sin}[x3]^2 - 0.0346595 \text{Sin}[x4] - 0.178977 \text{Cos}[x1] \text{Sin}[x4] - 0.0351477 \text{Cos}[x2] \text{Sin}[x4] + 0.020551 \text{Cos}[x3] \text{Sin}[x4] + 0.254286 \text{Cos}[x4] \text{Sin}[x4] - 0.195718 \text{Sin}[x1] \text{Sin}[x4] + 0.691313 \text{Sin}[x2] \text{Sin}[x4] - 0.0870805 \text{Sin}[x3] \text{Sin}[x4] - 0.0136081 \text{Sin}[x4]^2$
CS2-O1-SOTNR	$(1.32923 + 0.784048 \text{Cos}[x1] + 1.08715 \text{Cos}[x1]^2 + 0.918194 \text{Cos}[x2] + 1.02085 \text{Cos}[x1] \text{Cos}[x2] + 0.513729 \text{Cos}[x2]^2 + 0.697562 \text{Cos}[x3] + 1.18916 \text{Cos}[x1] \text{Cos}[x3] + 0.322659 \text{Cos}[x2] \text{Cos}[x3] + 0.390265 \text{Cos}[x3]^2 + 0.725108 \text{Cos}[x4] - 0.530004 \text{Cos}[x1] \text{Cos}[x4] + 0.890794 \text{Cos}[x2] \text{Cos}[x4] + 0.815914 \text{Cos}[x3] \text{Cos}[x4] + 1.70669 \text{Cos}[x4]^2 + 1.77049 \text{Sin}[x1] + 0.552361 \text{Cos}[x1] \text{Sin}[x1] - 1.7916 \text{Cos}[x2] \text{Sin}[x1] + 1.87712 \text{Cos}[x3] \text{Sin}[x1] + 3.62943 \text{Cos}[x4] \text{Sin}[x1] + 1.24208 \text{Sin}[x1]^2 + 4.42088 \text{Sin}[x2] - 0.929813 \text{Cos}[x1] \text{Sin}[x2] + 4.34449 \text{Cos}[x2] \text{Sin}[x2] + 4.06889 \text{Cos}[x3] \text{Sin}[x2] - 0.343603 \text{Cos}[x4] \text{Sin}[x2] + 0.816057 \text{Sin}[x1] \text{Sin}[x2] + 1.8155 \text{Sin}[x2]^2 + 0.707911 \text{Sin}[x3] + 1.03977 \text{Cos}[x1] \text{Sin}[x3] + 0.566736 \text{Cos}[x2] \text{Sin}[x3] - 0.010076 \text{Cos}[x3] \text{Sin}[x3] + 0.976918 \text{Cos}[x4] \text{Sin}[x3] + 0.829435 \text{Sin}[x1] \text{Sin}[x3] + 2.19861 \text{Sin}[x2] \text{Sin}[x3] + 1.93897 \text{Sin}[x3]^2 - 0.0907169 \text{Sin}[x4] - 0.0653061 \text{Sin}[x1] \text{Sin}[x4] - 0.393655 \text{Cos}[x2] \text{Sin}[x4] - 0.783297 \text{Cos}[x3] \text{Sin}[x4] + 2.21742 \text{Cos}[x4] \text{Sin}[x4] - 2.40278 \text{Sin}[x1] \text{Sin}[x4] + 3.53845 \text{Sin}[x2] \text{Sin}[x4] + 0.0709478 \text{Sin}[x3] \text{Sin}[x4] + 0.622539 \text{Sin}[x4]^2) / (2.22166 - 0.130365 \text{Cos}[x1] + 2.21535 \text{Cos}[x1]^2 + 2.29025 \text{Cos}[x2] - 0.166862 \text{Cos}[x1] \text{Cos}[x2] + 2.35768 \text{Cos}[x2]^2 + 2.27987 \text{Cos}[x3] - 0.188376 \text{Cos}[x1] \text{Cos}[x3] + 2.34212 \text{Cos}[x2] \text{Cos}[x3] + 2.28449 \text{Cos}[x3]^2 - 0.203042 \text{Cos}[x4] + 2.30913 \text{Cos}[x1] \text{Cos}[x4] - 0.224914 \text{Cos}[x2] \text{Cos}[x4] - 0.243835 \text{Cos}[x3] \text{Cos}[x4] + 1.78642 \text{Cos}[x4]^2 - 0.320064 \text{Sin}[x1] + 1.509 \text{Cos}[x1] \text{Sin}[x1] - 0.309165 \text{Cos}[x2] \text{Sin}[x1] - 0.135324 \text{Cos}[x3] \text{Sin}[x1] + 1.19436 \text{Cos}[x4] \text{Sin}[x1] + 1.0063 \text{Sin}[x1]^2 + 0.504044 \text{Sin}[x2] + 1.22901 \text{Cos}[x1] \text{Sin}[x2] + 0.517365 \text{Cos}[x2] \text{Sin}[x2] + 0.563242 \text{Cos}[x3] \text{Sin}[x2] + 1.10436 \text{Cos}[x4] \text{Sin}[x2] + 0.841879 \text{Sin}[x1] \text{Sin}[x2] + 0.863973 \text{Sin}[x2]^2 + 1.39188 \text{Sin}[x3] + 0.755207 \text{Cos}[x1] \text{Sin}[x3] + 1.4159 \text{Cos}[x2] \text{Sin}[x3] + 1.50026 \text{Cos}[x3] \text{Sin}[x3] + 0.861828 \text{Cos}[x4] \text{Sin}[x3] + 0.41527 \text{Sin}[x1] \text{Sin}[x3] + 0.81467 \text{Sin}[x2] \text{Sin}[x3] + 0.937164 \text{Sin}[x3]^2 + 1.46983 \text{Sin}[x4] + 0.975465 \text{Cos}[x1] \text{Sin}[x4] + 1.52603 \text{Cos}[x2] \text{Sin}[x4] + 1.42764 \text{Cos}[x3] \text{Sin}[x4] + 0.407702 \text{Cos}[x4] \text{Sin}[x4] + 1.07403 \text{Sin}[x1] \text{Sin}[x4] + 0.546363 \text{Sin}[x2] \text{Sin}[x4] + 1.61397 \text{Sin}[x3] \text{Sin}[x4] + 1.43523 \text{Sin}[x4]^2)$
CS2-O1-FOLN	$-0.738238 + 0.199067 \text{Log}[x1] + 0.0796313 \text{Log}[x2] + 0.018771 \text{Log}[x3] + 0.0567917 \text{Log}[x4]$
CS2-O1-FOLNR	$(5.58984 + 0.212759 \text{Log}[x1] + 1.71731 \text{Log}[x2] + 0.609255 \text{Log}[x3] - 0.0565823 \text{Log}[x4]) / (69.6447 - 8.29019 \text{Log}[x1] + 3.28113 \text{Log}[x2] + 1.34878 \text{Log}[x3] - 3.32055 \text{Log}[x4])$
CS2-O1-SOLN	$5.70788 - 1.89803 \text{Log}[x1] + 0.185923 \text{Log}[x1]^2 + 0.464449 \text{Log}[x2] + 0.00336089 \text{Log}[x1] \text{Log}[x2] + 0.0809967 \text{Log}[x2]^2 + 0.0743047 \text{Log}[x3] + 0.00938062 \text{Log}[x1] \text{Log}[x3] + 0.0194823 \text{Log}[x2] \text{Log}[x3] + 0.0241822 \text{Log}[x3]^2 - 0.513616 \text{Log}[x4] + 0.0877114 \text{Log}[x1] \text{Log}[x4] - 0.00624825 \text{Log}[x2] \text{Log}[x4] - 0.000171744 \text{Log}[x3] \text{Log}[x4] + 0.0288352 \text{Log}[x4]^2$
CS2-O1-SOLNR	$(-68.6687 - 176.77 \text{Log}[x1] + 46.7864 \text{Log}[x1]^2 + 75.8876 \text{Log}[x2] - 6.41293 \text{Log}[x1] \text{Log}[x2] + 3.41952 \text{Log}[x2]^2 + 34.1657 \text{Log}[x3] - 8.7705 \text{Log}[x1] \text{Log}[x3] + 29.5824 \text{Log}[x2] \text{Log}[x3] - 10.8057 \text{Log}[x3]^2 - 78.4473 \text{Log}[x4] + 33.589 \text{Log}[x1] \text{Log}[x4] + 34.7366 \text{Log}[x2] \text{Log}[x4] + 19.2674 \text{Log}[x3] \text{Log}[x4] + 15.2392 \text{Log}[x4]^2) / (20.1259 + 53.8335 \text{Log}[x1] + 30.8437 \text{Log}[x1]^2 - 24.9286 \text{Log}[x2] - 35.4348 \text{Log}[x1] \text{Log}[x2] + 24.9343 \text{Log}[x2]^2 - 13.5202 \text{Log}[x3] - 28.7896 \text{Log}[x1] \text{Log}[x3] + 12.9807 \text{Log}[x2] \text{Log}[x3] + 17.0419 \text{Log}[x3]^2 + 16.6879 \text{Log}[x4] - 30.5952 \text{Log}[x1] \text{Log}[x4] - 2.55745 \text{Log}[x2] \text{Log}[x4] - 8.79176 \text{Log}[x3] \text{Log}[x4] - 20.5788 \text{Log}[x4]^2)$
NOTATION	CS2-O2
CS2-O2-L	$0.336175 - 0.000970039 [x1] + 1.83652 [x2] + 0.0519202 [x3] + 0.0139923 [x4]$
CS2-O2-LN	$(8705.16 - 26.1522 [x1] + 5728.7 [x2] - 349.986 [x3] + 163.88 [x4]) / (21014.3 - 31.289 [x1] - 28079.9 [x2] - 2141.15 [x3] + 22.738 [x4])$
CS2-O2-SON	$0.778767 - 0.00458809 [x1] + 6.76248 \cdot 10^{-6} [x1]^2 + 1.0233 [x2] + 0.00165332 [x1] [x2] + 2.38618 [x2]^2 + 0.0894347 [x3] + 0.000227986 [x1] [x3] - 0.100069 [x2] [x3] - 0.0440976 [x3]^2 - 0.00429524 [x4] + 0.0000717317 [x1] [x4] + 0.00554415 [x2] [x4] - 0.00237944 [x3] [x4] + 0.000240068 [x4]^2$
CS2-O2-SONR	$(1.00042 + 0.509983 [x1] - 0.00145637 [x1]^2 + 1.03645 [x2] + 7.61163 [x1] [x2] + 1.00864 [x2]^2 + 1.00652 [x3] + 0.889895 [x1] [x3] + 1.01662 [x2] [x3] + 1.01178 [x3]^2 + 0.656177 [x4] + 0.0732689 [x1] [x4] + 1.27161 [x2] [x4] + 0.701786 [x3] [x4] + 0.706079 [x4]^2) / (1.01062 + 2.33516 [x1] + 0.00690492 [x1]^2 + 0.982407 [x2] - 2.14356 [x1] [x2] + 0.995681 [x2]^2 + 1.00006 [x3] + 1.32653 [x1] [x3] + 0.991843 [x2] [x3] + 0.995313 [x3]^2 + 1.19853 [x4] + 0.0225593 [x1] [x4] + 0.845968 [x2] [x4] + 1.18462 [x3] [x4] + 1.30399 [x4]^2)$
CS2-O2-TON	$0.388935 - 0.000622981 [x1] - 4.73937 \cdot 10^{-6} [x1]^2 - 5.24016 \cdot 10^{-9} [x1]^3 + 2.79176 [x2] - 0.0025846 [x1] [x2] + 0.000031875 [x1]^2 [x2] + 7.54858 [x2]^2 - 0.0252336 [x1] [x2]^2 - 57.1083 [x2]^3 - 0.117675 [x3] - 0.000261919 [x1] [x3] + 8.17044 \cdot 10^{-6} [x1]^2 [x3] - 1.22871 [x2] [x3] - 0.0116726 [x1] [x2] [x3] + 19.8828 [x2]^2 [x3] - 0.252142 [x3]^2 + 0.000492497 [x1] [x3]^2 - 1.30391 [x2] [x3]^2 + 0.648678 [x3]^3 + 0.00653039 [x4] - 0.00004739 [x1] [x4] + 6.94998 \cdot 10^{-7} [x1]^2 [x4] - 0.121123 [x2] [x4] - 0.000389687 [x1] [x2] [x4] - 0.227748 [x2]^2 [x4] + 0.0707932 [x3] [x4] - 0.000280667 [x1] [x3] [x4] + 0.0420322 [x2] [x3] [x4] - 0.0650911 [x3]^2 [x4] - 0.000370967 [x4]^2 - 8.23422 \cdot 10^{-7} [x1] [x4]^2 + 0.0101422 [x2] [x4]^2 + 0.00184249 [x3] [x4]^2 - 0.0000437656 [x4]^3$
CS2-O2-FOTN	$-10.8123 - 0.0568194 \text{Cos}[x1] + 11.2993 \text{Cos}[x2] + 0.00240194 \text{Cos}[x3] + 0.334645 \text{Cos}[x4] - 0.0936539 \text{Sin}[x1] + 3.26354 \text{Sin}[x2] + 0.0556643 \text{Sin}[x3] - 0.310466 \text{Sin}[x4]$
CS2-O2-FOTNR	$(-27.1288 - 0.124366 \text{Cos}[x1] + 30.196 \text{Cos}[x2] - 2.84838 \text{Cos}[x3] + 0.0856684 \text{Cos}[x4] - 0.0566939 \text{Sin}[x1] + 3.70066 \text{Sin}[x2] - 1.26574 \text{Sin}[x3] - 0.115184 \text{Sin}[x4]) / (-31.1975 - 0.232991 \text{Cos}[x1] + 37.4685 \text{Cos}[x2] - 5.74509 \text{Cos}[x3] - 0.0315811 \text{Cos}[x4] - 0.0565618 \text{Sin}[x1] + 3.48279 \text{Sin}[x2] - 2.56308 \text{Sin}[x3] - 0.0321899 \text{Sin}[x4])$
CS2-O2-SOTN	$0.0426917 - 0.00599215 \text{Cos}[x1] + 0.0212705 \text{Cos}[x1]^2 + 0.0433473 \text{Cos}[x2] + 0.00981929 \text{Cos}[x1] \text{Cos}[x2] + 0.0440079 \text{Cos}[x2]^2 + 0.041287 \text{Cos}[x3] - 0.0351535 \text{Cos}[x1] \text{Cos}[x3] + 0.0403354 \text{Cos}[x2] \text{Cos}[x3] + 0.0412422 \text{Cos}[x3]^2 + 0.1433 \text{Cos}[x4] + 0.741439 \text{Cos}[x1] \text{Cos}[x4] + 0.199815 \text{Cos}[x2] \text{Cos}[x4] - 0.112885 \text{Cos}[x3] \text{Cos}[x4] - 0.120209 \text{Cos}[x4]^2 - 0.541308 \text{Sin}[x1] + 0.805841 \text{Cos}[x1] \text{Sin}[x1] - 0.579977 \text{Cos}[x2] \text{Sin}[x1] + 1.40974 \text{Cos}[x3] \text{Sin}[x1] + 0.273313 \text{Cos}[x4] \text{Sin}[x1] +$

	$0.109114 \sin[x]^2 + 0.15448 \sin[x] + 2.59277 \cos[x] \sin[x] + 0.158687 \cos[x] \sin[x] + 2.79149 \cos[x] \sin[x] + 0.425849 \cos[x] \sin[x] + 0.0299422 \cos[x] \sin[x] + 0.0311294 \cos[x] \sin[x] - 0.120708 \cos[x] \sin[x] + 0.806552 \sin[x] \sin[x] + 1.89561 \sin[x] \sin[x] + 0.316726 \sin[x]^2 + 0.0996636 \sin[x] - 0.727978 \cos[x] \sin[x] + 0.134521 \cos[x] \sin[x] - 0.650117 \cos[x] \sin[x] + 0.4866 \cos[x] \sin[x] - 0.264627 \sin[x] \sin[x] - 0.161743 \sin[x] \sin[x] - 0.109077 \sin[x] \sin[x] + 0.133828 \sin[x]^2$
CS2-O2-SOTNR	$(1.38059 + 0.212403 \cos[x] + 2.07611 \cos[x]^2 + 0.770806 \cos[x] + 0.613143 \cos[x] \cos[x] + 0.170566 \cos[x]^2 + 1.13159 \cos[x] + 0.099207 \cos[x] \cos[x] + 0.578432 \cos[x] \cos[x] + 1.00333 \cos[x]^2 + 0.968378 \cos[x] + 0.0975409 \cos[x] \cos[x] + 1.28017 \cos[x] \cos[x] + 1.05676 \cos[x] \cos[x] + 1.66834 \cos[x]^2 + 0.190842 \sin[x] + 1.3629 \cos[x] \sin[x] + 0.0977381 \cos[x] \sin[x] + 0.668509 \cos[x] \sin[x] + 1.95371 \cos[x] \sin[x] + 0.304474 \sin[x]^2 + 6.13191 \sin[x] - 2.39019 \cos[x] \sin[x] + 6.01983 \cos[x] \sin[x] + 5.64594 \cos[x] \sin[x] - 1.58754 \cos[x] \sin[x] + 1.70603 \sin[x] \sin[x] + 2.21002 \sin[x]^2 + 0.979602 \sin[x] + 1.29812 \cos[x] \sin[x] + 0.742764 \cos[x] \sin[x] + 0.708977 \cos[x] \sin[x] + 0.543821 \cos[x] \sin[x] + 0.573992 \sin[x] \sin[x] + 2.98172 \sin[x] \sin[x] + 1.37726 \sin[x]^2 - 0.204813 \sin[x] - 0.615403 \cos[x] \sin[x] - 0.513757 \cos[x] \sin[x] - 0.456466 \cos[x] \sin[x] + 2.68618 \cos[x] \sin[x] - 1.38414 \sin[x] \sin[x] + 3.58019 \sin[x] \sin[x] - 0.12737 \sin[x] \sin[x] + 0.712245 \sin[x]^2 / (1.62722 + 0.237599 \cos[x] + 1.89568 \cos[x]^2 + 1.92735 \cos[x] + 0.0517225 \cos[x] \cos[x] + 2.22271 \cos[x]^2 + 1.68665 \cos[x] + 0.36899 \cos[x] \cos[x] + 1.95882 \cos[x] \cos[x] + 1.70807 \cos[x]^2 + 0.35175 \cos[x] + 2.22854 \cos[x] \cos[x] + 0.189176 \cos[x] \cos[x] + 0.436869 \cos[x] \cos[x] + 1.44204 \cos[x]^2 + 0.367444 \sin[x] + 1.23681 \cos[x] \sin[x] + 0.395856 \cos[x] \sin[x] + 0.201076 \cos[x] \sin[x] + 1.23168 \cos[x] \sin[x] + 0.731542 \sin[x]^2 + 1.46866 \sin[x] + 2.50135 \cos[x] \sin[x] - 1.41293 \cos[x] \sin[x] - 1.23357 \cos[x] \sin[x] + 2.30551 \cos[x] \sin[x] + 0.74821 \sin[x] \sin[x] + 0.404517 \sin[x]^2 + 1.17423 \sin[x] + 0.57438 \cos[x] \sin[x] + 1.29177 \cos[x] \sin[x] + 1.25575 \cos[x] \sin[x] + 0.90892 \cos[x] \sin[x] + 0.717964 \sin[x] \sin[x] + 0.0310416 \sin[x] \sin[x] + 0.91915 \sin[x]^2 + 1.18243 \sin[x] + 1.90151 \cos[x] \sin[x] + 1.31524 \cos[x] \sin[x] + 1.45154 \cos[x] \sin[x] + 0.723288 \cos[x] \sin[x] + 1.32933 \sin[x] \sin[x] - 0.127172 \sin[x] \sin[x] + 1.10176 \sin[x] \sin[x] + 1.18519 \sin[x]^2)$
CS2-O2-FOLN	$1.72358 - 0.179595 \log[x] + 0.196795 \log[x] + 0.00885818 \log[x] + 0.0857633 \log[x]$
CS2-O2-FOLNR	$(49.042 - 7.26401 \log[x] + 1.64912 \log[x] - 1.53796 \log[x] - 0.589898 \log[x]) / (61.6048 - 8.90007 \log[x] - 2.4697 \log[x] - 3.24573 \log[x] - 4.16443 \log[x])$
CS2-O2-SOLN	$6.57267 - 1.56969 \log[x] + 0.124082 \log[x]^2 + 0.802593 \log[x] + 0.0235149 \log[x] \log[x] + 0.155847 \log[x]^2 - 0.028019 \log[x] + 0.0218385 \log[x] \log[x] + 0.0223285 \log[x] \log[x] + 0.00251999 \log[x]^2 - 0.543118 \log[x] + 0.0812462 \log[x] \log[x] + 0.000782164 \log[x] \log[x] - 0.0039059 \log[x] \log[x] + 0.0602361 \log[x]^2$
CS2-O2-SOLNR	$(2.43678 + 4.58279 \log[x] - 0.459043 \log[x]^2 - 0.660744 \log[x] + 1.44509 \log[x] \log[x] + 1.51737 \log[x]^2 + 0.419429 \log[x] + 0.485504 \log[x] \log[x] + 1.3906 \log[x] \log[x] + 1.21484 \log[x]^2 + 1.43258 \log[x] + 0.264659 \log[x] \log[x] + 2.49872 \log[x] \log[x] + 0.168634 \log[x] \log[x] + 3.49259 \log[x]^2 / (0.449488 - 0.495229 \log[x] + 0.139511 \log[x]^2 + 1.44929 \log[x] + 0.0917736 \log[x] \log[x] + 1.55266 \log[x]^2 - 0.935742 \log[x] - 0.0955383 \log[x] \log[x] + 1.47406 \log[x] \log[x] + 1.77212 \log[x]^2 + 1.01743 \log[x] + 1.79782 \log[x] \log[x] - 0.579677 \log[x] \log[x] + 0.267749 \log[x] \log[x] + 0.313012 \log[x]^2)$
NOTATION	CS2-O3
CS2-O3-L	$23.495 - 0.253089 [x] + 393.366 [x] + 245.636 [x] + 5.5937 [x]$
CS2-O3-LN	$(-240208 - 1053.44 [x] + 5.48568 * 10^6 [x] + 1.47183 * 10^6 [x] + 22832.9 [x]) / (3643.19 + 2.17204 [x] + 18598.3 [x] + 265.061 [x] - 51.5007 [x])$
CS2-O3-SON	$18.7905 + 0.0425227 [x] - 0.000825846 [x]^2 - 183.221 [x] + 1.28148 [x] [x] + 3278.29 [x]^2 + 308.51 [x] - 0.273606 [x] [x] - 1311.84 [x] [x] + 182.451 [x]^2 + 2.25959 [x] + 0.000699861 [x] [x] + 7.63464 [x] [x] + 0.2026 [x] [x] + 0.116777 [x]^2$
CS2-O3-SONR	$(-99.1586 + 877.052 [x] - 1.88525 [x]^2 - 10.274 [x] + 4196. [x] [x] + 4.70316 [x]^2 + 253.587 [x] - 1385.93 [x] [x] + 7.20955 [x] [x] + 161.65 [x]^2 - 4699.6 [x] + 3.55688 [x] [x] + 1463.6 [x] [x] + 1347.44 [x] [x] + 149.247 [x]^2 / (1014.48 + 7.27704 [x] - 0.0120169 [x]^2 - 923.631 [x] + 23.0952 [x] [x] - 834.954 [x]^2 - 3621.27 [x] - 10.3712 [x] [x] + 2358.91 [x] [x] + 2881.59 [x]^2 - 70.4991 [x] + 0.0261176 [x] [x] - 91.6616 [x] [x] + 85.8505 [x] [x] + 1.08185 [x]^2)$
CS2-O3-TON	$-10.2819 + 0.0431226 [x] - 0.000702422 [x]^2 - 8.76071 * 10^{-6} [x]^3 + 594.248 [x] + 1.38006 [x] [x] + 0.0256762 [x]^2 [x] + 2000.72 [x]^2 - 5.46497 [x] [x]^2 - 28120.7 [x]^3 + 86.0859 [x] + 0.98158 [x] [x] - 0.00150101 [x]^2 [x] + 118.362 [x] [x] - 13.4605 [x] [x] + 2931.58 [x]^2 [x] + 57.2705 [x]^3 + 1.71091 [x] [x]^2 + 739.3 [x] [x]^2 - 220.285 [x]^3 - 0.655941 [x] - 0.0115659 [x] [x] + 0.000278799 [x]^2 [x] - 53.7733 [x] [x] - 0.544133 [x] [x] [x] + 696.802 [x]^2 [x] + 30.8943 [x] [x] - 0.0776189 [x] [x] [x] - 14.1185 [x] [x] [x] - 16.0989 [x]^3 [x] + 0.0386871 [x]^2 - 0.000684531 [x] [x]^2 + 1.05077 [x] [x]^2 + 0.126591 [x] [x]^2 - 0.00590462 [x]^3$
CS2-O3-FOTN	$10744.2 - 63.8367 \cos[x] - 10053.8 \cos[x] - 468.908 \cos[x] + 147.574 \cos[x] - 33.5963 \sin[x] - 814.414 \sin[x] + 72.8834 \sin[x] - 132.384 \sin[x]$
CS2-O3-FOTNR	$(-231.42 + 5.94595 \cos[x] + 117.089 \cos[x] + 104.327 \cos[x] - 5.20524 \cos[x] + 0.478435 \sin[x] + 42.0054 \sin[x] + 39.5273 \sin[x] + 1.42083 \sin[x]) / (-1.51596 + 0.0286113 \cos[x] + 0.929204 \cos[x] + 0.533172 \cos[x] - 0.0211013 \cos[x] + 0.0015522 \sin[x] + 0.255887 \sin[x] + 0.209668 \sin[x] + 0.0032783 \sin[x])$
CS2-O3-SOTN	$-49.9315 + 119.078 \cos[x] - 239.005 \cos[x]^2 - 51.0666 \cos[x] + 91.5707 \cos[x] \cos[x] - 52.2101 \cos[x]^2 - 76.3785 \cos[x] - 710.696 \cos[x] \cos[x] - 77.8508 \cos[x] \cos[x] - 99.4257 \cos[x]^2 + 393.662 \cos[x] + 275.761 \cos[x] \cos[x] + 350.194 \cos[x] \cos[x] - 1030.35 \cos[x] \cos[x] - 389.701 \cos[x]^2 + 376.542 \sin[x] + 540.945 \sin[x] \sin[x] + 340.968 \cos[x] \sin[x] - 912.007 \cos[x] \sin[x] + 146.21 \cos[x] \sin[x] + 108.806 \sin[x]^2 - 31.5844 \sin[x] - 1298.3 \cos[x] \sin[x] - 39.2884 \cos[x] \sin[x] + 113.821 \cos[x] \sin[x] - 102.722 \cos[x] \sin[x] + 223.431 \sin[x] \sin[x] + 2565.4 \sin[x]^2 - 95.2304 \sin[x] - 143.573 \cos[x] \sin[x] - 104.688 \cos[x] \sin[x] - 245.707 \cos[x] \sin[x] - 613.426 \cos[x] \sin[x] - 400.214 \sin[x] \sin[x] + 1393.81 \sin[x] \sin[x] + 419.876 \sin[x]^2 - 103.559 \sin[x] \sin[x] - 237.345 \cos[x] \sin[x] + 97.7519 \cos[x] \sin[x] - 148.154 \cos[x] \sin[x] + 495.867 \cos[x] \sin[x] - 73.5666 \sin[x] \sin[x] - 261.922 \sin[x] \sin[x] - 33.5657 \sin[x] \sin[x] + 102.345 \sin[x]^2$
CS2-O3-SOTNR	$(-3.01833 + 9.82447 \cos[x] - 9.0092 \cos[x]^2 - 2.96168 \cos[x] + 9.73881 \cos[x] \cos[x] - 2.9058 \cos[x]^2 - 2.60872 \cos[x] + 9.08346 \cos[x] \cos[x] - 2.56042 \cos[x] \cos[x] - 2.28793 \cos[x]^2 + 18.7299 \cos[x] - 17.4659 \cos[x] \cos[x] + 18.6053 \cos[x] \cos[x] + 17.1764 \cos[x] \cos[x] - 20.6315 \cos[x]^2 - 13.0298 \sin[x] + 8.90258 \cos[x] \sin[x] - 12.866 \cos[x] \sin[x] - 11.6562 \cos[x] \sin[x] + 21.4535 \cos[x] \sin[x] + 6.99087 \sin[x]^2 + 0.323367 \sin[x] + 2.17554 \cos[x] \sin[x] - 0.33269 \cos[x] \sin[x] + 0.414898 \cos[x] \sin[x] + 3.03286 \cos[x] \sin[x] - 1.16157 \sin[x] \sin[x] + 0.887471 \sin[x]^2 - 0.368271 \sin[x] + 3.94969 \cos[x] \sin[x] - 0.336947 \cos[x] \sin[x] - 0.112637 \cos[x] \sin[x] + 7.68457 \cos[x] \sin[x] - 4.22694 \sin[x] \sin[x] + 0.670142 \sin[x] \sin[x] + 0.269598 \sin[x]^2 + 30.1956 \sin[x] - 22.1023 \cos[x] \sin[x] + 30.0376 \cos[x] \sin[x] + 27.7626 \cos[x] \sin[x] - 14.0041 \cos[x] \sin[x] + 20.4351 \sin[x] \sin[x] + 3.98913 \sin[x] \sin[x] + 12.3957 \sin[x] \sin[x] + 18.6132 \sin[x]^2 / (1.09848 - 0.0589657 \cos[x] + 2.77529 \cos[x]^2 - 0.592397 \cos[x] + 1.39455 \cos[x] \cos[x] - 2.21068 \cos[x]^2 + 1.44061 \cos[x] + 3.62234 \cos[x] \cos[x] - 0.278169 \cos[x] \cos[x] + 1.59863 \cos[x]^2 - 0.759447 \cos[x] - 0.55272 \cos[x] \cos[x] - 0.478119 \cos[x] \cos[x] + 1.76491 \cos[x] \cos[x] + 1.5507 \cos[x]^2 - 1.34114 \sin[x] + 2.19695 \cos[x] \sin[x] - 1.29149 \cos[x] \sin[x] + 3.30651 \cos[x] \sin[x] + 0.240158 \cos[x] \sin[x] - 0.676802 \sin[x]^2 + 1.35881 \sin[x] + 0.45624 \cos[x] \sin[x] + 0.764782 \cos[x] \sin[x] + 3.06514 \cos[x] \sin[x] + 4.47796 \cos[x] \sin[x] + 0.804535 \sin[x] \sin[x] + 4.30917 \sin[x]^2 + 1.26769 \sin[x] + 0.248243 \cos[x] \sin[x] + 0.917765 \cos[x] \sin[x] + 1.67115 \cos[x] \sin[x] + 2.76428 \cos[x] \sin[x] + 1.85773 \sin[x] \sin[x] - 1.90989 \sin[x] \sin[x] + 0.499851 \sin[x]^2 + 1.59873 \sin[x] + 0.938841 \cos[x] \sin[x] + 0.890028 \cos[x] \sin[x] - 0.598242 \cos[x] \sin[x] - 1.62798 \cos[x] \sin[x] + 0.216816 \sin[x] \sin[x] - 4.2562 \sin[x] \sin[x] - 2.96625 \sin[x] \sin[x] + 0.547786 \sin[x]^2)$
CS2-O3-FOLN	$525.934 - 47.7582 \log[x] + 39.8252 \log[x] + 83.7567 \log[x] + 33.8643 \log[x]$
CS2-O3-FOLNR	$(-106603 + 6395.98 \log[x] - 21534.6 \log[x] - 5883.82 \log[x] - 3979.56 \log[x]) / (-317.148 - 1.23188 \log[x] - 88.5193 \log[x] + 50.1676 \log[x] + 6.42092 \log[x])$
CS2-O3-SOLN	$-600.018 + 486.673 \log[x] - 48.3636 \log[x]^2 + 172.524 \log[x] + 25.7164 \log[x] \log[x] + 75.0644 \log[x]^2 + 189.003 \log[x] - 13.6977 \log[x] \log[x] - 56.8657 \log[x] \log[x] + 70.3403 \log[x]^2 - 83.3071 \log[x] + 8.3474 \log[x] \log[x] + 5.063 \log[x] \log[x] - 0.30211 \log[x] \log[x] + 25.2066 \log[x]^2$
CS2-O3-SOLNR	$(7.1911 * 10^7 + 3.47723 * 10^8 \log[x] + 1.68071 * 10^9 \log[x]^2 - 1.35587 * 10^8 \log[x] - 6.42149 * 10^8 \log[x] \log[x] + 2.5302 * 10^8 \log[x]^2 - 4.40072 * 10^7 \log[x] - 1.99192 * 10^8 \log[x] \log[x] + 7.44692 * 10^7 \log[x] \log[x] + 4.07276 * 10^7 \log[x]^2 + 2.43394 * 10^8 \log[x] + 1.2282 * 10^9 \log[x] \log[x] - 4.99092 * 10^8 \log[x] \log[x] - 2.05972 * 10^8 \log[x] \log[x] + 6.37746 * 10^8 \log[x]^2 / (1.57925 * 10^8 + 5.00737 * 10^8 \log[x] + 9.19609 * 10^7 \log[x]^2 - 1.85127 * 10^8 \log[x] + 2.52156 * 10^8 \log[x] \log[x] - 3.09248 * 10^8 \log[x]^2 + 1.8948 * 10^8 \log[x] + 3.06056 * 10^8$

	$\text{Log}[x1] \text{Log}[x3] - 1.74921*10^8 \text{Log}[x2] \text{Log}[x3] - 4.10674*10^8 \text{Log}[x3]^2 - 5.53009*10^8 \text{Log}[x4] - 1.8855*10^8 \text{Log}[x1] \text{Log}[x4] - 1.098*10^9 \text{Log}[x2] \text{Log}[x4] - 1.27304*10^9 \text{Log}[x3] \text{Log}[x4] - 5.25958*10^8 \text{Log}[x4]^2$
NOTATION	CS2-O4
CS2-O4-L	$40.9741 - 0.349263 [x1] + 658.549 [x2] + 373.301 [x3] + 6.75743 [x4]$
CS2-O4-LN	$(-31978.3 - 109.463 [x1] + 573066. [x2] + 152997. [x3] + 2206.38 [x4]) / (171.677 + 0.044399 [x1] + 1309.43 [x2] + 75.4822 [x3] - 0.37337 [x4])$
CS2-O4-SON	$-207.812 + 2.81629 [x1] - 0.00725276 [x1]^2 - 42.055 [x2] - 0.25065 [x1] [x2] + 3923.14 [x2]^2 + 347.539 [x3] - 0.526574 [x1] [x3] - 1331.45 [x2] [x3] + 328.488 [x3]^2 + 5.47319 [x4] - 0.00268231 [x1] [x4] + 34.0286 [x2] [x4] + 2.85144 [x3] [x4] - 0.172817 [x4]^2$
CS2-O4-SONR	$(-2.19422*10^7 + 6.37827*10^6 [x1] - 73574.8 [x1]^2 - 1.11745*10^7 [x2] + 2.1146*10^8 [x1] [x2] - 535939. [x2]^2 + 3.42376*10^7 [x3] + 3.30265*10^7 [x1] [x3] + 682261. [x2] [x3] + 2.5958*10^7 [x3]^2 - 7.74834*10^7 [x4] + 128346. [x1] [x4] + 1.31179*10^6 [x2] [x4] + 1.1886*10^7 [x3] [x4] + 9.98765*10^6 [x4]^2) / (2.79548*10^7 - 112848. [x1] + 317.555 [x1]^2 + 2.84436*10^7 [x2] + 727256. [x1] [x2] - 3.6052*10^8 [x2]^2 - 3.24308*10^7 [x3] + 45554.8 [x1] [x3] + 1.13406*10^8 [x2] [x3] - 1.02332*10^6 [x3]^2 - 309970. [x4] - 2310.85 [x1] [x4] - 3.54363*10^6 [x2] [x4] + 133568. [x3] [x4] + 52502.1 [x4]^2)$
CS2-O4-TON	$-7.19318 + 0.379441 [x1] + 0.000324199 [x1]^2 - 0.0000101954 [x1]^3 - 542.9 [x2] + 3.40225 [x1] [x2] + 0.0101908 [x1]^2 [x2] - 1630.01 [x2]^2 - 6.77425 [x1] [x2]^2 + 24928.4 [x2]^3 + 371.202 [x3] + 0.484418 [x1] [x3] - 0.00326387 [x1]^2 [x3] + 433.651 [x2] [x3] - 5.85897 [x1] [x2] [x3] + 1961.63 [x2]^2 [x3] + 394.132 [x3]^2 + 0.813177 [x1] [x3]^2 - 2419.35 [x2] [x3]^2 - 313.716 [x3]^3 + 1.92498 [x4] + 0.0248292 [x1] [x4] + 0.0000205882 [x1]^2 [x4] + 90.242 [x2] [x4] - 0.172346 [x1] [x2] [x4] - 220.058 [x2]^2 [x4] - 38.0867 [x3] [x4] + 0.0606024 [x1] [x3] [x4] + 127.189 [x2] [x3] [x4] + 33.6505 [x3]^2 [x4] + 0.30598 [x4]^2 - 0.00256001 [x1] [x4]^2 - 2.06751 [x2] [x4]^2 - 0.748956 [x3] [x4]^2 + 0.0257708 [x4]^3$
CS2-O4-FOTN	$13068.7 - 160.778 \text{Cos}[x1] - 12096.1 \text{Cos}[x2] - 684.854 \text{Cos}[x3] + 253.946 \text{Cos}[x4] - 60.3033 \text{Sin}[x1] - 847.939 \text{Sin}[x2] + 119.725 \text{Sin}[x3] - 197.587 \text{Sin}[x4]$
CS2-O4-FOTNR	$(1666.57 - 5.09364 \text{Cos}[x1] - 1582.32 \text{Cos}[x2] - 70.228 \text{Cos}[x3] + 4.23689 \text{Cos}[x4] - 0.804445 \text{Sin}[x1] - 180.182 \text{Sin}[x2] - 12.2187 \text{Sin}[x3] - 1.96195 \text{Sin}[x4]) / (5.46074 - 0.00398739 \text{Cos}[x1] - 5.26852 \text{Cos}[x2] - 0.146426 \text{Cos}[x3] - 0.0127423 \text{Cos}[x4] + 0.00272598 \text{Sin}[x1] - 0.650568 \text{Sin}[x2] - 0.0346884 \text{Sin}[x3] + 0.0133909 \text{Sin}[x4])$
CS2-O4-SOTN	$-4.1437 - 3.45006 \text{Cos}[x1] - 19.875 \text{Cos}[x1]^2 - 5.2401 \text{Cos}[x2] - 15.5548 \text{Cos}[x1] \text{Cos}[x2] - 6.33664 \text{Cos}[x2]^2 - 20.4003 \text{Cos}[x3] - 115.185 \text{Cos}[x1] \text{Cos}[x3] - 21.2664 \text{Cos}[x2] \text{Cos}[x3] - 34.4976 \text{Cos}[x3]^2 + 6.06102 \text{Cos}[x4] + 153.109 \text{Cos}[x1] \text{Cos}[x4] - 23.7311 \text{Cos}[x2] \text{Cos}[x4] + 19.1117 \text{Cos}[x3] \text{Cos}[x4] + 24.1432 \text{Cos}[x4]^2 + 261.241 \text{Sin}[x1] - 403.278 \text{Sin}[x1] \text{Sin}[x2] + 275.387 \text{Cos}[x2] \text{Sin}[x1] - 646.675 \text{Cos}[x3] \text{Sin}[x1] + 111.339 \text{Cos}[x4] \text{Sin}[x1] + 9.07434 \text{Sin}[x1]^2 + 260.381 \text{Sin}[x2] + 323.129 \text{Cos}[x1] \text{Sin}[x2] + 246.416 \text{Cos}[x2] \text{Sin}[x2] - 566.335 \text{Cos}[x3] \text{Sin}[x2] + 742.113 \text{Cos}[x4] \text{Sin}[x2] - 114.287 \text{Sin}[x1] \text{Sin}[x2] + 7031.52 \text{Sin}[x2]^2 + 5.68712 \text{Sin}[x3] - 44.3514 \text{Cos}[x1] \text{Sin}[x3] + 14.3959 \text{Cos}[x2] \text{Sin}[x3] - 90.315 \text{Cos}[x3] \text{Sin}[x3] - 87.7639 \text{Sin}[x4] \text{Sin}[x3] - 341.185 \text{Sin}[x1] \text{Sin}[x4] + 199.726 \text{Sin}[x2] \text{Sin}[x4] + 440.064 \text{Sin}[x3]^2 - 33.5993 \text{Sin}[x4] - 89.6251 \text{Cos}[x1] \text{Sin}[x4] - 48.0407 \text{Cos}[x2] \text{Sin}[x4] + 253.596 \text{Cos}[x3] \text{Sin}[x4] + 277.918 \text{Cos}[x4] \text{Sin}[x4] - 47.2021 \text{Sin}[x1] \text{Sin}[x4] - 995.228 \text{Sin}[x2] \text{Sin}[x4] + 61.2597 \text{Sin}[x3] \text{Sin}[x4] - 19.0795 \text{Sin}[x4]^2$
CS2-O4-SOTNR	$(-3.80428*10^{10} + 2.12301*10^{10} \text{Cos}[x1] + 3.4779*10^9 \text{Cos}[x1]^2 - 3.87679*10^{10} \text{Cos}[x2] + 2.20193*10^{10} \text{Cos}[x1] \text{Cos}[x2] - 3.94835*10^{10} \text{Cos}[x2]^2 - 5.19562*10^{10} \text{Cos}[x3] + 2.78744*10^{10} \text{Cos}[x1] \text{Cos}[x3] - 5.26116*10^{10} \text{Cos}[x2] \text{Cos}[x3] - 6.3663*10^{10} \text{Cos}[x3]^2 + 1.36871*10^{11} \text{Cos}[x4] - 1.10344*10^{11} \text{Cos}[x1] \text{Cos}[x4] + 1.36656*10^{11} \text{Cos}[x2] \text{Cos}[x4] + 1.43527*10^{11} \text{Cos}[x3] \text{Cos}[x4] - 1.60784*10^{11} \text{Cos}[x4]^2 - 1.73035*10^{11} \text{Sin}[x1] + 9.53609*10^{10} \text{Cos}[x1] \text{Sin}[x1] - 1.72776*10^{11} \text{Cos}[x2] \text{Sin}[x1] - 1.5641*10^{11} \text{Cos}[x3] \text{Sin}[x1] + 1.94084*10^{11} \text{Cos}[x4] \text{Sin}[x1] - 4.15207*10^{10} \text{Sin}[x1]^2 + 5.0825*10^9 \text{Sin}[x2] - 6.19568*10^9 \text{Cos}[x1] \text{Sin}[x2] + 4.95738*10^9 \text{Cos}[x2] \text{Sin}[x2] + 3.6311*10^9 \text{Cos}[x3] \text{Sin}[x2] + 8.88824*10^9 \text{Cos}[x4] \text{Sin}[x2] - 1.13143*10^{10} \text{Sin}[x1] \text{Sin}[x2] + 1.44068*10^9 \text{Sin}[x2]^2 + 3.28828*10^{10} \text{Sin}[x3] - 1.70434*10^{10} \text{Cos}[x1] \text{Sin}[x3] + 3.25711*10^{10} \text{Cos}[x2] \text{Sin}[x3] + 2.51021*10^{10} \text{Cos}[x3] \text{Sin}[x3] + 3.64978*10^9 \text{Cos}[x4] \text{Sin}[x3] - 6.406*10^{10} \text{Sin}[x1] \text{Sin}[x3] + 4.85387*10^9 \text{Sin}[x2] \text{Sin}[x3] + 2.56202*10^{10} \text{Sin}[x3]^2 + 2.04503*10^{11} \text{Sin}[x4] - 1.82196*10^{11} \text{Cos}[x1] \text{Sin}[x4] + 2.02802*10^{11} \text{Cos}[x2] \text{Sin}[x4] + 1.95885*10^{11} \text{Cos}[x3] \text{Sin}[x4] - 1.00939*10^{11} \text{Cos}[x4] \text{Sin}[x4] + 1.01838*10^{11} \text{Sin}[x1] \text{Sin}[x4] + 2.62862*10^{10} \text{Sin}[x2] \text{Sin}[x4] + 5.70801*10^{10} \text{Sin}[x3] \text{Sin}[x4] + 1.22741*10^{11} \text{Sin}[x4]^2) / (6.97192*10^9 - 2.46207*10^8 \text{Cos}[x1] - 2.27965*10^9 \text{Cos}[x1]^2 - 4.85611*10^9 \text{Cos}[x2] + 6.99352*10^9 \text{Cos}[x1] \text{Cos}[x2] - 1.62258*10^{10} \text{Cos}[x2]^2 - 1.44165*10^9 \text{Cos}[x3] - 2.272*10^{10} \text{Cos}[x1] \text{Cos}[x3] - 1.1608*10^{10} \text{Cos}[x2] \text{Cos}[x3] - 6.19994*10^9 \text{Cos}[x3]^2 - 1.49555*10^9 \text{Cos}[x4] + 8.86821*10^9 \text{Cos}[x1] \text{Cos}[x4] - 6.72799*10^9 \text{Cos}[x2] \text{Cos}[x4] + 1.05055*10^9 \text{Cos}[x3] \text{Cos}[x4] + 2.12677*10^9 \text{Cos}[x4]^2 - 9.54693*10^9 \text{Sin}[x1] + 3.98634*10^9 \text{Cos}[x1] \text{Sin}[x1] - 1.01882*10^{10} \text{Cos}[x2] \text{Sin}[x1] + 1.53099*10^{10} \text{Cos}[x3] \text{Sin}[x1] + 4.99606*10^9 \text{Cos}[x4] \text{Sin}[x1] + 9.25157*10^9 \text{Sin}[x1]^2 + 1.75926*10^{10} \text{Sin}[x2] - 1.108*10^{10} \text{Cos}[x1] \text{Sin}[x2] + 1.37413*10^{10} \text{Cos}[x2] \text{Sin}[x2] + 1.5857*10^{10} \text{Cos}[x3] \text{Sin}[x2] + 5.01757*10^{10} \text{Cos}[x4] \text{Sin}[x2] + 1.0544*10^{10} \text{Sin}[x1] \text{Sin}[x2] + 2.31977*10^{10} \text{Sin}[x2]^2 + 2.44826*10^9 \text{Sin}[x3] - 1.14161*10^{10} \text{Cos}[x1] \text{Sin}[x3] - 5.66721*10^9 \text{Cos}[x2] \text{Sin}[x3] - 6.01111*10^9 \text{Cos}[x3] \text{Sin}[x3] + 8.61851*10^9 \text{Cos}[x4] \text{Sin}[x3] + 1.0694*10^{10} \text{Sin}[x1] \text{Sin}[x3] + 2.44855*10^{10} \text{Sin}[x2] \text{Sin}[x3] + 1.31719*10^{10} \text{Sin}[x3]^2 - 2.72578*10^9 \text{Sin}[x4] + 4.89946*10^9 \text{Cos}[x1] \text{Sin}[x4] - 3.4799*10^8 \text{Cos}[x2] \text{Sin}[x4] + 1.94428*10^{10} \text{Cos}[x3] \text{Sin}[x4] + 2.94413*10^9 \text{Cos}[x4] \text{Sin}[x4] + 5.77428*10^8 \text{Sin}[x1] \text{Sin}[x4] - 6.7738*10^{10} \text{Sin}[x2] \text{Sin}[x4] - 7.49599*10^9 \text{Sin}[x3] \text{Sin}[x4] + 4.84515*10^9 \text{Sin}[x4]^2)$
CS2-O4-FOLN	$800.176 - 64.3818 \text{Log}[x1] + 70.1943 \text{Log}[x2] + 129.549 \text{Log}[x3] + 42.7343 \text{Log}[x4]$
CS2-O4-FOLNR	$(682.656 - 39.6231 \text{Log}[x1] + 134.195 \text{Log}[x2] + 49.5497 \text{Log}[x3] + 26.8548 \text{Log}[x4]) / (1.28547 - 0.00325363 \text{Log}[x1] + 0.332541 \text{Log}[x2] - 0.174628 \text{Log}[x3] - 0.00123955 \text{Log}[x4])$
CS2-O4-SOLN	$-5743.16 + 2594.85 \text{Log}[x1] - 258.081 \text{Log}[x1]^2 + 338.321 \text{Log}[x2] - 1.3871 \text{Log}[x1] \text{Log}[x2] + 85.5284 \text{Log}[x2]^2 + 382.614 \text{Log}[x3] - 31.1345 \text{Log}[x1] \text{Log}[x3] - 65.851 \text{Log}[x2] \text{Log}[x3] + 110.772 \text{Log}[x3]^2 + 24.9408 \text{Log}[x4] + 4.73501 \text{Log}[x1] \text{Log}[x4] + 25.4227 \text{Log}[x2] \text{Log}[x4] + 5.20716 \text{Log}[x3] \text{Log}[x4] + 16.7191 \text{Log}[x4]^2$
CS2-O4-SOLNR	$(1.40617*10^{10} + 8.27366*10^{10} \text{Log}[x1] + 4.34122*10^{11} \text{Log}[x1]^2 + 1.42317*10^9 \text{Log}[x2] - 6.87779*10^{10} \text{Log}[x1] \text{Log}[x2] - 1.2685*10^{11} \text{Log}[x2]^2 + 2.35158*10^{11} \text{Log}[x3] + 1.24793*10^{12} \text{Log}[x1] \text{Log}[x3] - 5.14853*10^{11} \text{Log}[x2] \text{Log}[x3] - 5.18161*10^{11} \text{Log}[x3]^2 - 6.99879*10^{10} \text{Log}[x4] - 2.92016*10^{11} \text{Log}[x1] \text{Log}[x4] + 4.98272*10^{10} \text{Log}[x2] \text{Log}[x4] + 4.14611*10^{11} \text{Log}[x3] \text{Log}[x4] - 4.50227*10^{11} \text{Log}[x4]^2) / (6.12704*10^{10} - 4.10399*10^{10} \text{Log}[x1] + 4.88949*10^9 \text{Log}[x1]^2 + 1.56519*10^{10} \text{Log}[x2] - 1.17178*10^{10} \text{Log}[x1] \text{Log}[x2] - 8.18723*10^9 \text{Log}[x2]^2 - 8.05385*10^{10} \text{Log}[x3] + 7.75726*10^9 \text{Log}[x1] \text{Log}[x3] - 1.54765*10^{10} \text{Log}[x2] \text{Log}[x3] - 2.25162*10^{10} \text{Log}[x3]^2 + 3.37421*10^{10} \text{Log}[x4] - 9.35357*10^9 \text{Log}[x1] \text{Log}[x4] + 1.35654*10^9 \text{Log}[x2] \text{Log}[x4] + 1.75223*10^9 \text{Log}[x3] \text{Log}[x4] + 1.86101*10^9 \text{Log}[x4]^2)$
NOTATION	CS2-O5
CS2-O5-L	$77.7775 - 0.331437 [x1] + 597.933 [x2] + 429.188 [x3] + 9.28267 [x4]$
CS2-O5-LN	$(-39871. - 488.523 [x1] + 1.54303*10^6 [x2] + 593616. [x3] + 7237.07 [x4]) / (646.453 - 0.44235 [x1] + 2770.59 [x2] + 461.597 [x3] - 5.86192 [x4])$
CS2-O5-SON	$-24.7911 + 0.354084 [x1] - 0.00207788 [x1]^2 + 510.881 [x2] + 0.15584 [x1] [x2] + 3207.58 [x2]^2 + 689.506 [x3] + 0.0513194 [x1] [x3] - 2130.31 [x2] [x3] - 3.1741 [x3]^2 + 6.97633 [x4] + 0.011017 [x1] [x4] + 15.2474 [x2] [x4] + 0.15584 [x3] [x4] - 0.0725023 [x4]^2$
CS2-O5-SONR	$(-43.2719 + 20.5572 [x1] - 0.0658603 [x1]^2 - 34.0625 [x2] + 91.5096 [x1] [x2] - 4.04695 [x2]^2 + 40.1843 [x3] + 18.2179 [x1] [x3] + 1.47771 [x2] [x3] + 16.4379 [x3]^2 + 12.9752 [x4] + 0.154069 [x1] [x4] + 440.238 [x2] [x4] - 319.978 [x3] [x4] - 5.23875 [x4]^2) / (14.1571 + 0.0758793 [x1] - 0.0000608926 [x1]^2 - 3.45939 [x2] + 0.226469 [x1] [x2] - 168.437 [x2]^2 - 36.1652 [x3] - 0.0110439 [x1] [x3] + 74.4876 [x2] [x3] + 15.807 [x3]^2 - 0.727701 [x4] - 0.00223607 [x1] [x4] + 1.25248 [x2] [x4] + 0.312573 [x3] [x4] + 0.00862536 [x4]^2)$
CS2-O5-TON	$55.691 + 0.093647 [x1] - 0.000231862 [x1]^2 - 2.68834*10^{-6} [x1]^3 + 135.633 [x2] + 0.368702 [x1] [x2] - 0.00165559 [x1]^2 [x2] + 602.204 [x2]^2 + 3.19393 [x1] [x2]^2 + 9921.92 [x2]^3 + 294.336 [x3] + 0.384248 [x1] [x3] - 0.000658954 [x1]^2 [x3] + 751.301 [x2] [x3] - 3.40615 [x1] [x2] [x3] - 2616.51 [x2]^2 [x3] + 320.123 [x3]^2 - 0.0913195 [x1] [x3]^2 - 884.203 [x2] [x3]^2 - 59.7945 [x3]^3 + 4.15044 [x4] + 0.00972063 [x1] [x4] - 0.0000294032 [x1]^2 [x4] + 18.9223 [x2] [x4] + 0.0713014 [x1] [x2] [x4] + 22.0465 [x2]^2 [x4] + 10.27 [x3] [x4] + 0.0405527 [x1] [x3] [x4] - 81.8883 [x2] [x3] [x4] - 12.372 [x3]^2 [x4] + 0.0917715 [x4]^2 - 0.000688457 [x1] [x4]^2 + 0.10392 [x2] [x4]^2 + 0.0163552 [x3] [x4]^2 - 0.00181328 [x4]^3$
CS2-O5-FOTN	$8693.38 - 100.394 \text{Cos}[x1] - 8009.07 \text{Cos}[x2] - 303.982 \text{Cos}[x3] + 300.193 \text{Cos}[x4] - 47.9383 \text{Sin}[x1] - 382.422 \text{Sin}[x2] + 342.07 \text{Sin}[x3] - 246.049 \text{Sin}[x4]$
CS2-O5-FOTNR	$(3045.77 - 14.3631 \text{Cos}[x1] - 2598.14 \text{Cos}[x2] - 405.78 \text{Cos}[x3] + 10.8134 \text{Cos}[x4] - 1.1542 \text{Sin}[x1] - 343.732 \text{Sin}[x2] - 119.533 \text{Sin}[x3] - 2.09255 \text{Sin}[x4]) / (9.19309 - 0.0281607 \text{Cos}[x1] - 8.12752 \text{Cos}[x2] - 0.962011 \text{Cos}[x3] - 0.0187463 \text{Cos}[x4] + 0.0026635 \text{Sin}[x1] - 1.11306 \text{Sin}[x2] - 0.317976 \text{Sin}[x3] + 0.0299941 \text{Sin}[x4])$
CS2-O5-SOTN	$4.12489 + 3.18527 \text{Cos}[x1] - 21.3518 \text{Cos}[x1]^2 + 3.40528 \text{Cos}[x2] + 0.0728196 \text{Cos}[x1] \text{Cos}[x2] + 2.70245 \text{Cos}[x2]^2 - 4.96757 \text{Cos}[x3] - 169. \text{Cos}[x1] \text{Cos}[x3] - 6.25769 \text{Cos}[x2] \text{Cos}[x3] - 15.2431 \text{Cos}[x3]^2 + 101.414 \text{Cos}[x4] + 20.086 \text{Cos}[x1] \text{Cos}[x4] + 96.0381 \text{Cos}[x2] \text{Cos}[x4] - 198.907 \text{Cos}[x3] \text{Cos}[x4] - 86.4413 \text{Cos}[x4]^2 + 65.852 \text{Sin}[x1] - 106.059 \text{Sin}[x1] \text{Sin}[x2] + 56.7401 \text{Cos}[x2] \text{Sin}[x1] - 140.444 \text{Cos}[x3] \text{Sin}[x1] + 77.5427 \text{Cos}[x4] \text{Sin}[x1] + 36.3868 \text{Sin}[x1]^2 - 88.2755 \text{Sin}[x2] - 50.2981 \text{Cos}[x1] \text{Sin}[x2] - 110.72 \text{Cos}[x2] \text{Sin}[x2] + 151.119 \text{Cos}[x3] \text{Sin}[x2] - 83.3622 \text{Cos}[x4] \text{Sin}[x2] - 130.846 \text{Sin}[x1] \text{Sin}[x2] + 5268.84$

	$\text{Sin}[x2]^2 + 104.103 \text{Sin}[x3] - 60.3578 \text{Cos}[x1] \text{Sin}[x3] + 104.82 \text{Cos}[x2] \text{Sin}[x3] + 99.3177 \text{Cos}[x3] \text{Sin}[x3] - 240.428 \text{Cos}[x4] \text{Sin}[x3] - 72.8001 \text{Sin}[x1] \text{Sin}[x3] - 1374.08 \text{Sin}[x2] \text{Sin}[x3] + 327.462 \text{Sin}[x3]^2 + 35.9587 \text{Sin}[x4] - 7.05566 \text{Cos}[x1] \text{Sin}[x4] + 35.5736 \text{Cos}[x2] \text{Sin}[x4] - 51.8578 \text{Cos}[x3] \text{Sin}[x4] + 285.669 \text{Cos}[x4] \text{Sin}[x4] - 43.09 \text{Sin}[x1] \text{Sin}[x4] - 266.558 \text{Sin}[x2] \text{Sin}[x4] + 24.8241 \text{Sin}[x3] \text{Sin}[x4] + 49.4576 \text{Sin}[x4]^2$
CS2-O5-SOTNR	$(-1.37251*10^{12} + 1.28244*10^{12} \text{Cos}[x1] - 1.25286*10^{12} \text{Cos}[x1]^2 - 1.36099*10^{12} \text{Cos}[x2] + 1.27152*10^{12} \text{Cos}[x1] \text{Cos}[x2] - 1.3496*10^{12} \text{Cos}[x2]^2 - 1.22318*10^{12} \text{Cos}[x3] + 1.14304*10^{12} \text{Cos}[x1] \text{Cos}[x3] - 1.21296*10^{12} \text{Cos}[x2] \text{Cos}[x3] - 1.09464*10^{12} \text{Cos}[x3]^2 + 6.05071*10^{11} \text{Cos}[x4] - 5.67785*10^{11} \text{Cos}[x1] \text{Cos}[x4] + 6.01147*10^{11} \text{Cos}[x2] \text{Cos}[x4] + 5.41101*10^{11} \text{Cos}[x3] \text{Cos}[x4] - 2.15973*10^{11} \text{Cos}[x4]^2 + 8.54699*10^{10} \text{Sin}[x1] + 1.54555*10^{11} \text{Cos}[x1] \text{Sin}[x1] + 8.48597*10^{10} \text{Cos}[x2] \text{Sin}[x1] + 6.49139*10^{10} \text{Cos}[x3] \text{Sin}[x1] + 3.55243*10^{11} \text{Cos}[x4] \text{Sin}[x1] - 1.1965*10^{11} \text{Sin}[x1]^2 - 1.68637*10^{11} \text{Sin}[x2] + 1.59326*10^{11} \text{Cos}[x1] \text{Sin}[x2] - 1.66958*10^{11} \text{Cos}[x2] \text{Sin}[x2] - 1.49522*10^{11} \text{Cos}[x3] \text{Sin}[x2] + 6.58306*10^{10} \text{Cos}[x4] \text{Sin}[x2] + 1.33509*10^{10} \text{Sin}[x1] \text{Sin}[x2] - 2.29053*10^{10} \text{Sin}[x2]^2 - 5.92796*10^{11} \text{Sin}[x3] + 5.53911*10^{11} \text{Cos}[x1] \text{Sin}[x3] - 5.87736*10^{11} \text{Cos}[x2] \text{Sin}[x3] - 5.18499*10^{11} \text{Cos}[x3] \text{Sin}[x3] + 2.62333*10^{11} \text{Cos}[x4] \text{Sin}[x3] + 5.97992*10^{10} \text{Sin}[x1] \text{Sin}[x3] - 7.41673*10^{10} \text{Sin}[x2] \text{Sin}[x3] - 2.77869*10^{11} \text{Sin}[x3]^2 - 1.33409*10^{12} \text{Sin}[x4] + 1.16506*10^{12} \text{Cos}[x1] \text{Sin}[x4] - 1.32289*10^{12} \text{Cos}[x2] \text{Sin}[x4] - 1.19317*10^{12} \text{Cos}[x3] \text{Sin}[x4] + 6.52825*10^{11} \text{Cos}[x4] \text{Sin}[x4] + 4.46704*10^{11} \text{Sin}[x1] \text{Sin}[x4] - 1.63406*10^{11} \text{Sin}[x2] \text{Sin}[x4] - 5.60663*10^{11} \text{Sin}[x3] \text{Sin}[x4] - 1.15653*10^{12} \text{Sin}[x4]^2) / (-7.97646*10^{11} + 2.49942*10^{11} \text{Cos}[x1] + 4.72687*10^{10} \text{Cos}[x1]^2 - 1.03968*10^{12} \text{Cos}[x2] + 4.27846*10^{11} \text{Cos}[x1] \text{Cos}[x2] - 1.27831*10^{12} \text{Cos}[x2]^2 - 8.26633*10^{11} \text{Cos}[x3] + 4.30442*10^{11} \text{Cos}[x1] \text{Cos}[x3] - 1.02603*10^{12} \text{Cos}[x2] \text{Cos}[x3] - 8.69531*10^{11} \text{Cos}[x3]^2 + 7.99997*10^{11} \text{Cos}[x4] - 7.88596*10^{11} \text{Cos}[x1] \text{Cos}[x4] + 8.70652*10^{11} \text{Cos}[x2] \text{Cos}[x4] + 1.18959*10^{12} \text{Cos}[x3] \text{Cos}[x4] - 1.29042*10^{12} \text{Cos}[x4]^2 - 2.1094*10^{11} \text{Sin}[x1] + 2.22457*10^{11} \text{Cos}[x1] \text{Sin}[x1] - 3.73472*10^{11} \text{Cos}[x2] \text{Sin}[x1] - 3.08407*10^{10} \text{Cos}[x3] \text{Sin}[x1] - 1.08768*10^{12} \text{Cos}[x4] \text{Sin}[x1] - 8.44915*10^{11} \text{Sin}[x1]^2 + 2.10964*10^{12} \text{Sin}[x2] - 1.57701*10^{12} \text{Cos}[x1] \text{Sin}[x2] + 2.06736*10^{12} \text{Cos}[x2] \text{Sin}[x2] - 1.73821*10^{12} \text{Cos}[x3] \text{Sin}[x2] - 5.56318*10^{11} \text{Cos}[x4] \text{Sin}[x2] + 1.42536*10^{12} \text{Sin}[x1] \text{Sin}[x2] + 4.80659*10^{11} \text{Sin}[x2]^2 + 1.50062*10^{11} \text{Sin}[x3] - 5.0678*10^{11} \text{Cos}[x1] \text{Sin}[x3] + 9.36293*10^9 \text{Cos}[x2] \text{Sin}[x3] + 1.62601*10^{11} \text{Cos}[x3] \text{Sin}[x3] - 6.4459*10^{11} \text{Cos}[x4] \text{Sin}[x3] - 2.75199*10^{11} \text{Sin}[x1] \text{Sin}[x3] + 1.24024*10^{12} \text{Sin}[x2] \text{Sin}[x3] + 7.18852*10^{10} \text{Sin}[x3]^2 + 1.51033*10^{12} \text{Sin}[x4] - 1.43807*10^{12} \text{Cos}[x1] \text{Sin}[x4] + 1.26596*10^{12} \text{Cos}[x2] \text{Sin}[x4] + 1.39833*10^{12} \text{Cos}[x3] \text{Sin}[x4] - 1.56418*10^{12} \text{Cos}[x4] \text{Sin}[x4] - 8.20188*10^{10} \text{Sin}[x1] \text{Sin}[x4] + 2.25782*10^{12} \text{Sin}[x2] \text{Sin}[x4] + 7.8398*10^{11} \text{Sin}[x3] \text{Sin}[x4] + 4.92777*10^{11} \text{Sin}[x4]^2)$
CS2-O5-FOLN	$843.201 - 63.2653 \text{Log}[x1] + 61.4462 \text{Log}[x2] + 149.19 \text{Log}[x3] + 58.5033 \text{Log}[x4]$
CS2-O5-FOLNR	$(3368.01 - 253.045 \text{Log}[x1] + 472.296 \text{Log}[x2] + 325.724 \text{Log}[x3] + 117.077 \text{Log}[x4]) / (6.14916 - 0.284535 \text{Log}[x1] + 0.912987 \text{Log}[x2] - 0.242831 \text{Log}[x3] - 0.111715 \text{Log}[x4])$
CS2-O5-SOLN	$-1359.83 + 957.468 \text{Log}[x1] - 101.579 \text{Log}[x1]^2 + 366.788 \text{Log}[x2] - 1.55764 \text{Log}[x1] \text{Log}[x2] + 91.7247 \text{Log}[x2]^2 + 82.5432 \text{Log}[x3] + 9.45717 \text{Log}[x1] \text{Log}[x3] - 91.718 \text{Log}[x2] \text{Log}[x3] + 78.3405 \text{Log}[x3]^2 - 148.863 \text{Log}[x4] + 24.9328 \text{Log}[x1] \text{Log}[x4] + 10.2482 \text{Log}[x2] \text{Log}[x4] - 2.21353 \text{Log}[x3] \text{Log}[x4] + 29.2169 \text{Log}[x4]^2$
CS2-O5-SOLNR	$(151.416 + 406.726 \text{Log}[x1] + 30.9867 \text{Log}[x1]^2 - 196.967 \text{Log}[x2] + 166.498 \text{Log}[x1] \text{Log}[x2] - 53.4479 \text{Log}[x2]^2 - 36.7738 \text{Log}[x3] + 27.0893 \text{Log}[x1] \text{Log}[x3] + 76.8438 \text{Log}[x2] \text{Log}[x3] - 114.397 \text{Log}[x3]^2 - 64.3553 \text{Log}[x4] - 106.866 \text{Log}[x1] \text{Log}[x4] - 148.696 \text{Log}[x2] \text{Log}[x4] + 25.971 \text{Log}[x3] \text{Log}[x4] + 71.3355 \text{Log}[x4]^2) / (22.4875 - 10.7713 \text{Log}[x1] + 1.29278 \text{Log}[x1]^2 - 4.54229 \text{Log}[x2] + 0.207554 \text{Log}[x1] \text{Log}[x2] - 1.40103 \text{Log}[x2]^2 - 0.11864 \text{Log}[x3] - 0.392069 \text{Log}[x1] \text{Log}[x3] + 0.736343 \text{Log}[x2] \text{Log}[x3] - 0.858699 \text{Log}[x3]^2 + 2.7437 \text{Log}[x4] - 0.862574 \text{Log}[x1] \text{Log}[x4] - 0.490239 \text{Log}[x2] \text{Log}[x4] + 0.585385 \text{Log}[x3] \text{Log}[x4] + 0.116352 \text{Log}[x4]^2)$
NOTATION	CS3-O1
CS3-O1-L	$30.3668 - 0.189234 [x1] - 59.4892 [x2]$
CS3-O1-LN	$(1292.63 + 0.18814 [x1] - 5477.86 [x2]) / (-6.12838 + 1.35424 [x1] - 176.612 [x2])$
CS3-O1-SON	$58.549 - 1.0675 [x1] + 0.00609375 [x1]^2 - 22.1667 [x2] + 0.175 [x1] [x2] - 205. [x2]^2$
CS3-O1-SONR	$(4.97963*10^7 + 1.64719*10^9 [x1] + 7.98453*10^9 [x1]^2 + 5.64053*10^6 [x2] + 1.21709*10^8 [x1] [x2] + 607832. [x2]^2) / (-4.02954*10^8 - 1.28427*10^10 [x1] + 1.12123*10^9 [x1]^2 - 4.49194*10^7 [x2] - 8.61375*10^8 [x1] [x2] - 4.7134*10^6 [x2]^2)$
CS3-O1-TON	$35.16 + 0.00550599 [x1] - 0.0145795 [x1]^2 + 0.000883764 [x1]^3 + 32.4328 [x2] + 4.54374 [x1] [x2] + 0.0140946 [x1]^2 [x2] - 1920.05 [x2]^2 - 20.1738 [x1] [x2]^2 + 7447.27 [x2]^3$
CS3-O1-FOTN	$-3877.21 + 0.364141 \text{Cos}[x1] + 3865.2 \text{Cos}[x2] - 2.70456 \text{Sin}[x1] + 435.999 \text{Sin}[x2]$
CS3-O1-FOTNR	$(-4.67358 + 0.0353674 \text{Cos}[x1] + 12.5494 \text{Cos}[x2] - 0.407401 \text{Sin}[x1] - 47.7044 \text{Sin}[x2]) / (0.330978 + 0.00459497 \text{Cos}[x1] + 0.379639 \text{Cos}[x2] - 0.0117023 \text{Sin}[x1] - 4.40662 \text{Sin}[x2])$
CS3-O1-SOTN	$3.25849 - 0.214342 \text{Cos}[x1] + 8.27462 \text{Cos}[x1]^2 + 3.38253 \text{Cos}[x2] - 0.264635 \text{Cos}[x1] \text{Cos}[x2] + 3.50901 \text{Cos}[x2]^2 + 0.271854 \text{Sin}[x1] - 1.68262 \text{Cos}[x1] \text{Sin}[x1] + 0.299523 \text{Cos}[x2] \text{Sin}[x1] + 1.4002 \text{Sin}[x1]^2 - 6.09749 \text{Sin}[x2] + 10.2907 \text{Cos}[x1] \text{Sin}[x2] - 5.65877 \text{Cos}[x2] \text{Sin}[x2] - 8.58448 \text{Sin}[x1] \text{Sin}[x2] - 189.233 \text{Sin}[x2]^2$
CS3-O1-SOTNR	$(2.83056 + 0.127232 \text{Cos}[x1] + 2.16187 \text{Cos}[x1]^2 + 2.85304 \text{Cos}[x2] + 1.34935 \text{Cos}[x1] \text{Cos}[x2] + 2.87497 \text{Cos}[x2]^2 + 0.745468 \text{Sin}[x1] + 1.24278 \text{Cos}[x1] \text{Sin}[x1] + 0.766071 \text{Cos}[x2] \text{Sin}[x1] + 1.66869 \text{Sin}[x1]^2 + 0.949802 \text{Sin}[x2] + 1.01644 \text{Cos}[x1] \text{Sin}[x2] + 0.955376 \text{Cos}[x2] \text{Sin}[x2] + 0.816638 \text{Sin}[x1] \text{Sin}[x2] + 0.955587 \text{Sin}[x2]^2) / (0.256359 + 0.127232 \text{Cos}[x1] + 0.0525958 \text{Cos}[x1]^2 - 0.151432 \text{Cos}[x2] - 0.200073 \text{Cos}[x1] \text{Cos}[x2] - 0.551367 \text{Cos}[x2]^2 - 0.0349057 \text{Sin}[x1] + 0.317735 \text{Cos}[x1] \text{Sin}[x1] - 0.155819 \text{Cos}[x2] \text{Sin}[x1] + 1.20376 \text{Sin}[x1]^2 + 3.96625 \text{Sin}[x2] + 0.954938 \text{Cos}[x1] \text{Sin}[x2] + 3.88238 \text{Cos}[x2] \text{Sin}[x2] + 1.97487 \text{Sin}[x1] \text{Sin}[x2] + 1.80773 \text{Sin}[x2]^2)$
CS3-O1-FOLN	$50.1892 - 13.5141 \text{Log}[x1] - 8.00441 \text{Log}[x2]$
CS3-O1-FOLNR	$(-11.5029 - 2.23817 \text{Log}[x1] - 14.4088 \text{Log}[x2]) / (-4.36534 + 0.878534 \text{Log}[x1] - 0.761502 \text{Log}[x2])$
CS3-O1-SOLN	$376.552 - 188.471 \text{Log}[x1] + 20.7385 \text{Log}[x1]^2 - 47.2561 \text{Log}[x2] - 0.4629 \text{Log}[x1] \text{Log}[x2] - 9.96759 \text{Log}[x2]^2$
CS3-O1-SOLNR	$(1.66002*10^7 - 5.30954*10^7 \text{Log}[x1] - 9.3724*10^7 \text{Log}[x1]^2 - 8.11363*10^7 \text{Log}[x2] - 3.42678*10^8 \text{Log}[x1] \text{Log}[x2] + 1.09504*10^8 \text{Log}[x2]^2) / (-5.53193*10^7 - 5.10264*10^7 \text{Log}[x1] + 5.66958*10^7 \text{Log}[x1]^2 + 1.70728*10^8 \text{Log}[x2] + 1.01345*10^8 \text{Log}[x1] \text{Log}[x2] + 1.58492*10^8 \text{Log}[x2]^2)$
NOTATION	CS3-O2
CS3-O2-L	$74658. - 116.354 [x1] + 73329.3 [x2]$
CS3-O2-LN	$(1.68718*10^6 + 1129.86 [x1] - 1.17339*10^7 [x2]) / (21.7821 + 0.0136152 [x1] - 151.011 [x2])$
CS3-O2-SON	$299882. - 4664.24 [x1] + 24.9334 [x1]^2 - 860690. [x2] + 6913.51 [x1] [x2] + 1.55062*10^6 [x2]^2$
CS3-O2-SONR	$(1.00023 + 1.01507 [x1] + 2.01273 [x1]^2 + 1.00003 [x2] + 1.00223 [x1] [x2] + 1.00001 [x2]^2) / (0.99977 + 0.984925 [x1] - 0.0127263 [x1]^2 + 0.999966 [x2] + 0.997774 [x1] [x2] + 0.999995 [x2]^2)$
CS3-O2-TON	$174267. - 1411.34 [x1] + 7.07087 [x1]^2 + 0.046628 [x1]^3 + 97368.4 [x2] - 20395.5 [x1] [x2] + 53.8045 [x1]^2 [x2] + 1.97214*10^6 [x2]^2 + 66632.2 [x1] [x2]^2 - 1.22733*10^7 [x2]^3$
CS3-O2-FOTN	$-4.69669*10^6 + 331.54 \text{Cos}[x1] + 4.72999*10^6 \text{Cos}[x2] - 4852.39 \text{Sin}[x1] + 666048. \text{Sin}[x2]$
CS3-O2-FOTNR	$(-2.46462*10^6 + 345517. \text{Cos}[x1] + 1.39386*10^6 \text{Cos}[x2] + 650662. \text{Sin}[x1] + 4.34658*10^6 \text{Sin}[x2]) / (-11.3097 + 4.59612 \text{Cos}[x1] - 2.50146 \text{Cos}[x2] + 8.23695 \text{Sin}[x1] + 55.9117 \text{Sin}[x2])$
CS3-O2-SOTN	$16100.7 - 132.04 \text{Cos}[x1] + 26037.6 \text{Cos}[x1]^2 + 16502.1 \text{Cos}[x2] - 201.823 \text{Cos}[x1] \text{Cos}[x2] + 16910.6 \text{Cos}[x2]^2 + 1659.26 \text{Sin}[x1] - 10787.1 \text{Cos}[x1] \text{Sin}[x1] + 1807.59 \text{Cos}[x2] \text{Sin}[x1] + 21453.4 \text{Sin}[x1]^2 + 35969.2 \text{Sin}[x2] + 11073.5 \text{Cos}[x1] \text{Sin}[x2] + 37664.6 \text{Cos}[x2] \text{Sin}[x2] - 36218.4 \text{Sin}[x1] \text{Sin}[x2] - 143438. \text{Sin}[x2]^2$
CS3-O2-SOTNR	$(3.31183 + 1. \text{Cos}[x1] + 2.29142 \text{Cos}[x1]^2 + 3.28447 \text{Cos}[x2] + 0.485638 \text{Cos}[x1] \text{Cos}[x2] + 3.25746 \text{Cos}[x2]^2 + 0.813468 \text{Sin}[x1] + 1.46962 \text{Cos}[x1] \text{Sin}[x1] + 0.817972 \text{Cos}[x2] \text{Sin}[x1] + 2.02042 \text{Sin}[x1]^2 + 1.3509 \text{Sin}[x2] + 0.917552 \text{Cos}[x1] \text{Sin}[x2] + 1.34658 \text{Cos}[x2] \text{Sin}[x2] + 0.957 \text{Sin}[x1] \text{Sin}[x2] + 1.05437 \text{Sin}[x2]^2) / (-1.31183 + 1. \text{Cos}[x1] - 0.291416 \text{Cos}[x1]^2 - 1.28447 \text{Cos}[x2] + 1.51436 \text{Cos}[x1] \text{Cos}[x2] - 1.25746 \text{Cos}[x2]^2 + 1.18653 \text{Sin}[x1] + 0.530378 \text{Cos}[x1] \text{Sin}[x1] + 1.18203 \text{Cos}[x2] \text{Sin}[x1] - 0.020418 \text{Sin}[x1]^2 + 0.649103 \text{Sin}[x2] + 1.08245 \text{Cos}[x1] \text{Sin}[x2] + 0.653419 \text{Cos}[x2] \text{Sin}[x2] + 1.043 \text{Sin}[x1] \text{Sin}[x2] + 0.94563 \text{Sin}[x2]^2)$
CS3-O2-FOLN	$139559. - 10220.2 \text{Log}[x1] + 9848.3 \text{Log}[x2]$
CS3-O2-FOLNR	$(-225379. + 55301.2 \text{Log}[x1] + 5419.82 \text{Log}[x2]) / (-2.76137 + 0.680709 \text{Log}[x1] + 0.0739391 \text{Log}[x2])$
CS3-O2-SOLN	$1.70087*10^6 - 819893. \text{Log}[x1] + 111010. \text{Log}[x1]^2 - 139336. \text{Log}[x2] + 65857.2 \text{Log}[x1] \text{Log}[x2] + 33166. \text{Log}[x2]^2$
CS3-O2-SOLNR	$(1.03961 + 1.16666 \text{Log}[x1] + 1.70232 \text{Log}[x1]^2 + 0.923774 \text{Log}[x2] + 0.679294 \text{Log}[x1] \text{Log}[x2] + 1.14763 \text{Log}[x2]^2) / (0.960394 + 0.833338 \text{Log}[x1] + 0.297676 \text{Log}[x1]^2 + 1.07623 \text{Log}[x2] + 1.32071 \text{Log}[x1] \text{Log}[x2] + 0.852371 \text{Log}[x2]^2)$
NOTATION	CS4-O
CS4-O-L	$1.21719 + 0.00066308 [[x1]] + 6.67456 [x2] + 13.8992 [[x3]]$
CS4-O-LN	$(14104.4 - 3.33154 [x1] + 57411.5 [x2] - 59538.5 [x3]) / (5424.52 - 1.0734 [x1] + 4701.81 [x2] - 19146.5 [x3])$
CS4-O-SON	$11.0962 + 0.00628107 [x1] - 2.11334*10^{-6} [x1]^2 + 12.2932 [x2] + 0.000280782 [x1] [x2] - 8.06027 [x2]^2 - 200.66 [x3] - 0.00877092 [x1] [x3] + 11.5402 [x2] [x3] + 838.512 [x3]^2$

CS4-O-SONR	$(1.19171 \cdot 10^6 + 9007.12 [x1] - 3.90591 [x1]^2 + 2.26926 \cdot 10^6 [x2] + 2207.11 [x1] [x2] - 1.08533 \cdot 10^7 [x2]^2 - 6.19286 \cdot 10^7 [x3] - 15280.3 [x1] [x3] + 3.62137 \cdot 10^7 [x2] [x3] + 1.94542 \cdot 10^8 [x3]^2) / (698854 + 895.606 [x1] - 0.478325 [x1]^2 - 411380 [x2] + 527.968 [x1] [x2] - 1.36318 \cdot 10^6 [x2]^2 - 9.55882 \cdot 10^6 [x3] - 1869.75 [x1] [x3] + 7.32745 \cdot 10^6 [x2] [x3] + 2.25245 \cdot 10^7 [x3]^2)$
CS4-O-TON	$-50.6114 + 0.103749 [x1] + 0.0000669003 [x1]^2 - 6.33707 \cdot 10^{-8} [x1]^3 - 27.6247 [x2] - 0.0711413 [x1] [x2] + 0.0000498592 [x1]^2 [x2] + 16.1684 [x2]^2 + 0.0420459 [x1] [x2]^2 + 52.8303 [x2]^3 + 417.594 [x3] - 2.10435 [x1] [x3] + 0.000761538 [x1]^2 [x3] + 884.22 [x2] [x3] + 0.0320913 [x1] [x2] [x3] - 374.657 [x2]^2 [x3] + 3062.11 [x3]^2 [x2] - 2081.83 [x2] [x3]^2 - 7769.72 [x3]^3$
CS4-O-FOTN	$1685.06 + 1.79729 \cos[x1] + 12.1346 \cos[x2] - 1682.8 \cos[x3] - 0.843848 \sin[x1] + 13.6131 \sin[x2] - 206.049 \sin[x3]$
CS4-O-FOTNR	$(-21.227 - 0.0898775 \cos[x1] - 2.42298 \cos[x2] + 23.6419 \cos[x3] + 0.0463529 \sin[x1] - 0.137339 \sin[x2] + 1.78044 \sin[x3]) / (-4.00391 - 0.0293574 \cos[x1] - 0.209761 \cos[x2] + 4.21632 \cos[x3] + 0.0147841 \sin[x1] + 0.0160416 \sin[x2] + 0.283404 \sin[x3])$
CS4-O-SOTN	$-6977.17 - 3206.98 \cos[x1] - 14186.2 \cos[x1]^2 - 9891.8 \cos[x2] + 190.625 \cos[x1] \cos[x2] - 12084.6 \cos[x2]^2 - 7103.87 \cos[x3] - 8405.51 \cos[x1] \cos[x3] + 59788.6 \cos[x2] \cos[x3] - 7233.49 \cos[x3]^2 + 4228.29 \sin[x1] - 12305. \cos[x1] \sin[x1] - 90.02 \cos[x2] \sin[x1] + 3328.04 \cos[x3] \sin[x1] - 8905.55 \sin[x1]^2 - 9434.57 \sin[x2] + 95.0115 \cos[x1] \sin[x2] - 23232.4 \cos[x2] \sin[x2] + 34279.6 \cos[x3] \sin[x2] - 46.8915 \sin[x1] \sin[x2] + 5413.03 \sin[x2]^2 - 4840.79 \sin[x3] - 1195.76 \cos[x1] \sin[x3] + 8559.92 \cos[x2] \sin[x3] - 4717.21 \cos[x3] \sin[x3] + 457.87 \sin[x1] \sin[x3] + 4892.1 \sin[x2] \sin[x3] + 22550.5 \sin[x3]^2$
CS4-O-SOTNR	$(4.24255 \cdot 10^8 - 3.12831 \cdot 10^8 \cos[x1] + 2.58637 \cdot 10^8 \cos[x1]^2 - 1.91428 \cdot 10^8 \cos[x2] - 3.34875 \cdot 10^8 \cos[x1] \cos[x2] - 4.96575 \cdot 10^8 \cos[x2]^2 + 4.81297 \cdot 10^8 \cos[x3] - 3.99593 \cdot 10^8 \cos[x1] \cos[x3] - 1.46351 \cdot 10^8 \cos[x2] \cos[x3] + 5.43801 \cdot 10^8 \cos[x3]^2 - 2.40536 \cdot 10^7 \sin[x1] + 4.30742 \cdot 10^8 \cos[x1] \sin[x1] + 1.9125 \cdot 10^8 \cos[x2] \sin[x1] - 2.34405 \cdot 10^8 \cos[x3] \sin[x1] + 1.65618 \cdot 10^8 \sin[x1]^2 + 3.53918 \cdot 10^8 \sin[x2] + 1.19922 \cdot 10^7 \cos[x1] \sin[x2] - 2.63945 \cdot 10^8 \cos[x2] \sin[x2] + 3.34825 \cdot 10^8 \cos[x3] \sin[x2] + 8.39236 \cdot 10^8 \sin[x1] \sin[x2] + 9.2083 \cdot 10^8 \sin[x2]^2 - 1.92282 \cdot 10^9 \sin[x3] + 8.30417 \cdot 10^8 \cos[x1] \sin[x3] - 1.82305 \cdot 10^9 \cos[x2] \sin[x3] - 1.94831 \cdot 10^9 \cos[x3] \sin[x3] + 2.6785 \cdot 10^9 \sin[x1] \sin[x3] - 6.93195 \cdot 10^7 \sin[x2] \sin[x3] - 1.19546 \cdot 10^8 \sin[x3]^2) / (-5.25718 \cdot 10^8 - 1.83619 \cdot 10^8 \cos[x1] + 3.20827 \cdot 10^7 \cos[x1]^2 - 4.18315 \cdot 10^8 \cos[x2] + 2.76447 \cdot 10^8 \cos[x1] \cos[x2] - 3.63752 \cdot 10^8 \cos[x2]^2 + 2.90275 \cdot 10^8 \cos[x3] - 3.06785 \cdot 10^8 \cos[x1] \cos[x3] + 5.60152 \cdot 10^8 \cos[x2] \cos[x3] + 1.06369 \cdot 10^9 \cos[x3]^2 + 2.84574 \cdot 10^8 \sin[x1] + 3.64224 \cdot 10^6 \cos[x1] \sin[x1] - 5.19612 \cdot 10^7 \cos[x2] \sin[x1] - 2.93941 \cdot 10^8 \cos[x3] \sin[x1] - 5.578 \cdot 10^8 \sin[x1]^2 - 1.11938 \cdot 10^8 \sin[x2] + 5.4896 \cdot 10^8 \cos[x1] \sin[x2] - 6.62867 \cdot 10^6 \cos[x2] \sin[x2] + 3.37911 \cdot 10^7 \cos[x3] \sin[x2] - 1.16989 \cdot 10^8 \sin[x1] \sin[x2] - 1.61965 \cdot 10^8 \sin[x2]^2 + 2.66626 \cdot 10^8 \sin[x3] + 2.89703 \cdot 10^8 \cos[x1] \sin[x3] - 1.35021 \cdot 10^9 \cos[x2] \sin[x3] + 5.87417 \cdot 10^8 \cos[x3] \sin[x3] + 3.44164 \cdot 10^8 \sin[x1] \sin[x3] + 2.2236 \cdot 10^8 \sin[x2] \sin[x3] - 1.5894 \cdot 10^9 \sin[x3]^2)$
CS4-O-FOLN	$6.48267 + 0.898279 \log[x1] + 2.45972 \log[x2] + 1.64048 \log[x3]$
CS4-O-FOLNR	$(-1371.49 + 561.472 \log[x1] + 725.851 \log[x2] - 263.659 \log[x3]) / (-162.487 + 34.1357 \log[x1] - 20.2213 \log[x2] - 121.989 \log[x3])$
CS4-O-SOLN	$-32.4248 + 32.8416 \log[x1] - 2.46385 \log[x1]^2 + 3.25024 \log[x2] + 0.178855 \log[x1] \log[x2] + 0.138893 \log[x2]^2 + 71.363 \log[x3] - 1.19079 \log[x1] \log[x3] + 0.861838 \log[x2] \log[x3] + 14.6295 \log[x3]^2$
CS4-O-SOLNR	$(-987.96 + 345.98 \log[x1] - 25.4476 \log[x1]^2 - 28.0785 \log[x2] + 4.02031 \log[x1] \log[x2] - 5.01345 \log[x2]^2 + 210.026 \log[x3] - 6.87319 \log[x1] \log[x3] + 7.37762 \log[x2] \log[x3] + 32.7372 \log[x3]^2) / (-148.999 + 50.6345 \log[x1] - 3.7753 \log[x1]^2 - 4.91914 \log[x2] + 0.560567 \log[x1] \log[x2] - 0.506154 \log[x2]^2 + 26.6787 \log[x3] - 1.28271 \log[x1] \log[x3] + 0.347832 \log[x2] \log[x3] + 3.57015 \log[x3]^2)$
NOTATION	CS5-O
CS5-O-L	$0.266001 - 0.000944892 [x1] + 3.56356 [x2] + 0.163355 [x3]$
CS5-O-LN	$(-1188.43 + 14.954 [x1] + 21013.6 [x2] - 3693.17 [x3]) / (-298.01 + 31.1019 [x1] + 10922. [x2] - 5201.78 [x3])$
CS5-O-SON	$0.638954 - 0.0039915 [x1] + 0.000016325 [x1]^2 + 2.67406 [x2] - 0.006625 [x1] [x2] - 1.28906 [x2]^2 - 0.0955 [x3] - 0.005325 [x1] [x3] + 4.25 [x2] [x3] + 0.83125 [x3]^2$
CS5-O-SONR	$(5.16715 \cdot 10^7 - 1.08413 \cdot 10^9 [x1] + 6.67759 \cdot 10^7 [x1]^2 + 7.61179 \cdot 10^7 [x2] + 1.03926 \cdot 10^10 [x1] [x2] + 1.84809 \cdot 10^7 [x2]^2 + 9.82933 \cdot 10^7 [x3] + 5.28271 \cdot 10^9 [x1] [x3] + 3.91731 \cdot 10^7 [x2] [x3] + 7.19583 \cdot 10^7 [x3]^2) / (-6.73736 \cdot 10^7 - 2.24511 \cdot 10^9 [x1] + 1.67567 \cdot 10^8 [x1]^2 - 5.30761 \cdot 10^7 [x2] - 6.76463 \cdot 10^9 [x1] [x2] - 1.25389 \cdot 10^7 [x2]^2 - 8.45582 \cdot 10^7 [x3] - 5.87897 \cdot 10^9 [x1] [x3] - 2.8222 \cdot 10^7 [x2] [x3] - 5.77872 \cdot 10^7 [x3]^2)$
CS5-O-TON	$0.462598 + 0.00736519 [x1] - 0.0000127843 [x1]^2 + 1.26892 \cdot 10^{-8} [x1]^3 + 1.59219 [x2] - 0.0969112 [x1] [x2] + 0.000300162 [x1]^2 [x2] + 0.272799 [x2]^2 - 0.113776 [x1] [x2]^2 + 31.6255 [x2]^3 - 4.4517 [x3] - 0.00572297 [x1] [x3] - 0.0000423135 [x1]^2 [x3] + 58.7409 [x2] [x3] + 0.00173282 [x1] [x2] [x3] + 29.1331 [x2]^2 [x3] + 4.02726 [x3]^2 + 0.0222752 [x1] [x3]^2 - 87.4595 [x2] [x3]^2 + 2.8228 [x3]^3$
CS5-O-FOTN	$16.8452 + 1.33016 \cos[x1] - 11.3431 \cos[x2] - 3.61925 \cos[x3] - 0.676265 \sin[x1] + 1.56093 \sin[x2] - 1.17092 \sin[x3]$
CS5-O-FOTNR	$(15.2478 + 12.418 \cos[x1] + 9.11218 \cos[x2] + 1.80602 \cos[x3] - 6.86865 \sin[x1] + 60.0568 \sin[x2] - 14.4095 \sin[x3]) / (-4.30733 - 27.8217 \cos[x1] - 0.362341 \cos[x2] + 15.5677 \cos[x3] + 11.8851 \sin[x1] - 36.1481 \sin[x2] - 24.3313 \sin[x3])$
CS5-O-SOTN	$-0.0639075 - 0.133391 \cos[x1] - 0.0121638 \cos[x1]^2 - 0.0619371 \cos[x2] - 0.242969 \cos[x1] \cos[x2] - 0.0609355 \cos[x2]^2 - 0.0791639 \cos[x3] - 0.278073 \cos[x1] \cos[x3] - 0.0978803 \cos[x2] \cos[x3] - 0.0841373 \cos[x3]^2 - 0.297637 \sin[x1] - 1.92607 \cos[x1] \sin[x1] - 0.137322 \cos[x2] \sin[x1] - 1.17536 \cos[x3] \sin[x1] - 0.846473 \sin[x1]^2 + 11.5555 \sin[x2] + 40.6608 \cos[x1] \sin[x2] + 12.182 \cos[x2] \sin[x2] + 21.1941 \cos[x3] \sin[x2] - 15.0403 \sin[x1] \sin[x2] - 12.9987 \sin[x2]^2 - 0.00555919 \sin[x3] + 1.03838 \cos[x1] \sin[x3] + 0.075458 \cos[x2] \sin[x3] - 0.143923 \cos[x3] \sin[x3] - 0.368789 \sin[x1] \sin[x3] + 15.7945 \sin[x2] \sin[x3] + 0.0525024 \sin[x3]^2$
CS5-O-SOTNR	$(2.66419 + 0.11749 \cos[x1] + 3.6649 \cos[x1]^2 + 2.42171 \cos[x2] + 0.19882 \cos[x1] \cos[x2] + 2.15358 \cos[x2]^2 + 0.0437481 \cos[x3] + 3.13608 \cos[x1] \cos[x3] - 0.134358 \cos[x2] \cos[x3] - 1.38325 \cos[x3]^2 + 1.83297 \sin[x1] + 3.47455 \cos[x1] \sin[x1] + 1.94353 \cos[x2] \sin[x1] + 2.51155 \cos[x3] \sin[x1] - 0.000712622 \sin[x1]^2 + 10.9933 \sin[x2] - 6.61426 \cos[x1] \sin[x2] + 11.1184 \cos[x2] \sin[x2] + 9.84026 \cos[x3] \sin[x2] + 3.72506 \sin[x1] \sin[x2] + 1.51062 \sin[x2]^2 - 1.69653 \sin[x3] + 2.45319 \cos[x1] \sin[x3] - 1.94304 \cos[x2] \sin[x3] - 4.64931 \cos[x3] \sin[x3] - 3.73884 \sin[x1] \sin[x3] + 5.48351 \sin[x2] \sin[x3] + 5.04744 \sin[x3]^2) / (-0.144303 - 2.06368 \cos[x1] + 5.17821 \cos[x1]^2 - 0.48438 \cos[x2] - 1.68901 \cos[x1] \cos[x2] - 0.799847 \cos[x2]^2 + 1.48598 \cos[x3] - 3.61044 \cos[x1] \cos[x3] + 1.14025 \cos[x2] \cos[x3] + 2.74814 \sin[x1] \cos[x3]^2 - 2.8736 \sin[x1] - 6.30231 \cos[x1] \sin[x1] + 2.52581 \cos[x2] \sin[x1] + 2.4041 \cos[x3] \sin[x1] - 4.32251 \sin[x1]^2 - 0.868 \sin[x2] + 1.74149 \cos[x1] \sin[x2] - 1.03863 \cos[x2] \sin[x2] - 0.461525 \cos[x3] \sin[x2] + 1.9567 \sin[x1] \sin[x2] + 1.65554 \sin[x2]^2 - 1.5867 \sin[x3] + 2.46356 \cos[x1] \sin[x3] - 1.58172 \cos[x2] \sin[x3] - 0.440501 \cos[x3] \sin[x3] + 3.08948 \sin[x1] \sin[x3] - 0.676131 \sin[x2] \sin[x3] - 1.89244 \sin[x3]^2)$
CS5-O-FOLN	$2.37577 - 0.17412 \log[x1] + 0.387459 \log[x2] + 0.0477195 \log[x3]$
CS5-O-FOLNR	$(-969.309 + 355.901 \log[x1] + 210.975 \log[x2] - 110.673 \log[x3]) / (-3810.49 + 798.526 \log[x1] - 234.831 \log[x2] - 128.103 \log[x3])$
CS5-O-SOLN	$19.4923 - 5.88271 \log[x1] + 0.512939 \log[x1]^2 + 1.7057 \log[x2] - 0.0820015 \log[x1] \log[x2] + 0.139854 \log[x2]^2 + 2.75883 \log[x3] - 0.332141 \log[x1] \log[x3] + 0.343461 \log[x2] \log[x3] + 0.127371 \log[x3]^2$
CS5-O-SOLNR	$(12656.1 + 29859.9 \log[x1] - 1773.52 \log[x1]^2 - 11133.5 \log[x2] + 6136.07 \log[x1] \log[x2] - 2950.61 \log[x2]^2 - 5294.2 \log[x3] - 7937.57 \log[x1] \log[x3] + 1951.53 \log[x2] \log[x3] - 2051.13 \log[x3]^2) / (-10634.5 - 25038.6 \log[x1] + 5084.5 \log[x1]^2 + 8398.73 \log[x2] - 9571.46 \log[x1] \log[x2] + 7855. \log[x2]^2 + 1413.13 \log[x3] - 10640.7 \log[x1] \log[x3] + 5669.09 \log[x2] \log[x3] + 6785.5 \log[x3]^2)$
NOTATION	CS6-O
CS6-O-L	$3.29144 - 0.645897 [x1] - 0.993714 [x2] - 0.0689516 [x3] + 5.8672 [x4]$
CS6-O-LN	$(-1340.35 + 157.426 [x1] + 4083.11 [x2] + 184.659 [x3] + 1162.39 [x4]) / (-698.717 + 130.805 [x1] + 1962.14 [x2] + 93.1946 [x3] - 78.2296 [x4])$
CS6-O-SON	$3.33016 - 3.57571 [x1] + 0.493052 [x1]^2 - 2.38689 [x2] + 4.44193 [x1] [x2] + 17.188 [x2]^2 + 1.71293 [x3] - 0.15681 [x1] [x3] - 5.81525 [x2] [x3] + 0.0699914 [x3]^2 + 34.5991 [x4] - 2.96164 [x1] [x4] - 49.7241 [x2] [x4] - 1.5198 [x3] [x4] - 18.4565 [x4]^2$
CS6-O-SONR	$(-2.69866 + 2.49186 [x1] + 0.911059 [x1]^2 + 5.47291 [x2] + 15.8316 [x1] [x2] + 5.44027 [x2]^2 - 1.67789 [x3] - 9.14077 [x1] [x3] - 2.62593 [x2] [x3] + 12.2386 [x3]^2 + 3.28291 [x4] + 3.06258 [x1] [x4] - 0.227766 [x2] [x4] + 2.97087 [x3] [x4] - 1.10392 [x4]^2) / (1.43031 + 4.61876 [x1] + 0.00862041 [x1]^2 + 0.798422 [x2] - 4.05178 [x1] [x2] - 3.24333 [x2]^2 - 12.0464 [x3] - 2.17372 [x1] [x3] + 24.5034 [x2] [x3] + 6.37539 [x3]^2 - 3.13246 [x4] + 1.90158 [x1] [x4] + 6.83817 [x2] [x4] - 10.8392 [x3] [x4] + 6.16376 [x4]^2)$
CS6-O-TON	$2.88997 - 0.895935 [x1] - 0.203344 [x1]^2 + 0.0437755 [x1]^3 + 1.60703 [x2] - 1.00073 [x1] [x2] + 1.04422 [x1]^2 [x2] - 48.0132 [x2]^2 + 8.21629 [x1] [x2]^2 - 44.6298 [x2]^3 + 0.748038 [x3] - 0.163726 [x1] [x3] + 0.0678032 [x1]^2 [x3] + 7.54783 [x2] [x3] - 1.84589 [x1] [x2] [x3] + 25.5231 [x2]^2 [x3] - 0.734529 [x3]^2 + 0.0104098 [x1] [x3]^2 - 2.88398 [x2] [x3]^2 + 0.191167 [x3]^3$

	$+ 7.27838 [x4] - 4.22226 [x1] [x4] + 0.0688295 [x1]^2 [x4] + 38.5532 [x2] [x4] - 14.7777 [x1] [x2] [x4] + 190.703 [x2]^2 [x4] + 8.45577 [x3] [x4] - 0.304727 [x1] [x3] [x4] - 53.0528 [x2] [x3] [x4] + 1.53305 [x3]^2 [x4] + 28.6278 [x4]^2 + 13.7642 [x1] [x4]^2 - 83.7919 [x2] [x4]^2 - 3.4411 [x3] [x4]^2 - 118.788 [x4]^3$
CS6-O-FOTN	$3.51756 + 0.825705 \text{Cos}[x1] - 49.2935 \text{Cos}[x2] + 0.120483 \text{Cos}[x3] + 48.2858 \text{Cos}[x4] + 0.525366 \text{Sin}[x1] - 12.8594 \text{Sin}[x2] - 0.0907293 \text{Sin}[x3] + 15.2808 \text{Sin}[x4]$
CS6-O-FOTNR	$(222.997 + 5.5982 \text{Cos}[x1] - 120.556 \text{Cos}[x2] - 8.67136 \text{Cos}[x3] + 74.1852 \text{Cos}[x4] - 5.14218 \text{Sin}[x1] + 493.767 \text{Sin}[x2] - 242.027 \text{Sin}[x3] - 122.195 \text{Sin}[x4]) / (-154.925 + 5.54337 \text{Cos}[x1] + 353.011 \text{Cos}[x2] - 5.12501 \text{Cos}[x3] - 103.314 \text{Cos}[x4] - 9.12216 \text{Sin}[x1] + 317.801 \text{Sin}[x2] - 115.988 \text{Sin}[x3] - 147.714 \text{Sin}[x4])$
CS6-O-SOTN	$0.176082 + 0.0514894 \text{Cos}[x1] + 0.229238 \text{Cos}[x1]^2 + 0.149695 \text{Cos}[x2] + 0.21369 \text{Cos}[x1] \text{Cos}[x2] + 0.133418 \text{Cos}[x2]^2 - 0.453523 \text{Cos}[x3] + 0.347676 \text{Cos}[x1] \text{Cos}[x3] - 0.591507 \text{Cos}[x2] \text{Cos}[x3] + 0.315949 \text{Cos}[x3]^2 + 0.179092 \text{Cos}[x4] + 0.0588002 \text{Cos}[x1] \text{Cos}[x4] + 0.146787 \text{Cos}[x2] \text{Cos}[x4] - 0.484302 \text{Cos}[x3] \text{Cos}[x4] + 0.181228 \text{Cos}[x4]^2 + 0.398747 \text{Sin}[x1] + 1.85692 \text{Cos}[x1] \text{Sin}[x1] + 0.41894 \text{Cos}[x2] \text{Sin}[x1] - 0.352291 \text{Cos}[x3] \text{Sin}[x1] + 0.417607 \text{Cos}[x4] \text{Sin}[x1] + 0.299911 \text{Sin}[x1]^2 - 2.28472 \text{Sin}[x2] - 4.81942 \text{Cos}[x1] \text{Sin}[x2] - 3.23076 \text{Cos}[x2] \text{Sin}[x2] + 6.59279 \text{Cos}[x3] \text{Sin}[x2] - 1.9446 \text{Cos}[x4] \text{Sin}[x2] - 2.44162 \text{Sin}[x1] \text{Sin}[x2] + 17.3393 \text{Sin}[x2]^2 - 0.07451 \text{Sin}[x3] + 0.644516 \text{Cos}[x1] \text{Sin}[x3] - 0.214531 \text{Cos}[x2] \text{Sin}[x3] + 0.453743 \text{Cos}[x3] \text{Sin}[x3] - 0.0813581 \text{Cos}[x4] \text{Sin}[x3] + 0.986536 \text{Sin}[x1] \text{Sin}[x3] + 2.98252 \text{Sin}[x2] \text{Sin}[x3] + 0.226598 \text{Sin}[x3]^2 + 2.60629 \text{Sin}[x4] - 2.54052 \text{Cos}[x1] \text{Sin}[x4] + 3.02723 \text{Cos}[x2] \text{Sin}[x4] + 0.862086 \text{Cos}[x3] \text{Sin}[x4] + 2.81305 \text{Cos}[x4] \text{Sin}[x4] + 2.78504 \text{Sin}[x1] \text{Sin}[x4] - 38.2714 \text{Sin}[x2] \text{Sin}[x4] + 2.42438 \text{Sin}[x3] \text{Sin}[x4] + 4.01779 \text{Sin}[x4]^2$
CS6-O-SOTNR	$(5.59916 - 2.85727 \text{Cos}[x1] + 8.47811 \text{Cos}[x1]^2 + 4.69487 \text{Cos}[x2] - 1.29782 \text{Cos}[x1] \text{Cos}[x2] + 3.92256 \text{Cos}[x2]^2 + 0.133742 \text{Cos}[x3] - 0.770413 \text{Cos}[x1] \text{Cos}[x3] - 3.92577 \text{Cos}[x2] \text{Cos}[x3] + 3.52842 \text{Cos}[x3]^2 + 4.62631 \text{Cos}[x4] - 1.94913 \text{Cos}[x1] \text{Cos}[x4] + 3.69079 \text{Cos}[x2] \text{Cos}[x4] - 0.683182 \text{Cos}[x3] \text{Cos}[x4] + 3.67659 \text{Cos}[x4]^2 + 5.82862 \text{Sin}[x1] + 0.431351 \text{Cos}[x1] \text{Sin}[x1] + 6.48594 \text{Cos}[x2] \text{Sin}[x1] - 0.735967 \text{Cos}[x3] \text{Sin}[x1] + 5.98474 \text{Cos}[x4] \text{Sin}[x1] - 1.87895 \text{Sin}[x1]^2 + 3.10006 \text{Sin}[x2] - 3.81947 \text{Cos}[x1] \text{Sin}[x2] + 2.57668 \text{Cos}[x2] \text{Sin}[x2] + 18.2146 \text{Cos}[x3] \text{Sin}[x2] + 3.16194 \text{Cos}[x4] \text{Sin}[x2] - 1.6713 \text{Sin}[x1] \text{Sin}[x2] + 2.67661 \text{Sin}[x2]^2 + 1.65003 \text{Sin}[x3] + 2.4261 \text{Cos}[x1] \text{Sin}[x3] + 0.173826 \text{Cos}[x2] \text{Sin}[x3] - 0.0164027 \text{Cos}[x3] \text{Sin}[x3] + 0.780663 \text{Cos}[x4] \text{Sin}[x3] + 6.03817 \text{Sin}[x1] \text{Sin}[x3] + 5.07324 \text{Sin}[x2] \text{Sin}[x3] + 3.07075 \text{Sin}[x3]^2 + 8.03881 \text{Sin}[x4] - 5.48412 \text{Cos}[x1] \text{Sin}[x4] + 8.02115 \text{Cos}[x2] \text{Sin}[x4] + 5.23382 \text{Cos}[x3] \text{Sin}[x4] + 8.82206 \text{Cos}[x4] \text{Sin}[x4] + 1.13805 \text{Sin}[x1] \text{Sin}[x4] + 1.45636 \text{Sin}[x2] \text{Sin}[x4] + 7.04505 \text{Sin}[x3] \text{Sin}[x4] + 2.92257 \text{Sin}[x4]^2) / (8.02142 - 3.23979 \text{Cos}[x1] - 3.22289 \text{Cos}[x1]^2 + 0.853633 \text{Cos}[x2] - 5.16315 \text{Cos}[x1] \text{Cos}[x2] + 0.734179 \text{Cos}[x2]^2 + 0.287937 \text{Cos}[x3] + 5.73139 \text{Cos}[x1] \text{Cos}[x3] + 10.1475 \text{Cos}[x2] \text{Cos}[x3] + 4.78421 \text{Cos}[x3]^2 + 2.76107 \text{Cos}[x4] - 4.9509 \text{Cos}[x1] \text{Cos}[x4] + 2.93288 \text{Cos}[x2] \text{Cos}[x4] + 1.74357 \text{Cos}[x3] \text{Cos}[x4] + 4.66772 \text{Cos}[x4]^2 - 0.152487 \text{Sin}[x1] - 9.22323 \text{Cos}[x1] \text{Sin}[x1] - 3.72476 \text{Cos}[x2] \text{Sin}[x1] + 1.45625 \text{Cos}[x3] \text{Sin}[x1] - 0.530268 \text{Cos}[x4] \text{Sin}[x1] + 5.02503 \text{Sin}[x1]^2 + 5.21235 \text{Sin}[x2] + 4.26717 \text{Cos}[x1] \text{Sin}[x2] + 5.67068 \text{Cos}[x2] \text{Sin}[x2] - 4.1.1748 \text{Cos}[x3] \text{Sin}[x2] + 4.84278 \text{Cos}[x4] \text{Sin}[x2] + 16.89 \text{Sin}[x1] \text{Sin}[x2] + 1.06796 \text{Sin}[x2]^2 + 1.53499 \text{Sin}[x3] - 7.65639 \text{Cos}[x1] \text{Sin}[x3] + 3.29447 \text{Cos}[x2] \text{Sin}[x3] + 3.67344 \text{Cos}[x3] \text{Sin}[x3] + 3.33921 \text{Cos}[x4] \text{Sin}[x3] - 4.85271 \text{Sin}[x1] \text{Sin}[x3] - 1.96561 \text{Sin}[x2] \text{Sin}[x3] - 2.98207 \text{Sin}[x3]^2 - 12.085 \text{Sin}[x4] + 12.0315 \text{Cos}[x1] \text{Sin}[x4] - 12.4901 \text{Cos}[x2] \text{Sin}[x4] - 6.78271 \text{Cos}[x3] \text{Sin}[x4] - 11.6233 \text{Cos}[x4] \text{Sin}[x4] + 1.69573 \text{Sin}[x1] \text{Sin}[x4] + 2.07072 \text{Sin}[x2] \text{Sin}[x4] - 11.0358 \text{Sin}[x3] \text{Sin}[x4] - 2.86558 \text{Sin}[x4]^2)$
CS6-O-FOLN	$5.59397 - 1.81246 \text{Log}[x1] - 0.230811 \text{Log}[x2] - 0.0991312 \text{Log}[x3] + 1.0505 \text{Log}[x4]$
CS6-O-FOLNR	$(2.6275 - 0.0224973 \text{Log}[x1] + 2.18575 \text{Log}[x2] + 1.24909 \text{Log}[x3] - 0.0385969 \text{Log}[x4]) / (1.3596 - 0.0395996 \text{Log}[x1] + 1.065 \text{Log}[x2] + 0.607601 \text{Log}[x3] + 0.0075985 \text{Log}[x4])$
CS6-O-SOLN	$4.05695 - 5.25 \text{Log}[x1] + 2.78293 \text{Log}[x1]^2 - 3.33985 \text{Log}[x2] + 3.0976 \text{Log}[x1] \text{Log}[x2] + 0.951662 \text{Log}[x2]^2 - 3.07582 \text{Log}[x3] - 0.688445 \text{Log}[x1] \text{Log}[x3] - 1.95477 \text{Log}[x2] \text{Log}[x3] - 0.00596054 \text{Log}[x3]^2 - 0.48802 \text{Log}[x4] - 1.76772 \text{Log}[x1] \text{Log}[x4] - 2.19534 \text{Log}[x2] \text{Log}[x4] - 0.426249 \text{Log}[x3] \text{Log}[x4] - 0.0283658 \text{Log}[x4]^2$
CS6-O-SOLNR	$(0.876953 + 0.515023 \text{Log}[x1] + 0.502096 \text{Log}[x1]^2 + 0.767089 \text{Log}[x2] + 1.93999 \text{Log}[x1] \text{Log}[x2] + 1.89879 \text{Log}[x2]^2 + 0.326182 \text{Log}[x3] + 0.759354 \text{Log}[x1] \text{Log}[x3] + 1.00894 \text{Log}[x2] \text{Log}[x3] + 1.7903 \text{Log}[x3]^2 + 0.160736 \text{Log}[x4] + 1.80025 \text{Log}[x1] \text{Log}[x4] + 0.9205 \text{Log}[x2] \text{Log}[x4] + 1.55392 \text{Log}[x3] \text{Log}[x4] + 0.864499 \text{Log}[x4]^2) / (1.51101 + 1.3603 \text{Log}[x1] - 1.00906 \text{Log}[x1]^2 + 0.942904 \text{Log}[x2] - 0.420822 \text{Log}[x1] \text{Log}[x2] + 0.323479 \text{Log}[x2]^2 + 2.08135 \text{Log}[x3] + 0.341663 \text{Log}[x1] \text{Log}[x3] + 1.48955 \text{Log}[x2] \text{Log}[x3] + 0.90751 \text{Log}[x3]^2 + 3.1366 \text{Log}[x4] + 0.523403 \text{Log}[x1] \text{Log}[x4] + 1.12312 \text{Log}[x2] \text{Log}[x4] + 1.03579 \text{Log}[x3] \text{Log}[x4] + 1.11833 \text{Log}[x4]^2)$
NOTATION	CS7-O1
CS7-O1-L	$0.376918 - 0.0000284699 [x1] + 0.0899108 [x2] + 1.52794 [x3] - 0.183538 [x4]$
CS7-O1-LN	$(-5120.24 + 57.6129 [x1] + 121050. [x2] + 15154.4 [x3] + 2380.12 [x4]) / (564.199 + 1.13363 [x1] - 534.76 [x2] - 653.847 [x3] + 240.326 [x4])$
CS7-O1-SON	$0.591623 - 0.000245477 [x1] + 0.0000130693 [x1]^2 - 0.624861 [x2] + 0.000986062 [x1] [x2] + 0.247123 [x2]^2 + 3.91429 [x3] - 0.0202152 [x1] [x3] + 1.66667 [x2] [x3] - 6.50313 [x3]^2 - 0.684944 [x4] - 0.00216004 [x1] [x4] + 0.265869 [x2] [x4] + 1.875 [x3] [x4] + 0.280931 [x4]^2$
CS7-O1-SONR	$(5.72803*10^7 + 3.47232*10^9 [x1] + 1.94466*10^9 [x1]^2 + 2.07448*10^7 [x2] + 2.32538*10^9 [x1] [x2] + 5.95239*10^6 [x2]^2 + 1.69434*10^7 [x3] + 1.95292*10^9 [x1] [x3] + 4.44012*10^6 [x2] [x3] + 2.95826*10^6 [x3]^2 - 7.744*10^7 [x4] - 2.17366*10^10 [x1] [x4] - 3.03341*10^6 [x2] [x4] + 4.78648*10^6 [x3] [x4] - 2.43818*10^8 [x4]^2) / (-1.98127*10^7 - 1.1842*10^9 [x1] + 5.23134*10^9 [x1]^2 - 7.17336*10^6 [x2] - 8.00317*10^8 [x1] [x2] - 2.05906*10^6 [x2]^2 - 5.86915*10^6 [x3] - 6.74436*10^8 [x1] [x3] - 1.5373*10^6 [x2] [x3] - 1.02509*10^6 [x3]^2 + 2.66479*10^7 [x4] + 7.50797*10^9 [x1] [x4] + 1.02415*10^6 [x2] [x4] - 1.68151*10^6 [x3] [x4] + 8.40408*10^7 [x4]^2)$
CS7-O1-TON	$0.365638 - 0.000217673 [x1] + 5.65001*10^-7 [x1]^2 + 5.1423*10^-8 [x1]^3 - 0.240295 [x2] + 0.00988436 [x1] [x2] - 0.0000360403 [x1]^2 [x2] + 1.91598 [x2]^2 - 0.056559 [x1] [x2]^2 + 36.535 [x2]^3 + 3.5215 [x2]^4 - 0.0338682 [x1] [x3] - 0.0000158736 [x1]^2 [x3] + 20.9403 [x2] [x3] + 0.0376238 [x1] [x2] [x3] - 103.88 [x2]^2 [x3] + 4.81175 [x3]^2 + 0.070922 [x1] [x3]^2 + 128.658 [x2] [x3]^2 - 289.526 [x3]^3 - 0.152246 [x4] + 0.0024161 [x1] [x4] - 8.56533*10^6 [x1]^2 [x4] - 4.0295 [x2] [x4] + 0.013994 [x1] [x2] [x4] - 2.20918 [x2]^2 [x4] - 0.525514 [x3] [x4] - 0.00221421 [x1] [x3] [x4] - 10.7284 [x2] [x3] [x4] + 42.187 [x3]^2 [x4] - 0.0852983 [x4]^2 - 0.00159797 [x1] [x4]^2 + 1.56595 [x2] [x4]^2 - 1.80498 [x3] [x4]^2 - 0.154501 [x4]^3$
CS7-O1-FOTN	$-8.87775 - 0.114486 \text{Cos}[x1] - 0.817506 \text{Cos}[x2] + 10.3724 \text{Cos}[x3] - 0.017746 \text{Cos}[x4] + 0.0325899 \text{Sin}[x1] - 0.0468017 \text{Sin}[x2] + 2.68554 \text{Sin}[x3] - 0.519744 \text{Sin}[x4]$
CS7-O1-FOTNR	$(-915.704 + 11.6921 \text{Cos}[x1] + 203.412 \text{Cos}[x2] + 734.211 \text{Cos}[x3] + 5.31635 \text{Cos}[x4] - 2.78431 \text{Sin}[x1] + 51.3661 \text{Sin}[x2] + 30.8749 \text{Sin}[x3] - 36.634 \text{Sin}[x4]) / (232.46 + 40.0029 \text{Cos}[x1] + 746.851 \text{Cos}[x2] - 966.308 \text{Cos}[x3] + 31.9794 \text{Cos}[x4] - 9.50266 \text{Sin}[x1] + 177.35 \text{Sin}[x2] - 327.124 \text{Sin}[x3] - 36.1954 \text{Sin}[x4])$
CS7-O1-SOTN	$\text{Abs}[-0.428198 - 0.789724 \text{Cos}[x1] + 0.419809 \text{Cos}[x1]^2 - 1.14756 \text{Cos}[x2] - 4.20092 \text{Cos}[x1] \text{Cos}[x2] + 0.973106 \text{Cos}[x2]^2 + 0.0618098 \text{Cos}[x3] + 2.21932 \text{Cos}[x1] \text{Cos}[x3] + 2.36543 \text{Cos}[x2] \text{Cos}[x3] + 1.51433 \text{Cos}[x3]^2 - 4.12479 \text{Cos}[x4] + 0.444785 \text{Cos}[x1] \text{Cos}[x4] + 9.40322 \text{Cos}[x2] \text{Cos}[x4] - 4.77729 \text{Cos}[x3] \text{Cos}[x4] - 1.13648 \text{Cos}[x4]^2 - 1.67836 \text{Sin}[x1] - 1.36064 \text{Cos}[x1] \text{Sin}[x1] + 7.30472 \text{Cos}[x2] \text{Sin}[x1] - 4.48619 \text{Cos}[x3] \text{Sin}[x1] + 0.0744336 \text{Cos}[x4] \text{Sin}[x1] - 0.596695 \text{Sin}[x1]^2 - 1.1232 \text{Sin}[x2] - 1.25851 \text{Cos}[x1] \text{Sin}[x2] + 0.453946 \text{Cos}[x2] \text{Sin}[x2] + 0.0018139 \text{Cos}[x3] \text{Sin}[x2] + 3.0389 \text{Cos}[x4] \text{Sin}[x2] + 1.46066 \text{Sin}[x1] \text{Sin}[x2] - 1.18069 \text{Sin}[x2]^2 - 4.25857 \text{Sin}[x3] + 3.10668 \text{Cos}[x1] \text{Sin}[x3] - 4.48172 \text{Cos}[x2] \text{Sin}[x3] - 3.1809 \text{Cos}[x3] \text{Sin}[x3] + 4.6226 \text{Cos}[x4] \text{Sin}[x3] - 2.62635 \text{Sin}[x1] \text{Sin}[x3] - 2.70701 \text{Sin}[x2] \text{Sin}[x3] - 1.97363 \text{Sin}[x3]^2 - 1.21038 \text{Sin}[x4] + 0.295984 \text{Cos}[x1] \text{Sin}[x4] - 1.8804 \text{Cos}[x2] \text{Sin}[x4] + 1.26921 \text{Cos}[x3] \text{Sin}[x4] - 1.45892 \text{Cos}[x4] \text{Sin}[x4] - 0.0163039 \text{Sin}[x1] \text{Sin}[x4] + 1.62642 \text{Sin}[x2] \text{Sin}[x4] + 8.03857 \text{Sin}[x3] \text{Sin}[x4] + 0.431409 \text{Sin}[x4]^2)$
CS7-O1-SOTNR	$(-21.0006 - 13.3024 \text{Cos}[x1] - 8.78266 \text{Cos}[x1]^2 - 11.2099 \text{Cos}[x2] - 2.70142 \text{Cos}[x1] \text{Cos}[x2] - 2.53452 \text{Cos}[x2]^2 + 3.37456 \text{Cos}[x3] + 11.782 \text{Cos}[x1] \text{Cos}[x3] + 12.5127 \text{Cos}[x2] \text{Cos}[x3] + 26.8073 \text{Cos}[x3]^2 + 11.2785 \text{Cos}[x4] - 7.4413 \text{Cos}[x1] \text{Cos}[x4] - 28.533 \text{Cos}[x2] \text{Cos}[x4] + 23.3259 \text{Cos}[x3] \text{Cos}[x4] - 9.81214 \text{Cos}[x4]^2 + 4.01335 \text{Sin}[x1] + 0.398258 \text{Cos}[x1] \text{Sin}[x1] + 3.32662 \text{Cos}[x2] \text{Sin}[x1] - 3.50251 \text{Cos}[x3] \text{Sin}[x1] - 14.9324 \text{Cos}[x4] \text{Sin}[x1] - 11.2179 \text{Sin}[x1]^2 - 5.78824 \text{Sin}[x2] - 11.8168 \text{Cos}[x1] \text{Sin}[x2] - 0.41009 \text{Cos}[x2] \text{Sin}[x2] - 1.48041 \text{Cos}[x3] \text{Sin}[x2] - 21.5182 \text{Cos}[x4] \text{Sin}[x2] - 7.53805 \text{Sin}[x1] \text{Sin}[x2] - 17.4661 \text{Sin}[x2]^2 + 20.5088 \text{Sin}[x3] + 9.72364 \text{Cos}[x1] \text{Sin}[x3] + 21.6136 \text{Cos}[x2] \text{Sin}[x3] + 28.8247 \text{Cos}[x3] \text{Sin}[x3] + 18.5487 \text{Cos}[x4] \text{Sin}[x3] + 19.531 \text{Sin}[x1] \text{Sin}[x3] + 9.06954 \text{Sin}[x2] \text{Sin}[x3] - 46.8079 \text{Sin}[x3]^2 - 13.5937 \text{Sin}[x4] - 5.98883 \text{Cos}[x1] \text{Sin}[x4] + 22.0764 \text{Cos}[x2] \text{Sin}[x4] + 8.96384 \text{Cos}[x3] \text{Sin}[x4] + 19.399 \text{Cos}[x4] \text{Sin}[x4] - 6.84935 \text{Sin}[x1] \text{Sin}[x4] + 17.3045 \text{Sin}[x2] \text{Sin}[x4] - 4.02606 \text{Sin}[x3] \text{Sin}[x4] - 10.1884 \text{Sin}[x4]^2) / (-7.08261 - 7.16899 \text{Cos}[x1] - 6.73974 \text{Cos}[x1]^2 + 5.36201 \text{Cos}[x2] + 4.59392 \text{Cos}[x1] \text{Cos}[x2] + 16.4533 \text{Cos}[x2]^2 - 18.5307 \text{Cos}[x3] - 18.8114 \text{Cos}[x1] \text{Cos}[x3] - 5.87064 \text{Cos}[x2] \text{Cos}[x3] - 29.6103 \text{Cos}[x3]^2 + 7.96765 \text{Cos}[x4] + 11.3419 \text{Cos}[x1] \text{Cos}[x4] + 32.3905 \text{Cos}[x2] \text{Cos}[x4] + 2.10279 \text{Cos}[x3] \text{Cos}[x4] - 30.7114 \text{Cos}[x4]^2 - 5.25934 \text{Sin}[x1] - 3.12295 \text{Cos}[x1] \text{Sin}[x1] - 8.31908 \text{Cos}[x2] \text{Sin}[x1] - 1.9957 \text{Cos}[x3] \text{Sin}[x1] + 4.92172 \text{Cos}[x4] \text{Sin}[x1] + 0.657128 \text{Sin}[x1]^2 - 10.82 \text{Sin}[x2] - 7.74348 \text{Cos}[x1] \text{Sin}[x2] - 4.20835 \text{Cos}[x2] \text{Sin}[x2] - 12.9398 \text{Cos}[x3] \text{Sin}[x2] - 4.12261 \text{Cos}[x4] \text{Sin}[x2] + 5.03403 \text{Sin}[x1] \text{Sin}[x2] - 22.5359 \text{Sin}[x2]^2 + 19.6468 \text{Sin}[x3] + 23.0379 \text{Cos}[x1] \text{Sin}[x3] + 20.2574 \text{Cos}[x2] \text{Sin}[x3] + 16.238 \text{Cos}[x3] \text{Sin}[x3] + 8.04066 \text{Cos}[x4] \text{Sin}[x3] - 11.321 \text{Sin}[x1] \text{Sin}[x3] + 2.718 \text{Sin}[x2] \text{Sin}[x3] + 23.5277 \text{Sin}[x3]^2 + 13.7215 \text{Sin}[x4] + 14.3627 \text{Cos}[x1] \text{Sin}[x4] + 12.1859 \text{Cos}[x2] \text{Sin}[x4] + 3.37101 \text{Cos}[x3] \text{Sin}[x4] + 28.7 \text{Cos}[x4] \text{Sin}[x4] - 3.27066 \text{Sin}[x1] \text{Sin}[x4] - 5.39626 \text{Sin}[x2] \text{Sin}[x4] + 26.6586 \text{Sin}[x3] \text{Sin}[x4] + 24.6288 \text{Sin}[x4]^2)$
CS7-O1-FOLN	$0.892318 - 0.0216239 \text{Log}[x1] + 0.0181013 \text{Log}[x2] + 0.170684 \text{Log}[x3] - 0.209127 \text{Log}[x4]$

CS7-O1-FOLNR	$(63722.2 - 7301.54 \text{ Log}[x1] - 414.569 \text{ Log}[x2] + 9331.36 \text{ Log}[x3] + 3212.03 \text{ Log}[x4]) / (157598. - 19647.2 \text{ Log}[x1] - 1861.37 \text{ Log}[x2] + 19227.4 \text{ Log}[x3] + 18398.6 \text{ Log}[x4])$
CS7-O1-SOLN	$15.3302 - 4.78979 \text{ Log}[x1] + 0.38863 \text{ Log}[x1]^2 + 0.0929459 \text{ Log}[x2] + 0.0206937 \text{ Log}[x1] \text{ Log}[x2] + 0.0142898 \text{ Log}[x2]^2 + 2.28649 \text{ Log}[x3] - 0.390855 \text{ Log}[x1] \text{ Log}[x3] + 0.0592874 \text{ Log}[x2] \text{ Log}[x3] + 0.00940776 \text{ Log}[x3]^2 + 2.20848 \text{ Log}[x4] - 0.380807 \text{ Log}[x1] \text{ Log}[x4] + 0.0360404 \text{ Log}[x2] \text{ Log}[x4] + 0.188339 \text{ Log}[x3] \text{ Log}[x4] + 0.289678 \text{ Log}[x4]^2$
CS7-O1-SOLNR	$(7.16416 - 4.60073 \text{ Log}[x1] + 0.925216 \text{ Log}[x1]^2 + 0.311962 \text{ Log}[x2] + 0.818827 \text{ Log}[x1] \text{ Log}[x2] + 2.11508 \text{ Log}[x2]^2 - 3.949 \text{ Log}[x3] + 1.36591 \text{ Log}[x1] \text{ Log}[x3] - 0.985498 \text{ Log}[x2] \text{ Log}[x3] + 0.932753 \text{ Log}[x3]^2 + 4.0493 \text{ Log}[x4] - 1.98205 \text{ Log}[x1] \text{ Log}[x4] + 2.22104 \text{ Log}[x2] \text{ Log}[x4] - 3.26118 \text{ Log}[x3] \text{ Log}[x4] + 2.86624 \text{ Log}[x4]^2) / (-1.7651 + 3.30072 \text{ Log}[x1] + 0.910701 \text{ Log}[x1]^2 + 3.27111 \text{ Log}[x2] + 1.69126 \text{ Log}[x1] \text{ Log}[x2] + 6.07158 \text{ Log}[x2]^2 + 4.36868 \text{ Log}[x3] + 4.03968 \text{ Log}[x1] \text{ Log}[x3] - 3.30177 \text{ Log}[x2] \text{ Log}[x3] + 6.68117 \text{ Log}[x3]^2 - 1.21383 \text{ Log}[x4] - 2.75161 \text{ Log}[x1] \text{ Log}[x4] + 5.33047 \text{ Log}[x2] \text{ Log}[x4] - 8.35853 \text{ Log}[x3] \text{ Log}[x4] + 4.41779 \text{ Log}[x4]^2)$
NOTATION	CS7-O2
CS7-O2-L	$6.85614 + 0.0180162 [x1] + 164.894 [x2] + 56.0767 [x3] - 8.17055 [x4]$
CS7-O2-LN	$(-5120.24 + 57.6129 [x1] + 121050. [x2] + 15154.4 [x3] + 2380.12 [x4]) / (564.199 + 1.13363 [x1] - 534.76 [x2] - 653.847 [x3] + 240.326 [x4])$
CS7-O2-SON	$126.294 - 0.475251 [x1] + 0.000793595 [x1]^2 + 277.171 [x2] - 0.311186 [x1] [x2] + 117.332 [x2]^2 - 1475.07 [x3] + 3.12035 [x1] [x3] + 345.833 [x2] [x3] + 1709.16 [x3]^2 - 12.0307 [x4] - 0.074154 [x1] [x4] - 124.796 [x2] [x4] + 443.958 [x3] [x4] - 3.32805 [x4]^2$
CS7-O2-SONR	$(800042. + 6.24114*10^7 [x1] + 9.99557*10^8 [x1]^2 + 762527. [x2] + 1.09376*10^8 [x1] [x2] + 276661. [x2]^2 + 97075.6 [x3] + 9.34216*10^6 [x1] [x3] + 86055.5 [x2] [x3] + 12047.9 [x3]^2 + 479630. [x4] - 9.32005*10^6 [x1] [x4] + 784235. [x2] [x4] + 71449.9 [x3] [x4] - 18890.4 [x4]^2) / (-2.6796*10^7 - 1.98627*10^9 [x1] + 3.77268*10^7 [x1]^2 - 2.81261*10^7 [x2] - 4.08432*10^9 [x1] [x2] - 1.02935*10^7 [x2]^2 - 3.28879*10^6 [x3] - 3.1216*10^8 [x1] [x3] - 3.17561*10^6 [x2] [x3] - 412969. [x3]^2 - 1.41276*10^7 [x4] + 7.98758*10^8 [x1] [x4] - 2.87229*10^7 [x2] [x4] - 2.26756*10^6 [x3] [x4] + 5.3321*10^6 [x4]^2)$
CS7-O2-TON	$50.9898 - 0.0881894 [x1] - 0.000556629 [x1]^2 + 2.5417*10^-6 [x1]^3 + 222.171 [x2] + 4.92697 [x1] [x2] - 0.00729742 [x1]^2 [x2] + 561.297 [x2]^2 - 16.8931 [x1] [x2]^2 + 581.459 [x2]^3 - 86.0516 [x3] - 7.77996 [x1] [x3] + 0.00405426 [x1]^2 [x3] - 1666.63 [x2] [x3] + 0.264718 [x1] [x2] [x3] + 10995.2 [x2]^2 [x3] - 3035.31 [x3]^2 + 30.9947 [x1] [x3]^2 + 6356.49 [x2] [x3]^2 - 28501. [x3]^3 - 20.4969 [x4] + 0.17538 [x1] [x4] + 0.000675846 [x1]^2 [x4] - 610.044 [x2] [x4] + 2.87181 [x1] [x2] [x4] + 713.29 [x2]^2 [x4] + 791.616 [x3] [x4] + 0.96809 [x1] [x3] [x4] - 3193.52 [x2] [x3] [x4] + 7809.43 [x3]^2 [x4] + 0.11329 [x4]^2 - 0.477248 [x1] [x4]^2 - 1.00928 [x2] [x4]^2 - 668.009 [x3] [x4]^2 + 42.9845 [x4]^3$
CS7-O2-FOTN	$4549.36 - 11.9657 \text{ Cos}[x1] - 422.715 \text{ Cos}[x2] - 4093.54 \text{ Cos}[x3] + 11.8685 \text{ Cos}[x4] + 0.0700483 \text{ Sin}[x1] + 84.6656 \text{ Sin}[x2] - 406.382 \text{ Sin}[x3] + 5.95449 \text{ Sin}[x4]$
CS7-O2-FOTNR	$(719.601 - 0.230675 \text{ Cos}[x1] - 296.47 \text{ Cos}[x2] - 414.176 \text{ Cos}[x3] + 0.496492 \text{ Cos}[x4] - 0.305701 \text{ Sin}[x1] - 68.3702 \text{ Sin}[x2] - 49.7893 \text{ Sin}[x3] + 1.65748 \text{ Sin}[x4]) / (19.9595 - 0.00602815 \text{ Cos}[x1] - 10.8388 \text{ Cos}[x2] - 8.78003 \text{ Cos}[x3] + 0.00734544 \text{ Cos}[x4] - 0.00702344 \text{ Sin}[x1] - 2.62222 \text{ Sin}[x2] - 1.08536 \text{ Sin}[x3] + 0.0309919 \text{ Sin}[x4])$
CS7-O2-SOTN	$1.02001 + 26.9023 \text{ Cos}[x1] + 38.1478 \text{ Cos}[x1]^2 + 0.483021 \text{ Cos}[x2] + 204.017 \text{ Cos}[x1] \text{ Cos}[x2] + 0.0382832 \text{ Cos}[x2]^2 + 0.800524 \text{ Cos}[x3] + 12.9007 \text{ Cos}[x1] \text{ Cos}[x3] + 0.542383 \text{ Cos}[x2] \text{ Cos}[x3] + 0.601487 \text{ Cos}[x3]^2 - 240.817 \text{ Cos}[x4] - 171.952 \text{ Cos}[x1] \text{ Cos}[x4] + 1163.26 \text{ Cos}[x2] \text{ Cos}[x4] - 370.642 \text{ Cos}[x3] \text{ Cos}[x4] - 229.771 \text{ Cos}[x4]^2 + 539.522 \text{ Sin}[x1] + 762.825 \text{ Cos}[x1] \text{ Sin}[x1] - 2348.04 \text{ Cos}[x2] \text{ Sin}[x1] + 805.999 \text{ Cos}[x3] \text{ Sin}[x1] + 279.869 \text{ Cos}[x4] \text{ Sin}[x1] - 197.059 \text{ Sin}[x1]^2 - 100.421 \text{ Sin}[x2] + 578.817 \text{ Cos}[x1] \text{ Sin}[x2] - 120.519 \text{ Cos}[x2] \text{ Sin}[x2] - 107.957 \text{ Cos}[x3] \text{ Sin}[x2] + 246.058 \text{ Cos}[x4] \text{ Sin}[x2] - 327.639 \text{ Sin}[x1] \text{ Sin}[x2] + 441.009 \text{ Sin}[x2]^2 - 517.712 \text{ Sin}[x3] - 1524.23 \text{ Cos}[x1] \text{ Sin}[x3] - 731.981 \text{ Cos}[x2] \text{ Sin}[x3] - 540.462 \text{ Cos}[x3] \text{ Sin}[x3] + 517.42 \text{ Cos}[x4] \text{ Sin}[x3] - 477.931 \text{ Sin}[x1] \text{ Sin}[x3] + 195.343 \text{ Sin}[x2] \text{ Sin}[x3] + 2363.08 \text{ Sin}[x3]^2 + 11.9178 \text{ Sin}[x4] - 36.049 \text{ Cos}[x1] \text{ Sin}[x4] - 215.965 \text{ Cos}[x2] \text{ Sin}[x4] + 27.0229 \text{ Cos}[x3] \text{ Sin}[x4] - 348.311 \text{ Cos}[x4] \text{ Sin}[x4] + 456.316 \text{ Sin}[x1] \text{ Sin}[x4] - 296.579 \text{ Sin}[x2] \text{ Sin}[x4] + 2705.49 \text{ Sin}[x3] \text{ Sin}[x4] + 25.9728 \text{ Sin}[x4]^2$
CS7-O2-SOTNR	$(15.5646 - 0.578215 \text{ Cos}[x1] - 11.0622 \text{ Cos}[x1]^2 + 15.6218 \text{ Cos}[x2] - 0.68586 \text{ Cos}[x1] \text{ Cos}[x2] + 15.6331 \text{ Cos}[x2]^2 + 14.5114 \text{ Cos}[x3] - 1.59223 \text{ Cos}[x1] \text{ Cos}[x3] + 14.5331 \text{ Cos}[x2] \text{ Cos}[x3] + 13.4591 \text{ Cos}[x3]^2 - 36.4241 \text{ Cos}[x4] - 42.3399 \text{ Cos}[x1] \text{ Cos}[x4] - 35.0283 \text{ Cos}[x2] \text{ Cos}[x4] - 36.7201 \text{ Cos}[x3] \text{ Cos}[x4] - 22.0794 \text{ Cos}[x4]^2 + 27.4901 \text{ Sin}[x1] + 28.6445 \text{ Cos}[x1] \text{ Sin}[x1] + 28.8686 \text{ Cos}[x2] \text{ Sin}[x1] + 27.953 \text{ Cos}[x3] \text{ Sin}[x1] + 18.7672 \text{ Cos}[x4] \text{ Sin}[x1] + 27.6268 \text{ Sin}[x1]^2 + 4.52872 \text{ Sin}[x2] + 6.67319 \text{ Cos}[x1] \text{ Sin}[x2] + 4.70579 \text{ Cos}[x2] \text{ Sin}[x2] + 4.72815 \text{ Cos}[x3] \text{ Sin}[x2] - 9.89926 \text{ Cos}[x4] \text{ Sin}[x2] - 17.6148 \text{ Sin}[x1] \text{ Sin}[x2] + 0.931419 \text{ Sin}[x2]^2 + 16.0685 \text{ Sin}[x3] + 14.283 \text{ Cos}[x1] \text{ Sin}[x3] + 16.2993 \text{ Cos}[x2] \text{ Sin}[x3] + 15.9789 \text{ Cos}[x3] \text{ Sin}[x3] + 3.70099 \text{ Cos}[x4] \text{ Sin}[x3] - 0.581251 \text{ Sin}[x1] \text{ Sin}[x3] + 0.264823 \text{ Sin}[x2] \text{ Sin}[x3] + 3.10548 \text{ Sin}[x3]^2 + 28.9043 \text{ Sin}[x4] + 14.1757 \text{ Cos}[x1] \text{ Sin}[x4] + 28.688 \text{ Cos}[x2] \text{ Sin}[x4] + 27.5452 \text{ Cos}[x3] \text{ Sin}[x4] - 27.3868 \text{ Cos}[x4] \text{ Sin}[x4] + 23.177 \text{ Sin}[x1] \text{ Sin}[x4] + 7.17654 \text{ Sin}[x2] \text{ Sin}[x4] + 19.1664 \text{ Sin}[x3] \text{ Sin}[x4] + 38.6439 \text{ Sin}[x4]^2) / (16.2608 + 9.7636 \text{ Cos}[x1] + 7.09585 \text{ Cos}[x1]^2 + 10.3467 \text{ Cos}[x2] - 15.5139 \text{ Cos}[x1] \text{ Cos}[x2] + 5.3472 \text{ Cos}[x2]^2 - 4.14587 \text{ Cos}[x3] - 7.63937 \text{ Cos}[x1] \text{ Cos}[x3] - 8.81856 \text{ Cos}[x2] \text{ Cos}[x3] - 23.8556 \text{ Cos}[x3]^2 - 0.320913 \text{ Cos}[x4] + 6.75418 \text{ Cos}[x1] \text{ Cos}[x4] - 7.95355 \text{ Cos}[x2] \text{ Cos}[x4] - 6.06921 \text{ Cos}[x3] \text{ Cos}[x4] + 10.2395 \text{ Cos}[x4]^2 - 23.1079 \text{ Sin}[x1] - 14.3605 \text{ Cos}[x1] \text{ Sin}[x1] + 77.5809 \text{ Cos}[x2] \text{ Sin}[x1] - 31.4746 \text{ Cos}[x3] \text{ Sin}[x1] - 6.40251 \text{ Cos}[x4] \text{ Sin}[x1] + 10.1649 \text{ Sin}[x1]^2 - 11.18 \text{ Sin}[x2] - 16.9628 \text{ Cos}[x1] \text{ Sin}[x2] - 15.2896 \text{ Cos}[x2] \text{ Sin}[x2] - 22.9365 \text{ Cos}[x3] \text{ Sin}[x2] + 41.6317 \text{ Cos}[x4] \text{ Sin}[x2] - 3.48707 \text{ Sin}[x1] \text{ Sin}[x2] + 11.9136 \text{ Sin}[x2]^2 + 19.9729 \text{ Sin}[x3] + 12.4549 \text{ Cos}[x1] \text{ Sin}[x3] + 12.6283 \text{ Cos}[x2] \text{ Sin}[x3] + 13.6294 \text{ Cos}[x3] \text{ Sin}[x3] - 10.5336 \text{ Cos}[x4] \text{ Sin}[x3] + 30.9158 \text{ Sin}[x1] \text{ Sin}[x3] + 71.4241 \text{ Sin}[x2] \text{ Sin}[x3] + 41.1163 \text{ Sin}[x3]^2 + 10.2476 \text{ Sin}[x4] + 6.83289 \text{ Cos}[x1] \text{ Sin}[x4] - 0.700106 \text{ Cos}[x2] \text{ Sin}[x4] + 3.96596 \text{ Cos}[x3] \text{ Sin}[x4] - 6.19734 \text{ Cos}[x4] \text{ Sin}[x4] - 8.67069 \text{ Sin}[x1] \text{ Sin}[x4] + 19.3857 \text{ Sin}[x2] \text{ Sin}[x4] - 97.4617 \text{ Sin}[x3] \text{ Sin}[x4] + 7.02127 \text{ Sin}[x4]^2)$
CS7-O2-FOLN	$94.8219 + 0.975369 \text{ Log}[x1] + 27.7705 \text{ Log}[x2] + 5.71478 \text{ Log}[x3] - 8.67569 \text{ Log}[x4]$
CS7-O2-FOLNR	$(-576.942 - 281.272 \text{ Log}[x1] - 25.8397 \text{ Log}[x2] + 48.8377 \text{ Log}[x3] + 9286.96 \text{ Log}[x4]) / (-9.86873 - 5.46892 \text{ Log}[x1] + 6.859 \text{ Log}[x2] + 3.23311 \text{ Log}[x3] + 253.623 \text{ Log}[x4])$
CS7-O2-SOLN	$477.902 - 179.687 \text{ Log}[x1] + 27.1699 \text{ Log}[x1]^2 + 135.004 \text{ Log}[x2] - 3.65816 \text{ Log}[x1] \text{ Log}[x2] + 21.1135 \text{ Log}[x2]^2 - 135.212 \text{ Log}[x3] + 46.0311 \text{ Log}[x1] \text{ Log}[x3] + 4.01305 \text{ Log}[x2] \text{ Log}[x3] + 22.1493 \text{ Log}[x3]^2 + 126.8 \text{ Log}[x4] - 7.46425 \text{ Log}[x1] \text{ Log}[x4] - 23.4369 \text{ Log}[x2] \text{ Log}[x4] + 60.8721 \text{ Log}[x3] \text{ Log}[x4] - 10.3375 \text{ Log}[x4]^2$
CS7-O2-SOLNR	$(-8.35098*10^6 - 1.58747*10^7 \text{ Log}[x1] + 1.71499*10^8 \text{ Log}[x1]^2 - 1.42876*10^7 \text{ Log}[x2] - 1.89417*10^8 \text{ Log}[x1] \text{ Log}[x2] + 1.5735*10^8 \text{ Log}[x2]^2 - 2.25778*10^7 \text{ Log}[x3] - 1.34168*10^8 \text{ Log}[x1] \text{ Log}[x3] + 1.06709*10^8 \text{ Log}[x2] \text{ Log}[x3] + 9.79455*10^7 \text{ Log}[x3]^2 + 3.2159*10^7 \text{ Log}[x4] + 1.23662*10^8 \text{ Log}[x1] \text{ Log}[x4] - 8.6465*10^7 \text{ Log}[x2] \text{ Log}[x4] - 5.07652*10^7 \text{ Log}[x3] \text{ Log}[x4] + 6.26476*10^6 \text{ Log}[x4]^2) / (-1.69177*10^8 + 1.07582*10^8 \text{ Log}[x1] - 3.19056*10^7 \text{ Log}[x1]^2 - 7.50926*10^8 \text{ Log}[x2] + 2.06438*10^8 \text{ Log}[x1] \text{ Log}[x2] + 9.65616*10^7 \text{ Log}[x2]^2 + 7.34966*10^8 \text{ Log}[x3] - 2.66498*10^8 \text{ Log}[x1] \text{ Log}[x3] + 1.11981*10^8 \text{ Log}[x2] \text{ Log}[x3] - 1.78144*10^8 \text{ Log}[x3]^2 - 4.0934*10^8 \text{ Log}[x4] - 9.23484*10^7 \text{ Log}[x1] \text{ Log}[x4] + 5.89721*10^7 \text{ Log}[x2] \text{ Log}[x4] - 4.79194*10^8 \text{ Log}[x3] \text{ Log}[x4] + 2.06166*10^8 \text{ Log}[x4]^2)$
NOTATION	CS7-O3
CS7-O3-L	$-29.0391 + 0.0886171 [x1] + 324.678 [x2] + 385.258 [x3] + 16.1563 [x4]$
CS7-O3-LN	$(1.09058*10^6 - 5575.18 [x1] + 7103.93 [x2] + 8470. [x3] - 25609.7 [x4]) / (10289.9 - 50.1624 [x1] - 1194.99 [x2] - 987.313 [x3] - 311.248 [x4])$
CS7-O3-SON	$296.223 - 0.728934 [x1] + 0.000153748 [x1]^2 + 49.0626 [x2] - 1.15737 [x1] [x2] + 539.127 [x2]^2 - 2128.8 [x3] + 5.09599 [x1] [x3] + 476.667 [x2] [x3] + 5259.02 [x3]^2 - 136.122 [x4] + 0.352764 [x1] [x4] + 180.961 [x2] [x4] + 306.25 [x3] [x4] + 7.03021 [x4]^2$
CS7-O3-SONR	$(263.164 + 56189.3 [x1] + 1.40537*10^7 [x1]^2 + 1849.53 [x2] + 291211. [x1] [x2] + 727.988 [x2]^2 + 220.858 [x3] + 39787.8 [x1] [x3] + 243.35 [x2] [x3] + 47.5716 [x3]^2 + 592.171 [x4] + 151062. [x1] [x4] + 2237.28 [x2] [x4] + 303.324 [x3] [x4] + 962.949 [x4]^2) / (53098.9 + 5.01517*10^6 [x1] + 159887. [x1]^2 - 185696. [x2] - 2.96904*10^7 [x1] [x2] - 75834.7 [x2]^2 - 15194. [x3] - 3.16071*10^6 [x1] [x3] - 24725.4 [x2] [x3] - 4102.06 [x3]^2 + 33785.7 [x4] - 2.73246*10^6 [x1] [x4] - 224863. [x2] [x4] - 22418.2 [x3] [x4] + 17183.1 [x4]^2)$
CS7-O3-TON	$122.983 - 0.0806463 [x1] - 0.00110289 [x1]^2 + 1.91791*10^-6 [x1]^3 + 388.008 [x2] + 5.61377 [x1] [x2] - 0.0126331 [x1]^2 [x2] + 453.431 [x2]^2 - 19.6677 [x1] [x2]^2 - 2267.35 [x2]^3 + 319.979 [x3] - 13.1523 [x1] [x3] + 0.0249281 [x1]^2 [x3] - 1650.55 [x2] [x3] - 23.5131 [x1] [x2] [x3] + 12889.3 [x2]^2 [x3] - 3494.05 [x3]^2 + 40.8215 [x1] [x3]^2 + 26539.5 [x2] [x3]^2 - 70469.4 [x3]^3 - 79.7281 [x4] + 0.571859 [x1] [x4] - 0.000449922 [x1]^2 [x4] - 943.099 [x2] [x4] + 6.23819 [x1] [x2] [x4] + 2869.03 [x2]^2 [x4] + 778.269 [x3] [x4] + 3.38332 [x1] [x3] [x4] - 3823.16 [x2] [x3] [x4] + 17924.8 [x3]^2 [x4] - 17.0813 [x4]^2 - 0.644103 [x1] [x4]^2 - 316.453 [x2] [x4]^2 - 1777.75 [x3] [x4]^2 + 109.793 [x4]^3$
CS7-O3-FOTN	$13533.5 - 14.2805 \text{ Cos}[x1] - 948.935 \text{ Cos}[x2] - 12476.5 \text{ Cos}[x3] - 14.2927 \text{ Cos}[x4] - 5.91801 \text{ Sin}[x1] + 140.709 \text{ Sin}[x2] - 1004.18 \text{ Sin}[x3] + 5.68351 \text{ Sin}[x4]$
CS7-O3-FOTNR	$(-66.5007 + 154.903 \text{ Cos}[x1] - 6.30243 \text{ Cos}[x2] - 70.9691 \text{ Cos}[x3] - 0.147477 \text{ Cos}[x4] + 32.0143 \text{ Sin}[x1] - 1.27757 \text{ Sin}[x2] - 7.83822 \text{ Sin}[x3] - 0.379332 \text{ Sin}[x4]) / (-0.527083 + 1.3426 \text{ Cos}[x1] - 0.0586003 \text{ Cos}[x2] - 0.065987 \text{ Cos}[x3] - 0.00137123 \text{ Cos}[x4] + 0.277505 \text{ Sin}[x1] - 0.011879 \text{ Sin}[x2] - 0.0728798 \text{ Sin}[x3] - 0.00352702 \text{ Sin}[x4])$
CS7-O3-SOTN	$11.3843 + 53.19 \text{ Cos}[x1] + 71.0222 \text{ Cos}[x1]^2 + 10.6134 \text{ Cos}[x2] + 332.086 \text{ Cos}[x1] \text{ Cos}[x2] + 10.3315 \text{ Cos}[x2]^2 + 10.7604 \text{ Cos}[x3] + 29.5016 \text{ Cos}[x1] \text{ Cos}[x3] + 10.6961 \text{ Cos}[x2] \text{ Cos}[x3] + 10.19 \text{ Cos}[x3]^2 - 409.788 \text{ Cos}[x4] - 313.824 \text{ Cos}[x1] \text{ Cos}[x4]$

	$+ 1913.9 \cos[x_2] \cos[x_4] - 628.492 \cos[x_3] \cos[x_4] - 216.8 \cos[x_4]^2 + 857.271 \sin[x_1] + 1215.28 \cos[x_1] \sin[x_1] - 3761.12 \cos[x_2] \sin[x_1] + 1284.68 \cos[x_3] \sin[x_1] + 505.181 \cos[x_4] \sin[x_1] - 289.799 \sin[x_1]^2 - 642.465 \sin[x_2] + 1032.39 \cos[x_1] \sin[x_2] - 735.256 \cos[x_2] \sin[x_2] - 678.633 \cos[x_3] \sin[x_2] + 662.492 \cos[x_4] \sin[x_2] - 500.072 \sin[x_1] \sin[x_2] + 832.226 \sin[x_2]^2 - 1238.63 \sin[x_3] - 2417.74 \cos[x_1] \sin[x_3] - 1715.93 \cos[x_2] \sin[x_3] - 1298.99 \cos[x_3] \sin[x_3] + 1506.79 \cos[x_4] \sin[x_3] - 725.227 \sin[x_1] \sin[x_3] + 67.1806 \sin[x_2] \sin[x_3] + 7912.69 \sin[x_3]^2 + 22.3293 \sin[x_4] - 60.0119 \cos[x_1] \sin[x_4] - 369.344 \cos[x_2] \sin[x_4] + 45.3027 \cos[x_3] \sin[x_4] - 651.915 \cos[x_4] \sin[x_4] + 705.632 \sin[x_1] \sin[x_4] + 1010.47 \sin[x_2] \sin[x_4] + 4932.77 \sin[x_3] \sin[x_4] + 40.0795 \sin[x_4]^2$
CS7-O3-SOTNR	$(5.26591 \times 10^{11} + 4.08554 \times 10^{11} \cos[x_1] + 3.6531 \times 10^{11} \cos[x_1]^2 + 5.12392 \times 10^{11} \cos[x_2] + 3.9668 \times 10^{11} \cos[x_1] \cos[x_2] + 4.98639 \times 10^{11} \cos[x_2]^2 + 5.22781 \times 10^{11} \cos[x_3] + 4.05692 \times 10^{11} \cos[x_1] \cos[x_3] + 5.08678 \times 10^{11} \cos[x_2] \cos[x_3] + 5.19007 \times 10^{11} \cos[x_3]^2 + 3.66145 \times 10^{10} \cos[x_4] + 3.53341 \times 10^9 \cos[x_1] \cos[x_4] + 3.5311 \times 10^{10} \cos[x_2] \cos[x_4] + 3.62625 \times 10^{10} \cos[x_3] \cos[x_4] - 2.8198 \times 10^{10} \cos[x_4]^2 - 6.42714 \times 10^{11} \sin[x_1] - 4.46898 \times 10^{11} \cos[x_1] \sin[x_1] - 6.29846 \times 10^{11} \cos[x_2] \sin[x_1] - 6.38391 \times 10^{11} \cos[x_3] \sin[x_1] - 3.25199 \times 10^{11} \cos[x_4] \sin[x_1] + 1.61281 \times 10^{11} \sin[x_1]^2 + 1.19323 \times 10^{11} \sin[x_2] + 9.63699 \times 10^{10} \cos[x_1] \sin[x_2] + 1.15866 \times 10^{11} \cos[x_2] \sin[x_2] + 1.1851 \times 10^{11} \cos[x_3] \sin[x_2] + 1.06098 \times 10^{10} \cos[x_4] \sin[x_2] - 1.26457 \times 10^{11} \sin[x_1] \sin[x_2] + 2.79518 \times 10^{10} \sin[x_2]^2 + 6.06127 \times 10^{10} \sin[x_3] + 4.5857 \times 10^{10} \cos[x_1] \sin[x_3] + 5.90563 \times 10^{10} \cos[x_2] \sin[x_3] + 6.01076 \times 10^{10} \cos[x_3] \sin[x_3] + 4.09657 \times 10^9 \cos[x_4] \sin[x_3] - 7.36855 \times 10^{10} \sin[x_1] \sin[x_3] + 1.32368 \times 10^{10} \sin[x_2] \sin[x_3] + 7.58395 \times 10^9 \sin[x_3]^2 + 5.47137 \times 10^{11} \sin[x_4] + 4.36095 \times 10^{11} \cos[x_1] \sin[x_4] + 5.32136 \times 10^{11} \cos[x_2] \sin[x_4] + 5.43165 \times 10^{11} \cos[x_3] \sin[x_4] + 6.1997 \times 10^{10} \cos[x_4] \sin[x_4] - 5.24939 \times 10^{11} \sin[x_1] \sin[x_4] + 1.24692 \times 10^{11} \sin[x_2] \sin[x_4] + 6.35528 \times 10^{10} \sin[x_3] \sin[x_4] + 5.54789 \times 10^{11} \sin[x_4]^2 + (2.90776 \times 10^{10} + 4.33135 \times 10^{10} \cos[x_1] + 5.67005 \times 10^{10} \cos[x_1]^2 - 9.63384 \times 10^9 \cos[x_2] - 7.19833 \times 10^9 \cos[x_1] \cos[x_2] - 4.33118 \times 10^{10} \cos[x_2]^2 + 3.6196 \times 10^{10} \cos[x_3] + 5.28352 \times 10^{10} \cos[x_1] \cos[x_3] - 2.34029 \times 10^9 \cos[x_2] \cos[x_3] + 4.31399 \times 10^{10} \cos[x_3]^2 - 4.40786 \times 10^{11} \cos[x_4] + 1.62915 \times 10^{12} \cos[x_1] \cos[x_4] - 5.45841 \times 10^{11} \cos[x_2] \cos[x_4] - 4.49693 \times 10^{11} \cos[x_3] \cos[x_4] - 2.72459 \times 10^{11} \cos[x_4]^2 - 1.22936 \times 10^{11} \sin[x_1] - 1.01152 \times 10^{11} \cos[x_1] \sin[x_1] - 1.47229 \times 10^{11} \cos[x_2] \sin[x_1] - 1.23816 \times 10^{11} \cos[x_3] \sin[x_1] - 1.11991 \times 10^{12} \cos[x_4] \sin[x_1] - 2.76229 \times 10^{10} \sin[x_1]^2 - 1.90662 \times 10^{10} \sin[x_2] + 1.01318 \times 10^{11} \cos[x_1] \sin[x_2] - 4.25775 \times 10^{10} \cos[x_2] \sin[x_2] - 1.93194 \times 10^{10} \cos[x_3] \sin[x_2] + 1.26082 \times 10^{10} \cos[x_4] \sin[x_2] + 4.07536 \times 10^{10} \sin[x_1] \sin[x_2] + 7.23894 \times 10^{10} \sin[x_2]^2 - 3.17416 \times 10^{10} \sin[x_3] - 4.83222 \times 10^{10} \cos[x_1] \sin[x_3] - 3.90555 \times 10^{10} \cos[x_2] \sin[x_3] - 2.99885 \times 10^{10} \cos[x_3] \sin[x_3] + 1.03819 \times 10^{11} \cos[x_4] \sin[x_3] - 1.60499 \times 10^{10} \sin[x_1] \sin[x_4] + 2.05953 \times 10^{10} \sin[x_2] \sin[x_4] - 1.40623 \times 10^{10} \sin[x_3] \sin[x_4] + 1.86403 \times 10^{11} \sin[x_4] - 8.97728 \times 10^{11} \cos[x_1] \sin[x_4] + 2.51997 \times 10^{11} \cos[x_2] \sin[x_4] + 2.00988 \times 10^{11} \cos[x_3] \sin[x_4] - 3.34633 \times 10^{11} \cos[x_4] \sin[x_4] + 9.1372 \times 10^{11} \sin[x_1] \sin[x_4] - 3.25031 \times 10^{11} \sin[x_2] \sin[x_4] - 1.06285 \times 10^{11} \sin[x_3] \sin[x_4] + 3.01536 \times 10^{11} \sin[x_4]^2$
CS7-O3-POLN	$221.771 + 13.2967 \log[x_1] + 54.8639 \log[x_2] + 39.6562 \log[x_3] + 18.6689 \log[x_4]$
CS7-O3-POLNR	$(-20973.9 + 454.123 \log[x_1] - 166.801 \log[x_2] + 493.49 \log[x_3] + 112375. \log[x_4]) / (-199.098 + 1.67924 \log[x_1] - 7.25009 \log[x_2] + 0.391617 \log[x_3] + 1035.13 \log[x_4])$
CS7-O3-SOLN	$1034.22 - 157.236 \log[x_1] + 24.8797 \log[x_1]^2 + 349.653 \log[x_2] - 22.3943 \log[x_1] \log[x_2] + 50.8858 \log[x_2]^2 + 140.587 \log[x_3] + 59.3118 \log[x_1] \log[x_3] + 0.115295 \log[x_2] \log[x_3] + 92.1476 \log[x_3]^2 - 289.108 \log[x_4] + 90.3136 \log[x_1] \log[x_4] + 29.2882 \log[x_2] \log[x_4] + 52.5423 \log[x_3] \log[x_4] + 5.52687 \log[x_4]^2$
CS7-O3-SOLNR	$(-2.38864 \times 10^8 - 7.84263 \times 10^8 \log[x_1] - 2.00031 \times 10^9 \log[x_1]^2 - 3.3241 \times 10^8 \log[x_2] - 1.99944 \times 10^9 \log[x_1] \log[x_2] + 1.18602 \times 10^9 \log[x_2]^2 - 2.11821 \times 10^8 \log[x_3] - 2.31906 \times 10^9 \log[x_1] \log[x_3] + 8.70587 \times 10^8 \log[x_2] \log[x_3] + 1.88254 \times 10^9 \log[x_3]^2 + 8.52436 \times 10^8 \log[x_4] + 4.5209 \times 10^9 \log[x_1] \log[x_4] - 2.09749 \times 10^9 \log[x_2] \log[x_4] - 2.01797 \times 10^9 \log[x_3] \log[x_4] + 9.72 \times 10^8 \log[x_4]^2) / (2.82823 \times 10^8 + 6.58068 \times 10^7 \log[x_1] + 4.12761 \times 10^6 \log[x_1]^2 + 7.73791 \times 10^7 \log[x_2] + 8.71225 \times 10^7 \log[x_1] \log[x_2] + 7.50179 \times 10^7 \log[x_2]^2 + 3.71028 \times 10^8 \log[x_3] + 4.41599 \times 10^7 \log[x_1] \log[x_3] + 2.06689 \times 10^8 \log[x_2] \log[x_3] + 1.08116 \times 10^8 \log[x_3]^2 - 3.08887 \times 10^8 \log[x_4] + 4.09485 \times 10^7 \log[x_1] \log[x_4] - 1.32523 \times 10^8 \log[x_2] \log[x_4] - 8.68155 \times 10^7 \log[x_3] \log[x_4] - 7.70466 \times 10^7 \log[x_4]^2)$
NOTATION	CS7-O4
CS7-O4-L	$-30.6415 - 0.0416669 [x_1] + 343.929 [x_2] + 411.51 [x_3] + 14.0065 [x_4]$
CS7-O4-LN	$(1.39859 \times 10^7 - 16349. [x_1] + 8.08612 \times 10^7 [x_2] - 1.21548 \times 10^8 [x_3] + 8.58197 \times 10^6 [x_4]) / (493331. - 104.06 [x_1] - 64135.1 [x_2] - 2.45258 \times 10^6 [x_3] + 62113.7 [x_4])$
CS7-O4-SON	$185.476 - 0.631289 [x_1] + 0.000535502 [x_1]^2 - 39.8502 [x_2] - 0.294205 [x_1] [x_2] + 235.804 [x_2]^2 - 1871.6 [x_3] + 4.52075 [x_1] [x_3] + 3380.83 [x_2] [x_3] + 4262.12 [x_3]^2 + 9.79693 [x_4] - 0.0542013 [x_1] [x_4] - 28.9436 [x_2] [x_4] - 105.208 [x_3] [x_4] + 13.0136 [x_4]^2$
CS7-O4-SONR	$(87356.2 + 1.03231 \times 10^7 [x_1] + 1.26779 \times 10^9 [x_1]^2 + 114327. [x_2] + 1.74521 \times 10^7 [x_1] [x_2] + 41971.6 [x_2]^2 + 19290.7 [x_3] + 2.90857 \times 10^6 [x_1] [x_3] + 14806.5 [x_2] [x_3] + 3357.9 [x_3]^2 + 102779. [x_4] + 1.13624 \times 10^7 [x_1] [x_4] + 133047. [x_2] [x_4] + 22831.3 [x_3] [x_4] + 112677. [x_4]^2) / (-3.71145 \times 10^6 - 2.40597 \times 10^8 [x_1] + 1.84131 \times 10^7 [x_1]^2 - 9.49525 \times 10^6 [x_2] - 1.43373 \times 10^9 [x_1] [x_2] - 3.6102 \times 10^6 [x_2]^2 - 1.27777 \times 10^6 [x_3] - 1.85392 \times 10^8 [x_1] [x_3] - 1.24524 \times 10^6 [x_2] [x_3] - 249362. [x_3]^2 - 4.17886 \times 10^6 [x_4] - 1.52168 \times 10^8 [x_1] [x_4] - 1.10395 \times 10^7 [x_2] [x_4] - 1.49915 \times 10^6 [x_3] [x_4] - 3.63441 \times 10^6 [x_4]^2)$
CS7-O4-TON	$69.6149 - 0.0904271 [x_1] - 0.000582866 [x_1]^2 + 4.0113 \times 10^{-6} [x_1]^3 + 218.988 [x_2] - 2.42505 [x_1] [x_2] + 0.0022651 [x_1]^2 [x_2] - 220.427 [x_2]^2 + 9.82682 [x_1] [x_2]^2 - 5368.12 [x_2]^3 - 387.395 [x_3] + 5.02725 [x_1] [x_3] - 0.0163158 [x_1]^2 [x_3] - 1533.37 [x_2] [x_3] + 16.6419 [x_1] [x_2] [x_3] + 8334.96 [x_2]^2 [x_3] - 1694.34 [x_3]^2 + 5.31044 [x_1] [x_3]^2 - 7582.95 [x_2] [x_3]^2 + 53578.7 [x_3]^3 + 57.8693 [x_4] - 0.504978 [x_1] [x_4] + 0.000484384 [x_1]^2 [x_4] + 387.597 [x_2] [x_4] - 3.2465 [x_1] [x_2] [x_4] + 955.69 [x_2]^2 [x_4] - 725.118 [x_3] [x_4] + 0.341593 [x_1] [x_3] [x_4] + 183.034 [x_2] [x_3] [x_4] - 9995.96 [x_3]^2 [x_4] + 2.58097 [x_4]^2 + 0.361992 [x_1] [x_4]^2 - 68.1976 [x_2] [x_4]^2 + 1133.43 [x_3] [x_4]^2 - 45.7669 [x_4]^3$
CS7-O4-FOTN	$11404.2 - 9.58609 \cos[x_1] - 543.189 \cos[x_2] - 10787.1 \cos[x_3] - 17.5084 \cos[x_4] + 4.86905 \sin[x_1] + 240.609 \sin[x_2] - 788.465 \sin[x_3] - 7.48081 \sin[x_4]$
CS7-O4-FOTNR	$(89.286 - 0.470082 \cos[x_1] + 105.349 \cos[x_2] - 195.085 \cos[x_3] - 0.730505 \cos[x_4] + 0.0422696 \sin[x_1] + 32.4091 \sin[x_2] - 27.9325 \sin[x_3] - 1.72774 \sin[x_4]) / (0.574088 - 0.00507038 \cos[x_1] + 2.31519 \cos[x_2] - 2.92252 \cos[x_3] - 0.00872547 \cos[x_4] + 0.000416657 \sin[x_1] + 0.643575 \sin[x_2] - 0.386777 \sin[x_3] - 0.0207799 \sin[x_4])$
CS7-O4-SOTN	$12.0104 + 9.74583 \cos[x_1] + 6.35322 \cos[x_1]^2 + 12.3361 \cos[x_2] + 28.8058 \cos[x_1] \cos[x_2] + 12.923 \cos[x_2]^2 + 11.4575 \cos[x_3] + 5.47576 \cos[x_1] \cos[x_3] + 11.9034 \cos[x_2] \cos[x_3] + 10.9277 \cos[x_3]^2 - 50.7521 \cos[x_4] - 8.35961 \cos[x_1] \cos[x_4] + 180.461 \cos[x_2] \cos[x_4] - 74.7475 \cos[x_3] \cos[x_4] - 22.3749 \cos[x_4]^2 + 49.7959 \sin[x_1] + 95.74 \cos[x_1] \sin[x_1] - 312.814 \cos[x_2] \sin[x_1] + 84.1933 \cos[x_3] \sin[x_1] + 75.3578 \cos[x_4] \sin[x_1] + 63.3979 \sin[x_1]^2 - 359.46 \sin[x_2] + 154.046 \cos[x_1] \sin[x_2] - 404.145 \cos[x_2] \sin[x_2] - 384.092 \cos[x_3] \sin[x_2] + 520.488 \cos[x_4] \sin[x_2] - 33.0409 \sin[x_1] \sin[x_2] + 42.5234 \sin[x_2]^2 - 363.903 \sin[x_3] + 476.406 \cos[x_1] \sin[x_3] - 421.111 \cos[x_2] \sin[x_3] - 394.408 \cos[x_3] \sin[x_3] - 353.606 \cos[x_4] \sin[x_3] - 394.772 \sin[x_1] \sin[x_3] + 3348.83 \sin[x_2] \sin[x_3] + 7406.27 \sin[x_3]^2 + 15.7928 \sin[x_4] + 17.9726 \cos[x_1] \sin[x_4] - 30.5845 \cos[x_2] \sin[x_4] + 19.4147 \cos[x_3] \sin[x_4] - 81.8803 \cos[x_4] \sin[x_4] + 137.445 \sin[x_1] \sin[x_4] + 834.427 \sin[x_2] \sin[x_4] - 1186.24 \sin[x_3] \sin[x_4] + 20.3274 \sin[x_4]^2$
CS7-O4-SOTNR	$(48.0074 + 242.591 \cos[x_1] + 344.357 \cos[x_1]^2 + 46.9746 \cos[x_2] + 238.615 \cos[x_1] \cos[x_2] + 46.056 \cos[x_2]^2 + 49.6996 \cos[x_3] + 242.639 \cos[x_1] \cos[x_3] + 48.6849 \cos[x_2] \cos[x_3] + 51.3928 \cos[x_3]^2 - 282.189 \cos[x_4] - 202.218 \cos[x_1] \cos[x_4] - 278.33 \cos[x_2] \cos[x_4] - 279.408 \cos[x_3] \cos[x_4] - 158.494 \cos[x_4]^2 + 83.2665 \sin[x_1] - 46.5772 \cos[x_1] \sin[x_1] + 80.7571 \cos[x_2] \sin[x_1] + 81.5161 \cos[x_3] \sin[x_1] + 95.6204 \cos[x_4] \sin[x_1] - 295.35 \sin[x_1]^2 + 4.63432 \sin[x_2] + 33.8028 \cos[x_1] \sin[x_2] + 4.09298 \cos[x_2] \sin[x_2] + 4.51878 \cos[x_3] \sin[x_2] - 40.8348 \cos[x_4] \sin[x_2] + 41.0959 \sin[x_1] \sin[x_2] + 2.95141 \sin[x_2]^2 - 21.3657 \sin[x_3] + 4.48221 \cos[x_1] \sin[x_3] - 21.3783 \cos[x_2] \sin[x_3] - 21.2321 \cos[x_3] \sin[x_3] - 43.3378 \cos[x_4] \sin[x_3] + 20.0717 \sin[x_1] \sin[x_3] + 0.399869 \sin[x_2] \sin[x_3] - 2.38538 \sin[x_3]^2 + 139.062 \sin[x_4] + 316.822 \cos[x_1] \sin[x_4] + 136.296 \cos[x_2] \sin[x_4] + 140.613 \cos[x_3] \sin[x_4] - 223.545 \cos[x_4] \sin[x_4] + 57.1888 \sin[x_1] \sin[x_4] + 19.4634 \sin[x_2] \sin[x_4] - 14.2544 \sin[x_3] \sin[x_4] + 207.502 \sin[x_4]^2) / (-37.6597 - 17.3885 \cos[x_1] - 9.57813 \cos[x_1]^2 - 80.1226 \cos[x_2] + 26.291 \cos[x_1] \cos[x_2] - 117.805 \cos[x_2]^2 + 63.6727 \cos[x_3] + 82.9791 \cos[x_1] \cos[x_3] + 19.3904 \cos[x_2] \cos[x_3] + 161.521 \cos[x_3]^2 + 14.8947 \cos[x_4] - 23.1574 \cos[x_1] \cos[x_4] - 78.9037 \cos[x_2] \cos[x_4] + 32.0844 \cos[x_3] \cos[x_4] - 17.2771 \cos[x_4]^2 + 82.8488 \sin[x_1] + 53.3192 \cos[x_1] \sin[x_1] - 227.047 \cos[x_2] \sin[x_1] + 88.148 \cos[x_3] \sin[x_1] + 15.7198 \cos[x_4] \sin[x_1] - 27.0815 \sin[x_1]^2 + 26.2613 \sin[x_2] - 88.4534 \cos[x_1] \sin[x_2] + 3.09839 \cos[x_2] \sin[x_2] + 62.5915 \cos[x_3] \sin[x_2] - 54.8352 \cos[x_4] \sin[x_2] - 61.1949 \sin[x_1] \sin[x_2] + 81.1452 \sin[x_2]^2 - 82.8222 \sin[x_3] - 139.692 \cos[x_1] \sin[x_3] - 89.6145 \cos[x_2] \sin[x_3] - 51.1636 \cos[x_3] \sin[x_3] + 223.493 \cos[x_4] \sin[x_3] + 50.917 \sin[x_1] \sin[x_3] - 149.662 \sin[x_2] \sin[x_3] - 198.181 \sin[x_3]^2 - 25.2907 \sin[x_4] - 24.618 \cos[x_1] \sin[x_4] + 17.9789 \cos[x_2] \sin[x_4] + 14.9605 \cos[x_3] \sin[x_4] + 28.1112 \cos[x_4] \sin[x_4] + 16.7019 \sin[x_1] \sin[x_4] - 146.914 \sin[x_2] \sin[x_4] + 375.615 \sin[x_3] \sin[x_4] - 19.3825 \sin[x_4]^2)$
CS7-O4-POLN	$327.053 - 8.74788 \log[x_1] + 58.6878 \log[x_2] + 42.0835 \log[x_3] + 15.916 \log[x_4]$
CS7-O4-POLNR	$(-4669.91 - 3130.83 \log[x_1] - 2090.08 \log[x_2] - 3800.93 \log[x_3] + 48024.1 \log[x_4]) / (-56.9238 - 34.3138 \log[x_1] - 23.3934 \log[x_2] - 42.131 \log[x_3] + 548.843 \log[x_4])$
CS7-O4-SOLN	$224.488 + 95.7997 \log[x_1] + 10.194 \log[x_1]^2 + 386.68 \log[x_2] - 7.48795 \log[x_1] \log[x_2] + 41.7608 \log[x_2]^2 - 61.0096 \log[x_3] + 100.028 \log[x_1] \log[x_3] + 62.3673 \log[x_2] \log[x_3] + 67.7425 \log[x_3]^2 + 55.9507 \log[x_4] - 15.384 \log[x_1] \log[x_4] - 5.25805 \log[x_2] \log[x_4] - 10.9839 \log[x_3] \log[x_4] + 29.3582 \log[x_4]^2$

CS7-O4-SOLNR	$(-1.59095*10^7 + 1.75785*10^8 \text{ Log}[x1] - 1.28025*10^9 \text{ Log}[x1]^2 - 3.89794*10^8 \text{ Log}[x2] - 1.97373*10^9 \text{ Log}[x1] \text{ Log}[x2] + 1.41657*10^9 \text{ Log}[x2]^2 - 1.00393*10^7 \text{ Log}[x3] - 5.5339*10^8 \text{ Log}[x1] \text{ Log}[x3] + 1.82864*10^9 \text{ Log}[x2] \text{ Log}[x3] - 8.48438*10^8 \text{ Log}[x3]^2 + 2.28789*10^8 \text{ Log}[x4] + 1.09314*10^9 \text{ Log}[x1] \text{ Log}[x4] - 4.4472*10^9 \text{ Log}[x2] \text{ Log}[x4] + 3.10116*10^8 \text{ Log}[x3] \text{ Log}[x4] + 4.80376*10^9 \text{ Log}[x4]^2) / (1.78803*10^8 + 1.97885*10^8 \text{ Log}[x1] - 2.02103*10^7 \text{ Log}[x1]^2 + 5.47717*10^8 \text{ Log}[x2] + 2.16755*10^7 \text{ Log}[x1] \text{ Log}[x2] + 1.82896*10^8 \text{ Log}[x2]^2 + 1.77967*10^8 \text{ Log}[x3] + 2.20619*10^7 \text{ Log}[x1] \text{ Log}[x3] + 1.20904*10^8 \text{ Log}[x2] \text{ Log}[x3] + 2.00366*10^7 \text{ Log}[x3]^2 - 4.01268*10^8 \text{ Log}[x4] + 3.43039*10^7 \text{ Log}[x1] \text{ Log}[x4] - 9.5291*10^7 \text{ Log}[x2] \text{ Log}[x4] - 9.48432*10^7 \text{ Log}[x3] \text{ Log}[x4] + 3.6973*10^7 \text{ Log}[x4]^2)$
NOTATION	CS8-O1
CS8-O1-L	$-54.9044 + 0.0126924 [x1] + 110.385 [x2] + 112.152 [x3]$
CS8-O1-LN	$(-3215.51 + 0.180968 [x1] + 14213.7 [x2] + 9181.29 [x3]) / (123.248 - 0.0178031 [x1] + 77.4951 [x2] - 17.4485 [x3])$
CS8-O1-SON	$-41.748 - 0.00861179 [x1] + 1.3402*10^6 [x1]^2 + 363.464 [x2] + 0.0182704 [x1] [x2] - 681.286 [x2]^2 + 60.009 [x3] + 0.0213713 [x1] [x3] - 36.4502 [x2] [x3] + 11.8511 [x3]^2$
CS8-O1-SONR	$(-3.34635*10^8 + 67236.5 [x1] - 14.468 [x1]^2 + 7.26487*10^8 [x2] - 348769. [x1] [x2] - 2.04232*10^9 [x2]^2 + 8.37234*10^8 [x3] + 55656.9 [x1] [x3] + 1.55003*10^9 [x2] [x3] - 1.05179*10^9 [x3]^2) / (-4.1996*10^6 - 61.9614 [x1] - 0.166786 [x1]^2 + 5.65691*10^6 [x2] - 4998.6 [x1] [x2] - 2.51451*10^7 [x2]^2 + 1.69691*10^7 [x3] + 1969.77 [x1] [x3] + 2.62236*10^7 [x2] [x3] - 2.2464*10^7 [x3]^2)$
CS8-O1-TON	$-102.263 + 0.101074 [x1] + 0.0000326033 [x1]^2 - 1.32129*10^8 [x1]^3 + 686.167 [x2] - 1.69116 [x1] [x2] + 0.000276816 [x1]^2 [x2] + 2716.61 [x2]^2 + 1.2192 [x1] [x2]^2 + 7356.17 [x2]^3 - 143.511 [x3] - 0.0126298 [x1] [x3] - 5.03831*10^7 [x1]^2 [x3] + 2883.2 [x2] [x3] + 0.118927 [x1] [x2] [x3] - 3197.7 [x2]^2 [x3] - 68.4451 [x3]^2 + 0.00595785 [x1] [x3]^2 - 1652.55 [x2] [x3]^2 + 233.957 [x3]^3$
CS8-O1-FOTN	$-1375.27 + 12.9017 \text{ Cos}[x1] + 1393.95 \text{ Cos}[x2] - 69.4043 \text{ Cos}[x3] - 2.18913 \text{ Sin}[x1] + 395.32 \text{ Sin}[x2] + 88.8538 \text{ Sin}[x3]$
CS8-O1-FOTNR	$(-24421.5 + 91.0349 \text{ Cos}[x1] + 38330.7 \text{ Cos}[x2] - 13331.9 \text{ Cos}[x3] + 89.9866 \text{ Sin}[x1] + 11414.8 \text{ Sin}[x2] - 5101.26 \text{ Sin}[x3]) / (167.925 - 4.09915 \text{ Cos}[x1] + 101.566 \text{ Cos}[x2] - 210.074 \text{ Cos}[x3] + 2.38993 \text{ Sin}[x1] + 33.8889 \text{ Sin}[x2] - 135.191 \text{ Sin}[x3])$
CS8-O1-SOTN	$5474.21 + 4778.91 \text{ Cos}[x1] + 11516.2 \text{ Cos}[x1]^2 + 5725.02 \text{ Cos}[x2] - 3329.92 \text{ Cos}[x1] \text{ Cos}[x2] + 5987.71 \text{ Cos}[x2]^2 + 8276.19 \text{ Cos}[x3] - 7.76545 \text{ Cos}[x1] \text{ Cos}[x3] - 44156.3 \text{ Cos}[x2] \text{ Cos}[x3] + 11099.3 \text{ Cos}[x3]^2 - 0.0769973 \text{ Sin}[x1] + 64.2828 \text{ Cos}[x1] \text{ Sin}[x1] + 299.84 \text{ Cos}[x2] \text{ Sin}[x1] + 7.41486 \text{ Cos}[x3] \text{ Sin}[x1] + 6836.25 \text{ Sin}[x1]^2 + 3411.25 \text{ Sin}[x2] - 658.597 \text{ Cos}[x1] \text{ Sin}[x2] + 3512.04 \text{ Cos}[x2] \text{ Sin}[x2] - 5957.66 \text{ Cos}[x3] \text{ Sin}[x2] + 22.0273 \text{ Sin}[x1] \text{ Sin}[x2] - 16553.2 \text{ Sin}[x2]^2 + 6636.33 \text{ Sin}[x3] + 16.9182 \text{ Cos}[x1] \text{ Sin}[x3] - 21152. \text{ Cos}[x2] \text{ Sin}[x3] + 14290.1 \text{ Cos}[x3] \text{ Sin}[x3] + 0.401215 \text{ Sin}[x1] \text{ Sin}[x3] - 2430.51 \text{ Sin}[x2] \text{ Sin}[x3] - 3399.73 \text{ Sin}[x3]^2$
CS8-O1-SOTNR	$(5.61809 - 4.89851 \text{ Cos}[x1] + 3.35654 \text{ Cos}[x1]^2 + 4.56512 \text{ Cos}[x2] + 1.33823 \text{ Cos}[x1] \text{ Cos}[x2] + 3.59182 \text{ Cos}[x2]^2 - 15.9506 \text{ Cos}[x3] + 29.0657 \text{ Cos}[x1] \text{ Cos}[x3] - 16.1078 \text{ Cos}[x2] \text{ Cos}[x3] - 29.9305 \text{ Cos}[x3]^2 + 0.0112405 \text{ Sin}[x1] + 6.25136 \text{ Cos}[x1] \text{ Sin}[x1] + 4.27691 \text{ Cos}[x2] \text{ Sin}[x1] - 26.5073 \text{ Cos}[x3] \text{ Sin}[x1] + 3.26155 \text{ Sin}[x1]^2 + 4.24964 \text{ Sin}[x2] - 42.4631 \text{ Cos}[x1] \text{ Sin}[x2] + 3.80504 \text{ Cos}[x2] \text{ Sin}[x2] - 2.71585 \text{ Cos}[x3] \text{ Sin}[x2] + 9.59915 \text{ Sin}[x1] \text{ Sin}[x2] + 3.02627 \text{ Sin}[x2]^2 + 34.1665 \text{ Sin}[x3] - 80.6674 \text{ Cos}[x1] \text{ Sin}[x3] + 32.7964 \text{ Cos}[x2] \text{ Sin}[x3] + 16.6412 \text{ Cos}[x3] \text{ Sin}[x3] + 40.1578 \text{ Sin}[x1] \text{ Sin}[x3] + 12.2129 \text{ Sin}[x2] \text{ Sin}[x3] + 36.5486 \text{ Sin}[x3]^2) / (2.03067 - 31.0368 \text{ Cos}[x1] + 10.5803 \text{ Cos}[x1]^2 - 2.06543 \text{ Cos}[x2] + 58.6839 \text{ Cos}[x1] \text{ Cos}[x2] - 5.82386 \text{ Cos}[x2]^2 + 1.15014 \text{ Cos}[x3] - 1.89377 \text{ Cos}[x1] \text{ Cos}[x3] + 5.57631 \text{ Cos}[x2] \text{ Cos}[x3] - 0.392916 \text{ Cos}[x3]^2 - 4.5638 \text{ Sin}[x1] + 26.6791 \text{ Cos}[x1] \text{ Sin}[x1] - 2.31314 \text{ Cos}[x2] \text{ Sin}[x1] + 2.83204 \text{ Cos}[x3] \text{ Sin}[x1] - 7.54967 \text{ Sin}[x1]^2 + 10.6327 \text{ Sin}[x2] + 12.9086 \text{ Cos}[x1] \text{ Sin}[x2] + 8.79435 \text{ Cos}[x2] \text{ Sin}[x2] - 20.4759 \text{ Cos}[x3] \text{ Sin}[x2] - 0.352126 \text{ Sin}[x1] \text{ Sin}[x2] + 8.85453 \text{ Sin}[x2]^2 + 5.99362 \text{ Sin}[x3] - 1.77241 \text{ Cos}[x1] \text{ Sin}[x3] - 6.50825 \text{ Cos}[x2] \text{ Sin}[x3] + 6.35969 \text{ Cos}[x3] \text{ Sin}[x3] + 2.71826 \text{ Sin}[x1] \text{ Sin}[x3] - 15.6222 \text{ Sin}[x2] \text{ Sin}[x3] + 3.42359 \text{ Sin}[x3]^2)$
CS8-O1-FOLN	$-69.0858 + 25.8706 \text{ Log}[x1] + 22.0159 \text{ Log}[x2] + 59.3364 \text{ Log}[x3]$
CS8-O1-FOLNR	$(20881.7 + 3320.68 \text{ Log}[x1] + 13107.1 \text{ Log}[x2] + 9800.06 \text{ Log}[x3]) / (1140.28 - 97.7874 \text{ Log}[x1] + 102.726 \text{ Log}[x2] - 192.526 \text{ Log}[x3])$
CS8-O1-SOLN	$861.546 - 249.435 \text{ Log}[x1] + 19.5013 \text{ Log}[x1]^2 - 72.9782 \text{ Log}[x2] + 5.24073 \text{ Log}[x1] \text{ Log}[x2] - 16.2545 \text{ Log}[x2]^2 - 69.5473 \text{ Log}[x3] + 22.0348 \text{ Log}[x1] \text{ Log}[x3] - 1.59238 \text{ Log}[x2] \text{ Log}[x3] + 32.8321 \text{ Log}[x3]^2$
CS8-O1-SOLNR	$(-1600.31 + 608.411 \text{ Log}[x1] - 53.4357 \text{ Log}[x1]^2 + 690.544 \text{ Log}[x2] - 106.579 \text{ Log}[x1] \text{ Log}[x2] - 56.7454 \text{ Log}[x2]^2 - 382.359 \text{ Log}[x3] + 48.189 \text{ Log}[x1] \text{ Log}[x3] + 104.791 \text{ Log}[x2] \text{ Log}[x3] - 183.62 \text{ Log}[x3]^2) / (-17.174 + 6.59564 \text{ Log}[x1] - 0.587407 \text{ Log}[x1]^2 + 9.31083 \text{ Log}[x2] - 1.39029 \text{ Log}[x1] \text{ Log}[x2] - 0.698194 \text{ Log}[x2]^2 - 16.0809 \text{ Log}[x3] + 1.90223 \text{ Log}[x1] \text{ Log}[x3] + 1.85584 \text{ Log}[x2] \text{ Log}[x3] - 4.21193 \text{ Log}[x3]^2)$
NOTATION	CS8-O2
CS8-O2-L	$-0.161913 - 0.000169284 [x1] + 1.33365 [x2] + 2.03907 [x3]$
CS8-O2-LN	$(-9099.52 + 2.42355 [x1] + 480.522 [x2] + 31463.2 [x3]) / (8374.93 + 5.87661 [x1] - 23371.2 [x2] - 576.207 [x3])$
CS8-O2-SON	$(-1.06474 + 0.000368836 [x1] + 3.1887*10^8 [x1]^2 - 0.697321 [x2] - 0.00121531 [x1] [x2] + 7.90143 [x2]^2 + 3.88423 [x3] - 0.000779298 [x1] [x3] + 2.58773 [x2] [x3] - 0.601544 [x3]^2$
CS8-O2-SONR	$(5.47974*10^6 - 1276.66 [x1] + 0.0902109 [x1]^2 - 2.59031*10^7 [x2] - 1105.55 [x1] [x2] + 9.66269*10^7 [x2]^2 - 4.23768*10^6 [x3] + 1883.88 [x1] [x3] + 7.75058*10^6 [x2] [x3] - 2.61702*10^6 [x3]^2) / (1.13371*10^7 - 2176.35 [x1] + 0.113614 [x1]^2 - 1.18305*10^7 [x2] + 2948.63 [x1] [x2] + 7.76606*10^7 [x2]^2 - 2.23725*10^7 [x3] + 2302.11 [x1] [x3] - 1.92947*10^7 [x2] [x3] + 1.34367*10^7 [x3]^2)$
CS8-O2-TON	$0.748471 - 0.000497874 [x1] - 2.15117*10^7 [x1]^2 + 2.08581*10^11 [x1]^3 - 3.20839 [x2] - 0.00106559 [x1] [x2] + 3.26141*10^7 [x1]^2 [x2] - 7.41009 [x2]^2 + 0.00146437 [x1] [x2]^2 + 111.478 [x2]^3 - 3.2989 \text{ Cos}[x1] \text{ Sin}[x2] + 0.00446856 [x1] [x3] + 9.03065*10^8 [x1]^2 [x3] + 20.5139 [x2] [x3] - 0.00346656 [x1] [x2] [x3] - 103.993 [x2]^2 [x3] - 2.65454 [x3]^2 - 0.00462583 [x1] [x3]^2 + 28.5218 [x2] [x3]^2 + 3.67474 [x3]^3$
CS8-O2-FOTN	$18.7608 - 0.172815 \text{ Cos}[x1] - 18.5391 \text{ Cos}[x2] - 0.443039 \text{ Cos}[x3] + 0.0238901 \text{ Sin}[x1] - 2.41475 \text{ Sin}[x2] + 2.15031 \text{ Sin}[x3]$
CS8-O2-FOTNR	$(12.3052 + 30.2998 \text{ Cos}[x1] - 18.9099 \text{ Cos}[x2] + 0.00245014 \text{ Cos}[x3] - 30.9792 \text{ Sin}[x1] - 1.7451 \text{ Sin}[x2] - 0.00608492 \text{ Sin}[x3]) / (33.4234 - 4.5816 \text{ Cos}[x1] - 32.3015 \text{ Cos}[x2] - 0.0288057 \text{ Cos}[x3] + 4.6736 \text{ Sin}[x1] - 2.92552 \text{ Sin}[x2] - 0.0114868 \text{ Sin}[x3])$
CS8-O2-SOTN	$346.113 + 206.382 \text{ Cos}[x1] + 826.643 \text{ Cos}[x1]^2 + 361.963 \text{ Cos}[x2] - 11.5092 \text{ Cos}[x1] \text{ Cos}[x2] + 378.477 \text{ Cos}[x2]^2 + 522.896 \text{ Cos}[x3] + 10.2185 \text{ Cos}[x1] \text{ Cos}[x3] - 2799.72 \text{ Cos}[x2] \text{ Cos}[x3] + 692.371 \text{ Cos}[x3]^2 - 1.79344 \text{ Sin}[x1] + 112.065 \text{ Cos}[x1] \text{ Sin}[x1] + 11.9158 \text{ Cos}[x2] \text{ Sin}[x1] - 1.45843 \text{ Cos}[x3] \text{ Sin}[x1] + 426.103 \text{ Sin}[x1]^2 + 342.337 \text{ Sin}[x2] - 3.2989 \text{ Cos}[x1] \text{ Sin}[x2] + 362.439 \text{ Cos}[x2] \text{ Sin}[x2] - 622.12 \text{ Cos}[x3] \text{ Sin}[x2] + 2.4493 \text{ Sin}[x1] \text{ Sin}[x2] - 998.513 \text{ Sin}[x2]^2 + 476.843 \text{ Sin}[x3] + 5.06658 \text{ Cos}[x1] \text{ Sin}[x3] - 1524.83 \text{ Cos}[x2] \text{ Sin}[x3] + 1012.13 \text{ Cos}[x3] \text{ Sin}[x3] - 0.717988 \text{ Sin}[x1] \text{ Sin}[x3] - 338.147 \text{ Sin}[x2] \text{ Sin}[x3] - 161.489 \text{ Sin}[x3]^2$
CS8-O2-SOTNR	$(6.15373*10^6 - 873368. \text{ Cos}[x1] + 2.55917*10^6 \text{ Cos}[x1]^2 - 1.91004*10^6 \text{ Cos}[x2] - 2.68963*10^6 \text{ Cos}[x1] \text{ Cos}[x2] - 8.9804*10^6 \text{ Cos}[x2]^2 + 3.56523*10^6 \text{ Cos}[x3] + 210469. \text{ Cos}[x1] \text{ Cos}[x3] - 5.10549*10^6 \text{ Cos}[x2] \text{ Cos}[x3] + 2.49582*10^6 \text{ Cos}[x3]^2 - 2.18875*10^7 \text{ Sin}[x1] - 2.16294*10^6 \text{ Cos}[x1] \text{ Sin}[x1] + 3.10375*10^7 \text{ Cos}[x2] \text{ Sin}[x1] - 1.786481*10^6 \text{ Cos}[x3] \text{ Sin}[x1] + 3.59456*10^6 \text{ Sin}[x1]^2 - 2.03594*10^6 \text{ Sin}[x2] + 1.06371*10^6 \text{ Cos}[x1] \text{ Sin}[x2] - 6.84992*10^6 \text{ Cos}[x2] \text{ Sin}[x2] + 2.33335*10^6 \text{ Cos}[x3] \text{ Sin}[x2] + 3.67331*10^6 \text{ Sin}[x1] \text{ Sin}[x2] + 1.51341*10^7 \text{ Sin}[x2]^2 + 2.89357*10^6 \text{ Sin}[x3] - 3.47287*10^6 \text{ Cos}[x1] \text{ Sin}[x3] + 2.4948*10^6 \text{ Cos}[x2] \text{ Sin}[x3] + 173589. \text{ Cos}[x3] \text{ Sin}[x3] - 8.81812*10^6 \text{ Sin}[x1] \text{ Sin}[x3] - 1.20848*10^7 \text{ Sin}[x2] \text{ Sin}[x3] + 3.65791*10^6 \text{ Sin}[x3]^2) / (-2.83161*10^6 + 19406.3 \text{ Cos}[x1] - 1.43141*10^6 \text{ Cos}[x1]^2 + 417494. \text{ Cos}[x2] - 2.63245*10^6 \text{ Cos}[x1] \text{ Cos}[x2] + 3.30312*10^6 \text{ Cos}[x2]^2 - 920977. \text{ Cos}[x3] - 3.67434*10^6 \text{ Cos}[x1] \text{ Cos}[x3] + 2.46097*10^6 \text{ Cos}[x2] \text{ Cos}[x3] - 823027. \text{ Cos}[x3]^2 + 1.54071*10^7 \text{ Sin}[x1] + 2.18986*10^6 \text{ Cos}[x1] \text{ Sin}[x1] - 2.64996*10^7 \text{ Cos}[x2] \text{ Sin}[x1] + 5.77591*10^6 \text{ Cos}[x3] \text{ Sin}[x1] - 1.40019*10^6 \text{ Sin}[x1]^2 - 1.58901*10^6 \text{ Sin}[x2] + 1.1351*10^7 \text{ Cos}[x1] \text{ Sin}[x2] + 216492. \text{ Cos}[x2] \text{ Sin}[x2] - 775614. \text{ Cos}[x3] \text{ Sin}[x2] - 5.83601*10^6 \text{ Sin}[x1] \text{ Sin}[x2] - 6.13472*10^6 \text{ Sin}[x2]^2 + 668247. \text{ Sin}[x3] + 4.82631*10^6 \text{ Cos}[x1] \text{ Sin}[x3] + 652703. \text{ Cos}[x2] \text{ Sin}[x3] + 3.45586*10^6 \text{ Cos}[x3] \text{ Sin}[x3] + 6.9781*10^6 \text{ Sin}[x1] \text{ Sin}[x3] + 2.31405*10^6 \text{ Sin}[x2] \text{ Sin}[x3] - 2.00858*10^6 \text{ Sin}[x3]^2)$
CS8-O2-FOLN	$4.6161 - 0.347544 \text{ Log}[x1] + 0.253734 \text{ Log}[x2] + 1.09447 \text{ Log}[x3]$
CS8-O2-FOLNR	$(-0.0787832 + 0.0513044 \text{ Log}[x1] + 0.0112032 \text{ Log}[x2] + 0.162951 \text{ Log}[x3]) / (-1.05078 + 0.147808 \text{ Log}[x1] - 0.053971 \text{ Log}[x2] - 0.108558 \text{ Log}[x3])$
CS8-O2-SOLN	$14.0524 - 1.07758 \text{ Log}[x1] - 0.0387908 \text{ Log}[x1]^2 + 5.71676 \text{ Log}[x2] - 0.502417 \text{ Log}[x1] \text{ Log}[x2] + 0.449427 \text{ Log}[x2]^2 + 8.21411 \text{ Log}[x3] - 0.809514 \text{ Log}[x1] \text{ Log}[x3] + 0.237863 \text{ Log}[x2] \text{ Log}[x3] + 0.408757 \text{ Log}[x3]^2$
CS8-O2-SOLNR	$(-1.0964*10^6 + 311793. \text{ Log}[x1] - 22028.8 \text{ Log}[x1]^2 + 75836.7 \text{ Log}[x2] - 5098.39 \text{ Log}[x1] \text{ Log}[x2] + 10272. \text{ Log}[x2]^2 - 24379.1 \text{ Log}[x3] - 10870. \text{ Log}[x1] \text{ Log}[x3] - 5615.6 \text{ Log}[x2] \text{ Log}[x3] - 52010.1 \text{ Log}[x3]^2) / (-1.451*10^6 + 398931. \text{ Log}[x1] - 27320.5 \text{ Log}[x1]^2 + 14203.9 \text{ Log}[x2] + 1266.51 \text{ Log}[x1] \text{ Log}[x2] + 5372.02 \text{ Log}[x2]^2 + 90882.1 \text{ Log}[x3] - 18638.5 \text{ Log}[x1] \text{ Log}[x3] + 1207.75 \text{ Log}[x2] \text{ Log}[x3] - 2711.44 \text{ Log}[x3]^2)$
NOTATION	CS9-O
CS9-O-L	$1.87061 - 0.0114886 [x1] + 18.6868 [x2] + 8.59617 [x3]$
CS9-O-LN	$(1025.43 - 4.62856 [x1] + 3190.93 [x2] + 2843.28 [x3]) / (388.229 - 0.307063 [x1] - 396.992 [x2] + 109.113 [x3])$

CS9-O-SON	$2.45847 - 0.00189348 [x1] - 0.0000472941 [x1]^2 + 6.83888 [x2] - 0.00445045 [x1] [x2] + 26.9872 [x2]^2 + 5.36516 [x3] + 0.0504367 [x1] [x3] + 14.1845 [x2] [x3] - 33.5635 [x3]^2$
CS9-O-SONR	$(-4.83879*10^7 + 334703. [x1] - 970.747 [x1]^2 + 4.31651*10^8 [x2] + 173035. [x1] [x2] - 1.3449*10^9 [x2]^2 - 2.481*10^8 [x3] + 1.68804*10^6 [x1] [x3] + 3.16572*10^8 [x2] [x3] - 3.47965*10^8 [x3]^2) / (-1.34979*10^7 + 116309. [x1] - 59.305 [x1]^2 + 9.65931*10^7 [x2] - 254863. [x1] [x2] - 2.28429*10^8 [x2]^2 - 5.53139*10^7 [x3] + 190145. [x1] [x3] + 1.32223*10^8 [x2] [x3] - 4.64206*10^7 [x3]^2)$
CS9-O-TON	$5.00377 - 0.0297535 [x1] - 0.000125448 [x1]^2 + 8.46711*10^{-7} [x1]^3 - 5.28511 [x2] + 0.317552 [x1] [x2] - 0.001358 [x1]^2 [x2] - 24.4649 [x2]^2 + 0.148298 [x1] [x2]^2 + 40.943 [x2]^3 - 3.66636 [x3] + 0.120226 [x1] [x3] - 0.000284089 [x1]^2 [x3] + 44.1969 [x2] [x3] + 0.216464 [x1] [x2] [x3] + 23.4036 [x2]^2 [x3] - 50.0952 [x3]^2 - 0.089525 [x1] [x3]^2 - 348.211 [x2] [x3]^2 + 371.271 [x3]^3$
CS9-O-FOTN	$33.6794 + 3.25945 \text{Cos}[x1] - 53.0319 \text{Cos}[x2] + 17.9063 \text{Cos}[x3] - 0.235264 \text{Sin}[x1] + 8.38796 \text{Sin}[x2] + 10.1466 \text{Sin}[x3]$
CS9-O-FOTNR	$(-2.74413 - 1.11619 \text{Cos}[x1] + 9.37171 \text{Cos}[x2] - 4.33852 \text{Cos}[x3] + 1.86827 \text{Sin}[x1] + 1.39322 \text{Sin}[x2] + 1.19265 \text{Sin}[x3]) / (2.25733 - 0.234437 \text{Cos}[x1] - 0.888403 \text{Cos}[x2] - 0.778967 \text{Cos}[x3] + 0.32135 \text{Sin}[x1] - 0.694225 \text{Sin}[x2] + 0.0858866 \text{Sin}[x3])$
CS9-O-SOTN	$-3057. - 2533.53 \text{Cos}[x1] - 5313.11 \text{Cos}[x1]^2 - 3210.44 \text{Cos}[x2] - 979.447 \text{Cos}[x1] \text{Cos}[x2] - 3367.12 \text{Cos}[x2]^2 - 3096.24 \text{Cos}[x3] - 2690.49 \text{Cos}[x1] \text{Cos}[x3] + 27771. \text{Cos}[x2] \text{Cos}[x3] - 3135.89 \text{Cos}[x3]^2 + 2551.31 \text{Sin}[x1] - 4579.93 \text{Cos}[x1] \text{Sin}[x1] + 1124.17 \text{Cos}[x2] \text{Sin}[x1] + 2824.07 \text{Cos}[x3] \text{Sin}[x1] - 5099.13 \text{Sin}[x1]^2 - 2728.05 \text{Sin}[x2] - 114.567 \text{Cos}[x1] \text{Sin}[x2] - 3039.53 \text{Cos}[x2] \text{Sin}[x2] + 5914.08 \text{Cos}[x3] \text{Sin}[x2] + 142.708 \text{Sin}[x1] \text{Sin}[x2] + 8106.65 \text{Sin}[x2]^2 - 1376.24 \text{Sin}[x3] - 283.03 \text{Cos}[x1] \text{Sin}[x3] + 3062.18 \text{Cos}[x2] \text{Sin}[x3] - 1345.98 \text{Cos}[x3] \text{Sin}[x3] + 285.278 \text{Sin}[x1] \text{Sin}[x3] + 651.119 \text{Sin}[x2] \text{Sin}[x3] + 7533.46 \text{Sin}[x3]^2$
CS9-O-SOTNR	$(-3.92521*10^8 + 1.53157*10^8 \text{Cos}[x1] - 1.60347*10^8 \text{Cos}[x1]^2 + 4.97553*10^8 \text{Cos}[x2] + 9.78375*10^8 \text{Cos}[x1] \text{Cos}[x2] + 1.27289*10^9 \text{Cos}[x2]^2 - 7.29291*10^8 \text{Cos}[x3] + 2.16472*10^8 \text{Cos}[x1] \text{Cos}[x3] + 1.36872*10^8 \text{Cos}[x2] \text{Cos}[x3] - 1.05888*10^9 \text{Cos}[x3]^2 - 7.41999*10^7 \text{Sin}[x1] - 8.90709*10^8 \text{Cos}[x1] \text{Sin}[x1] - 2.76628*10^8 \text{Cos}[x2] \text{Sin}[x1] + 4.66975*10^8 \text{Cos}[x3] \text{Sin}[x1] - 2.32174*10^8 \text{Sin}[x1]^2 + 3.8723*10^8 \text{Sin}[x2] - 2.17496*10^9 \text{Cos}[x1] \text{Sin}[x2] - 9.24341*10^8 \text{Cos}[x2] \text{Sin}[x2] + 6.21756*10^8 \text{Cos}[x3] \text{Sin}[x2] - 1.89656*10^9 \text{Sin}[x1] \text{Sin}[x2] - 1.66541*10^9 \text{Sin}[x2]^2 + 1.08192*10^9 \text{Sin}[x3] - 1.76775*10^9 \text{Cos}[x1] \text{Sin}[x3] + 1.35933*10^9 \text{Cos}[x2] \text{Sin}[x3] + 9.96431*10^8 \text{Cos}[x3] \text{Sin}[x3] - 2.33182*10^9 \text{Sin}[x1] \text{Sin}[x3] - 1.93759*10^9 \text{Sin}[x2] \text{Sin}[x3] + 6.66359*10^8 \text{Sin}[x3]^2) / (4.97674*10^8 + 6.31884*10^8 \text{Cos}[x1] + 9.12452*10^8 \text{Cos}[x1]^2 - 5.02313*10^8 \text{Cos}[x2] + 3.9769*10^8 \text{Cos}[x1] \text{Cos}[x2] - 1.4037*10^9 \text{Cos}[x2]^2 + 2.10347*10^8 \text{Cos}[x3] - 5.98445*10^7 \text{Cos}[x1] \text{Cos}[x3] - 9.15476*10^8 \text{Cos}[x2] \text{Cos}[x3] - 6.83767*10^7 \text{Cos}[x3]^2 + 3.7223*10^8 \text{Sin}[x1] + 3.05938*10^8 \text{Cos}[x1] \text{Sin}[x1] - 2.64988*10^9 \text{Cos}[x2] \text{Sin}[x1] - 6.40091*10^8 \text{Cos}[x3] \text{Sin}[x1] - 4.14778*10^8 \text{Sin}[x1]^2 + 1.63137*10^9 \text{Sin}[x2] - 4.88708*10^9 \text{Cos}[x1] \text{Sin}[x2] + 1.13633*10^9 \text{Cos}[x2] \text{Sin}[x2] + 1.55664*10^9 \text{Cos}[x3] \text{Sin}[x2] + 4.86541*10^9 \text{Sin}[x1] \text{Sin}[x2] + 1.90137*10^9 \text{Sin}[x2]^2 + 1.8855*10^8 \text{Sin}[x3] - 9.29985*10^8 \text{Cos}[x1] \text{Sin}[x3] + 8.39588*10^8 \text{Cos}[x2] \text{Sin}[x3] + 1.05482*10^8 \text{Cos}[x3] \text{Sin}[x3] + 7.34043*10^8 \text{Sin}[x1] \text{Sin}[x3] + 6.72778*10^8 \text{Sin}[x2] \text{Sin}[x3] + 5.66051*10^8 \text{Sin}[x3]^2)$
CS9-O-FOLN	$20.8118 - 1.71118 \text{Log}[x1] + 3.25274 \text{Log}[x2] + 0.841874 \text{Log}[x3]$
CS9-O-FOLNR	$(5713.73 - 820.72 \text{Log}[x1] - 7.52008 \text{Log}[x2] + 274.444 \text{Log}[x3]) / (417.637 - 85.7276 \text{Log}[x1] - 167.258 \text{Log}[x2] + 19.295 \text{Log}[x3])$
CS9-O-SOLN	$-22.0274 + 18.0308 \text{Log}[x1] - 1.85005 \text{Log}[x1]^2 + 13.6973 \text{Log}[x2] - 0.0907937 \text{Log}[x1] \text{Log}[x2] + 2.66101 \text{Log}[x2]^2 - 1.45112 \text{Log}[x3] + 0.665054 \text{Log}[x1] \text{Log}[x3] + 0.237988 \text{Log}[x2] \text{Log}[x3] + 0.125756 \text{Log}[x3]^2$
CS9-O-SOLNR	$(9226.03 - 3068.42 \text{Log}[x1] + 229.836 \text{Log}[x1]^2 - 1259.4 \text{Log}[x2] - 248.645 \text{Log}[x1] \text{Log}[x2] - 114.064 \text{Log}[x2]^2 - 291.941 \text{Log}[x3] + 2.48311 \text{Log}[x1] \text{Log}[x3] + 101.66 \text{Log}[x2] \text{Log}[x3] - 70.4194 \text{Log}[x3]^2) / (390.008 - 163.437 \text{Log}[x1] + 14.3741 \text{Log}[x1]^2 - 202.621 \text{Log}[x2] + 28.5322 \text{Log}[x1] \text{Log}[x2] - 55.3072 \text{Log}[x2]^2 - 61.227 \text{Log}[x3] + 8.64552 \text{Log}[x1] \text{Log}[x3] + 31.1755 \text{Log}[x2] \text{Log}[x3] - 9.8847 \text{Log}[x3]^2)$
NOTATION	CS10-O
CS10-O-L	$0.251182 - 0.00144178 [x1] + 6.62437 [x2] + 0.435294 [x3]$
CS10-O-LN	$(21657.7 - 78.8542 [x1] + 123533. [x2] + 12662.4 [x3]) / (50907.5 - 39.4659 [x1] - 116947. [x2] - 2428.04 [x3])$
CS10-O-SON	$0.453663 - 0.000881992 [x1] - 3.16061*10^{-6} [x1]^2 + 1.3658 [x2] + 0.00275818 [x1] [x2] + 22.4719 [x2]^2 + 0.400263 [x3] + 0.000512137 [x1] [x3] + 1.84199 [x2] [x3] - 0.548697 [x3]^2$
CS10-O-SONR	$(-1.51743*10^6 - 4313.8 [x1] + 25.0776 [x1]^2 + 6.13139*10^7 [x2] - 164735. [x1] [x2] - 3.98271*10^7 [x2]^2 + 145643. [x3] - 7244.03 [x1] [x3] + 1.92314*10^7 [x2] [x3] - 365824. [x3]^2) / (-1.69699*10^6 - 14057.4 [x1] + 14.9905 [x1]^2 + 9.96623*10^7 [x2] - 45528.1 [x1] [x2] - 3.36541*10^8 [x2]^2 - 144811. [x3] - 3484.54 [x1] [x3] + 5.82639*10^6 [x2] [x3] - 177545. [x3]^2)$
CS10-O-TON	$0.342304 - 0.000712382 [x1] - 4.30783*10^{-6} [x1]^2 + 5.43672*10^{-9} [x1]^3 + 3.70106 [x2] + 0.000404573 [x1] [x2] - 0.0000303288 [x1]^2 [x2] + 14.208 [x2]^2 + 0.0289683 [x1] [x2]^2 - 18.2639 [x2]^3 + 0.849465 [x3] - 0.00041336 [x1] [x3] + 9.92063*10^{-6} [x1]^2 [x3] - 13.3843 [x2] [x3] + 0.00833333 [x1] [x2] [x3] + 49.4444 [x2]^2 [x3] + 0.3869112 [x3]^2 - 0.00704365 [x1] [x3]^2 + 10.1389 [x2] [x3]^2 - 2.0873 [x3]^3$
CS10-O-FOTN	$41.916 - 0.0584334 \text{Cos}[x1] - 43.2762 \text{Cos}[x2] + 1.50779 \text{Cos}[x3] - 0.126368 \text{Sin}[x1] + 2.32259 \text{Sin}[x2] + 0.765818 \text{Sin}[x3]$
CS10-O-FOTNR	$(-12467.5 - 33.6798 \text{Cos}[x1] + 11945. \text{Cos}[x2] + 540.7 \text{Cos}[x3] - 26.4287 \text{Sin}[x1] + 1519.46 \text{Sin}[x2] + 193.773 \text{Sin}[x3]) / (-9530.12 - 23.0435 \text{Cos}[x1] + 9256.82 \text{Cos}[x2] + 490.338 \text{Cos}[x3] - 13.5252 \text{Sin}[x1] - 24.3464 \text{Sin}[x2] + 115.817 \text{Sin}[x3])$
CS10-O-SOTN	$132.913 + 121.111 \text{Cos}[x1] + 166.77 \text{Cos}[x1]^2 + 134.487 \text{Cos}[x2] - 0.912689 \text{Cos}[x1] \text{Cos}[x2] + 136.076 \text{Cos}[x2]^2 + 139.074 \text{Cos}[x3] - 2.13561 \text{Cos}[x1] \text{Cos}[x3] - 970.6 \text{Cos}[x2] \text{Cos}[x3] + 145.362 \text{Cos}[x3]^2 - 122.236 \text{Sin}[x1] + 103.888 \text{Cos}[x1] \text{Sin}[x1] - 4.3683 \text{Cos}[x2] \text{Sin}[x1] + 4.49655 \text{Cos}[x3] \text{Sin}[x1] + 163.193 \text{Sin}[x1]^2 + 59.2229 \text{Sin}[x2] + 0.397924 \text{Cos}[x1] \text{Sin}[x2] + 57.3592 \text{Cos}[x2] \text{Sin}[x2] - 111.862 \text{Cos}[x3] \text{Sin}[x2] - 0.643514 \text{Sin}[x1] \text{Sin}[x2] - 272.449 \text{Sin}[x2]^2 + 136.657 \text{Sin}[x3] - 0.464571 \text{Cos}[x1] \text{Sin}[x3] - 285.077 \text{Cos}[x2] \text{Sin}[x3] + 149.187 \text{Cos}[x3] \text{Sin}[x3] + 1.01049 \text{Sin}[x1] \text{Sin}[x3] - 29.7852 \text{Sin}[x2] \text{Sin}[x3] - 256.588 \text{Sin}[x3]^2$
CS10-O-SOTNR	$(1.65154 - 0.200336 \text{Cos}[x1] - 0.247817 \text{Cos}[x1]^2 - 0.513085 \text{Cos}[x2] - 1.26013 \text{Cos}[x1] \text{Cos}[x2] - 2.64677 \text{Cos}[x2]^2 + 2.16864 \text{Cos}[x3] + 0.447981 \text{Cos}[x1] \text{Cos}[x3] + 0.0471976 \text{Cos}[x2] \text{Cos}[x3] + 2.59939 \text{Cos}[x3]^2 - 1.29838 \text{Sin}[x1] + 0.460317 \text{Cos}[x1] \text{Sin}[x1] + 0.0531127 \text{Cos}[x2] \text{Sin}[x1] - 1.21455 \text{Cos}[x3] \text{Sin}[x1] + 2.89936 \text{Sin}[x1]^2 + 20.4875 \text{Sin}[x2] - 10.4561 \text{Cos}[x1] \text{Sin}[x2] + 20.1084 \text{Cos}[x2] \text{Sin}[x2] + 20.1454 \text{Cos}[x3] \text{Sin}[x2] - 11.5998 \text{Sin}[x1] \text{Sin}[x2] + 5.29832 \text{Sin}[x2]^2 + 2.61784 \text{Sin}[x3] + 1.05522 \text{Cos}[x1] \text{Sin}[x3] + 2.18985 \text{Cos}[x2] \text{Sin}[x3] + 3.00055 \text{Cos}[x3] \text{Sin}[x3] + 0.0247163 \text{Sin}[x1] \text{Sin}[x3] + 4.81525 \text{Sin}[x2] \text{Sin}[x3] + 0.0521569 \text{Sin}[x3]^2) / (2.2813 + 0.576247 \text{Cos}[x1] + 0.488278 \text{Cos}[x1]^2 + 4.23255 \text{Cos}[x2] + 1.49316 \text{Cos}[x1] \text{Cos}[x2] + 6.15625 \text{Cos}[x2]^2 + 1.88422 \text{Cos}[x3] + 0.36157 \text{Cos}[x1] \text{Cos}[x3] + 3.7926 \text{Cos}[x2] \text{Cos}[x3] + 1.55397 \text{Cos}[x3]^2 - 1.14143 \text{Sin}[x1] + 0.461044 \text{Cos}[x1] \text{Sin}[x1] - 2.35283 \text{Cos}[x2] \text{Sin}[x1] - 1.0289 \text{Cos}[x3] \text{Sin}[x1] + 2.79302 \text{Sin}[x1]^2 - 16.686 \text{Sin}[x2] - 7.38075 \text{Cos}[x1] \text{Sin}[x2] - 16.3467 \text{Cos}[x2] \text{Sin}[x2] - 16.327 \text{Cos}[x3] \text{Sin}[x2] + 12.1179 \text{Sin}[x1] \text{Sin}[x2] - 2.87495 \text{Sin}[x2]^2 - 0.171404 \text{Sin}[x3] - 0.221273 \text{Cos}[x1] \text{Sin}[x3] + 0.236108 \text{Cos}[x2] \text{Sin}[x3] - 0.466636 \text{Cos}[x3] \text{Sin}[x3] + 0.831807 \text{Sin}[x1] \text{Sin}[x3] - 2.70476 \text{Sin}[x2] \text{Sin}[x3] + 1.72732 \text{Sin}[x3]^2)$
CS10-O-FOLN	$3.22177 - 0.188847 \text{Log}[x1] + 0.577315 \text{Log}[x2] + 0.0729146 \text{Log}[x3]$
CS10-O-FOLNR	$(12313.7 - 1781.66 \text{Log}[x1] + 13.799 \text{Log}[x2] + 387.706 \text{Log}[x3]) / (2911.64 - 1229.97 \text{Log}[x1] - 3084.04 \text{Log}[x2] + 134.397 \text{Log}[x3])$
CS10-O-SOLN	$1.8152 + 1.57951 \text{Log}[x1] - 0.17023 \text{Log}[x1]^2 + 2.93379 \text{Log}[x2] + 0.0371877 \text{Log}[x1] \text{Log}[x2] + 0.505582 \text{Log}[x2]^2 + 0.118748 \text{Log}[x3] + 0.0162065 \text{Log}[x1] \text{Log}[x3] + 0.0239209 \text{Log}[x2] \text{Log}[x3] + 0.0179176 \text{Log}[x3]^2$
CS10-O-SOLNR	$(31.3262 + 1.1301 \text{Log}[x1] - 0.351823 \text{Log}[x1]^2 + 20.5004 \text{Log}[x2] - 0.721451 \text{Log}[x1] \text{Log}[x2] + 2.80885 \text{Log}[x2]^2 + 4.67867 \text{Log}[x3] - 0.62241 \text{Log}[x1] \text{Log}[x3] - 0.036012 \text{Log}[x2] \text{Log}[x3] + 0.153038 \text{Log}[x3]^2) / (29.6691 - 6.97013 \text{Log}[x1] + 0.395307 \text{Log}[x1]^2 + 7.42315 \text{Log}[x2] - 1.41839 \text{Log}[x1] \text{Log}[x2] + 0.103803 \text{Log}[x2]^2 + 0.830043 \text{Log}[x3] - 0.615859 \text{Log}[x1] \text{Log}[x3] - 1.49745 \text{Log}[x2] \text{Log}[x3] - 0.016376 \text{Log}[x3]^2)$
NOTATION	CS11-O
CS11-O-L	$1.20594 - 0.000842242 [x1] + 8.84648 [x2] + 0.377371 [x3]$
CS11-O-LN	$(11512.2 + 28.1025 [x1] + 111732. [x2] + 20233.4 [x3]) / (12214.6 + 21.3522 [x1] - 16048.8 [x2] + 7136.86 [x3])$
CS11-O-SON	$0.860886 + 0.00189385 [x1] - 3.49112*10^{-6} [x1]^2 + 6.84863 [x2] - 0.00890827 [x1] [x2] + 19.4497 [x2]^2 + 1.31281 [x3] - 0.00273723 [x1] [x3] - 4.85873 [x2] [x3] - 0.213422 [x3]^2$
CS11-O-SONR	$(-278216. + 2533.55 [x1] - 2.7704 [x1]^2 + 6.62198*10^6 [x2] - 4176.86 [x1] [x2] - 5.99393*10^7 [x2]^2 - 5960.26 [x3] + 205.525 [x1] [x3] - 361857. [x2] [x3] - 88239.9 [x3]^2) / (-126615. + 1614.71 [x1] - 1.03956 [x1]^2 + 2.59297*10^6 [x2] - 6407.37 [x1] [x2] - 2.32609*10^7 [x2]^2 - 31090.2 [x3] - 9.36626 [x1] [x3] + 226784. [x2] [x3] - 33059.4 [x3]^2)$
CS11-O-TON	$0.863228 + 0.00237367 [x1] + 1.45859*10^{-6} [x1]^2 - 1.53188*10^{-8} [x1]^3 + 8.5126 [x2] - 0.0341579 [x1] [x2] + 2.67996*10^{-6} [x1]^2 [x2] + 35.1865 [x2]^2 + 0.108444 [x1] [x2]^2 - 68.9457 [x2]^3 + 0.886979 [x3] - 0.00256499 [x1] [x3] + 6.15732*10^{-6} [x1]^2 [x3] + 0.300029 [x2] [x3] + 0.0184408 [x1] [x2] [x3] - 52.4859 [x2]^2 [x3] + 0.520234 [x3]^2 - 0.00578699 [x1] [x3]^2 + 1.53804 [x2] [x3]^2 - 0.0381871 [x3]^3$
CS11-O-FOTN	$31.9759 - 0.383414 \text{Cos}[x1] - 31.2254 \text{Cos}[x2] + 0.0823114 \text{Cos}[x3] - 0.0819917 \text{Sin}[x1] + 6.29993 \text{Sin}[x2] + 0.417234 \text{Sin}[x3]$

CS11-O-FOTNR	$(120.894 + 0.162011 \cos[x1] - 120.665 \cos[x2] + 0.0701416 \cos[x3] + 0.0798184 \sin[x1] - 3.94732 \sin[x2] - 0.0678742 \sin[x3]) / (39.5546 + 0.117583 \cos[x1] - 39.3533 \cos[x2] - 0.0279373 \cos[x3] + 0.0499025 \sin[x1] - 0.820916 \sin[x2] - 0.079732 \sin[x3])$
CS11-O-SOTN	$589.179 - 661.849 \cos[x1] + 714.284 \cos[x1]^2 + 593.843 \cos[x2] - 666.271 \cos[x1] \cos[x2] + 598.537 \cos[x2]^2 + 686.922 \cos[x3] + 3.29596 \cos[x1] \cos[x3] - 5294.32 \cos[x2] \cos[x3] + 783.506 \cos[x3]^2 + 18.1328 \sin[x1] + 144.658 \cos[x1] \sin[x1] + 119.493 \cos[x2] \sin[x1] + 3.93067 \cos[x3] \sin[x1] + 1433.31 \sin[x1]^2 + 212.959 \sin[x2] - 56.3309 \cos[x1] \sin[x2] + 204.527 \cos[x2] \sin[x2] - 451.477 \cos[x3] \sin[x2] + 7.98157 \sin[x1] \sin[x2] - 1477.92 \sin[x2]^2 + 563.878 \sin[x3] + 0.201012 \cos[x1] \sin[x3] - 1442.89 \cos[x2] \sin[x3] + 895.133 \cos[x3] \sin[x3] + 0.812013 \sin[x1] \sin[x3] - 129.737 \sin[x2] \sin[x3] - 1468.38 \sin[x3]^2$
CS11-O-SOTNR	$(4.02378*10^6 - 1.56609*10^7 \cos[x1] + 2.45883*10^7 \cos[x1]^2 + 9.07528*10^6 \cos[x2] - 1.95503*10^7 \cos[x1] \cos[x2] + 1.40521*10^7 \cos[x2]^2 - 1.39366*10^7 \cos[x3] - 4.0127*10^7 \cos[x1] \cos[x3] - 1.30813*10^7 \cos[x2] \cos[x3] - 3.15744*10^7 \cos[x3]^2 + 6.01959*10^7 \sin[x1] - 6.34565*10^7 \cos[x1] \sin[x1] + 3.74733*10^7 \cos[x1] \sin[x1] - 9.02454*10^6 \cos[x3] \sin[x1] - 2.05645*10^7 \sin[x1]^2 - 2.70613*10^7 \sin[x2] - 8.76674*10^7 \cos[x1] \sin[x2] - 2.60929*10^7 \cos[x2] \sin[x2] - 3.94473*10^7 \cos[x3] \sin[x2] - 1.87729*10^8 \sin[x1] \sin[x2] - 1.00283*10^7 \sin[x2]^2 + 1.01335*10^8 \sin[x3] + 3.21045*10^8 \cos[x1] \sin[x3] + 1.09962*10^8 \cos[x2] \sin[x3] + 9.68718*10^7 \cos[x3] \sin[x3] - 4.43289*10^6 \sin[x1] \sin[x3] + 4.73597*10^7 \sin[x2] \sin[x3] + 3.55981*10^7 \sin[x3]^2 / (1.05062*10^7 + 1.31488*10^7 \cos[x1] - 3.0226*10^7 \cos[x1]^2 - 5.71932*10^6 \cos[x2] + 3.7197*10^7 \cos[x1] \cos[x2] - 2.16036*10^7 \cos[x2]^2 - 2.87474*10^7 \cos[x3] - 2.68331*10^8 \cos[x1] \cos[x3] - 3.146*10^7 \cos[x2] \cos[x3] - 5.96274*10^7 \cos[x3]^2 + 1.2184*10^7 \sin[x1] + 2.71347*10^6 \cos[x1] \sin[x1] + 1.15813*10^8 \cos[x2] \sin[x1] - 2.05096*10^7 \cos[x3] \sin[x1] + 4.07322*10^7 \sin[x1]^2 - 1.85471*10^7 \sin[x2] + 9.15744*10^7 \cos[x1] \sin[x2] - 2.25835*10^7 \cos[x2] \sin[x2] - 5.23251*10^7 \cos[x3] \sin[x2] - 3.83656*10^8 \sin[x1] \sin[x2] + 3.21098*10^7 \sin[x2]^2 + 5.38876*10^7 \sin[x3] + 1.15605*10^8 \cos[x1] \sin[x3] + 2.37438*10^7 \cos[x2] \sin[x3] + 2.68331*10^7 \cos[x3] \sin[x3] - 9.32161*10^6 \sin[x1] \sin[x3] + 2.82455*10^7 \sin[x2] \sin[x3] + 7.01337*10^7 \sin[x3]^2)$
CS11-O-FOLN	$4.25238 - 0.114716 \log[x1] + 0.630051 \log[x2] + 0.102734 \log[x3]$
CS11-O-FOLNR	$(4015.87 + 321.938 \log[x1] - 1676.71 \log[x2] + 1573.97 \log[x3]) / (-2702.3 + 346.217 \log[x1] - 2340.15 \log[x2] + 620.524 \log[x3])$
CS11-O-SOLN	$5.89864 + 0.762761 \log[x1] - 0.126814 \log[x1]^2 + 3.34653 \log[x2] - 0.0902669 \log[x1] \log[x2] + 0.442772 \log[x2]^2 + 0.38678 \log[x3] - 0.0855129 \log[x1] \log[x3] - 0.0745112 \log[x2] \log[x3] + 0.0253648 \log[x3]^2$
CS11-O-SOLNR	$(-7405.89 + 1485.56 \log[x1] - 183.686 \log[x1]^2 - 2212.49 \log[x2] - 203.088 \log[x1] \log[x2] - 505.449 \log[x2]^2 + 43.0452 \log[x3] + 0.303946 \log[x1] \log[x3] - 6.02522 \log[x2] \log[x3] + 22.4723 \log[x3]^2) / (-2280.91 + 462.786 \log[x1] - 79.0686 \log[x1]^2 - 482.679 \log[x2] - 167.886 \log[x1] \log[x2] - 190.77 \log[x2]^2 + 65.4047 \log[x3] - 3.00364 \log[x1] \log[x3] + 11.3626 \log[x2] \log[x3] + 10.1023 \log[x3]^2)$
NOTATION	CS12-O1
CS12-O1-L	$451.961 - 111.656 [x1] - 15.5536 [x2] + 80.5217 [x3]$
CS12-O1-LN	$(1600.97 - 117.493 [x1] - 320.795 [x2] + 723.95 [x3]) / (3.68603 + 0.485964 [x1] - 0.973039 [x2] + 0.689693 [x3])$
CS12-O1-SON	$467.721 - 98.1342 [x1] + 1.54016 [x1]^2 + 57.4265 [x2] - 37.5645 [x1] [x2] - 21.7474 [x2]^2 + 117.685 [x3] - 9.70768 [x1] [x3] + 56.987 [x2] [x3] - 37.8996 [x3]^2$
CS12-O1-SONR	$(5.4976 + 68.419 [x1] - 147.207 [x1]^2 - 4.78413 [x2] + 25.0111 [x1] [x2] - 17.8943 [x2]^2 + 74.4273 [x3] + 32.2713 [x1] [x3] - 9.00437 [x2] [x3] - 38.5109 [x3]^2) / (0.0117603 - 0.0349209 [x1] - 0.316558 [x1]^2 + 0.0292642 [x2] - 0.0495718 [x1] [x2] - 0.0584004 [x2]^2 + 0.413368 [x3] + 0.159041 [x1] [x3] + 0.0581923 [x2] [x3] - 0.23618 [x3]^2)$
CS12-O1-TON	$467.47 - 39.5951 [x1] + 2.92493 [x1]^2 - 20.0114 [x1]^3 + 14.4604 [x2] - 6.0832 [x1] [x2] - 1.64961 [x1]^2 [x2] - 15.7949 [x2]^2 - 25.4768 [x1] [x2]^2 + 13.242 [x2]^3 + 47.3894 [x3] - 20.7727 [x1] [x3] + 29.1811 [x1]^2 [x3] + 25.5057 [x2] [x3] + 29.9393 [x1] [x2] [x3] + 29.1811 [x2]^2 [x3] - 36.5148 [x3]^2 - 25.4768 [x1] [x3]^2 - 1.64961 [x2] [x3]^2 + 24.2311 [x3]^3$
CS12-O1-FOTN	$365.718 - 0.0958139 \cos[x1] + 3.0546 \cos[x2] + 100.339 \cos[x3] - 139.028 \sin[x1] + 31.4459 \sin[x2] + 164.776 \sin[x3]$
CS12-O1-FOTNR	$(-157.756 + 429.993 \cos[x1] + 85.439 \cos[x2] + 776.737 \cos[x3] - 81.8429 \sin[x1] - 292.042 \sin[x2] - 16.2092 \sin[x3]) / (0.373035 + 0.838453 \cos[x1] + 0.00162818 \cos[x2] + 1.21359 \cos[x3] + 0.339726 \sin[x1] - 0.962061 \sin[x2] - 0.625617 \sin[x3])$
CS12-O1-SOTN	$60.7754 + 37.3454 \cos[x1] + 51.0848 \cos[x1]^2 + 64.9164 \cos[x2] + 11.897 \cos[x1] \cos[x2] + 76.9012 \cos[x2]^2 + 58.4406 \cos[x3] - 5.73472 \cos[x1] \cos[x3] + 39.2186 \cos[x2] \cos[x3] + 72.6253 \cos[x3]^2 - 34.1501 \sin[x1] + 10.269 \cos[x1] \sin[x1] - 63.7706 \cos[x2] \sin[x1] - 63.7706 \cos[x3] \sin[x1] + 108.402 \sin[x1]^2 + 21.9792 \sin[x2] + 79.0787 \cos[x1] \sin[x2] - 79.3105 \cos[x2] \sin[x2] + 79.0787 \cos[x3] \sin[x2] - 50.874 \sin[x1] \sin[x2] + 60.4866 \sin[x2]^2 + 41.8277 \sin[x3] + 76.7693 \cos[x1] \sin[x3] + 76.7693 \cos[x2] \sin[x3] - 7.75658 \cos[x3] \sin[x3] + 10.922 \sin[x1] \sin[x3] + 78.304 \sin[x2] \sin[x3] + 71.4314 \sin[x3]^2$
CS12-O1-SOTNR	$(-1.98123*10^8 + 9.54733*10^7 \cos[x1] + 1.16627*10^8 \cos[x1]^2 - 8.90454*10^7 \cos[x2] + 1.66622*10^8 \cos[x1] \cos[x2] - 4.7415*10^7 \cos[x2]^2 - 2.74532*10^8 \cos[x3] - 1.88647*10^7 \cos[x1] \cos[x3] - 2.03383*10^8 \cos[x2] \cos[x3] - 2.12318*10^8 \cos[x3]^2 - 3.50207*10^8 \sin[x1] - 7.01659*10^7 \cos[x1] \sin[x1] - 2.73249*10^8 \cos[x2] \sin[x1] - 2.73249*10^8 \cos[x3] \sin[x1] - 3.14749*10^8 \sin[x1]^2 + 3.16105*10^8 \sin[x2] + 1.59866*10^8 \cos[x1] \sin[x2] + 1.86272*10^8 \cos[x2] \sin[x2] + 1.59866*10^8 \cos[x3] \sin[x2] + 3.24737*10^8 \sin[x1] \sin[x2] - 1.50708*10^8 \sin[x2]^2 - 1.48771*10^8 \sin[x3] - 2.96306*10^6 \cos[x1] \sin[x3] - 2.96306*10^6 \cos[x2] \sin[x3] - 1.90064*10^8 \cos[x3] \sin[x3] - 2.53116*10^8 \sin[x1] \sin[x3] + 1.41468*10^8 \sin[x2] \sin[x3] + 1.41949*10^7 \sin[x3]^2 / (-1.54263*10^8 + 3.5483*10^7 \cos[x1] + 3.75423*10^7 \cos[x1]^2 - 5.66071*10^7 \cos[x2] + 1.16823*10^8 \cos[x1] \cos[x2] - 4.43281*10^7 \cos[x2]^2 - 5.06138*10^7 \cos[x3] + 1.22816*10^8 \cos[x1] \cos[x3] + 3.07261*10^7 \cos[x2] \cos[x3] - 3.9*10^7 \cos[x3]^2 + 8.6064*10^7 \sin[x1] + 7.03123*10^7 \cos[x1] \sin[x1] + 2.96933*10^7 \cos[x2] \sin[x1] + 2.96933*10^7 \cos[x3] \sin[x1] - 1.91806*10^8 \sin[x1]^2 + 1.10563*10^8 \sin[x2] + 3.41746*10^7 \cos[x1] \sin[x2] + 9.59532*10^7 \cos[x2] \sin[x2] + 3.41746*10^7 \cos[x3] \sin[x2] + 1.72127*10^8 \sin[x1] \sin[x2] - 1.09935*10^8 \sin[x2]^2 - 8.54593*10^7 \sin[x3] + 5.52421*10^7 \cos[x1] \sin[x3] + 5.52421*10^7 \cos[x2] \sin[x3] + 3.33264*10^7 \cos[x3] \sin[x3] - 1.02545*10^8 \sin[x1] \sin[x3] - 9.14107*10^7 \sin[x2] \sin[x3] - 1.15263*10^8 \sin[x3]^2)$
CS12-O1-FOLN	$250.413 - 264.44 \log[3 + x1] + 99.9729 \log[3 + x2] + 332.948 \log[3 + x3]$
CS12-O1-FOLNR	$(334.318 - 161.656 \log[3 + x1] - 121.833 \log[3 + x2] + 170.947 \log[3 + x3]) / (0.983758 - 0.0741898 \log[3 + x1] - 0.41197 \log[3 + x2] + 0.0321328 \log[3 + x3])$
CS12-O1-SOLN	$-58.3689 + 308.898 \log[3 + x1] - 109.724 \log[3 + x1]^2 + 480.845 \log[3 + x2] - 320.946 \log[3 + x1] \log[3 + x2] - 224.92 \log[3 + x2]^2 - 12.308 \log[3 + x3] - 6.40404 \log[3 + x1] \log[3 + x3] + 478.35 \log[3 + x2] \log[3 + x3] - 91.247 \log[3 + x3]^2$
CS12-O1-SOLNR	$(5598.15 + 2619.97 \log[3 + x1] + 5264.89 \log[3 + x1]^2 + 1844.11 \log[3 + x2] + 703.164 \log[3 + x1] \log[3 + x2] - 8307.52 \log[3 + x2]^2 - 975.686 \log[3 + x3] + 1977.01 \log[3 + x1] \log[3 + x3] - 3639.2 \log[3 + x2] \log[3 + x3] - 835.166 \log[3 + x3]^2) / (35.4919 + 44.4286 \log[3 + x1] + 37.799 \log[3 + x1]^2 - 57.184 \log[3 + x2] - 18.3575 \log[3 + x1] \log[3 + x2] + 10.9463 \log[3 + x2]^2 - 17.8365 \log[3 + x3] - 48.8357 \log[3 + x1] \log[3 + x3] + 1.13301 \log[3 + x2] \log[3 + x3] + 22.1222 \log[3 + x3]^2)$
NOTATION	CS12-O2
CS12-O2-L	$655.39 - 85.8367 [x1] + 144.037 [x2] + 199.148 [x3]$
CS12-O2-LN	$(-82276.3 + 160666. [x1] - 9569.6 [x2] + 135256. [x3]) / (-132.622 + 220.396 [x1] + 8.54386 [x2] + 247.275 [x3])$
CS12-O2-SON	$645.983 - 82.5137 [x1] + 6.60931 [x1]^2 + 145.528 [x2] - 52.7183 [x1] [x2] - 6.41306 [x2]^2 + 193.784 [x3] - 10.7642 [x1] [x3] + 60.1183 [x2] [x3] - 4.60535 [x3]^2$
CS12-O2-SONR	$(1.35779*10^8 + 2.70948*10^6 [x1] - 1.35101*10^7 [x1]^2 - 2.62912*10^8 [x2] + 9.17382*10^7 [x1] [x2] - 1.11117*10^7 [x2]^2 - 1.93878*10^8 [x3] - 1.23997*10^7 [x1] [x3] + 1.25305*10^8 [x2] [x3] + 2.89203*10^8 [x3]^2) / (207925. + 5.31325*10^7 [x1] + 3.15617*10^7 [x1]^2 - 627529. [x2] - 4.35706*10^7 [x1] [x2] + 162689. [x2]^2 - 5.36299*10^7 [x3] - 9.46748*10^6 [x1] [x3] + 4.40811*10^7 [x2] [x3] - 2.16728*10^7 [x3]^2)$
CS12-O2-TON	$645.983 - 17.9656 [x1] + 30.8338 [x1]^2 - 8.41339 [x1]^3 + 59.6104 [x2] - 38.4745 [x1] [x2] + 36.7616 [x1]^2 [x2] - 6.41306 [x2]^2 - 18.9309 [x1] [x2]^2 + 30.4681 [x2]^3 + 62.3999 [x3] - 25.008 [x1] [x3] + 36.3025 [x1]^2 [x3] + 45.8745 [x2] [x3] - 18.4718 [x1] [x2] [x3] + 36.3025 [x2]^2 [x3] - 14.5861 [x3]^2 - 18.9309 [x1] [x3]^2 + 36.7616 [x2] [x3]^2 + 40.5059 [x3]^3$
CS12-O2-FOTN	$365.718 - 0.0958139 \cos[x1] + 3.0546 \cos[x2] + 100.339 \cos[x3] - 139.028 \sin[x1] + 31.4459 \sin[x2] + 164.776 \sin[x3]$
CS12-O2-FOTNR	$(6549.68 - 5487.8 \cos[x1] + 15876.6 \cos[x2] + 12261.6 \cos[x3] + 862.824 \sin[x1] + 343.805 \sin[x2] + 5782.2 \sin[x3]) / (13.6318 - 2.15514 \cos[x1] + 21.3531 \cos[x2] + 12.3728 \cos[x3] + 4.76292 \sin[x1] - 7.8951 \sin[x2] - 0.56944 \sin[x3])$
CS12-O2-SOTN	$84.5859 + 72.6917 \cos[x1] + 69.9171 \cos[x1]^2 + 59.3903 \cos[x2] + 18.188 \cos[x1] \cos[x2] + 57.049 \cos[x2]^2 + 90.5128 \cos[x3] + 62.201 \cos[x1] \cos[x3] + 43.6009 \cos[x2] \cos[x3] + 87.8466 \cos[x3]^2 - 31.5962 \sin[x1] + 65.0846 \cos[x1] \sin[x1] - 94.266 \cos[x2] \sin[x1] - 94.266 \cos[x3] \sin[x1] + 172.793 \sin[x1]^2 + 57.1509 \sin[x2] + 96.0011 \cos[x1] \sin[x2] + 21.4356 \cos[x2] \sin[x2] + 96.0011 \cos[x3] \sin[x2] - 73.7799 \sin[x1] \sin[x2] + 174.985 \sin[x2]^2 + 62.6994 \sin[x3] + 60.8804 \cos[x1]$

	$\sin[x3] + 60.8804 \cos[x2] \sin[x3] + 188.859 \cos[x3] \sin[x3] - 15.8753 \sin[x1] \sin[x3] + 84.2308 \sin[x2] \sin[x3] + 129.985 \sin[x3]^2$
CS12-O2-SOTNR	$(-3.14704*10^8 - 1.23524*10^8 \cos[x1] - 6.80297*10^7 \cos[x1]^2 - 1.43514*10^8 \cos[x2] - 6.48024*10^6 \cos[x1] \cos[x2] - 8.58012*10^7 \cos[x2]^2 - 1.61641*10^8 \cos[x3] - 2.46072*10^7 \cos[x1] \cos[x3] - 4.4597*10^7 \cos[x2] \cos[x3] - 1.01917*10^8 \cos[x3]^2 + 4.54692*10^8 \sin[x1] + 2.02911*10^8 \cos[x1] \sin[x1] + 2.75853*10^8 \cos[x2] \sin[x1] + 2.75853*10^8 \cos[x3] \sin[x1] - 2.46675*10^8 \sin[x1]^2 - 4.72325*10^7 \sin[x2] - 744339. \cos[x1] \sin[x2] - 6.06205*10^7 \cos[x2] \sin[x2] - 744339. \cos[x3] \sin[x2] + 3.65654*10^8 \sin[x1] \sin[x2] - 2.28903*10^8 \sin[x2]^2 - 6.36203*10^6 \sin[x3] + 1.10696*10^7 \cos[x1] \sin[x3] + 1.10696*10^7 \cos[x2] \sin[x3] - 2.39902*10^7 \cos[x3] \sin[x3] + 2.74778*10^8 \sin[x1] \sin[x3] - 9.05486*10^7 \sin[x2] \sin[x3] - 2.12788*10^8 \sin[x3]^2) / (-1.66261*10^8 - 3.04755*10^7 \cos[x1] - 1.57382*10^7 \cos[x1]^2 - 4.73918*10^6 \cos[x2] + 1.10008*10^8 \cos[x1] \cos[x2] + 7.14201*10^6 \cos[x2]^2 - 4.32485*10^7 \cos[x3] + 7.1499*10^7 \cos[x1] \cos[x3] + 9.72353*10^7 \cos[x2] \cos[x3] - 2.70937*10^7 \cos[x3]^2 + 7.74442*10^7 \sin[x1] - 1.06025*10^7 \cos[x1] \sin[x1] + 7.88617*10^7 \cos[x2] \sin[x1] + 7.88617*10^7 \cos[x3] \sin[x1] - 1.50523*10^8 \sin[x1]^2 + 9.48581*10^7 \sin[x2] + 1.50736*10^8 \cos[x1] \sin[x2] - 8.96919*10^7 \cos[x2] \sin[x2] + 1.50736*10^8 \cos[x3] \sin[x2] - 9.45945*10^7 \sin[x1] \sin[x2] - 1.73403*10^8 \sin[x2]^2 + 2.10841*10^8 \sin[x3] + 1.45683*10^8 \cos[x1] \sin[x3] + 1.45683*10^8 \cos[x2] \sin[x3] + 6.89134*10^7 \cos[x3] \sin[x3] - 1.13284*10^7 \sin[x1] \sin[x3] - 1.53759*10^8 \sin[x2] \sin[x3] - 1.39168*10^8 \sin[x3]^2)$
CS12-O2-FOLN	$-96.0311 - 192.853 \log[3 + x1] + 406.479 \log[3 + x2] + 496.73 \log[3 + x3]$
CS12-O2-FOLNR	$(78.0083 + 53.3557 \log[3 + x1] + 102.699 \log[3 + x2] + 221.217 \log[3 + x3]) / (1.13834 + 0.267557 \log[3 + x1] - 0.359047 \log[3 + x2] - 0.249265 \log[3 + x3])$
CS12-O2-SOLN	$163.04 + 540.035 \log[3 + x1] - 110.002 \log[3 + x1]^2 + 47.4836 \log[3 + x2] - 485.091 \log[3 + x1] \log[3 + x2] + 148.158 \log[3 + x2]^2 - 485.988 \log[3 + x3] - 42.9964 \log[3 + x1] \log[3 + x3] + 547.569 \log[3 + x2] \log[3 + x3] + 250.164 \log[3 + x3]^2$
CS12-O2-SOLNR	$(3.87025*10^11 + 4.23851*10^11 \log[3 + x1] + 5.25064*10^11 \log[3 + x1]^2 + 2.51079*10^11 \log[3 + x2] + 2.77671*10^11 \log[3 + x1] \log[3 + x2] + 1.78823*10^11 \log[3 + x2]^2 + 3.37261*10^11 \log[3 + x3] + 3.70373*10^11 \log[3 + x1] \log[3 + x3] + 2.0055*10^11 \log[3 + x2] \log[3 + x3] + 3.87217*10^11 \log[3 + x3]^2) / (-1.75823*10^11 + 1.43995*10^11 \log[3 + x1] - 5.71238*10^10 \log[3 + x1]^2 + 2.05856*10^11 \log[3 + x2] - 2.71849*10^10 \log[3 + x1] \log[3 + x2] - 8.30011*10^10 \log[3 + x2]^2 - 2.03781*10^10 \log[3 + x3] - 2.0405*10^10 \log[3 + x1] \log[3 + x3] + 2.2224*10^10 \log[3 + x2] \log[3 + x3] + 2.25747*10^10 \log[3 + x3]^2)$
NOTATION	CS12-O3
CS12-O3-L	$50.6645 - 19.2266 [x1] - 0.0812922 [x2] + 4.60251 [x3]$
CS12-O3-LN	$(3243.63 + 7281.16 [x1] + 28.439 [x2] + 1039.5 [x3]) / (73.4957 + 128.53 [x1] + 0.435249 [x2] + 21.742 [x3])$
CS12-O3-SON	$43.74 - 16.5126 [x1] + 5.92969 [x1]^2 + 0.857342 [x2] - 8.4844 [x1] [x2] + 4.49432 [x2]^2 + 1.84508 [x3] - 4.0281 [x1] [x3] + 3.5319 [x2] [x3] - 1.13342 [x3]^2$
CS12-O3-SONR	$(7.34529 - 3.21108 [x1] + 6.35982 [x1]^2 - 1.9949 [x2] - 2.92642 [x1] [x2] + 10.0896 [x2]^2 + 0.235389 [x3] + 5.12158 [x1] [x3] - 3.84886 [x2] [x3] + 3.83959 [x3]^2) / (0.167931 + 0.0823192 [x1] + 0.112646 [x1]^2 - 0.0515308 [x2] - 0.0338567 [x1] [x2] + 0.166656 [x2]^2 + 0.062387 [x3] + 0.110284 [x1] [x3] - 0.116589 [x2] [x3] + 0.145939 [x3]^2)$
CS12-O3-TON	$43.74 - 5.70345 [x1] + 5.81405 [x1]^2 - 3.88941 [x1]^3 + 0.595432 [x2] - 7.22599 [x1] [x2] + 0.411133 [x1]^2 [x2] + 4.49432 [x2]^2 - 2.82975 [x1] [x2]^2 + 0.294937 [x2]^3 + 0.963195 [x3] - 5.28651 [x1] [x3] - 0.75348 [x1]^2 [x3] + 2.27349 [x2] [x3] - 1.66514 [x1] [x2] [x3] - 0.75348 [x2]^2 [x3] + 0.240629 [x3]^2 - 2.82975 [x1] [x3]^2 + 0.411133 [x2] [x3]^2 + 1.12863 [x3]^3$
CS12-O3-FOTN	$70.6744 - 21.1499 \cos[x1] - 10.7875 \cos[x2] + 5.12185 \cos[x3] - 19.8337 \sin[x1] + 1.02756 \sin[x2] + 1.97377 \sin[x3]$
CS12-O3-FOTNR	$(-4426.9 + 1211.27 \cos[x1] - 7058.62 \cos[x2] - 5279.61 \cos[x3] - 6794.99 \sin[x1] + 4893.12 \sin[x2] + 6773.08 \sin[x3]) / (-85.871 - 71.4512 \cos[x1] - 193.587 \cos[x2] - 4.68836 \cos[x3] - 162.297 \sin[x1] + 92.6967 \sin[x2] + 88.8338 \sin[x3])$
CS12-O3-SOTN	$7.55219 + 5.36792 \cos[x1] + 5.74776 \cos[x1]^2 + 3.33793 \cos[x2] - 3.08531 \cos[x1] \cos[x2] + 3.79634 \cos[x2]^2 + 8.09002 \cos[x3] + 3.65031 \cos[x1] \cos[x3] + 0.796415 \cos[x2] \cos[x3] + 8.48642 \cos[x3]^2 - 6.28251 \sin[x1] + 7.92129 \cos[x1] \sin[x1] - 16.7518 \cos[x2] \sin[x1] - 16.7518 \cos[x3] \sin[x1] + 16.6089 \sin[x1]^2 + 0.203156 \sin[x2] + 0.984117 \cos[x1] \sin[x2] - 2.23976 \cos[x2] \sin[x2] + 0.984117 \cos[x3] \sin[x2] - 10.8707 \sin[x1] \sin[x2] + 17.8499 \sin[x2]^2 + 0.480891 \sin[x3] - 2.7552 \cos[x1] \sin[x3] - 2.7552 \cos[x2] \sin[x3] + 9.56924 \cos[x3] \sin[x3] - 6.80051 \sin[x1] \sin[x3] + 3.87635 \sin[x2] \sin[x3] + 10.0701 \sin[x3]^2$
CS12-O3-SOTNR	$(-3.95553*10^9 + 4.70515*10^9 \cos[x1] + 1.13343*10^10 \cos[x1]^2 - 7.58998*10^9 \cos[x2] - 4.28678*10^9 \cos[x1] \cos[x2] + 4.03579*10^8 \cos[x2]^2 + 2.66512*10^9 \cos[x3] + 5.96831*10^9 \cos[x1] \cos[x3] - 6.32681*10^9 \cos[x2] \cos[x3] + 9.52062*10^9 \cos[x3]^2 - 1.83263*10^10 \sin[x1] - 8.15762*10^9 \cos[x1] \sin[x1] - 1.11328*10^10 \cos[x2] \sin[x1] - 1.1328*10^10 \cos[x3] \sin[x1] - 1.52898*10^10 \sin[x1]^2 + 1.91589*10^10 \sin[x2] + 5.59424*10^9 \cos[x1] \sin[x2] + 1.70916*10^10 \cos[x2] \sin[x2] + 5.59424*10^9 \cos[x3] \sin[x2] + 9.73234*10^9 \sin[x1] \sin[x2] - 4.35911*10^9 \sin[x2]^2 + 2.55602*10^10 \sin[x3] + 1.17402*10^10 \cos[x1] \sin[x3] + 1.17402*10^10 \cos[x2] \sin[x3] + 1.67429*10^10 \cos[x3] \sin[x3] + 1.73721*10^10 \sin[x1] \sin[x3] - 2.5591*10^10 \sin[x2] \sin[x3] - 1.34761*10^10 \sin[x3]^2) / (3.72646*10^8 - 1.52909*10^9 \cos[x1] + 3.61182*10^9 \cos[x1]^2 - 2.45515*10^7 \cos[x2] - 5.40598*10^9 \cos[x1] \cos[x2] + 4.94939*10^9 \cos[x2]^2 + 6.68079*10^8 \cos[x3] - 4.71335*10^9 \cos[x1] \cos[x3] - 3.20881*10^9 \cos[x2] \cos[x3] + 5.56515*10^9 \cos[x3]^2 + 7.27201*10^9 \sin[x1] + 9.44704*10^9 \cos[x1] \sin[x1] + 3.42802*10^7 \cos[x2] \sin[x1] + 3.42802*10^7 \cos[x3] \sin[x1] - 3.23917*10^9 \sin[x1]^2 + 1.08733*10^10 \sin[x2] - 4.08593*10^9 \cos[x1] \sin[x2] + 1.99869*10^10 \cos[x2] \sin[x2] - 4.08593*10^9 \cos[x3] \sin[x2] - 7.57416*10^9 \sin[x1] \sin[x2] - 4.57674*10^9 \sin[x2]^2 + 2.85648*10^9 \sin[x3] - 1.44791*10^9 \cos[x1] \sin[x3] - 1.44791*10^9 \cos[x2] \sin[x3] + 5.78125*10^9 \cos[x3] \sin[x3] - 7.04587*10^9 \sin[x1] \sin[x3] - 1.21876*10^10 \sin[x2] \sin[x3] - 5.19251*10^9 \sin[x3]^2)$
CS12-O3-FOLN	$94.9346 - 50.0312 \log[3 + x1] - 1.31431 \log[3 + x2] + 9.69568 \log[3 + x3]$
CS12-O3-FOLNR	$(2460.73 - 425.199 \log[3 + x1] - 985.267 \log[3 + x2] - 160.022 \log[3 + x3]) / (41.0678 + 3.63551 \log[3 + x1] - 22.0109 \log[3 + x2] - 4.79815 \log[3 + x3])$
CS12-O3-SOLN	$66.1866 + 53.2899 \log[3 + x1] + 3.92426 \log[3 + x1]^2 - 13.3013 \log[3 + x2] - 95.9268 \log[3 + x1] \log[3 + x2] + 28.9572 \log[3 + x2]^2 - 44.1087 \log[3 + x3] - 6.29202 \log[3 + x1] \log[3 + x3] + 58.6023 \log[3 + x2] \log[3 + x3] - 3.73752 \log[3 + x3]^2$
CS12-O3-SOLNR	$(5.96755*10^9 + 7.69851*10^9 \log[3 + x1] + 9.12399*10^9 \log[3 + x1]^2 + 5.69235*10^9 \log[3 + x2] + 5.02216*10^9 \log[3 + x1] \log[3 + x2] + 4.80552*10^9 \log[3 + x2]^2 + 6.0077*10^9 \log[3 + x3] + 8.7341*10^9 \log[3 + x1] \log[3 + x3] + 2.8382*10^9 \log[3 + x2] \log[3 + x3] + 7.64914*10^9 \log[3 + x3]^2) / (1.35754*10^9 - 3.61339*10^9 \log[3 + x1] + 1.09847*10^9 \log[3 + x1]^2 + 1.82407*10^9 \log[3 + x2] + 1.53903*10^9 \log[3 + x1] \log[3 + x2] - 8.44337*10^8 \log[3 + x2]^2 - 1.44095*10^9 \log[3 + x3] + 1.68755*10^9 \log[3 + x1] \log[3 + x3] - 1.42948*10^9 \log[3 + x2] \log[3 + x3] + 3.87635 \log[3 + x3]^2)$

Curriculum Vitae

Name Surname : Emre Görkem ÖZTÜRK

Education:

2012 – 2017 B.Sc. / Izmir Katip Celebi University, Dept. of Mechanical Eng.

2018 – 2021 MSc. / Izmir Katip Celebi University, Dept. of Mechanical Eng.

Work Experience:

2017 – 2018 Oerlikon Kaynak Elektrodları A.S. – Project Engineer

2019 – 2021 Ed-Van Vantilator San. Tic. Ltd. Sti. – Sales Engineer

2021 – Cont. Bonfiglioli Turkey – Application Engineer